Collected Papers

of the

"DIELECTRICS"

SYMPOSIUM

DEPARTMENT OF DEFENSE
PLASTICS TECHNICAL EVALUATION CENTER
PICATINNY ARSENAL, DOVER, N. J.

JUNE 25-26, 1963

at the

Westinghouse Research Laboratories
Beulah Road - Churchill Boro
Pittsburgh 35, Pennsylvania

Note in Insulation, Jan 1964 - avail. fr. D. T. W. Parker, Westinghouse Research Lab., Pittsburgh 35, Pa. @ $5.00 ea.

Was not published

DISCLAIMER NOTICE

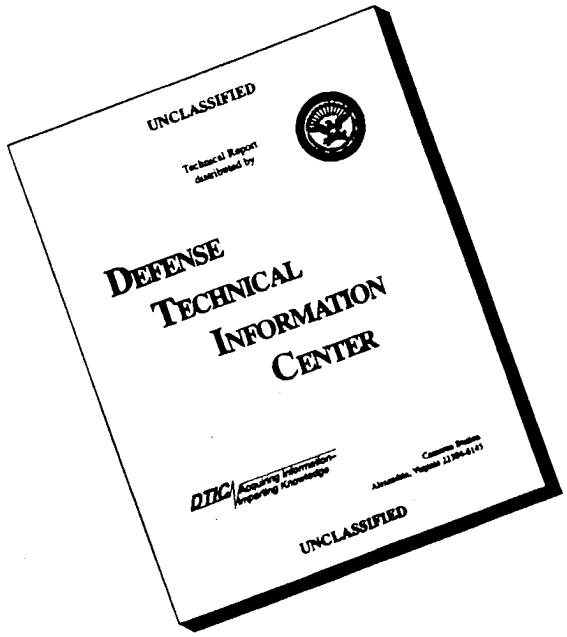

THIS DOCUMENT IS BEST QUALITY AVAILABLE. THE COPY FURNISHED TO DTIC CONTAINED A SIGNIFICANT NUMBER OF PAGES WHICH DO NOT REPRODUCE LEGIBLY.

@dtr@
add435240
7f
end
c

-- 1 OF 1
-- ***DTIC DOES NOT HAVE THIS ITEM***
-- 1 - AD NUMBER: D435240
-- 5 - CORPORATE AUTHOR: WESTINGHOUSE RESEARCH LABS PITTSBURGH PA
-- 6 - UNCLASSIFIED TITLE: DIELECTRICS IN SPACE.
--11 - REPORT DATE: JUN 25, 1963
--12 - PAGINATION: 210P
--20 - REPORT CLASSIFICATION: UNCLASSIFIED
--21 - SUPPLEMENTARY NOTE: PROCEEDINGS: 'DIELECTRICS IN SPACE', 25-26
-- JUN 63, PITTSBURGH, PA. SPONSORED BY WESTINGHOUSE RESEARCH LABS.
-- (SEE PL-42484 - PL-42488).
--22 - LIMITATIONS (ALPHA): APPROVED FOR PUBLIC RELEASE; DISTRIBUTION
-- UNLIMITED. [redacted].
--33 - [redacted]1

--END << ENTER NEXT COMMAND >> END --

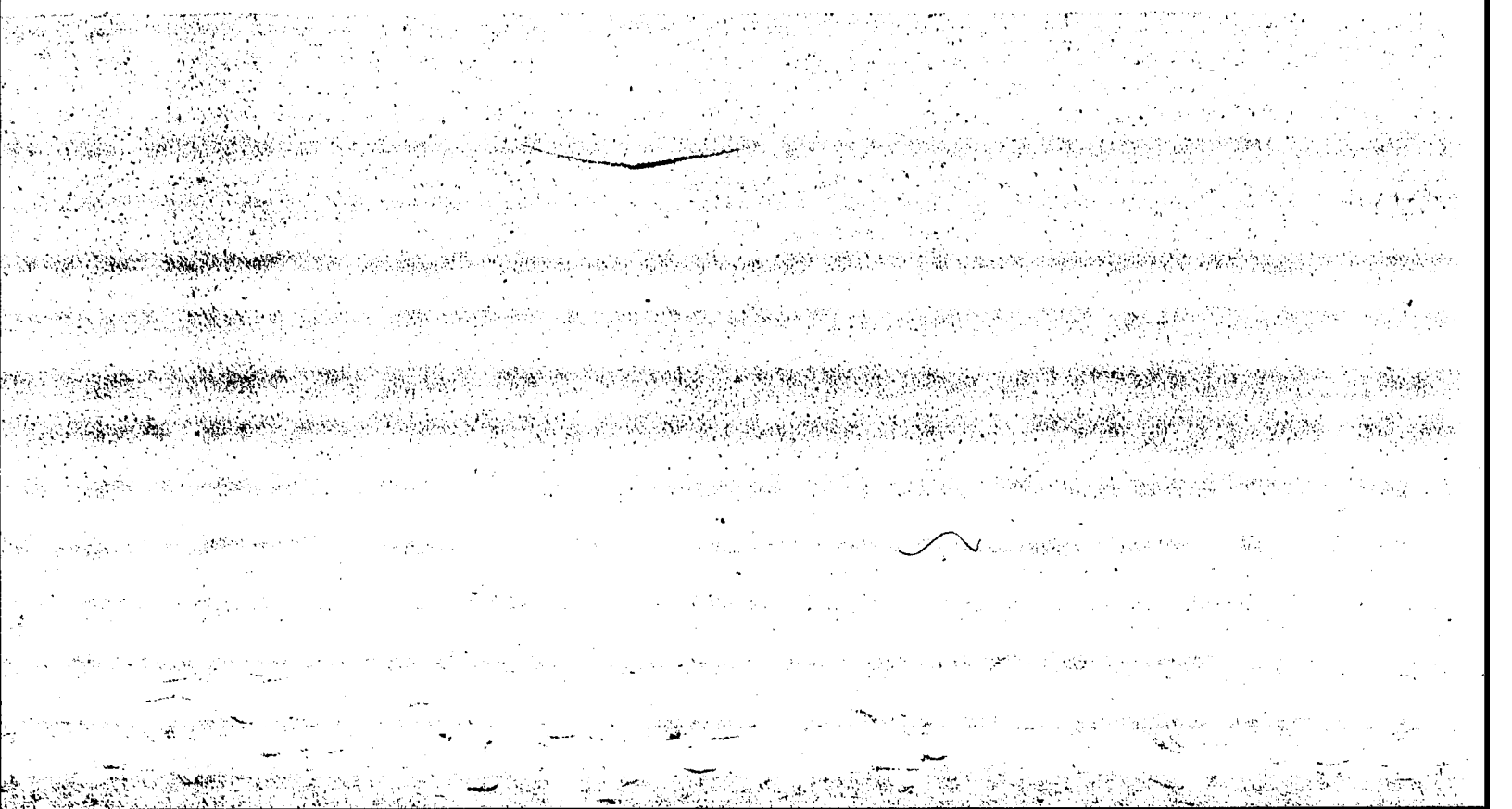

FORWARD

This conference on "Dielectrics in Space" was organized with the intention of reviewing research and problems of dielectric applications in the space program. It brought together research scientists in the field of dielectrics, who were doing, or anticipated doing research, which was applicable to the peculiar environment of space flight,and space engineers or scientists who were confronted with problems which were of a dielectric nature. The conference was attended by 140 scientists and engineers, 20 of whom represented Government agencies, N.A.S.A., Air Force, Navy, which are interested in the space exploration and flight program.

The fourteen papers presented at the Conference, thirteen of which are collected in this book, together with other brief reports and the recorded round table discussion, offer a good cross section of the present dielectric research effort in this field and indicate many of the problems which are still to be satisfactorily solved. The organizers of the Conference have been gratified by the enthusiastic interest of the participants and those attending and by the many favorable comments. These seem to indicate that the Conference's objective was achieved.

Daniel Berg

Thomas W. Dakin

LIST OF PAPERS

1. "The Space Environment as a Dielectric" by A. S. Denholm, Ion Physics Corporation.

2. "Gas Discharges in Insulating Systems at Pressures Between Atmospheric and High Vacuum" by T. W. Dakin and C. N. Works, Westinghouse Research Laboratories.

3. "Current Flow Between Electrodes Immersed in a Low Gas Pressure Plasma" by M. J. Kofoid, Boeing Scientific Research Laboratories.

4. "Some Effects of Simulated Space Environment on the Electrical Properties of Dielectrics" by L. J. Frisco, A. M. Muhlbaum and E. A. Szymkowiak, The Johns Hopkins University.

"A Brief Summary of Space Nuclear Radiations and Effects" by K. H. Sun, Westinghouse Research Laboratories.

5. "High Energy Electron Irradiation of Plastics for Communication Satellites" by J. V. Pascale, D. B. Herrmann and R. J. Miner, Bell Telephone Laboratories, Inc.

6. "Radiation Induced Conductivity in Dielectric Materials" by A. W. Snyder, Sandia Corporation.

7. "The Effects of High Energy Radiation on the Polarization Currents in Some Glasses" by R. A. Weeks and E. Lell, Oak Ridge National Laboratory.

8. "Space Simulation and Its Effects on Materials" by G. R. Blair, Hughes Aircraft Company.

9. "Failure Mechanisms in Dielectrics Under Space Conditions and Techniques for Their Investigation in the Laboratory" by S. M. Skinner, W. J. Lytle and J. W. Merck, Westinghouse Baltimore Air Arm Division.

10. "Properties of Dielectrics at Cryogenic Temperatures" by K. N. Mathes, General Electric Company.

11. "Thermal Behavior of Newer Types of High Stability Polymers" by G. R. Sprengling, Westinghouse Research Laboratories.

12. "Analysis of Solar Energy Conversion Using Thin Dielectric Films" by B. H. Beam, NASA, Ames Research Center.

13. "Evaluation of Inorganic Motor Insulation Under Space Environment" by O. P. Steele, III, Atomics International, Division of North American Aviation, Inc.

14. "Beryllium Oxide Dielectric Components in Aerospace Applications" by P. S. Hessinger and B. Haura, National Beryllia Corporation.

"The Electronic Properties Information Center" by Emil Schafer, Hughes Aircraft Company.

Round Table Panel Discussions and Questions and Answers.

THE SPACE ENVIRONMENT AS A DIELECTRIC

By: A. S. Denholm

Ion Physics Corporation
Burlington, Massachusetts

Abstract: There are many uses for high voltages in space, and in some cases it will be convenient, or necessary, to use the vacuum environment as a dielectric. The limitations of this dielectric are discussed before proceeding to the mechanisms which have been proposed to account for these limitations. The several factors which have to be considered when utilizing vacuum as a dielectric are enumerated. Other considerations when using the space vacuum should include the solar corona and micro-meteoroid bombardment.

Introduction:

Existing or potential requirements for high voltage in space are listed in Table 1. In some of these applications it is convenient, desirable or necessary to utilize the space environment as a dielectric. It is the purpose of this paper to discuss the utility of using the space vacuum to this end and to create an awareness of the areas in which problems exist, some of which are peculiar to the space environment.

The vacuum of deep space is commonly quoted in the 10^{-14} - 10^{-16} torr range with pressures obviously increasing in the vicinity of the earth. This paper will not discuss the transitional pressure regime where Paschen's Law holds and where long path discharges occur at p x d values below that for minimum breakdown voltage, but will confine discussion to altitudes above the earth where the mean free path is longer than typical system dimensions. At pressures below approximately 10^{-3} torr (altitude > 50 miles) avalanche ionization processes become unimportant and the environmental conditions consistent with vacuum discharge phenomena exist.

Table 1 The Use of High Voltage in Space

Primary Objective		Potential Application
electron beams	-	welding re-entry signalling directed energy weapons x-ray production, materials analysis
ion beams	-	thrustors (propulsion and orientation) neutron production-activation analysis directed energy weapons radiation belt studies, auroral investigation, etc.
colloid particle beams	-	thrustors (propulsion)
lasers	-	communication and guidance welding directed energy weapons
high power e.m. radiation	-	radar power transmission (long range) high intensity light sources (beacons, geodesy, etc.)
electrostatic shielding against energetic charged particles		
electrostatic gyros, bearings, etc.		

Vacuum Conduction Phenomena

At low voltages, for example, several thousand volts across a uniform field gap of 1 mm, the vacuum gap behaves like a perfect insulator. Unfortunately, as the voltage is raised there is an increasing probability of a complete collapse of the insulating properties of the gap, and the vacuum arc associated with this collapse is maintained by self-produced vapor from the electrodes. The cause of the transition from the perfect to the imperfect state (breakdown) is obviously a matter of some importance.

It is convenient to separate the discussion of the electrical conduction between electrodes in vacuum into two gap regimes; one below about 1 mm and one above. At the smaller gaps, the most obvious conduction is by the field emission of electrons, which requires no amplification here. However, as the voltage across such a gap is increased, there is eventually a complete collapse of the insulating properties of the gap, and the interelectrode current is determined essentially by the supply characteristics. It is not necessarily the case that a detectible field emission current precedes breakdown. In this gap regime, the breakdown voltage increases approximately linearly with gap (Fig. 1).

Complete breakdown occurs also at large gaps, but there is the further probability of pulsed conduction or current loading taking place. With small electrode areas, small pulses of charge of the order microcoulombs for milliseconds cross the gap at a specific threshold voltage.[1] With large structures, the integrated effect of these small pulses gives a steady current loading such as that indicated on Fig. 2. The continuous application of voltage in the current loading regime can condition a structure so that the voltage limit by current loading is raised to a maximum value. The voltage at which conduction takes place at large gaps increases slowly with increasing gap, and this has been called the total voltage effect.

Having noted briefly the discharge phenomena which can exist when high voltages are applied in vacuum, it is pertinent to discuss the processes which <u>may</u> account for these effects. Reviews of the many mechanisms which have been proposed to account for vacuum breakdown have been given elsewhere[2, 3] and only those which appear of most interest at the present time are discussed here.

Breakdown Mechanisms:

At the smaller gaps there is good evidence that in many cases breakdown is linked directly with field emission processes. In a recent publication[4] Alpert and Lee compare their data with that of others[5,6] to show that breakdown takes place at a critical microscopic electric field of almost 10^8 v/cm for tungsten. However, the data which is presented has two common pecularities which exclude the premise from applying to small vacuum gaps in general. These are that the experiments were made under ultra high vacuum conditions and that the prebreakdown current from the point at which breakdown was initiated was apparently of the order of milliamperes. Apart from the doubt that a gap conducting milliamperes is of utility in an insulating structure, the author and his colleagues have noted breakdown at small gaps at 10^{-6} torr when the prebreakdown current was 10^{-13} amperes or less, and further, with large diameter electrodes noted a current approaching 1 milliampere apparently flowing from one glowing point in the gap when a breakdown occurred in a dark diametrically opposite region. The critical cathode field criterion also discounts the results of the many investigators who found that the anode material is significant in determining breakdown voltage. It appears from this, that if the situation allows very high current from a point, breakdown will occur at a critical field at the point.

Maitland[7] proposed that breakdown occurs because of ionization effects in the vapor produced at the anode by an electron beam. This is consistent with the anode material influencing the breakdown voltage, but again does not account for breakdowns where no detectible prebreakdown current exists.

When those mechanisms for breakdown at small gaps which depend on field emission effects are excluded, there appears to remain only one plausible mechanism. This mechanism was proposed by Cranberg[8] and depends upon the removal of a small charged clump of material from one electrode, and its acceleration and impingement on the other where a cloud of vapor is generated. It was derived that, in general, the relationship

$$VE = C \qquad (1)$$

should hold, where V is the breakdown voltage, E is the gradient at the parent electrode, and C is a constant. For a uniform field gap with spacing d, this becomes

$$V = Cd^{1/2} \qquad (2)$$

Slivkov,[9] examining in more detail the action in the vapor, postulated that

$$V = Cd^{5/8} \qquad (3)$$

was a better relationship. These expressions do not agree well with most plots of breakdown voltage against small gaps, but it is likely that the majority of the published information is for electrodes between which significant field emission currents were flowing, which would permit field emission related mechanisms to act. However, recent experiments suggest that clumps do not cause breakdown at low voltage.[10]

There is good evidence that the current loading phenomenon which occurs at large gaps is related to anode/cathode interactions involving negative and positive ions, which are enhanced by the presence of organic contamination of the electrode surfaces.[11] It is interesting to speculate whether the current loading phenomenon would exist in ultra high vacuum conditions with really clean surfaces.

Probably the most broadly accepted mechanism for breakdown at very high voltages (> 100 kv) is that of Cranberg. This is supported by the voltage to gap relationship for the uniform field condition which tends to follow relation (2). However, Cranberg's non uniform field relationship (1) from which expression (2) was derived does not seem to hold.[12]

It can be seen from the above, that apart from special situations, the situation with regard to vacuum conduction mechanisms is far from clear.

Designing for Vacuum Insulation:

The various factors which should be considered in using the vacuum as a dielectric are itemized and discussed briefly below. References are given for further reading.

Materials: As might be expected from the preceding discussion, breakdown depends strongly on the materials of which the electrically stressed surfaces are made. The better metals include tungsten, nickel and some steel and titanium alloys. It is highly desirable to use metals in which there are no dielectric inclusions. Such impurities are present in many alloys to improve machining properties or to control other material characteristics. The significance of electrode material is indicated by the values in Table 2.

Table 2 Insulation Strength at 1 mm Gap for Several Metals

Metal	Strength kv/mm
304 Stainless Steel	60
Udimet A	55
Nickel, Inconel-718	50
303 Stainless Steel	44
Inconel	44
Inconel-X, Molybdenum	40
Haynes-25	30
Udimet-41	28
Hastelloy B	15
Multimet	10

Surface Finish: The effect of surface finish is less than might be expected and has been discussed elsewhere.[13] It appears that extensive and meticulous polishing gives small gains in insulation strength. Presumably, macroscopic polishing has little effect on the micro projections which may initiate vacuum breakdown. This suggests that electro polishing may be effective, but results have been unpromising. Mechanical polishing produces a hardened surface layer which, it is postulated,[14] inhibits breakdown. This layer is not present after electro polishing.

Gap: As already noted, the breakdown voltage is approximately proportional to gap below about 1 mm. This is illustrated by the plot of insulation strength against gap which is shown on Fig. 3. At large gaps where voltages of the order 10^5 volts can be insulated, the voltage gap relationship follows expression (2) with the constant C about 3 $Mv/m^{\frac{1}{2}}$.[17] At a fixed gap much higher voltages can be insulated for some non uniform field situations, such as a positive sphere opposing a plane, than for uniform field conditions.[12]

Electrode Area: It has long been known from bitter experience that it is more difficult to support high fields over large surface areas than small. But until recently no experiments had been made to determine the extent of this effect.[13] Undoubtedly, the area effect is largely related to the increasing probability with area of weaknesses existing which give low breakdown voltages. Such effects yield to the application of extreme value statistics,[15] which have been applied to similar phenomena in other dielectrics.[16] To give a measure of the effect, an electrode of 20 cm^2 area which can insulate 40 kv across a 1 mm gap can be compared with one of 1000 cm^2 which can insulate only 25 kv. This problem is being studied intensively at the present time.

Temperature: The effect of surface temperature on vacuum breakdown has not been studied extensively, and further work is required in this area. It appears from experiments by Slivkov[18] that for nickel there is no deterioration in vacuum insulation properties up to about 800 ° C. Recent studies at the Naval Research Laboratories by Little and Whitney[19] appear to confirm this.

Pressure: Again, it is necessary to discriminate between the gap regimes below and above 1 mm. At the smaller gaps there is no change in breakdown voltage as the pressure is changed from 10^{-3} torr down to 10^{-9} torr. Some improvement might be expected in the pressure range below 10^{-10} torr with surfaces kept free of adsorbed gas or vapor.

At the larger gaps there is a very definite pressure effect as can be seen on Fig. 4. At first sight, a qualitative explanation of the pressure effect based on mean free path, charge exchange collisions, and gap dimensions, appears reasonable, but closer examination of the numbers involved does not seem to confirm this. The reason for the improvement in vacuum breakdown strength at pressures in the micron range is being studied at the present time.

Structural Stability: Although this is not a vacuum breakdown phenomenon, it is worth noting since the closing of a gap by electric forces may lead to breakdown. The consideration is particularly pertinent to small gaps where high fields can be developed. The surface pressure tending to close a gap stressed at 80 kv/mm is 4 psi. Instability can result because any decrease in gap spacing increases the field ($\frac{V}{d}$) and consequently the force which is tending to decrease the gap. This problem has been treated elsewhere with regard to blade systems in electrostatic generators.[20]

Design Data: In culling values from the literature for the design of equipment, the above should be borne in mind. In most cases, one, or more, of these factors was not appreciated; and also the values are usually breakdown voltages rather than insulation strength. This is particularly important for vacuum breakdown, because of the vacuum gap's unfortunate quality of breaking down a long time after the application of voltage.[2] The time lag with delayed breakdown can be hours, or longer, but the situation is ameliorated by the self-healing property of the vacuum dielectric. In general, a spark does not reduce insulation strength, and in fact there is often a conditioning effect with sparking. The exception is where the discharge causes excessive surface damage. The energy in the discharge can obviously influence this, but the significance of discharge energy, or power, to surface damage is not yet known.

In designing, it is possible to use breakdown voltage values with a suitable factor of safety—if one knew what a suitable factor of safety was! At Ion Physics Corporation the concept of insulation strength has been used extensively, which is defined as the maximum voltage which the vacuum specimen will withstand for a 5 minute period. This is believed to be a more satisfactory criterion than actual breakdown voltage, because in many instances one spark in 5 minutes would be quite tolerable.

Surface Flashover:

It is impossible to stress electrically a vacuum gap without also stressing a dielectric surface in vacuum. There are few papers on the subject.[20-23] For the best performance, attention to the termination of the dielectric at metal surfaces, particularly at the negative end, is essential. The insulation strength of alumina has been plotted against length in Fig. 5. Above about 100 kv, a total voltage effect exists, as in the case of the gap, and again expression (2) appears to apply, but with C having a value around 0.6 $Mv/m^{\frac{1}{2}}$. To obtain dielectric surfaces to support voltages in the megavolt range without excessive dimensions, the dielectric surface is broken up into a series of steps with controlled potential. This is the technique used in accelerator tubes and in the bushing shown in Fig. 6.[24] Typically, a glass accelerator tube would have 50 kv across each one inch dielectric surface.

Pecularities of Space:

With regard to the support of voltage the space environment is not just another vacuum. Before discussing the features which prompt this remark, it is pertinent to qualify the earlier comment that the vacuum of deep space was in the range 10^{-14} to 10^{-16} torr. The presence of the space vehicle will influence the local environment, and the pressure at the surface of the craft, particularly in any re-entrant region, may be relatively high because of material outgassing. As an illustration, two examples have been calculated using commonly quoted outgassing rates. On Fig. 7 the values are for a spherical re-entrant volume evacuated to space through a small opening. Figure 8 is based on a disk of material facing out into space; the pressure being for the point one radius removed from the surface of the disk along the median. Pressure is much higher closer to the surface.

It is now known that the solar corona, at least in a weak form, extends beyond the orbit of the earth. This corona is essentially a very diffuse plasma of electrons and protons, and since it has a bulk velocity away from the sun, it has been called the solar wind. Gold[25] states that there are probably from 100 to 1000 ionized particles/cm^3 in quiet periods. With chromospheric outbursts (solar flares) there are particle densities > 1000 cm^3 with bulk velocities from 500 to 2000 km/sec. For a good discussion of solar emanations see Ref. 26.

To determine the significance of the plasma with regard to voltage support, it was assumed that there were 1000 particles/cm^3 moving with a bulk velocity of 2000 km/sec, which is probably a relatively severe condition. If an electric field system is suddenly applied to a volume containing such a plasma, there is a very brief pulse of current associated with the flushing of the electrons from the volume and the same charge in a longer pulse due to the ion movement and removal. The charge and duration of these pulses depend on the volume and the field, can readily be calculated to a reasonable approximation, and in most instances would be insignificant. Because of the influx of the plasma the field system is fed a continuous load which is of the order 3×10^{-8} amperes/cm^2. The total load thus depends on the effective area of collection, which has to be determined for the specific field system, its orientation with regard to the 'wind' velocity and the kinetic energy of the incoming particles. For small or largely enclosed systems the solar corona is not a significant load, but for more grandiose concepts such as electrostatic shielding it is a major problem.

Less frequent but higher energy particles than the above will produce secondary particles in a vacuum gap, but since these are present in many cases in earthbound high voltage vacuum systems without causing breakdown. it is not thought that they will present a problem in space. The reverse may well be true for micrometeoroid bombardment of the electrically stressed surfaces, about which one can only speculate until the appropriate experiments have been made.

Concluding Remarks:

In spite of all the problems which have been arrayed, it was the intention to encourage rather than to discourage the use of the space environment as a dielectric. If the utility of dielectrics for space were gauged on an electric strength to mass ratio, the natural environment would stand alone. This is certainly not the case on a strength to volume basis. In many cases, it will be inconvenient, or impossible, to use the environment for insulation; in some cases, it will be essential. It is hoped that the information presented will provide for specific applications the first step towards determining the utility of the natural environment for electrical insulation in space.

Acknowledgment:

The author has pirated freely the talents and experimental data of various colleagues. He humbly begs their pardon, In particular, he appreciates the support in this article of K. W. Arnold, R. B. Britton, W. C. Courtney, F. J. McCoy and S. C. Zanon.

Although this is essentially a review article, it is fitting to acknowledge USAF support through contracts AF08(635)-2166 and AF33(616)-7230, which is directed at understanding and controlling the vacuum insulation problem.

References:

1. Calvert, W.J.R., "Pre-Breakdown Current and Vacuum Breakdown," Proc. Phys. Soc. B, 69, 651, 1956.

2. Denholm, A.S., "The Electrical Breakdown of Small Gaps in Vacuum," Can. Jour. Phys. 36, 476, 1958.

3. Hawley, R., "Vacuum as an Insulator," Vacuum, 10, 310, 1960.

4. Alpert,D. and Lee, D., "Electrical Breakdown in High Vacuum," Coordinated Science Laboratory, University of Illinois, Report R-129, 1962.

5. Boyle, W.S., Kisluik, P. and Germer, L.H., "Electrical Breakdown in High Vacuum," J. Appl. Phys. 26, 720, 1955.

6. Dyke, W.P., Trolan, J.K., Martin, E.E., and Barbour, J.P., "The Field Emission Initiated Vacuum Arc," Phys. Rev. 91, 1043, 1953.

7. Maitland, A., "Electrical Breakdown at Low Pressure," M.S. Thesis, London University, 1960.

8. Cranberg, L., "The Initiation of Electrical Breakdown in Vacuum," J. Appl. Phys., 23, 518, 1952.

9. Slivkov, I.N., "Mechanism for Electrical Discharge in Vacuum,"Soviet Physics - Technical Physics, 2, 1928, 1957.

10. Raether, M., "Experimental Test of the Clump Hypothesis of Vacuum Breakdown for Low Voltages," Cordinated Science Laboratory, University of Illinois, Report R-148, 1962.

11. Mansfield, W.K., "Pre-Breakdown Conduction in Continuously-Pumped Vacuum Systems," British J. Appl. Phys. 11, 454, 1960.

12. Arnold, K.W., Britton, R.B., Zanon, S.C., and Denholm, A.S., "Electrical Breakdown Between a Sphere and a Plane in Vacuum," Proc. of 6th International Conference on Ionization Phenomena in Gases, Paris, 1963.

13. Denholm, A.S., McCoy, F.J., and Coenraads, C.N., "The Variable Capacitance Vacuum Insulated Generator-a Progress Report, "Proc. of the Symposium on Electrostatic Energy Conversion, 1963,PIC-ELE 209/1.

14. Germain, C., CERN, Geneva – private communication.

15. Gumbel, E.J., "Statistical Theory of Extreme Values and Some Practical Applications," NBS Applied Mathematics Series, No. 33, Washington, Government Printing Office, 1954.

16. Hill, L.R. and Schmidt, P.L., "Insulation Breakdown as a Function of Area," AIEE Transactions 67, 442, 1948.

17. Trump, J.G. and Van de Graaff, R.J., "The Insulation of High Voltages in Vacuum," J. Appl. Phys. 18, 327, 1947.

18. Slivkov, I.N., "The Influence of the Electrode Temperature on the Electrical Breakdown Strength of a Vacuum Gap," Soviet Physics - Technical Physics 3, No. 4, 708, 1958.

19. Little, R.P. and Whitney, W.T., "Studies of the Initiation of Electrical Breakdown in Vacuum," NRL Report 5944, May, 1963.

20. Coenraads, C., Denholm, A. S., Lavelle, J. and McCoy, F., "Electrostatic Power Generators for Space," Space Power Systems Conference, Santa Monica, American Rocket Society Preprint 2555-62.

21. Gleichauf, P.H., "Electrical Breakdown over Insulators in High Vacuum," J. Appl. Phys., 22, 535 and 766, 1951.

22. Borovik, L.S. and Batrakov, B.P., "Investigation of Breakdown in Vacuum," Soviet Physics - Technical Physics 3, 1811, 1958.

23. Kofoid, M. J., "Effect of Metal-Dielectric Junction Phenomena on High Voltage Breakdown over Insulators in Vacuum," AIEE Transactions III, 79, 999, 1960.

24. Britton, R.B., Arnold, K.W., and Denholm, A.S., "Ability of a Voltage-Graded Surface to Support a High Voltage in Vacuum and in a Pressurized Gas," Rev. Sci. Inst. 34, 185, 1963.

25. Gold, T., "Plasma and Magnetic Fields in the Solar System," J. Geoph. Res., 64, 1665, 1959.

26. Snyder, C., Anderson, H.R., Neugebauer, M. and Smith, J. S., "Interplanetary Space Physics," Proc. NASA-University Conference on the Science and Technology of Space Exploration, Vol. I, Chicago, 1962, p. 163.

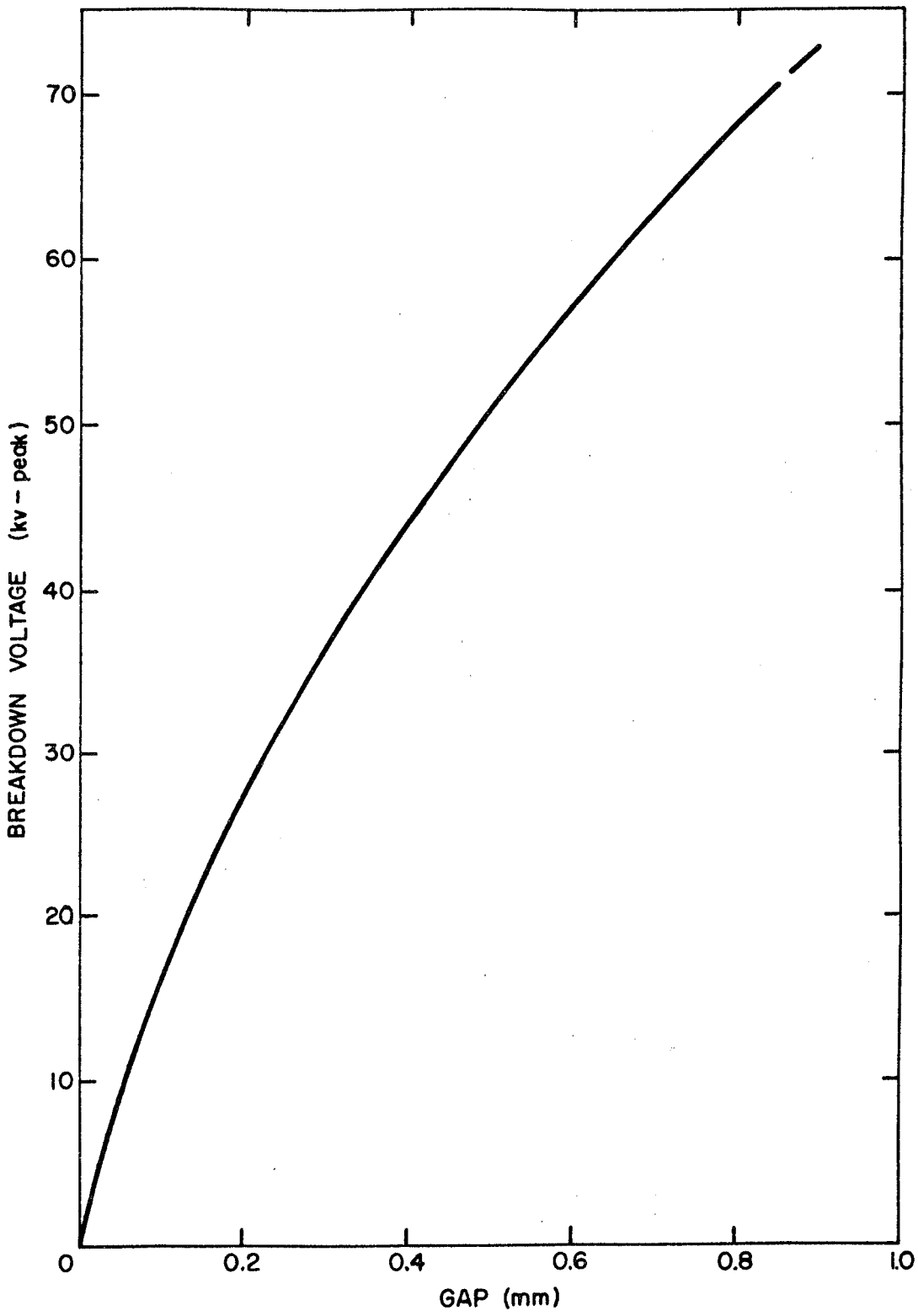

FIG. 1 MAXIMUM BREAKDOWN VOLTAGE (50c/s) FOR ALUMINUM ELECTRODES
(REF. 2)

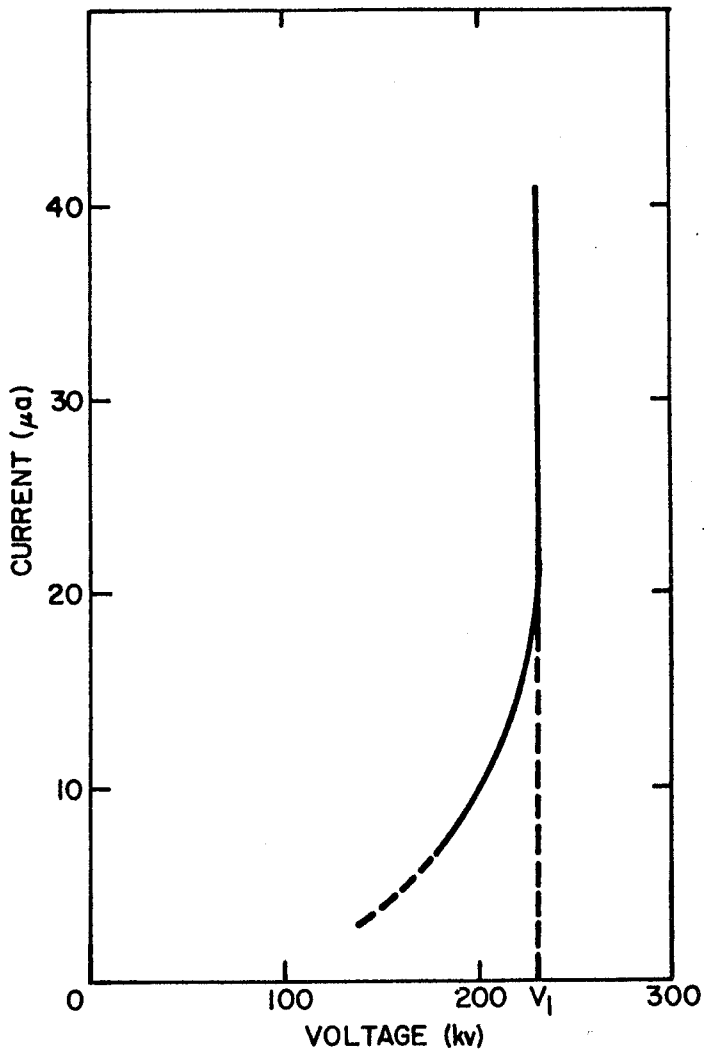

FIG. 2 CURRENT/VOLTAGE CHARACTERISTIC FOR UNCONDITIONED VACUUM BUSHING

(V_1 – VOLTAGE LIMIT BY CURRENT LOADING)

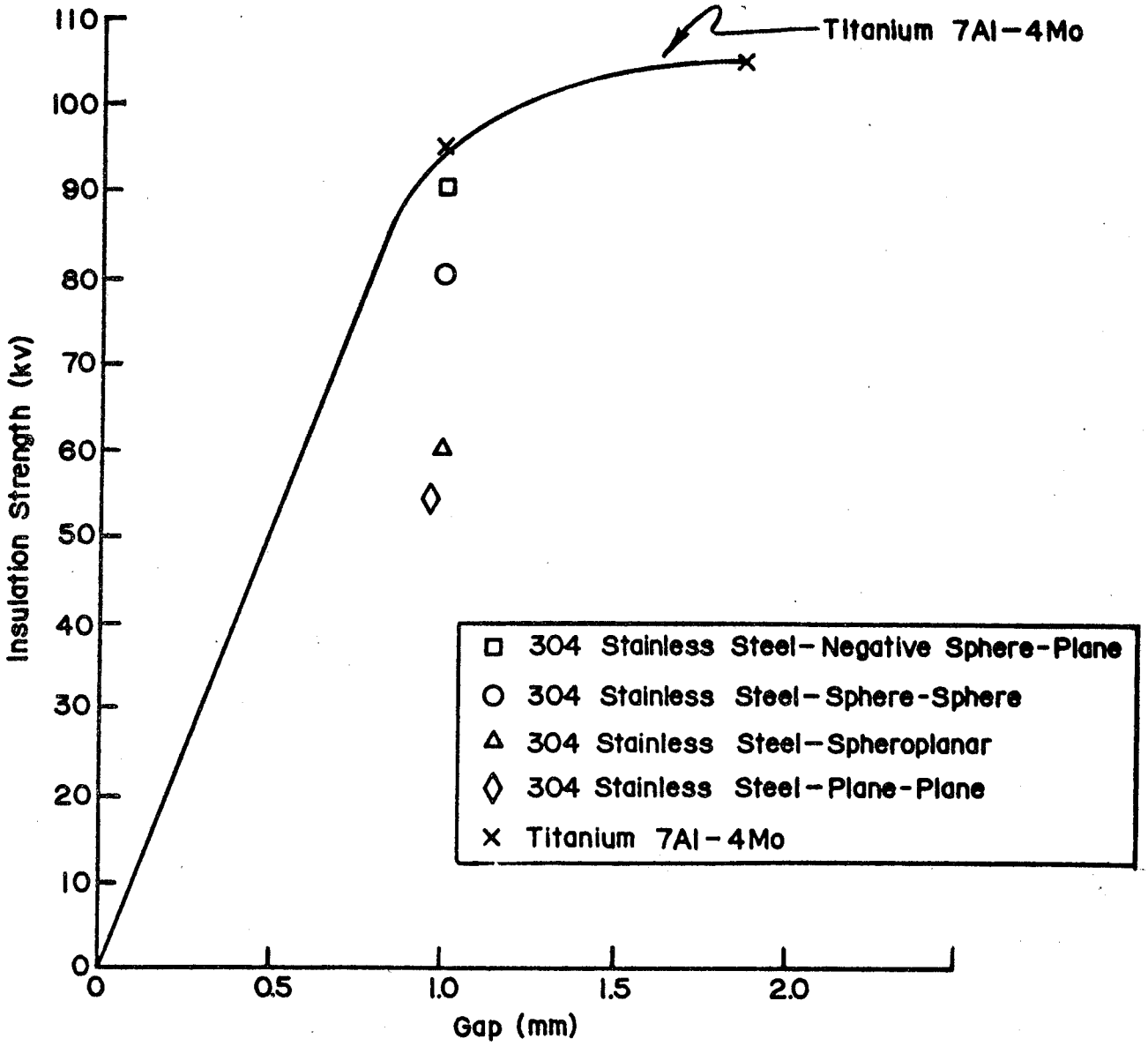

I-335

FIG. 3 RESULTS OF INSULATION STRENGTH TESTS

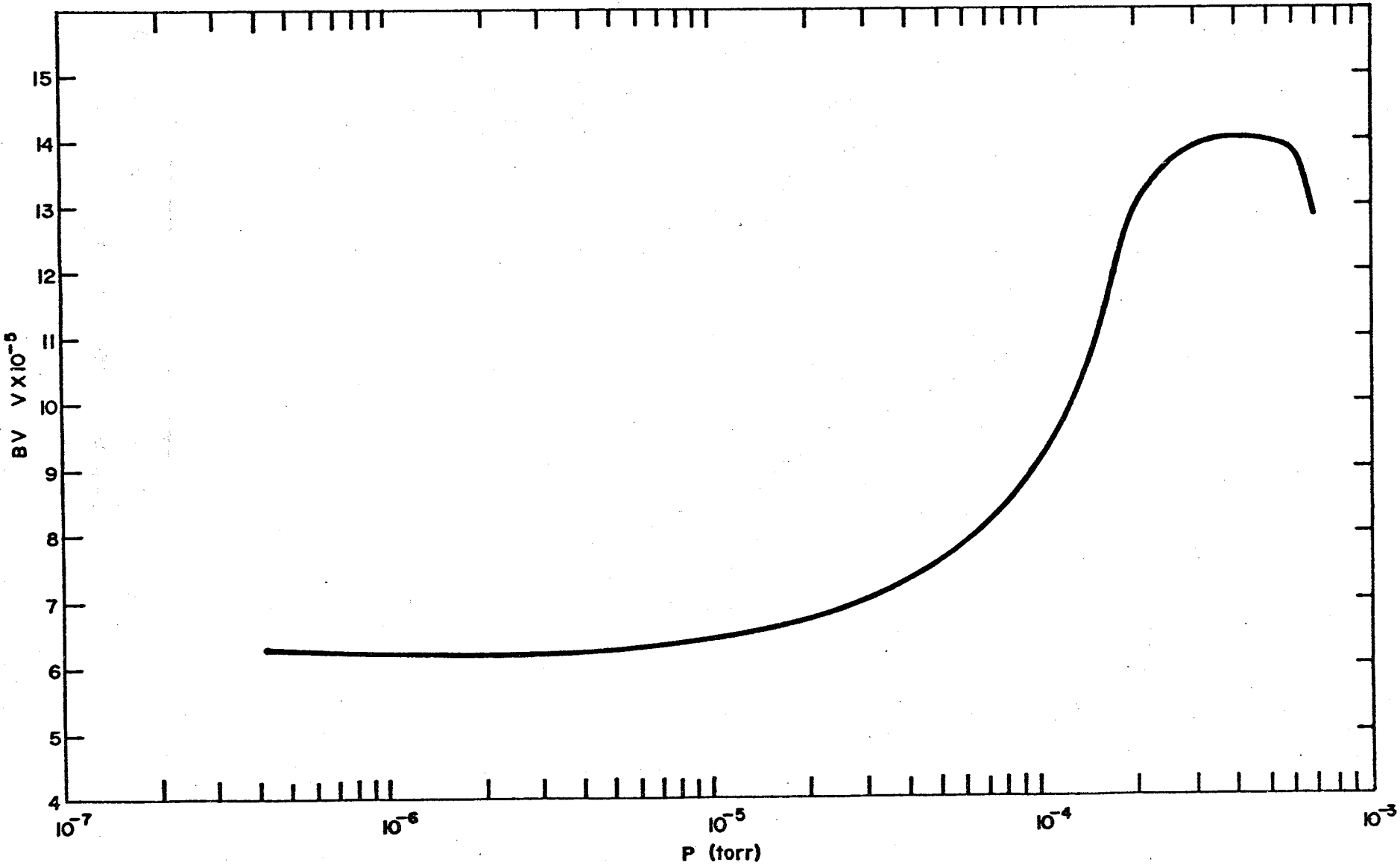

FIG. 4 BREAKDOWN VOLTAGES VS. PRESSURE FOR ANODE SPHERE TO CATHODE PLANE
(SPACING OF 20 cm — SPHERE 0.16 cm DIAMETER)
(REF. 12)

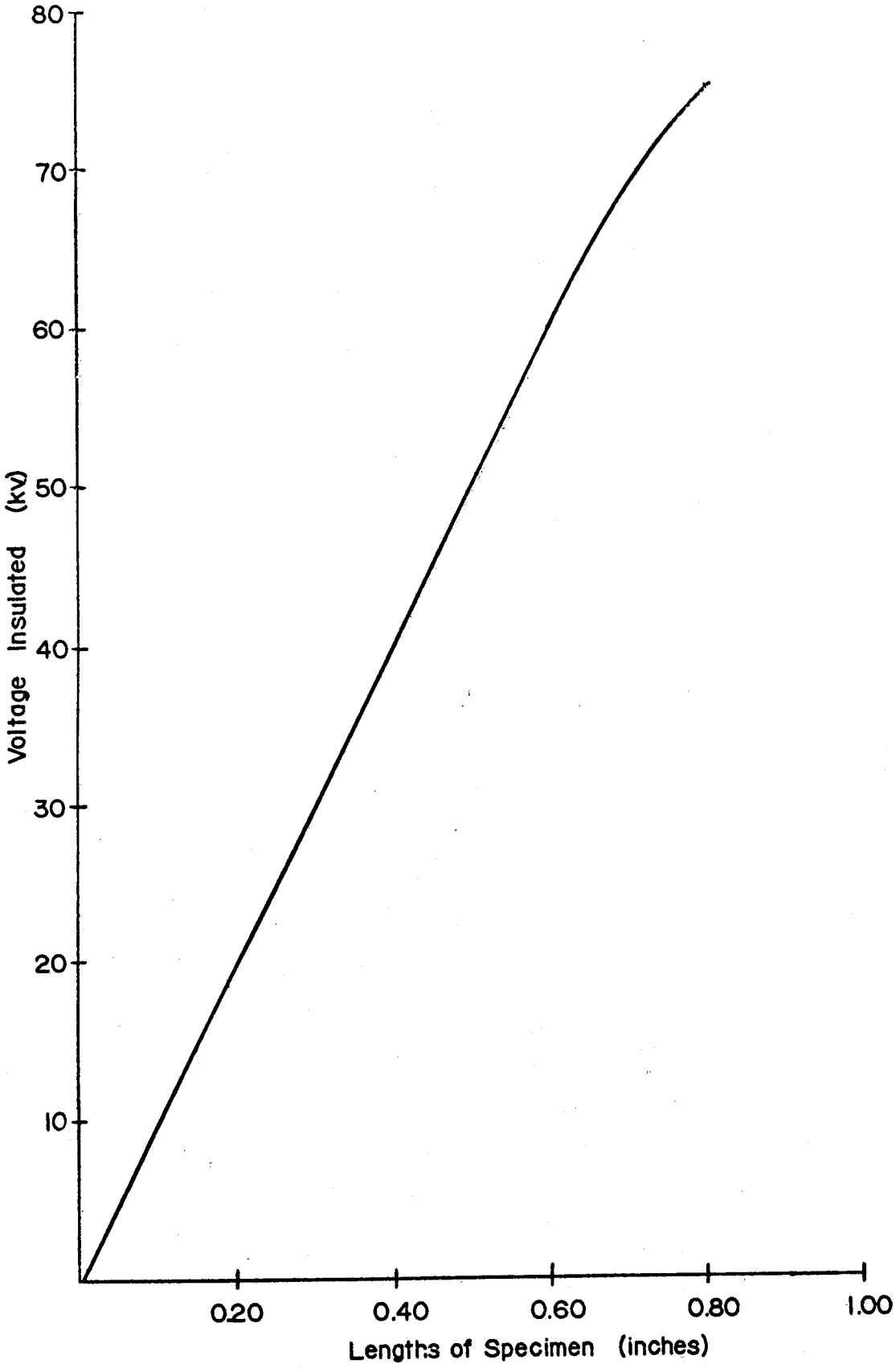

I-336

FIG. 5 INSULATION STRENGTHS OVER AL_2O_3 SURFACES IN VACUUM

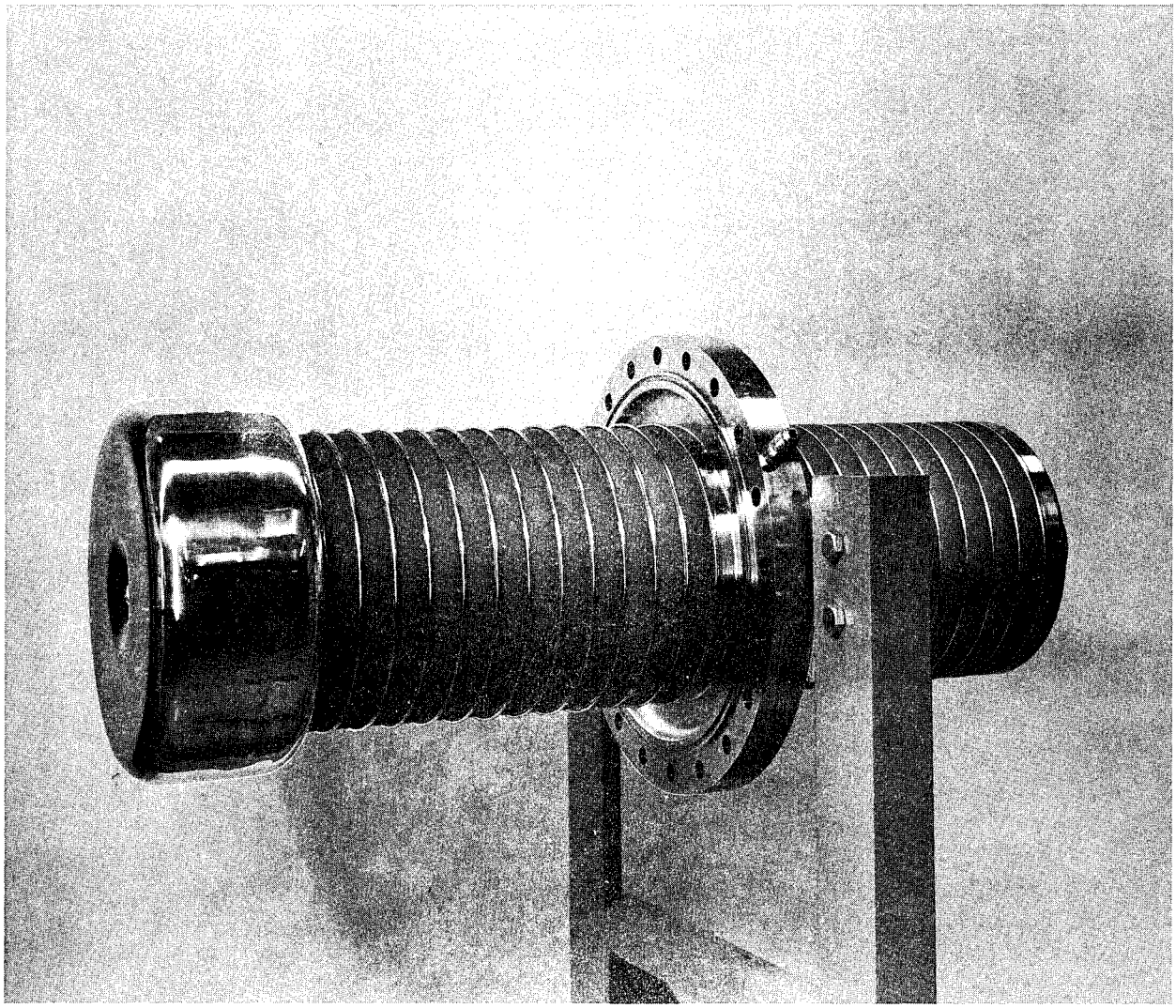

FIG. 6 CONTROLLED GRADIENT HIGH PRESSURE TO HIGH VACUUM BUSHING
(REF. 24)

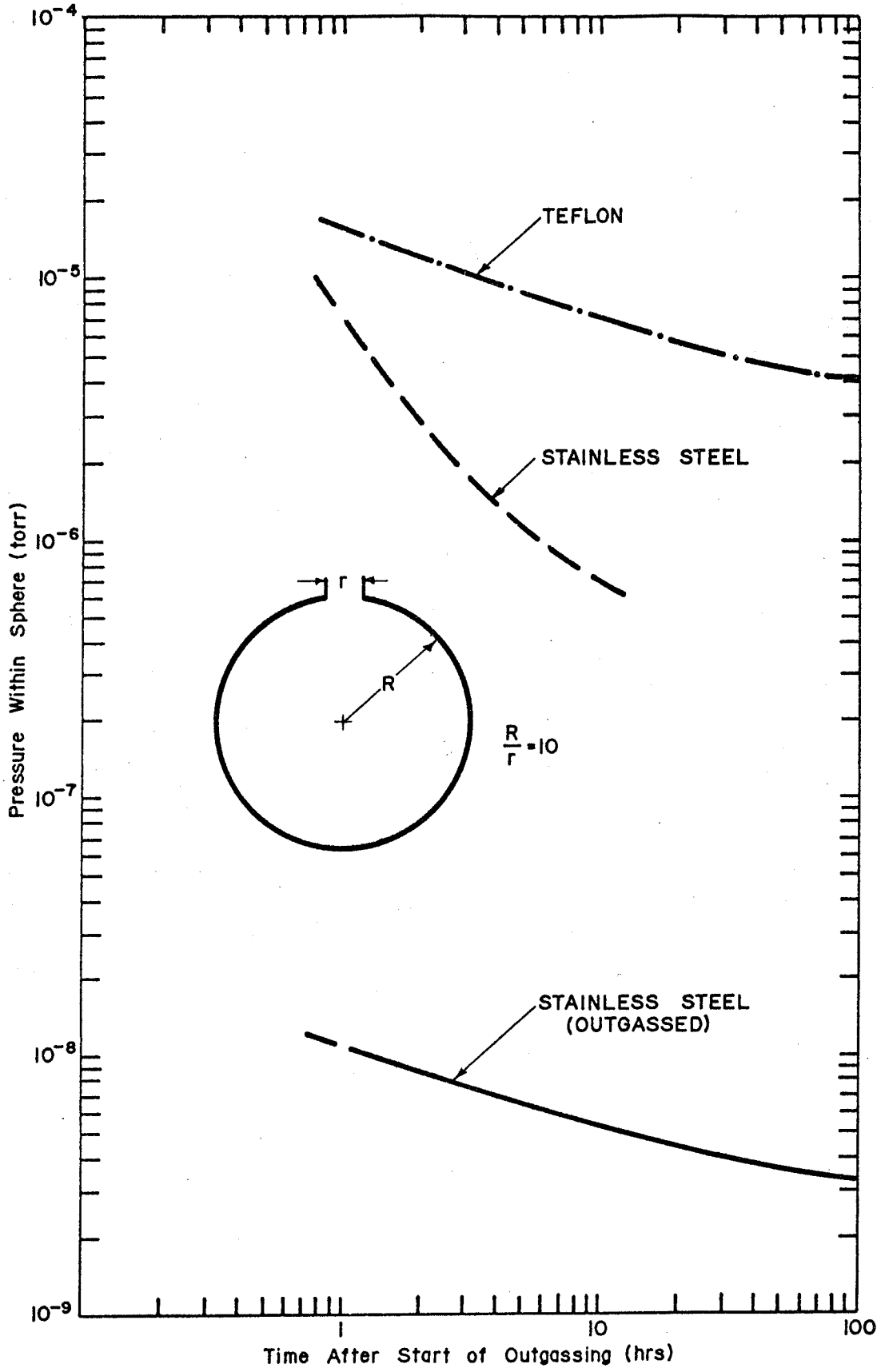

FIG. 7 PRESSURE INSIDE AN OUTGASSING SPHERE

I-337

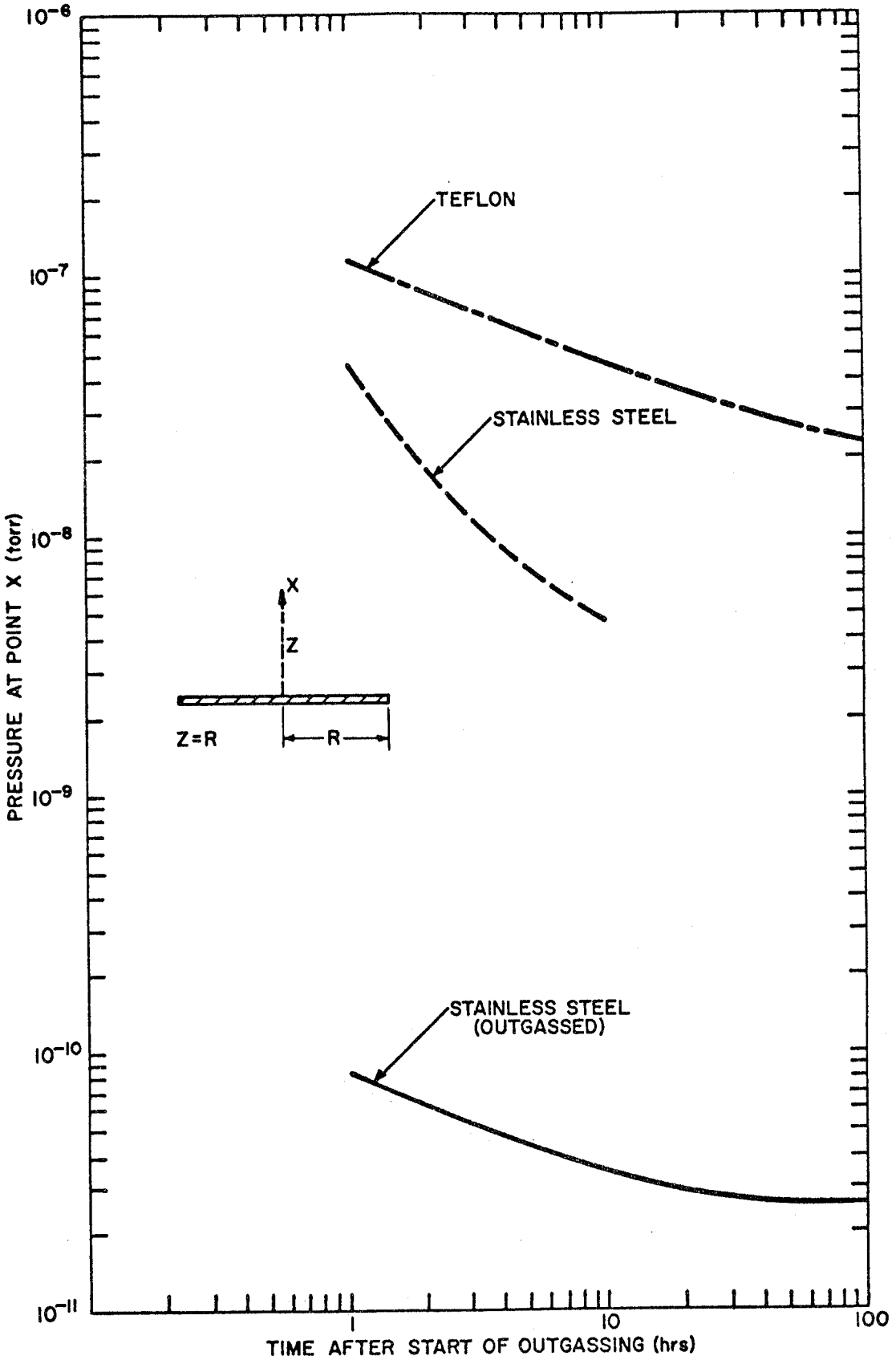

FIG. 8 PRESSURE ON THE MEDIAN OF AN OUTGASSING DISC AT Z=R

I-338

GAS DISCHARGES IN INSULATING SYSTEMS AT PRESSURES BETWEEN ATMOSPHERIC AND HIGH VACUUM

T. W. Dakin and C. N. Works
Westinghouse Research Laboratories
Pittsburgh 35, Pennsylvania

This paper will present a survey of the gas discharge situation which exposed-energized electrical systems will encounter as they pass from atmospheric pressure through the low pressure regions at high altitudes and on to the vacuum of outer space. Part of the presentation will be based on a scrutiny of well-known low pressure discharges phenomena as they apply to electrical system environments at high altitude. The discharge behavior of gaps and simple insulation systems in the low pressure glow discharge region is illustrated by experiments made on such systems. Finally some observations made on discharges with insulating barriers in vacuum will be discussed.

Fig. 1 orients us as to the relation of pressure and altitude. The most critical region of altitude is in the range of 10 to 50 miles, about 100 to 0.01 torr (mm. Hg.), where the minimum breakdown voltage of air occurs for typical spacings likely to be encountered in electrical systems. At higher altitudes the situation for smaller systems improves markedly, since the breakdown voltage increases toward high vacuum.

The problem of reduced breakdown voltages at high altitudes has been recognized and dealt with in connection with high flying aircraft where altitudes of the order of 10-14 miles maximum were encountered but now the altitude is unlimited in spacecraft, which encounter the very minimum air breakdown voltages possible. Thus a broader view must be taken for high altitude aircraft.

The relation of breakdown voltage to pressure and spacing with uniform field is shown in the familiar Paschen's curve, Fig. 2.[1,2] It should be noted particularly that the minimum value is at about 0.6 mm. Hg. for a 1 cm spacing. Correspondingly for 10 cm it would be .06 mm. Hg., etc. Also it should be noted that the minimum value is at about 330 volts crest. This would correspond to about 230 volts r.m.s. for sinusoidal a-c voltage, since the minimum breakdown would occur on the crest of such a varying voltage. The behavior in this curve is typical of a breakdown in any gas resulting from the castastrophic-avalanche build-up of ionization by collisions of electrons with atoms or molecules and kept going by a secondary ionization process such as photoionization or cathode photoemission. At lower pressures, below the Paschen's minimum, higher voltages are required to increase the electron energy and the probability of ionization due to the fewer collisions of electrons in each avalanche resulting from the reduced gas density (or spacing).

If now we examine in Fig. 3 actual experimental data taken on a 0.25 cm (0.1 inch) sphere gap in a low pressure cell, we note a similarity between the Paschen's curve, but there is one notable difference. The curve does not rise sharply after passing through the minimum. This is simply due to the fact that there are larger available spacings for discharges to occur in most practical systems. Discharge does not start at the closest spacing between the spheres but at some greater distance from the sides of the spheres or their supporting rods.

There is another notable difference. In the low pressure region the "breakdown" does not result in an arc and a sudden drop in voltage but results in a glow discharge which will maintain a substantial voltage if the current is not driven too high. This raises the question: What condition really constitutes breakdown in this region? At higher pressures it is difficult to avoid an arc discharge which will draw unlimited currents usually at a localized point on the conductor after a spark starts the breakdown. In that case the question of the criterion of breakdown current is not so critical. But in the low pressures glow discharge region, a few, up to several hundred, milliamperes of current may flow without an arc developing. Such glow currents may or may not be at all serious to the performance of an electrical system, or only temporarily disabling. They would, however, cause substantial radio noise.

The behavior of the glow discharge in a simple sphere gap cell should be illustrative and of some interest. For example, the current which flows in the glow may be partly determined by the impedance of the circuit supplying the voltage. We have worked with both very low and high impedance sources. If, at a particular pressure, the gap cell is connected to a very low impedance source and the current allowed to reach whatever level it wishes, one will find that, after the glow once starts, a higher voltage is required to produce an arc. Note the line in Fig. 3 for the limit of voltage for a d-c arc.

The currents flowing in the system at various pressures in the glow region are shown in Fig. 4. It will be noted that, near the Paschen's minimum pressure, the overvoltage tolerated by the glow for this clear small gap is small. But at lower pressures, where the glow has spread to larger spacings the overvoltage is considerable before an arc develops. The arc condition corresponds to a negative voltage current characteristic where the voltage drops as the current increases. With this system the highest stable glow current was about .2 ampere.

The appearance of the glow discharge in this system is fascinating as shown in the photos of Fig. 5. Only a color photo, however, can capture the beauty of the discharge. Only in 5a, at a pressure not far below the Paschen's minimum are seen clearly some of the typical characteristics of the classical glow discharge which has been studied and described about 100 years ago by Crookes and Faraday and others[3,4]. The cathode glow is seen uniformly sheathing the upper negative electrode and its supporting shaft. Must of the voltage drop in the glow appears between the cathode and this glow. This cathode drop in normal glows in gases depends on the cathode

metal and varies from 230 volts for Al to 375 volts for copper, being 270 volts for iron. The Faraday dark space outside the cathode glow and the anode glow as a ring around the lower electrode are evident, but the positive column which in the classical discharge tube with a single uniform spacing between electrodes, is a fainter striated columnar glow is not very evident here. In the other photos taken at lower pressures the nature of the glow is very indistinct, but the bright spots in the photo 5c are the precussors of an arc breakdown. The glow current here is quite high and fills the whole vessel. At still lower pressures the size of the vessel is too small to sustain a discharge and it disappears, unless the voltage is increased.

With a-c voltages a dynamic characteristic is noted, as shown in the oscillograms of Fig. 6. In Fig. 6, the horizontal axis is proportional to the voltage driven back and forth, in phase with the sinusoidal voltage applied to the test cell. The vertical axis corresponds to the current flowing through the cell at each value of the voltage. An overshoot of the voltage can be noted particularly at low pressures (as in 6a) before the glow begins, after which the voltage drops as the glow starts and then it rises again as the glow current builds up. At higher pressures as much as an ampere of glow current has been observed without the development of an arc. In Fig. 6b a substantial glow current is flowing, but without an arc breakdown. No overshoot of the voltage is observed, presumably because the electrodes have been heated by the discharge current. The development of an arc was caught as shown in 6c.

When solid insulation is introduced into the spacing, we have at higher pressures the possibility of a corona discharge between the electrodes and the conductors, where the gas gap is stressed higher than the breakdown voltage, but not sufficiently high to flash around the solid barrier or to puncture it. A typical situation is an insulated wire adjacent to a metal ground plane as in Fig. 7, which shows a decreasing corona starting voltage as the pressure decreases. This discharge threshold is a function of the ratio of the solid dielectric thickness to the dielectric constant. The threshold voltage decreases toward the Paschen's minimum voltage but generally levels off somewhat above it, for reasons connected with the geometry of the discharge, which is occurring in an essentially divergent field. As the pressure drops, the corona pulses increase in charge and spreading distance, until at low pressures the corona discharge takes on the character of a glow discharge, which now fills the entire vessel.

Fig. 8 shows the behavior of pulse magnitude with a-c overvoltage. It can be seen that the pulse magnitude becomes tremendous at low pressures. It is believed that the decline in apparent pulse size with increasing voltage at low pressure is due to the fact there is such a large glow current the gas space is so conducting as to diminish the apparent size of pulses. A somewhat similar effect is observed with highly overvolted point corona sources in air at atmospheric pressure. The pulse voltage which develops as a result of such corona can be estimated by dividing the picocoulomb charge by the picofarads of capacitance directly attached to the corona source.

Pulses amounting to hundreds of volts may be anticipated if the capacitance is not large. This could cause serious interference with radio circuits.

The presence of solid insulation in the system causes surface charges to develop, which, with d-c voltage,prevents successive pulses until the charge leaks away or the voltage is raised further. A typical behavior with increasing d-c voltage is a succession of pulses as long as the voltage is increasing, but, which nearly stop when the voltage is steady. If there is the possibility of a complete flashover between conductors a glow discharge current will occur at low pressures.

Another situation which we have studied is represented by parallel enamel insulated wires, each of which had a deliberately prepared defect, a bare spot. The bare spots were separated in the direction of the wire axes by about 1/2 inch. As the pressure was lowered, the corona threshold voltage dropped to about 300 volts r.m.s. and a glow developed which eventually filled much of the chamber. The effect of this glow on the dissipation factor of this system is shown in Fig. 9. It is notable, however, that an arc did not develop between the bare spots until the a-c voltage was raised to 500-600 volts, r.m.s. This illustrates the overvoltage capability of such systems. Furthermore, it was possible in the pressure range below 1 mm. to apply as high as 1300 volt impulse overvoltages without developing an arc breakdown, while the system was glowing with 450-470 volts, but at 5 mm. pressure a 300 volt overvoltage pulse caused an arc. The pulses applied here had decay times of the order of a millisecond.

A somewhat more dramatic indication of the glow discharge is shown in Fig. 10, which is a photo of a motor stator first with a negative d-c applied to the winding at a pressure in the glow.region. In these experiments which were carried on for hours,no arc breakdown of the insulation occurred. Defects in the insulation are indicated by the brightly glowing points.

A short investigation of the impulse overvoltage behavior of gaps in the low pressure region has been made. Tests with an enameled wire were described in the previous paragraph. The tests with a clear sphere gap were of two types: first, starting from an a-c voltage below the glow discharge voltage, i.e., 230 volts r.m.s., and secondly, with a d-c glow occurring and superimposing an overvoltage pulse. It was the intention of these tests to determine when impulse overvoltages would result in a power follow arc.

In the tests with 230 volts r.m.s., from a low impedance source, applied to a 0.25 cm sphere gap with no discharges occurring, many pulses were applied with voltages up to 3000 volts without initiating an arc breakdown. These pulses had a decay time of about 0.2 milliseconds to half voltage. In these tests the gap was not irradiated, however. It is fairly well known that low pressure breakdowns have a long statistical time lag.

In impulse overvoltage tests of gaps already having a glow discharge, two problems arose. The d-c source had to have an adequate current capability to support an arc and the impulse overvoltage source had to be of

a high capacitance capability to overcome the shunting effect of the glow discharge on the d-c source. Impulse overvoltages of a few hundred volts were achieved, but without any persistent power arc breakdown occurring.

In these experiments an impulse voltage was applied to discharge operating at 400 to 500 volts. This output of the d-c source was shunted by 2.3 microfarads and it was capable of delivering several amperes. The impulse voltage was obtained by switching a capacitor of 0.5 to 2.7 microfarads charged to a high voltage, from 2000 to 10,000 volts, onto the glow discharge cell, while a d-c glow current was flowing through the cell from the d-c source. Since both the d-c source and the glow discharge served to shunt the applied impulse voltage, the actual voltage rise on the gap was much less than the applied voltage.

Figs. 11 (a)(b)(c) are traces of oscillograms of the current and voltage in a glow discharge between sphere gaps at 0.254 cm spacing. A steady d-c current was flowing in each case prior to the overvoltage pulse. Three typical different conditions are shown. In case (a) the current rises in the glow, and the voltage rises as in an abnormal glow discharge characteristic. In case (b) the current rises along with the voltage but subsequently both voltage and current drop, with apparently a sort of arc characteristic developing which extinguishes. After this the gap recovers voltage and the process is repeated. In case (c) the overvoltage impulse causes a very high a-c current pulse to develop and the voltage drops. In both cases (b) and (c) the voltage appears to swing somewhat to the opposite polarity before it recovers. It is notable that in all cases no persistent power follow arc, driven by the d-c supply, developed.

There is an insulation system for high voltage d-c which can be recommended as fairly secure against breakdown over the entire pressure range from atmospheric pressure to high vacuum. This is a system in which all of the conductor parts of at least one polarity are completely enclosed in a coating of insulation which will withstand the highest voltage to be applied. This gives no possibility for discharges around the insulation barrier. The efficacy of such a system has been checked by tests on vinyl and polyethylene insulated wire which have been carried into a low pressure chamber and around bare metal rods of the opposite polarity, as in Fig. 12. Such an arrangement cannot conduct a d-c current except the insulation leakage current. This system has withstood high voltage close to the d-c breakdown voltage of the wire insulation without apparent distress or very obvious discharges over the entire pressure range down to high vacuum. If the voltage is raised, however, in the low pressure range a few discharges between the bare metal and the insulation surface occur, but these are not serious. A few discharges would also occur if the pressure is reduced while the voltage is applied. Such discharges transfer the potential of the metal to much of the surface of the wire insulation. As this charge is conducted slowly through the insulation, occasional subsequent discharges will occur. It would possibly be fatal to this system if a single break in the insulation occurred. This would permit a glow and possibly an arc to develop.

As it was mentioned previously, the breakdown voltages increase greatly as the pressure is reduced toward high vacuum, since collision ionization of electrons with gas molecules no longer occurs within the dimensions of the system.

Since electron-gas collisions do not occur in high vacuum, electrode processes are responsible for breakdown, and the metal of the electrodes affect the result. Vacuum breakdown stresses are of the order of 1 megavolt/cm.[5,6] It is not the purpose of this paper, however, to discuss the vacuum breakdown process, except as it applies to the phenomena the authors have been observing in arrangements involving dielectric barriers between electrodes in high vacuum.

A common arrangement in insulation systems in air is one involving a conductor edge on an insulation barrier with an extended conductor (plane or cylinder) on the opposite side of the insulation. In air, corona discharges occur at the conductor edge at a critical threshold voltage, depending on the thickness/dielectric constant ratio. Since this is a fairly typical insulation arrangement, the authors have been studying the behavior of such a system in vacuum, as in Fig. 13.

Typical corona detection equipment has been used to detect pulses in vacuum with a-c voltage applied to a sphere electrode resting in the center of flat insulation specimens and placed on a larger flat electrode.

Tests on mica, glass and Mylar have all indicated small discharges of the order of a few hundred to a few thousand picocoulombs prior to much larger pulses which are visible and which eventually lead to flashover. These pulses usually occurred in bursts, and with a-c voltage pulses occurring on the negative half cycle were followed by ones on the positive half cycle, the polarity referring to the small upper electrode. With mica, the more reproducible pulses occurred at a stress of about 1000 to 1500 volts r.m.s./mil as referred to the mica thickness although less reproducible pulses occurred at lower voltages. Complete flashover of the specimen surface occurred at about twice this stress. The stress in the vacuum gap depended on the gap where the discharges were occurring. In gaps of the order of 1 mil this would have been as high as a megavolt/cm for the pulses at 1000 to 1500 volts/mil.

At the voltage near complete specimen flashover and development of a high current breakdown visible diffuse streamer like discharges were seen to spread over the surface, some of which drew many milliamperes of current, but without tripping the overload relay. These larger flashovers usually occurred on the negative half cycle. Under these conditions the sample sometimes punctured, possibly due to the heat of the discharge.

The most interesting results were obtained with d-c voltage. With 2" x 2" glass specimens ($\epsilon' = 8.7$) 31 mils thick, with the upper electrode negative, pulses of similar magnitude to those seen on a-c were seen occasionally as the voltage was raised. At higher voltage they came in bursts, and complete flashover occurred at 31-37 prior to glass puncture. But with

positive voltage on the upper electrode, no pulses were observed until near breakdown between 40 and 50 KV at which time the sample appeared to breakdown thermally.

Similar tests in vacuum with polyethylene insulated wires in an arrangement similar to Fig. 12, but with a hole through the insulation at a point remote from the ground plane, indicate a substantially lower flashover voltage when the exposed ground plane is negative, as compared to the arrangement with the insulated wire negative.

These experiments indicate that cathode emitted current pulses are observable in situations where dielectric barriers occur between electrodes in vacuum and they initiate flashover of the insulation barrier. These current pulses develop surface charges and reverse pulses with voltage reversal. Thus a repetitive pulse phenomena is observed with a-c voltages, similar to that observed in the same arrangement in gases. These discharges reduce the breakdown voltage of dielectric barriers with a-c applied voltage in vacuum.

SUMMARY

This paper has outlined the discharge behavior to be expected in passing from atmospheric pressure to high vacuum.

It has shown that complete insulation of conductors at at least one terminal voltage can lead to high d-c electric strengths (and with a minimum number of discharges), corresponding to the d-c insulation strength, throughout the low pressure range and at high vacuum. With high a-c voltage such a system would have discharges which would reduce the electric strength of the solid.

To avoid all discharges it would be necessary to completely enclose the system in a sealed capsule, or avoid high stresses across solid insulation where series gaps may occur.

REFERENCES

1. J. M. Meek and J. D. Craggs, Electrical Breakdown of Gases, Oxford Univ. Press, London, 1953.

2. T. W. Dakin and D. Berg, Theory of Gas Breakdown.

3. A. Von Engel, Ionized Gases, Oxford Univ. Press, London, 1955.

4. J. D. Cobine, Gaseous Conductors, McGraw-Hill Co., New York, 1941.

5. A. S. Denholm, The Space Environment as a Dielectric, Dielectrics in Space Symposium, Westinghouse Research Laboratories, June 1963.

6. R. Hawley, Vacuum as an Insulator, VACUUM, Vol. 10, No. 4, pp. 310-318, 1961.

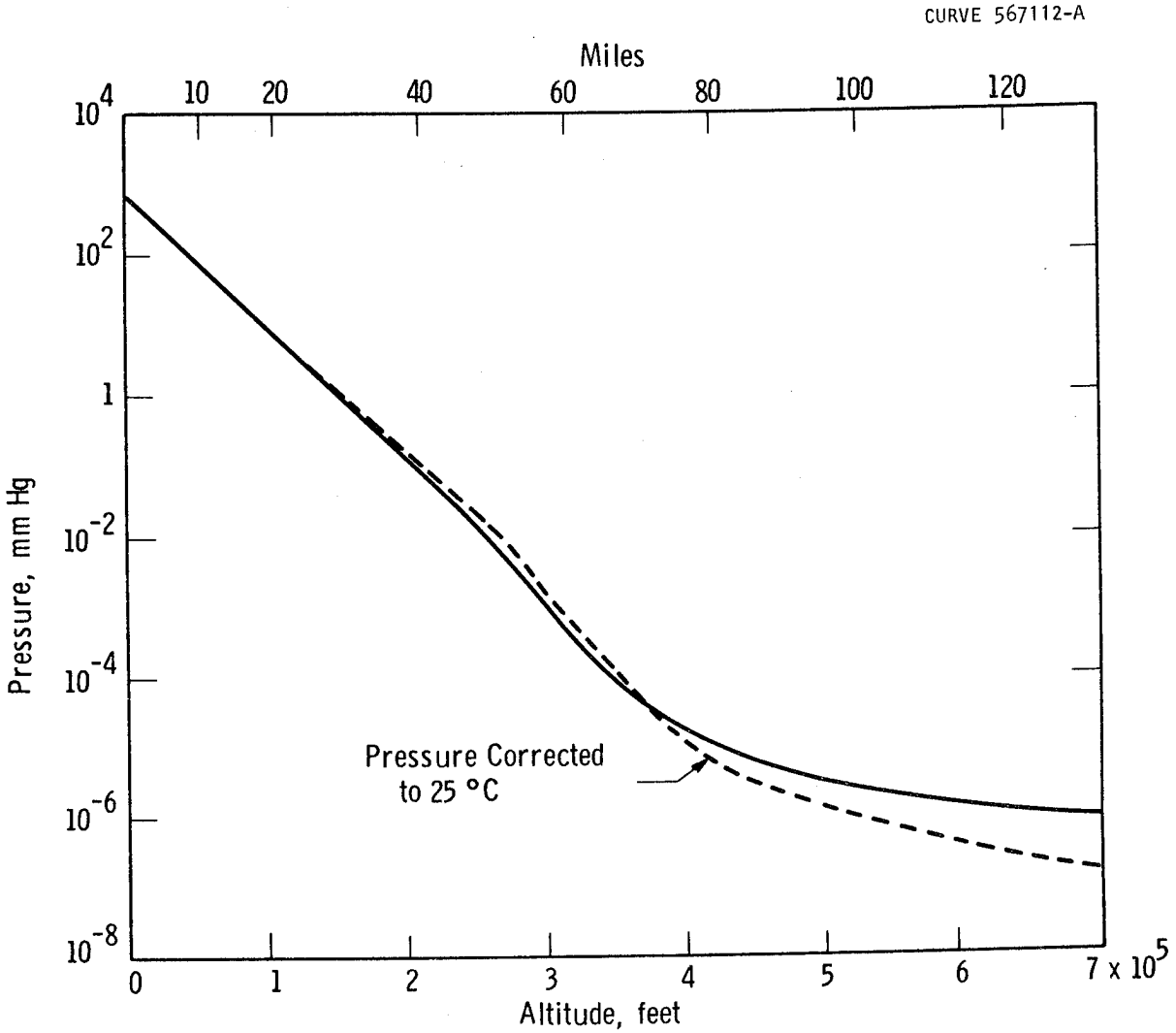

Fig. 1– Pressure - altitude curve (NASA, U. S. Std. Atm., 1962)

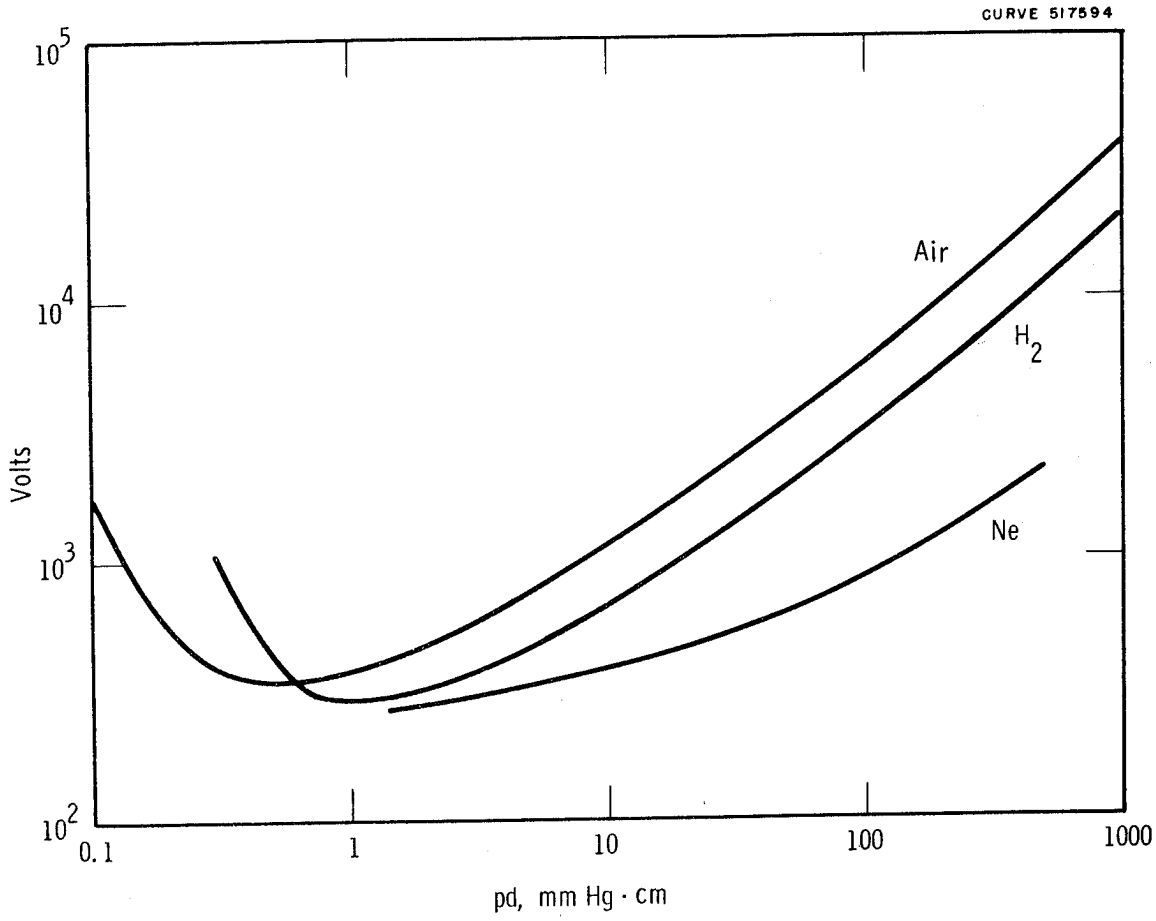

Fig. 2 --Uniform field breakdown voltage of gases. Air (Carr), H_2 (Ehrenkrantz, Carr), Ne (Penning and Addink)

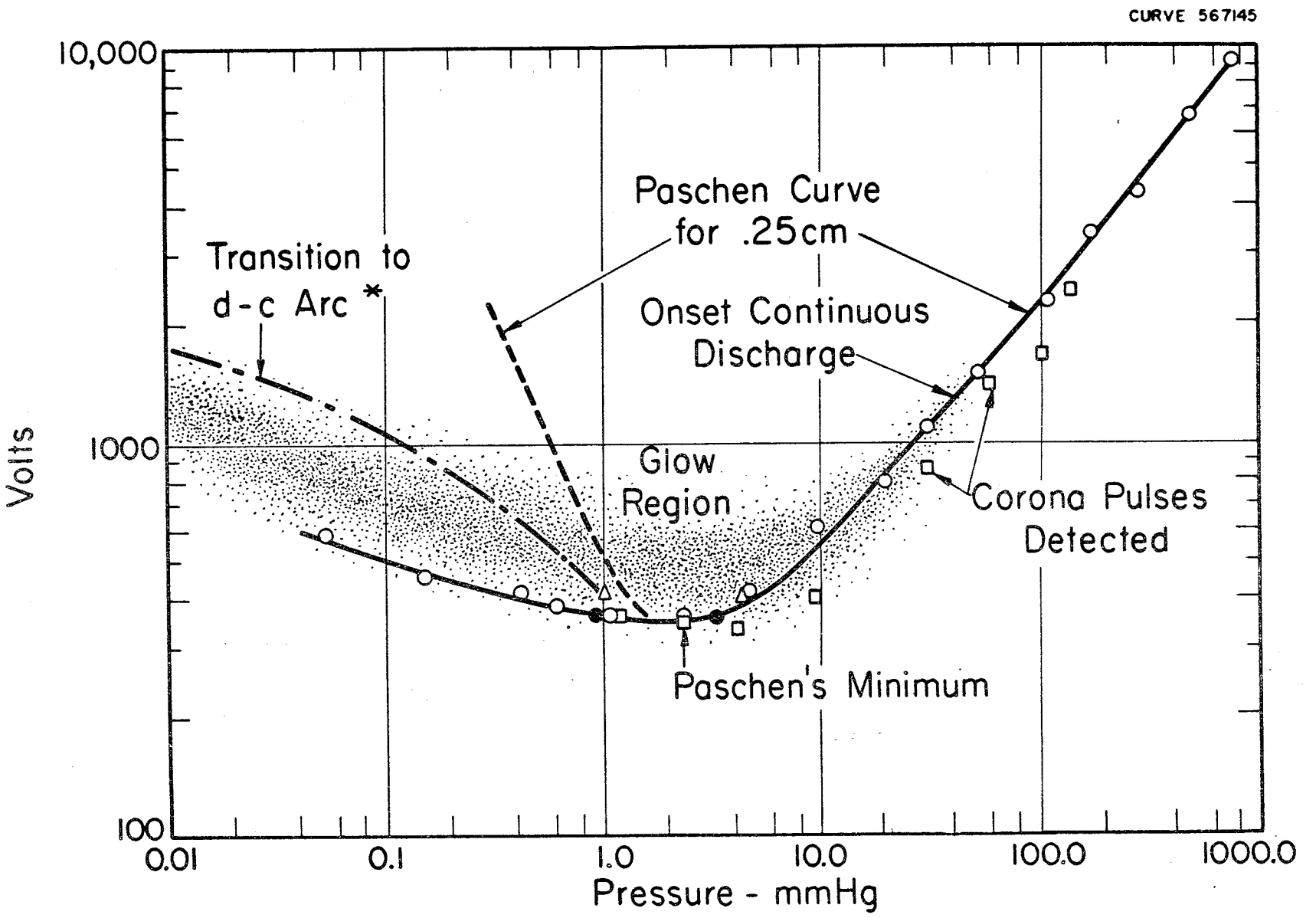

Fig. 3 - Discharge characteristics of air between 3/4" brass spheres for 0.25 cm gap.

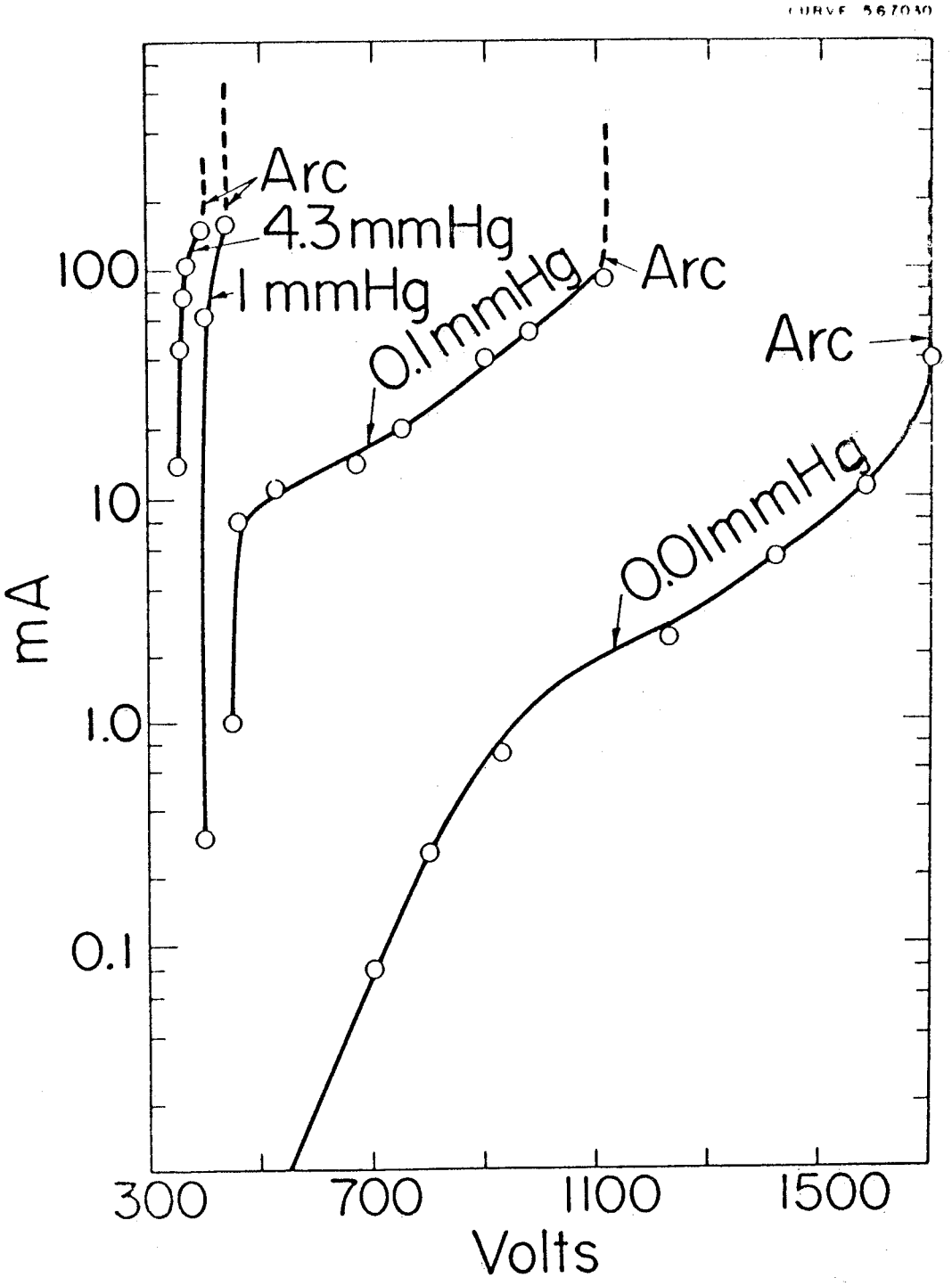

Fig. 4 - D-c glow current characteristic of air between 3/4" brass spheres for 2½ cm gap with U.V. radiation.

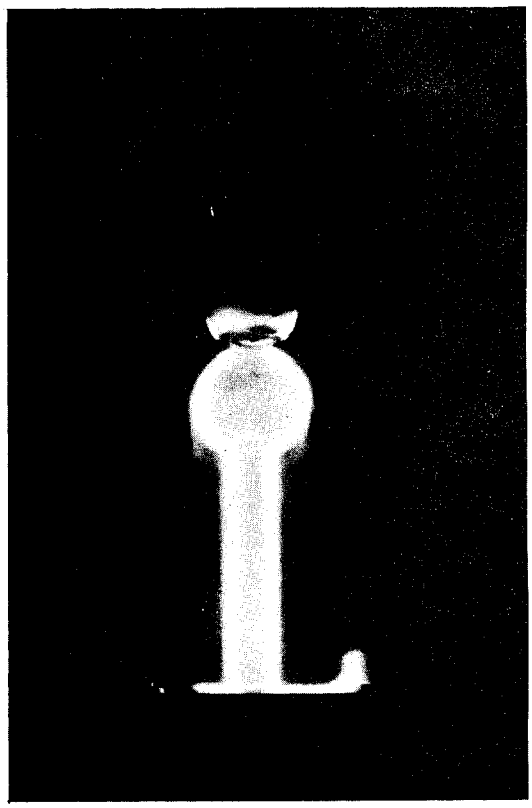

a.) 0.95mm Hg, 420V, 6.5ma

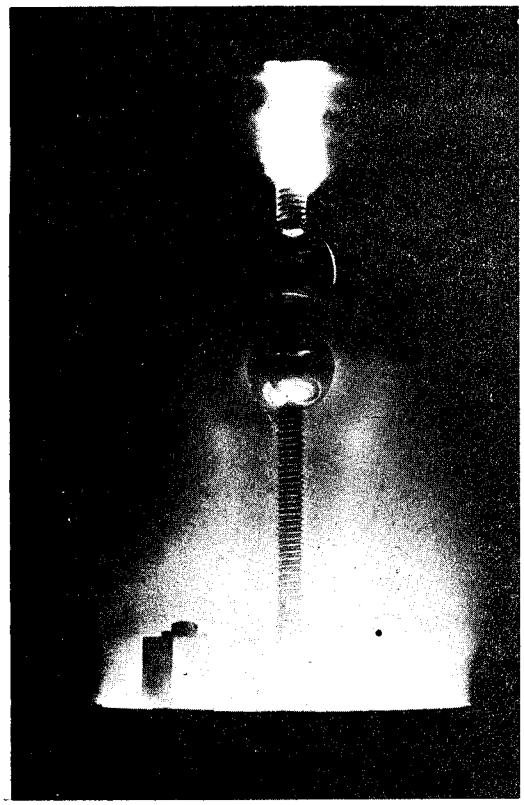

b.) 0.55mm Hg, 450V, 10ma

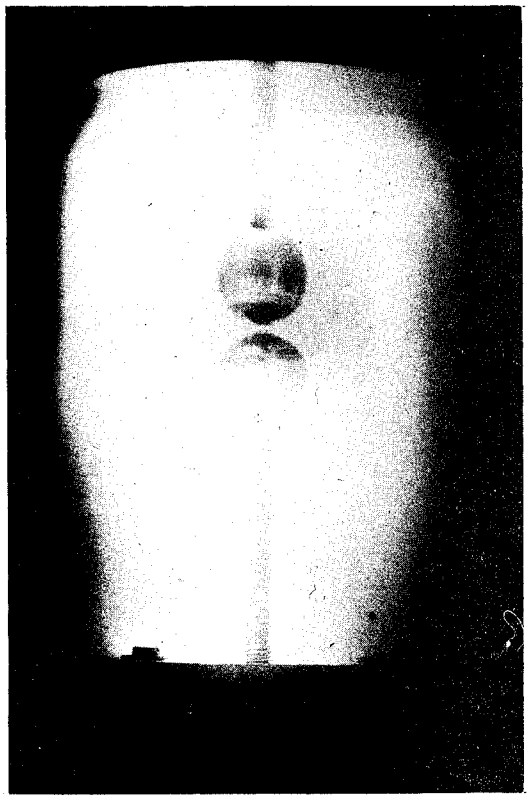

c.) 0.05mm Hg, 620V, 70ma

Fig. 5—Photographs of the d-c glow discharge in a low pressure chamber with a sphere gap at 0.25cm spacing

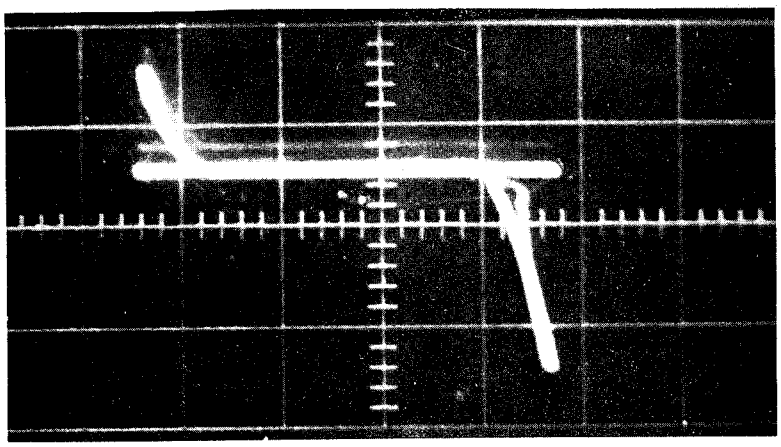

a.) 0.5mm Hg, 453V Crest, 100ma Crest

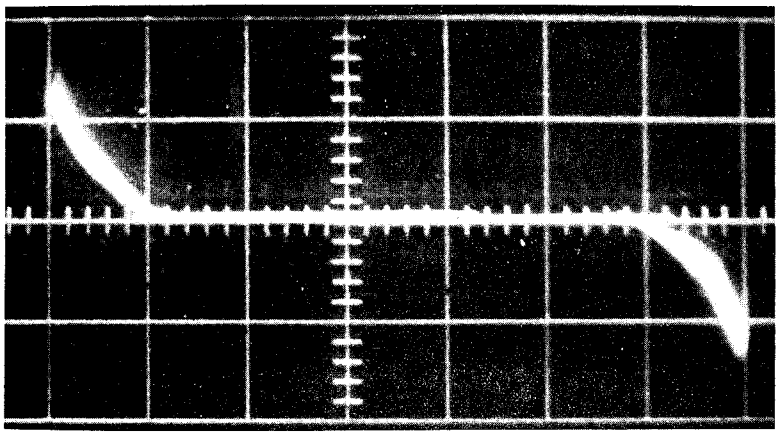

b.) 2.6mm Hg, 700V Crest, 1.5A Crest

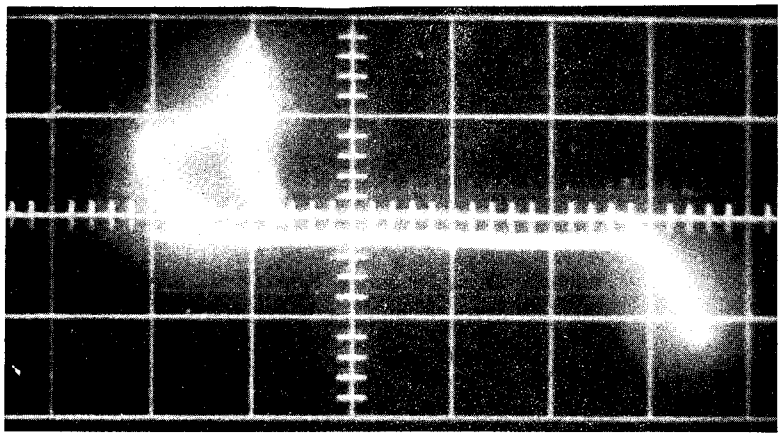

c.) 9 mm Hg, 525V Crest, 2A Crest

Fig. 6—Oscillograms of a-c dynamic glow current - voltage characteristics, 1.9cm spheres at 0.25cm spacing

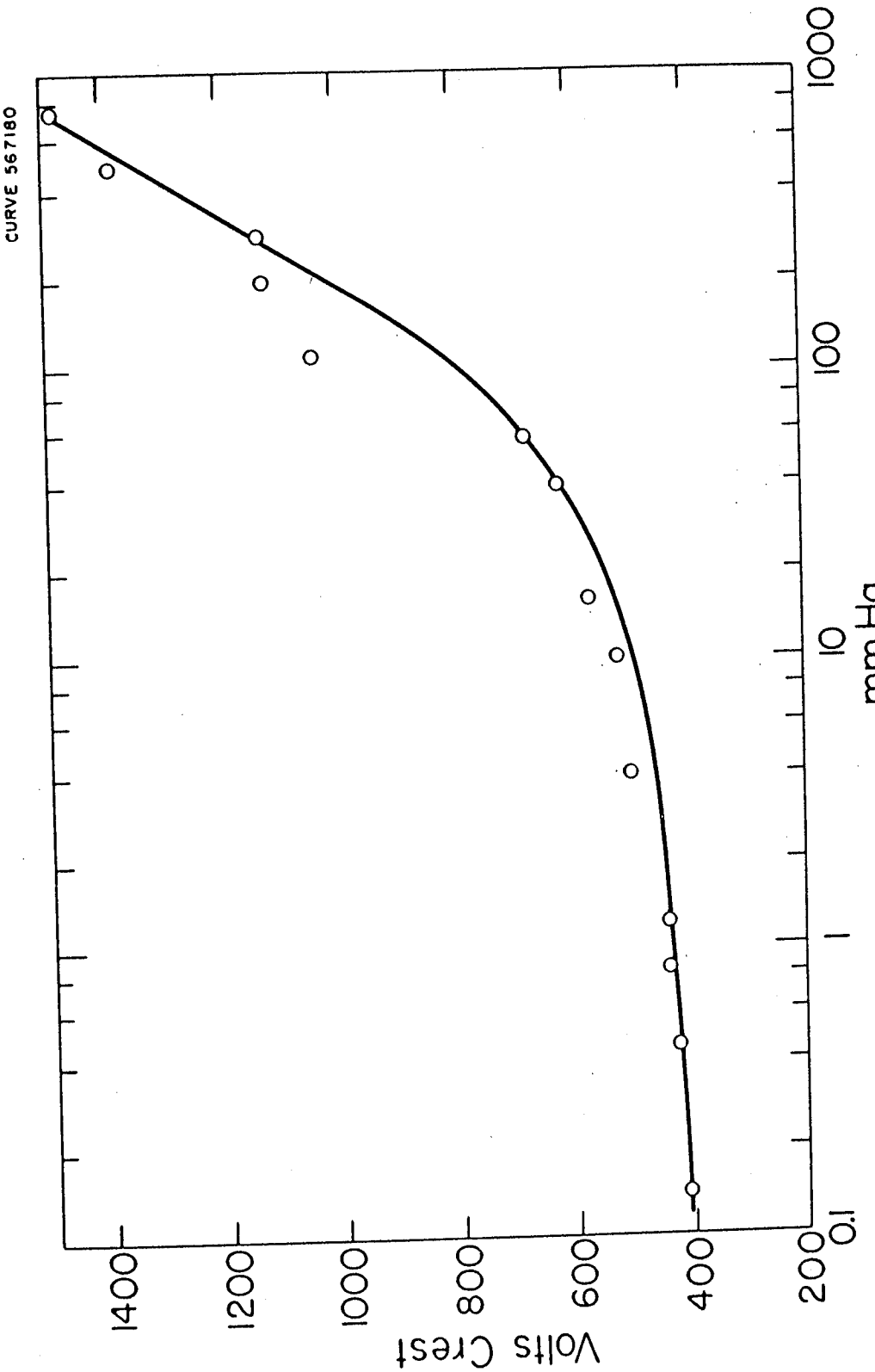

Fig. 7 - A-c corona inception voltage vs press for insulated wire (0.056" stranded conductor with 20 mils of vinyl insulation) twisted around 1/8" steel rod.

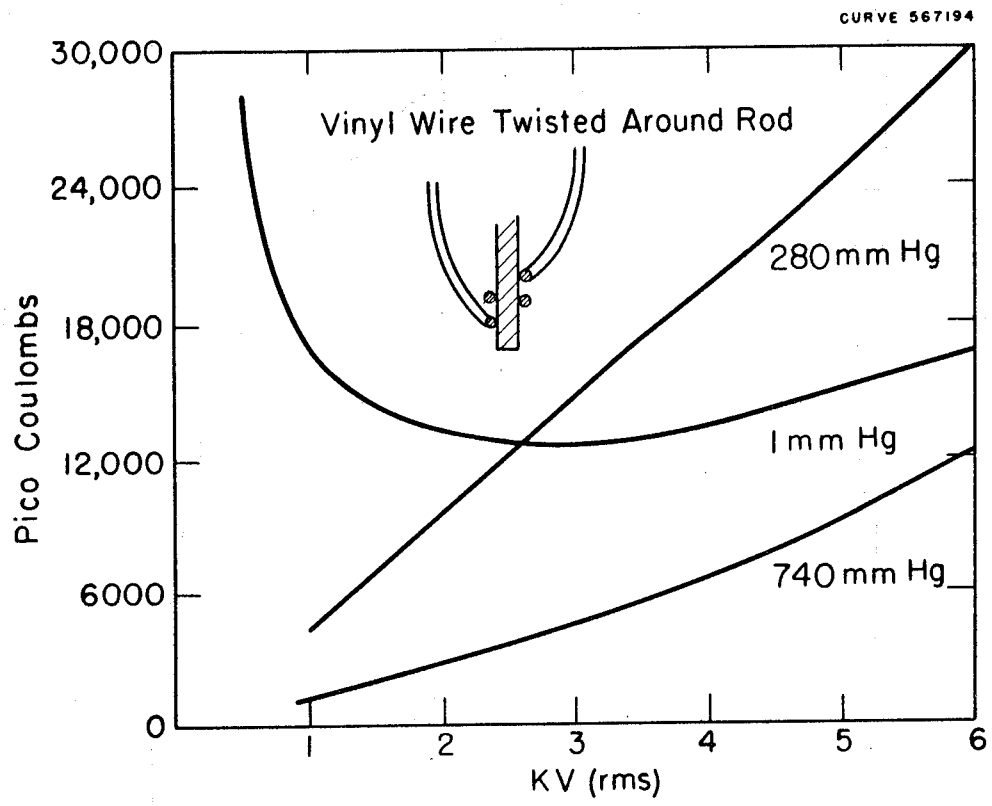

Fig. 8-Magnitude of corona pulses between a .056 " dia +.020" wall vinyl insulated wire and a rod.

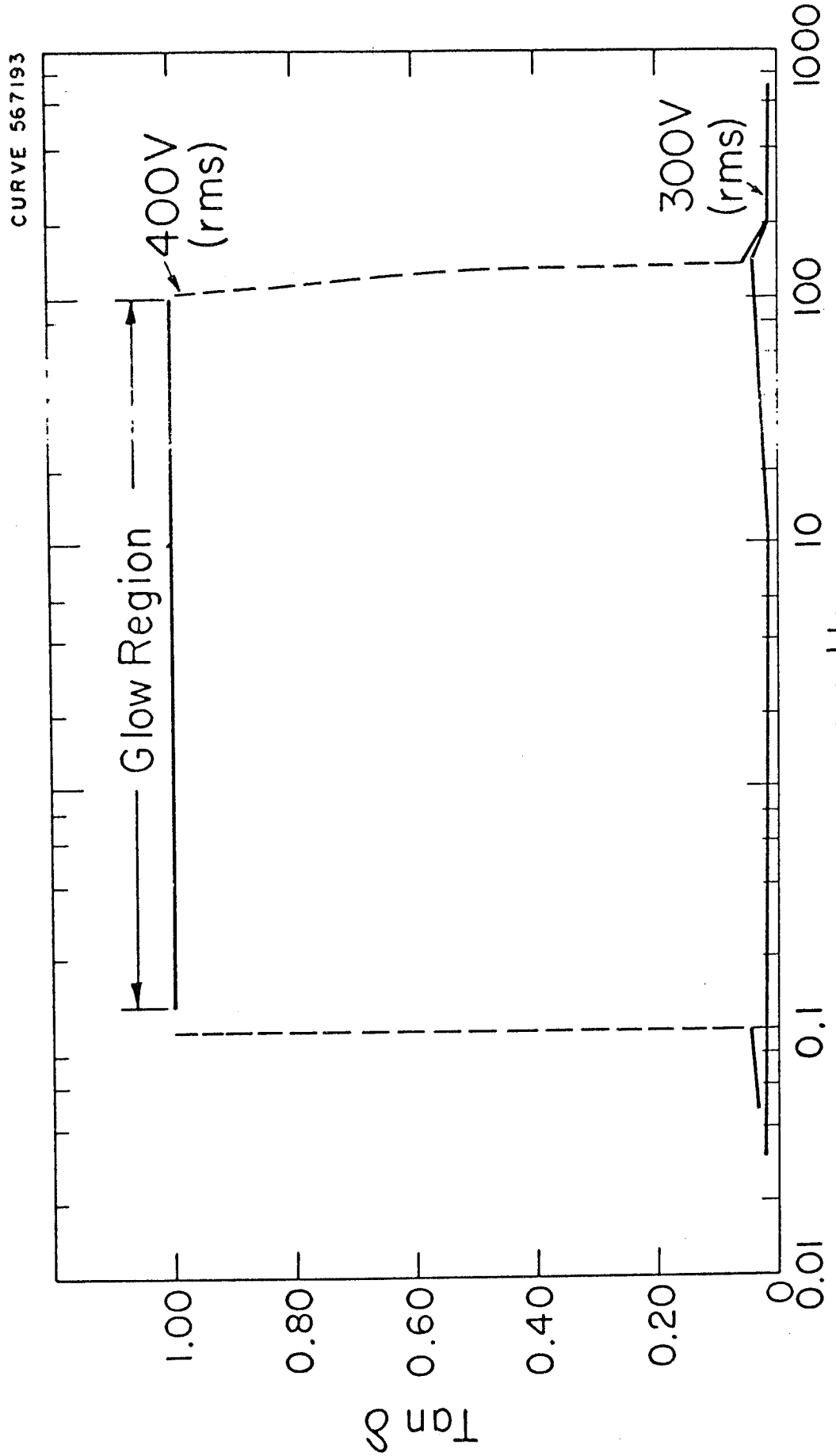

Fig. 9 - Tan δ vs press. for a twisted pair of enameled wires.

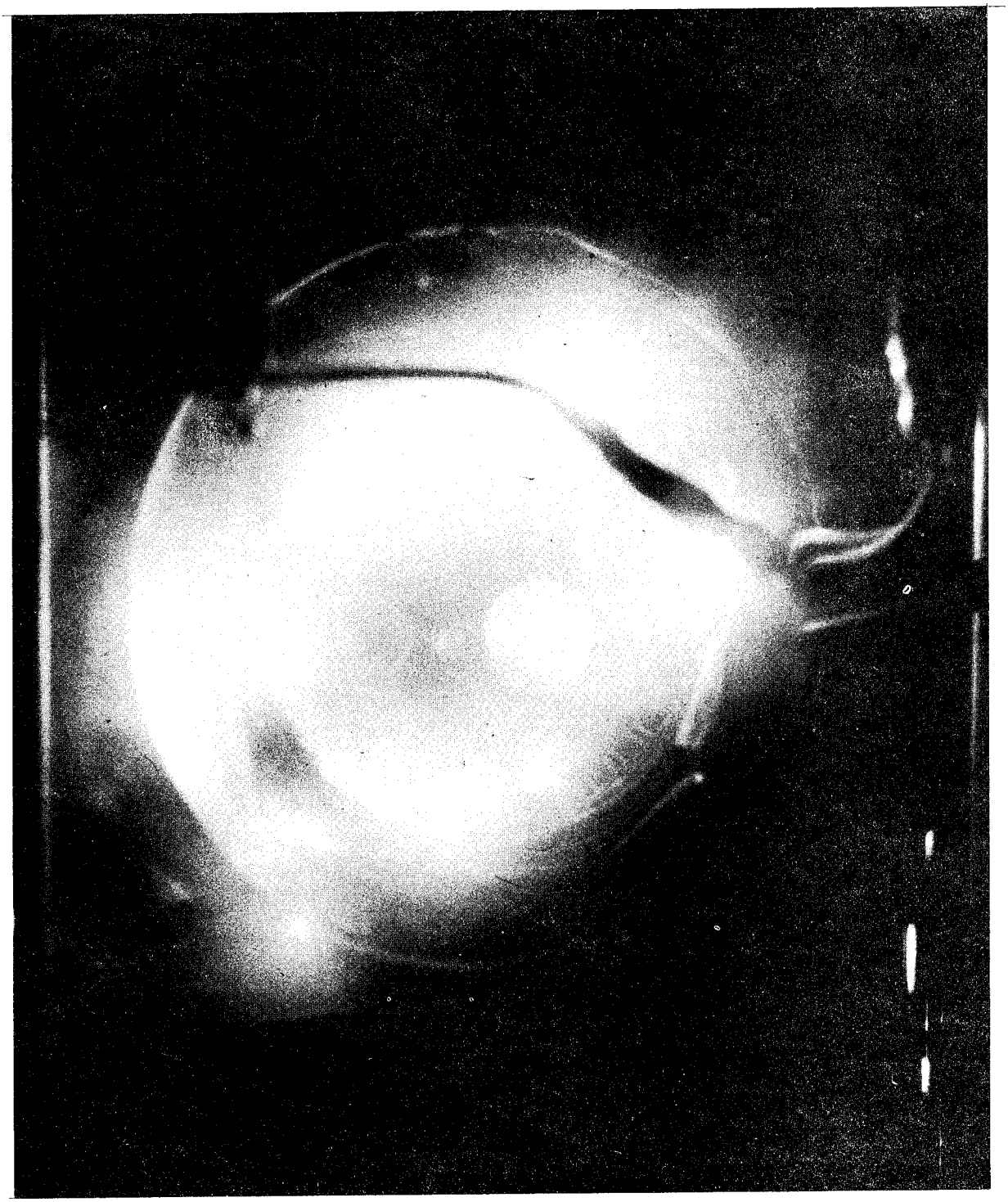

Fig. 10—Photograph of the d-c glow discharge in a motor stator at low pressure, 0.15mm Hg, 680 V with the iron positive

CURVE 567704-A

(a) p = 0.8mm Hg
V_0 = 455
I_0 = 35ma

(b) p = 1.3mm Hg
V_0 = 420
I_0 = 50ma

(c) p = 1.7mm Hg
V_0 = 470
I_0 = 46ma

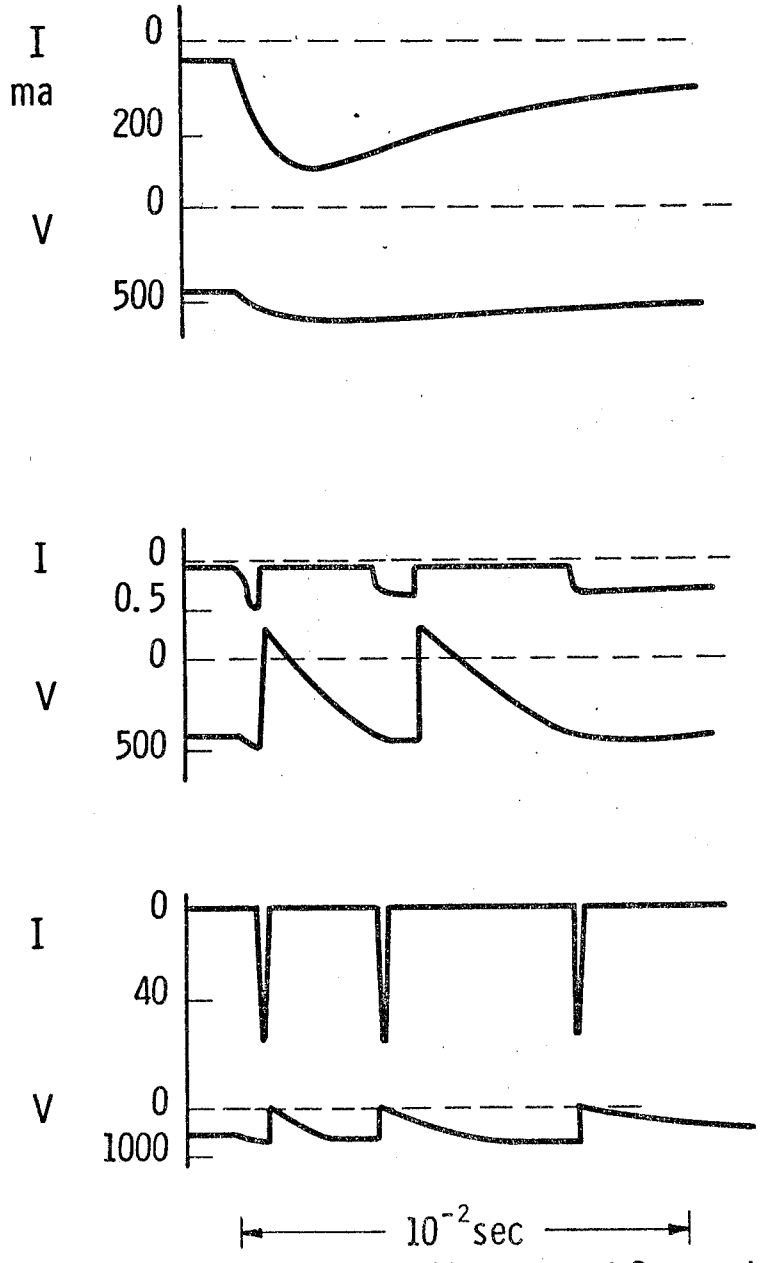

Fig. 11—Current and voltage oscillograms of a d-c glow discharge between spheres (0.254cm spacing) with overvoltage pulses

DWG. 626A832

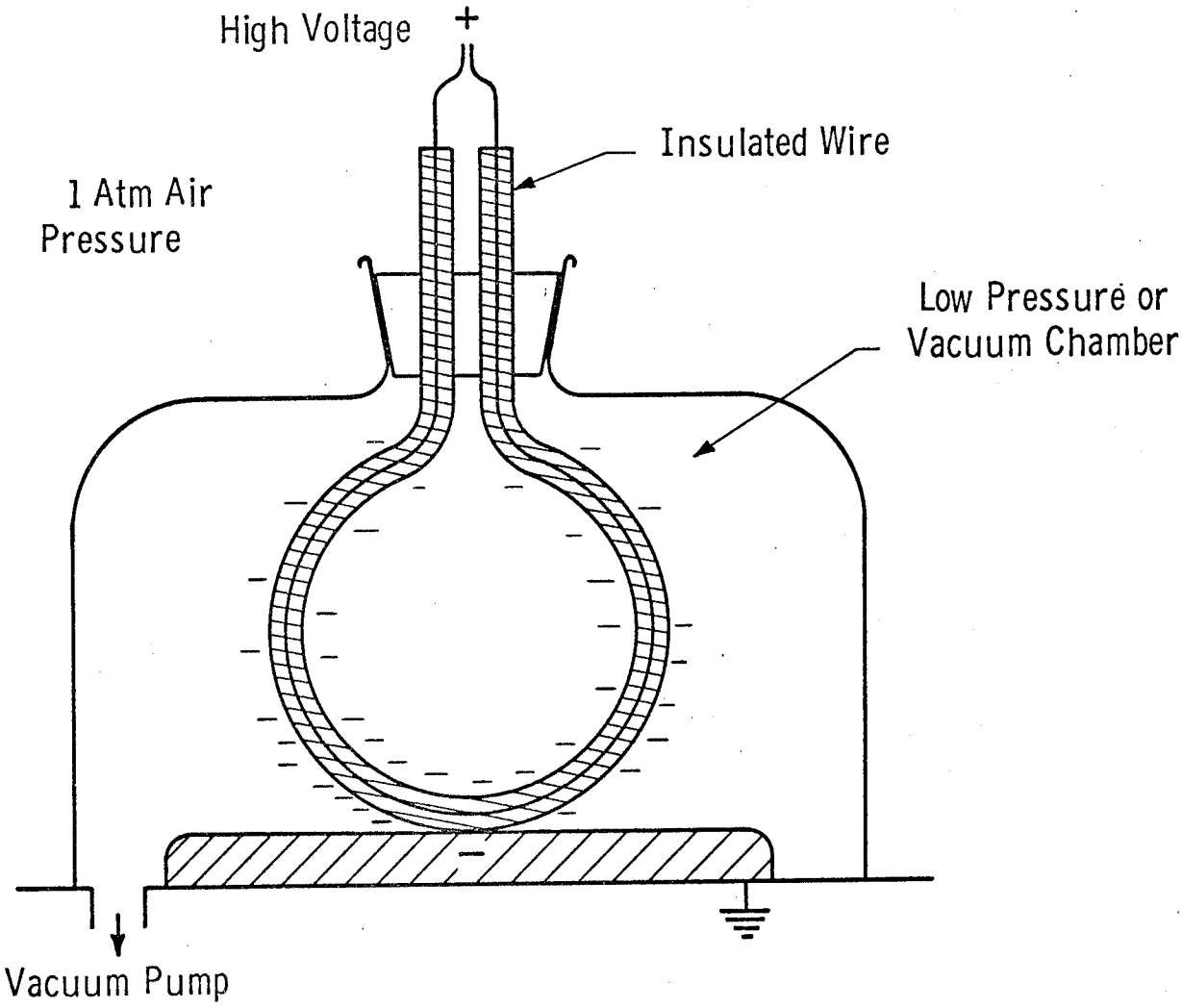

Fig. 12 —Illustration of charge transfer to an insulation surface by a low pressure discharge or field emission in vacuum

DWG. 626A656

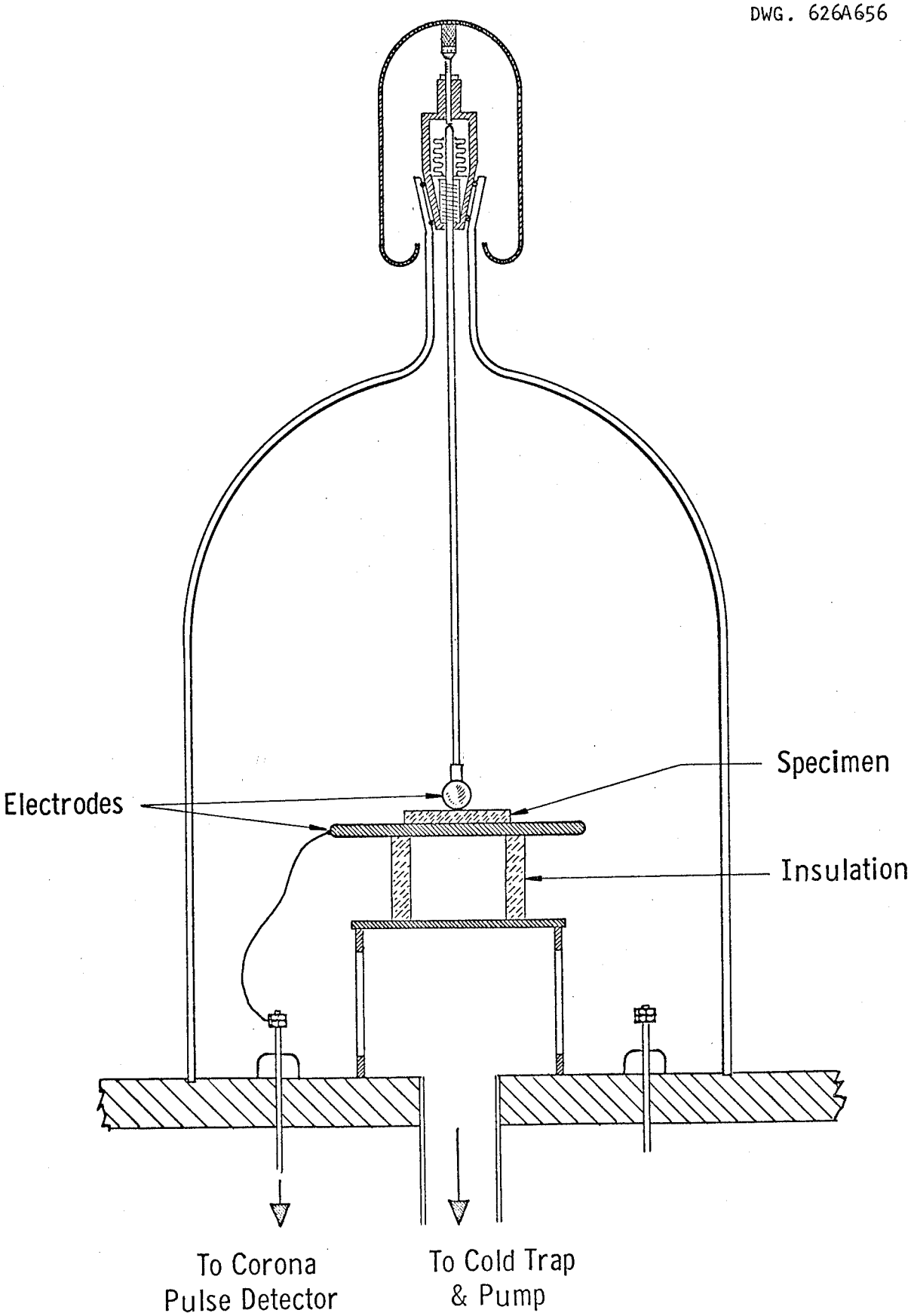

Fig. 13—High voltage vacuum test chamber

CURRENT FLOW BETWEEN ELECTRODES IMMERSED IN A LOW GAS PRESSURE PLASMA

M. J. Kofoid

Boeing Scientific Research Laboratories
Seattle, Washington

INTRODUCTION

This paper is concerned with the question of what can happen when a voltage is applied between electrodes immersed in a plasma in a gas of low density. Primary attention is given to the case of two highly unequal area electrodes with a d-c potential difference of up to 150 volts. The question is encountered, for example, with the Dyna-Soar glider vehicle when it is shrouded in a plasma sheath during re-entry. Typical of the conditions when at an altitude of 200,000 feet might be a plasma temperature of 4400°K, an ionization density of $n_e = 10^{11}$, an air density equivalent to 0.1 mm Hg at N.T.P.

An initial question is can electric breakdown, in the ordinary sense of a large maintained increase in current limited principally by the metallic-circuit impedance, occur between electrodes inserted into a plasma. The theoretical answer is that breakdown cannot occur with voltages smaller than the minimum value of the Paschen breakdown voltage curve for the particular gas and cathode material. It is here assumed that the electrodes are at too low a temperature to thermally emit electrons. The minimum of Paschen's curve for air with electrodes of ordinary metal is about 300 volts. Therefore, it is believed that in practice breakdown in the ordinary sense will not take place in air between electrodes of commonly used metals with d-c or power-frequency voltages of up to 150 volts. It is worthy of emphasis that this conclusion applies to any electrode separation, any gas density, and in particular to any degree of ionization.

If breakdown cannot occur, will there be an appreciable leakage current through the plasma in which the electrodes are immersed? It is with this remaining question that this paper is concerned. On a theoretical basis it will be concluded that the current can become appreciable only if the cathode area is large; it can then become large only if the anode conditions permit.

THEORY

Consider immersed and electrically floating in a plasma two small, and for this initial discussion, identical exposed terminals of a circuit which is to be energized with not more than a few tens of volts d-c. Refer to Fig. 1.

Initially, with zero voltage applied between them, the terminals will each assume the same small negative potential with respect to the plasma. This potential will be the voltage drop across the sheath of positive ions which will form to surround the electrodes -- just as with the well-known Langmuir single probe, or any floating electrode. Each electrode will assume the same floating potential and will collect zero net current. Since there is no net potential acting in the loop, the circuit current $i_d = 0$.

With electrodes of equal area, these actions which will occur when the d-c circuit voltage is applied will be identical to those encountered with classical double probes used in plasma diagnosis, the theory for which has been discussed in detail by Johnson and Malter. Fundamental in the situation is the demand that the instantaneous net current of positive ions and electrons flowing to the system from the plasma must always be zero. It is also basic that the flow of positive ions to each electrode will be essentially unaffected by the application of the voltage, as long as the voltages are not great.

The potentials of the electrodes with respect to the plasma must adjust so that the basic current relations are satisfied. Let a small battery voltage be applied, with the positive terminal connected to probe No. 2. Probe No. 2 must shift closer to the plasma potential and collect more electrons, while probe No. 1 shifts away from the plasma potential and collects less electrons. The deficiency at probe No. 1 is made up by the passage through the circuit of extra electrons flowing to probe No. 2. This flow will be referred to as the deficiency current. It is always identically the circuit current.

As the voltage is increased probe No. 2 shifts still closer to plasma potential. It collects the entire electron current to the system when probe No. 1 becomes so highly negative with respect to the plasma that no electrons from the gas can reach it. Half of the electrons arriving at probe No. 2 now travel through the metal circuit to probe No. 1.

Increasing V_d still more cannot produce an increase in i_d since probe No. 2 is already collecting sufficient electron current to balance the total ion current to the system. Probe No. 2 therefore stays fixed in potential and probe No. 1 goes negative along with V_d. This probe can be considered saturated with respect to positive ions.

The point of high interest of the double-probe theory for the present studies is that with equal-area electrodes a relatively very small applied circuit voltage the anode can attract all of the electrons reaching the two-electrode floating system from the plasma.

Theoretical Consequences of Large and Unequal Electrode Areas

In the simple picture which has been presented, if the cathode surface is small very little circuit current can flow even if the anode surface is made very large. The positive ion current to the cathode will be the

have been the original plasma value n_+; the maximum deficiency current would have been some value indicated as the "original n_+ saturation level". However, when the situation demands an applied electric field so large as to cause appreciable ionization in the plasma near the anode, not only are extra electrons made available to flow to the anode but also extra positive ions are created which flow to the cathode. Furthermore, the applied field can make the general flow of ions a much larger value than existed with simply ambipolar diffusion; in the ensuing diffusion process, we do not have in the plasma just a field due to the positive charges restraining the flow of electrons. The application of voltage alters the field causing increased flow of the positive ions. In this paper this process of effecting increased ion flow will be termed "enhanced diffusion". The increase of the ion population due to an anode discharge and also the enhanced ion flow due to the applied field result in an augmentation of the ion density in the plasma at the cathode, and therefore of the plasma-to-cathode saturation ion current. If a deficiency current equal to the normal plasma ion saturation current cannot be collected with a low circuit voltage, the augmentation can be large. As in the situation of Fig. 2, the current may be increased to some value such as indicated as the "augmented n_+ saturation level".

Several important questions arise regarding the leakage-current problem when the anode area is very much smaller than that of the cathode. Quantitatively, how large a current will flow if the applied voltage is not great enough to cause an appreciable increase in the ionization intensity in the anode fall region or enhanced mobility? At what critical voltage V_c will the current start to increase rapidly due to the onset of discharge phenomena which will effect a negative resistance condition? Also, what must the circuit voltage be to obtain the maximum deficiency current, i.e., circuit current? Further, what will be the magnitude of this saturation current? To gain further insight to the answers to these questions an experimental study was made.

EXPERIMENTAL RESULTS AND DISCUSSION

The experimental results were found to be in agreement with the theoretical considerations discussed. They will now be mentioned only very briefly. A comprehensive paper concerning this study has been accepted for publication in the A.I.E.E. Transactions later this year; this paper is currently available as Boeing Scientific Research Laboratories report No. D1-82-0238.

The general apparatus arrangement is indicated in Fig. 3. The investigation was conducted with a cylindrical test electrode C and a very much smaller area rod electrode A immersed in the central section of the positive column of a long d-c low pressure arc between cathode C' and anode A'.

The study, in almost its entirety, was made with the smaller electrode as the anode, since with the reverse polarity an insignificant current flowed. Therefore, for convenience, the small electrode will be referred to as the anode and the large electrode as the cathode. The ratio of the cathode

area to the anode area was made large to clearly display the unequal-area deficiency current phenomena. The general features of the voltage-current characteristics are evident in some curves taken with nitrogen.

The phenomena can be conveniently considered as developing in three stages. Refer to Fig. 4. In stage A, as the applied voltage was increased the current increased monotonously until a critical voltage V_c was reached. During this phase, the cathode potential did not shift a detectable amount; the rise in the anode potential with respect to the plasma was equal to the total applied voltage. Stage B was entered with the attainment of voltage V_c; the electric field had then increased to the point where in the plasma, in the immediate vicinity of the small anode electrode, there was the onset of anode discharge phenomena characterized by effectively negative resistance properties. In stage B, with applied voltages greater than V_c, there occurred a very rapid increase in current due to the increased ionization density about the anode and to enhanced diffusion; this was accompanied by a small decrease in anode potential. The current ceased its high rate of increase at the start of stage C; here the condition had been attained where the flow of electrons to the cathode had become practically zero. Essentially all of any further increase in circuit voltage appeared as an increase in the departure of the potential of the cathode from that of the plasma.

At a lower pressure, the mean free path of an ionizing electron is greater, or stated differently, the macroscopic collision cross-section for ionization is less. Therefore, at a lower pressure a larger electric field, hence larger V_c, is required to cause an anode discharge. With only 10 microns pressure (i.e., p = 10 μ) the discharge condition was not attained. See Fig. 5.

The onset of the anode discharge occurred at a lower voltage in the higher-density gas, as should be expected. That the saturation current was greater at the lower pressure is attributed to increased diffusion produced by the higher electric fields.

Data were also taken to determine the effects of a change in the degree of ionization of the background plasma, of different gases, with different ionization potentials and molecular mass, and of increasing the anode area. Of these data, only the curves for the effect of change of gas were selected for presentation in this talk. Refer to Fig. 6.

Prediction of Leakage Currents

A few simple calculations have been made for an orbiting vehicle. Live electrical terminals may be exposed to the plasma surrounding the vehicle during high-speed re-entry into the earth's atmosphere. With the typical conditions given at the start of the talk for the Dyna-Soar glider vehicle, where the positive ion temperature was 4400°K the positive ion current density was calculated to be 1.3×10^{-3} amperes per square cm. A positive ion current with a density of at least this order flows from the plasma through the positive ion sheath to every exterior area of the vehicle -- except to

that of the small positive terminal, or terminals, at the back of the vehicle.

If the exposed area of negative electrode, say a cable connector terminal, is only 1.0 square cm, the maximum leakage current is of the order of 1.3×10^{-3} amperes, regardless of the anode area -- which might be most of the remainder of the exterior vehicle surface of, say, 500 square feet. However, if the polarity is reversed, for the same areas the saturation leakage current could be of the order of 620 amperes before a cathode ion current limitation would be reached. To what extent this saturation leakage current would be approached would depend primarily on the ability of the small anode to collect the deficiency current electrons from the plasma and on the limitations of the power supply.

Minimization of Leakage Currents

If it is not possible to make the small electrode negative the d-c leakage current often can be kept small, i.e., to a few milliamperes, or less, by taking advantage of simple design considerations.

The collection of electrons from the plasma by the anode should be made as difficult as possible in order to increase V_c.

As a practical expedient, the critical voltage V_c can be increased to above the circuit voltage by placing the anode in a recessed location where the ion temperature and in particular the ionization density will be very much reduced. The effectiveness of this simple expedient was demonstrated by a laboratory test. Except for the recessing of the electrode, the test was the same as that of the 100 microns pressure curve of Fig. 6. The rod electrode, instead of having its end flush with the end of the covering glass sleeve, was withdrawn into the glass sleeve just a distance equal to one rod diameter. The leakage current was thereby reduced from more than 20 ma to less than 100 microamperes with 150 volts applied.

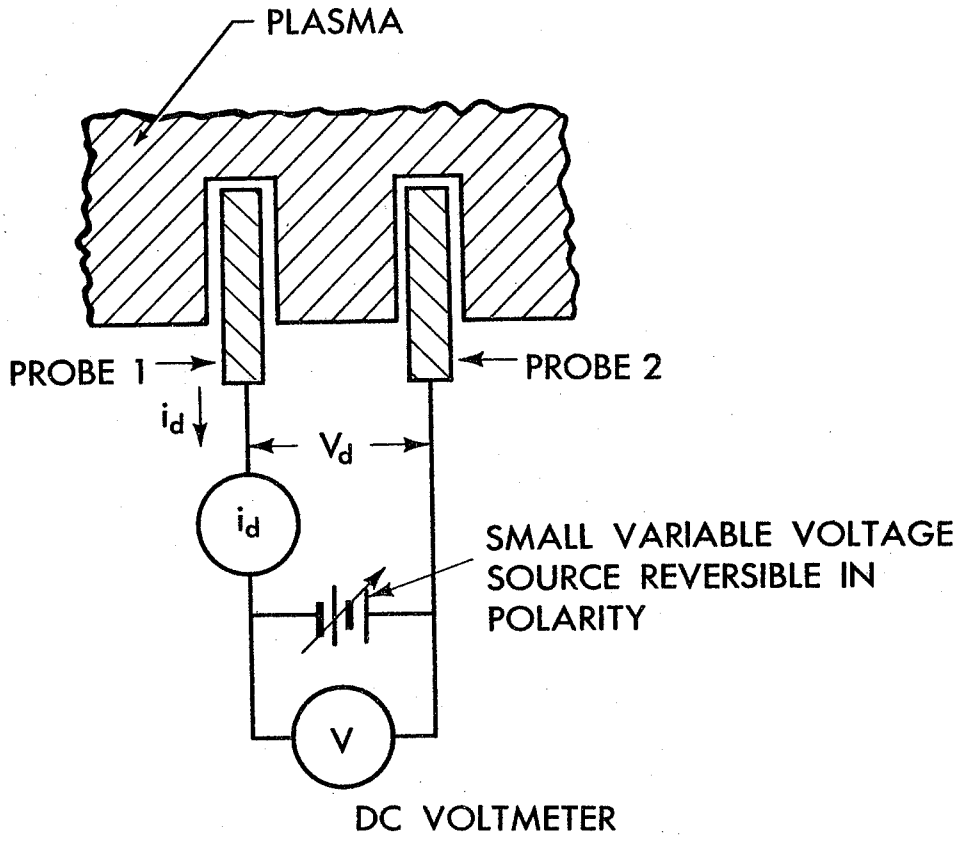

Fig. 1. Basic double-probe circuit

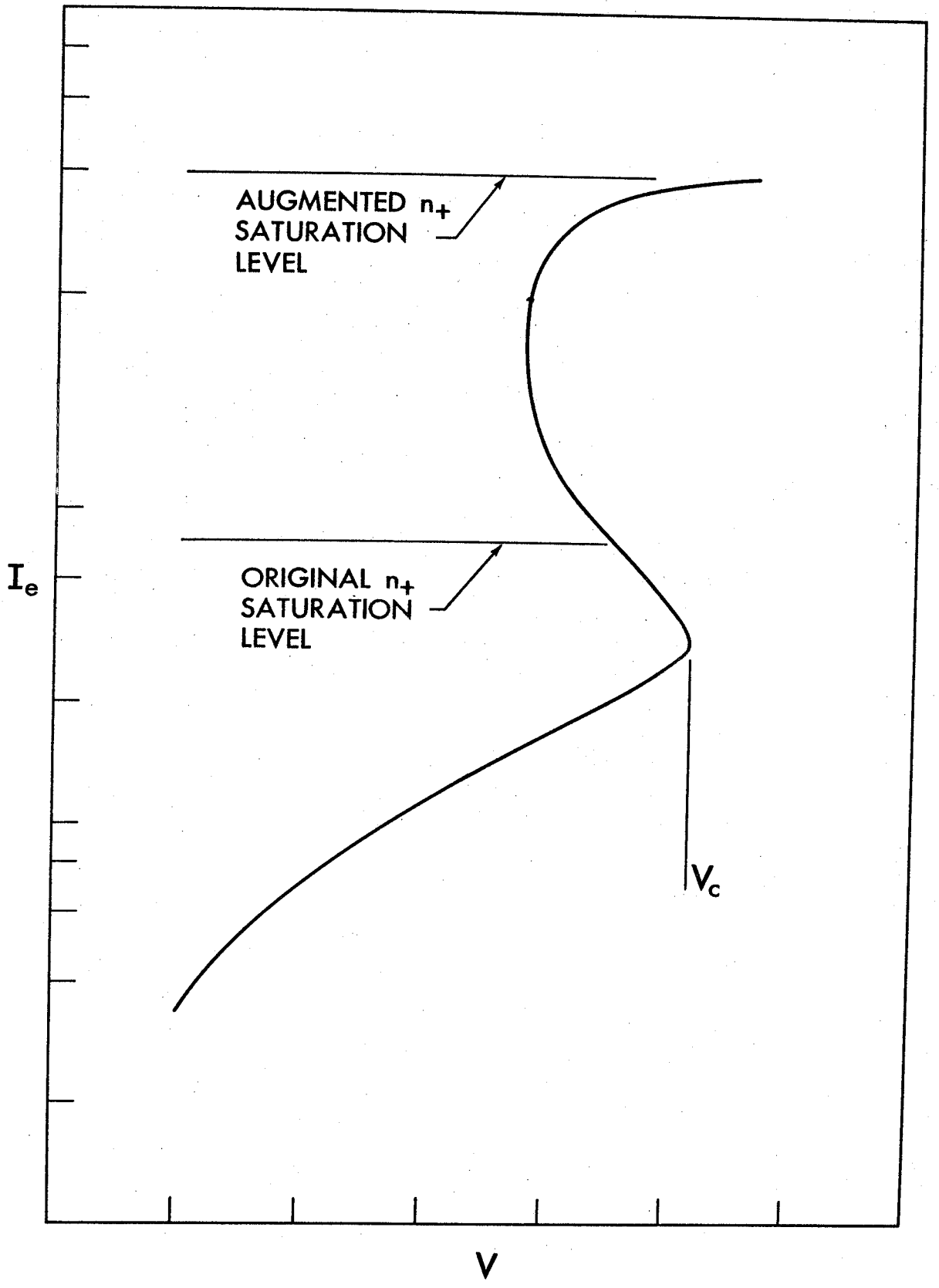

Fig. 2. Increase in leakage current due to augmented ionization.

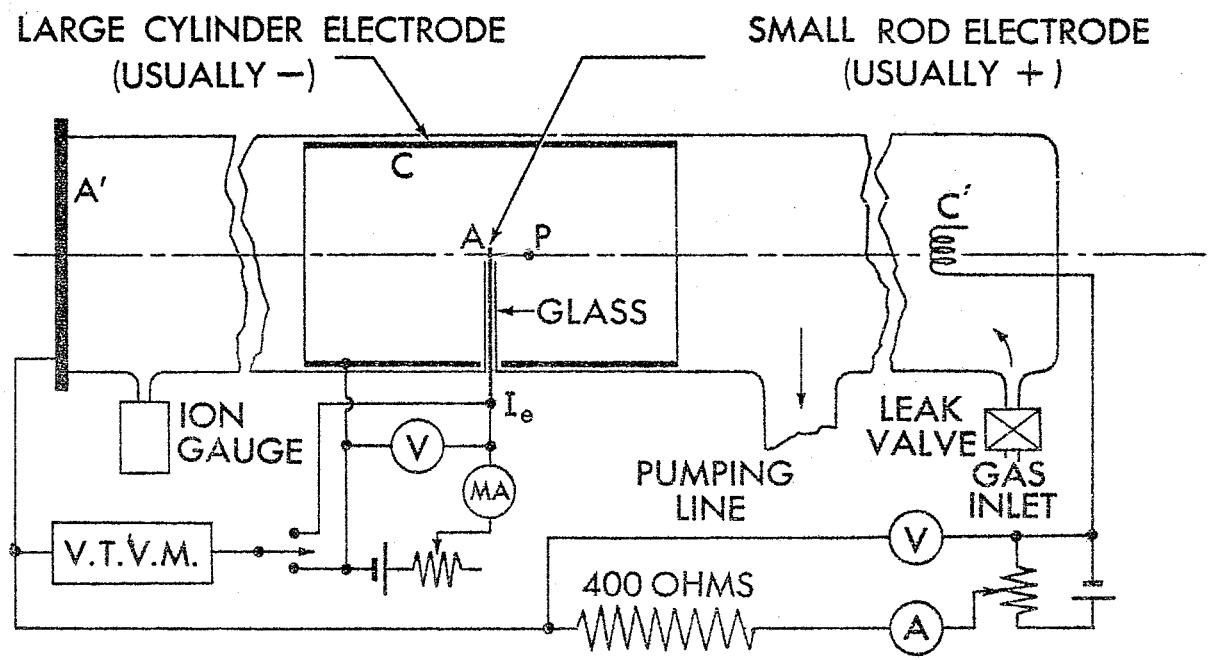

Fig. 3. Test apparatus arrangement.

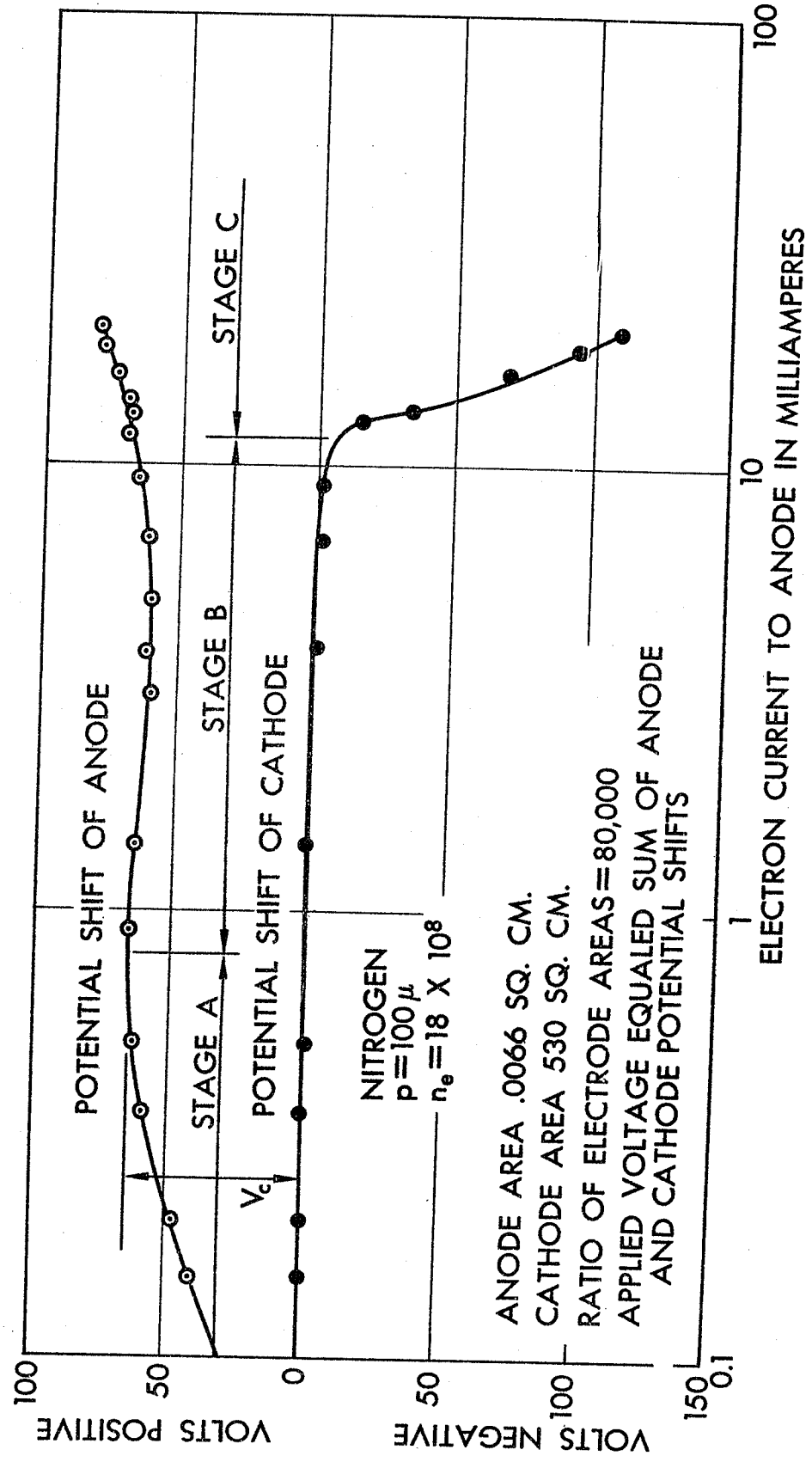

Fig. 4. Changes in electrode potentials from their floating potential caused by applied voltage.

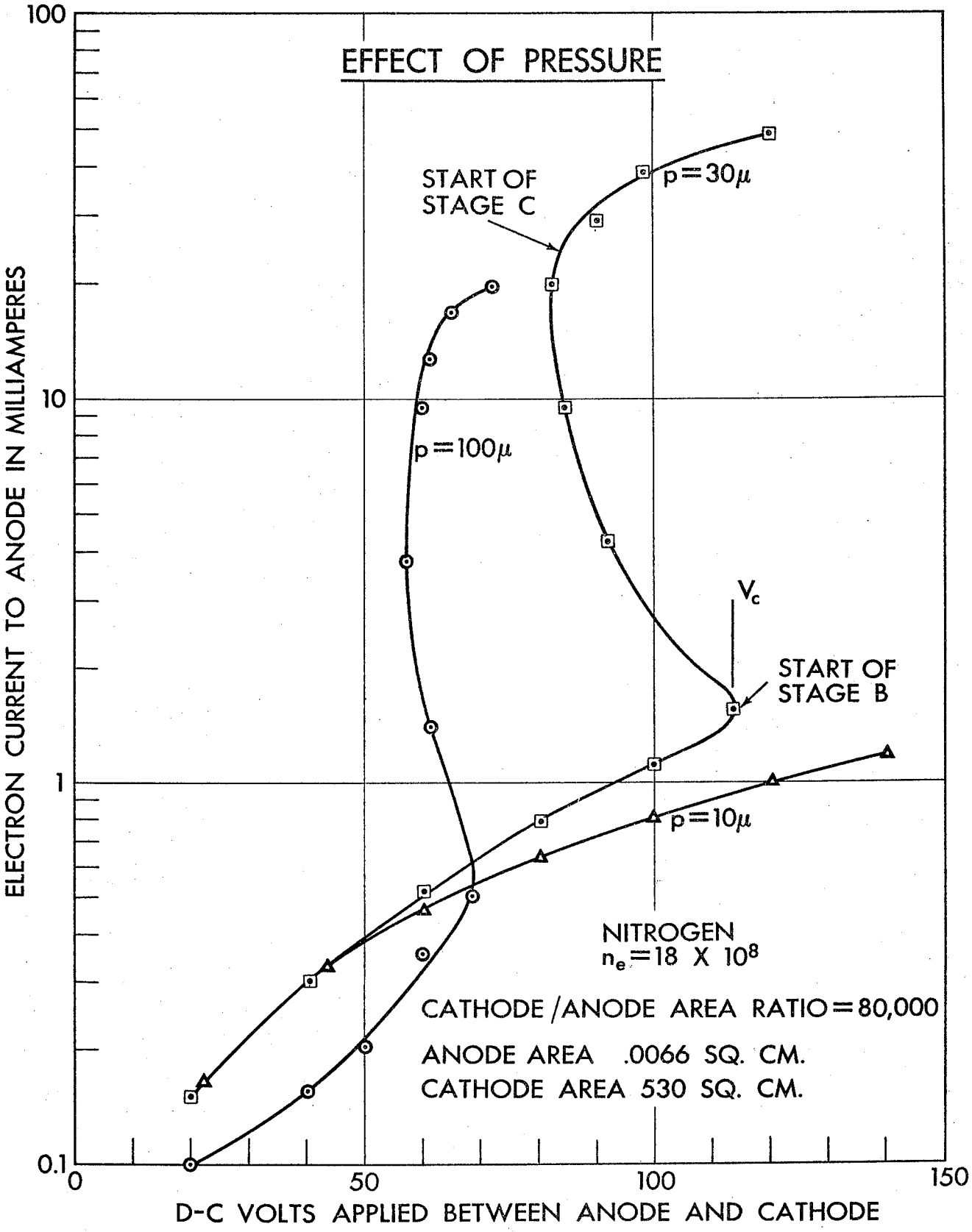

Fig. 7. Leakage current as a function of gas pressure.

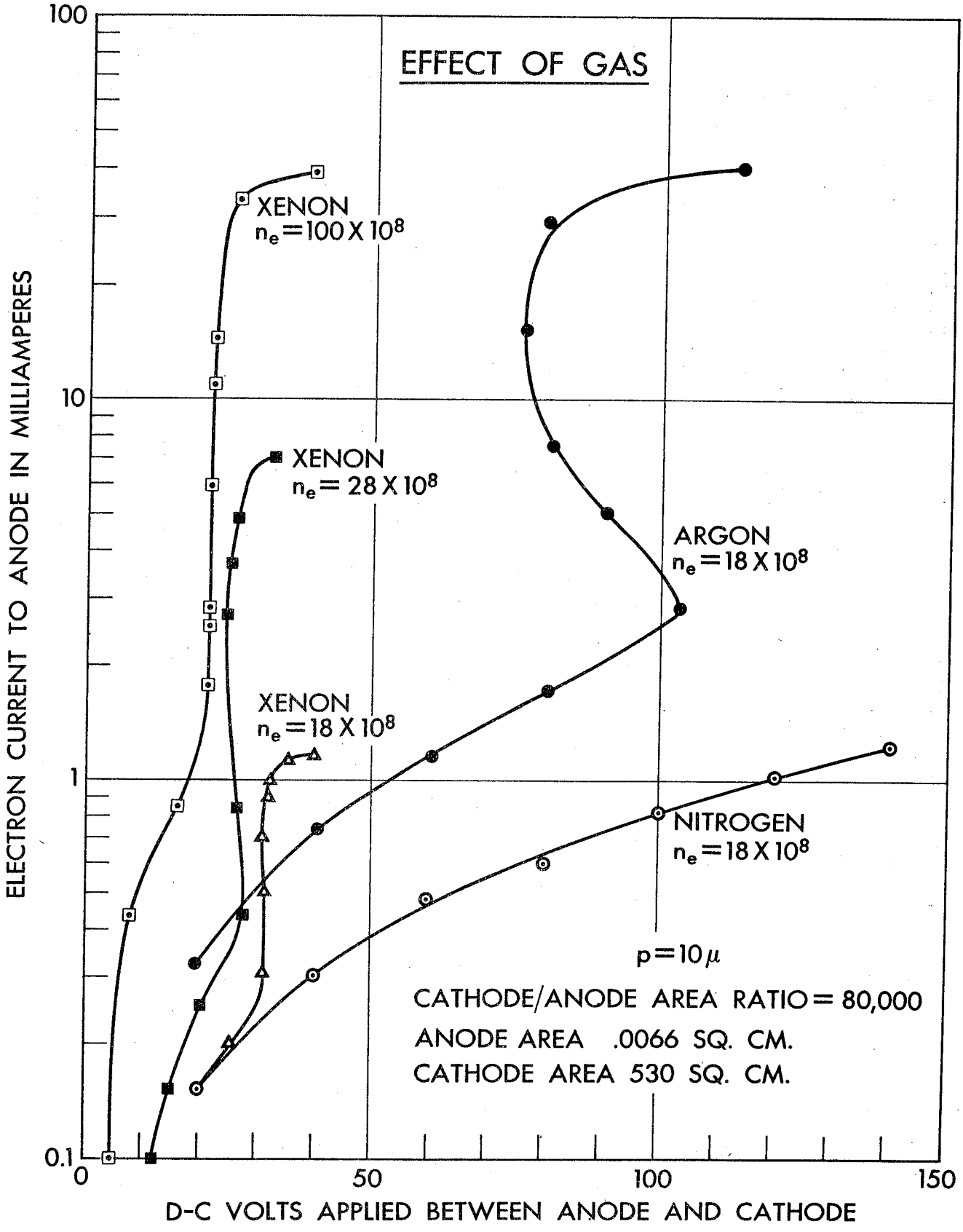

Fig. 6. Results with gases differing in their ease of ionization.

SOME EFFECTS OF SIMULATED SPACE ENVIRONMENT ON THE ELECTRICAL PROPERTIES OF DIELECTRICS

L. J. Frisco, A. M. Muhlbaum and E. A. Szymkowiak

The Johns Hopkins University
Dielectrics Laboratory
Baltimore, Maryland

Introduction.

In 1959 the Dielectrics Laboratory began an investigation of the effects of simulated space environment on the electrical properties of insulating materials. Until recently the program was sponsored by the U.S. Army Electronics Research and Development Laboratory, Fort Monmouth, New Jersey. Certain phases of the program are being continued under the sponsorship of the National Aeronautics and Space Administration, George C. Marshall Space Flight Center, Huntsville, Alabama.

In this brief presentation, it will be possible to give only a general description of the program, mention a few of the experimental results, and describe the current work in progress. There will be no attempt made here to define the space environment or to be concerned with the correlation between simulated and actual environmental conditions.

Detailed results have been presented in two Final Reports that are available from ASTIA[1][2]. A discussion of the flashover and sparkover studies has been published in the Proc. of the 1963 Electronics Components Conference[3]. These publications contain complete descriptions of apparatus, specimens and experimental techniques - details that cannot be presented in this brief report.

Exposure Conditions.

In the initial study, specimens were irradiated with x-ray (50KVP) or ultraviolet radiation during vacuum exposure at pressures in the 10^{-6} torr range. All measurements were made at room temperature, i.e. no attempt was made to control temperature.

Properties.

The properties that have been studied include a-c loss (ϵ' and $\tan\delta$); d-c conductivity; flashover strength (d-c and 60 cps to 18 Mc); and electric strength (d-c and 60 cps to 18 Mc). These properties were measured before, during, and after exposure.

Uniform field sparkover measurements were also made in the high vacuum medium with and without x-ray irradiation.

Materials.

The following materials have been included in the program:

Polyethylene.

Polytetrafluoroethylene extrusion resin (TFE-6).

Polytetrafluoroethylene molding resin (TFE-7).

Copolymer of tetrafluoroethylene and hexafluoropropylene (FEP-100).

Polychlorotrifluoroethylene.

Copolymer of chlorotrifluorethylene and vinylidene fluoride.

Polystyrene, crosslinked.

Polyethylene terephthalate.

Polyurethane foam.

Methyl styrene with dimethyl siloxane additive.

Glass-cloth polyester-resin laminate.

Copper-clad epoxy laminate printed circuit board.

Forsterite (2MgO. SiO2) ceramic.

Steatite (MgO. SiO2) ceramic.
Alumina (Al_2O_3) ceramic.
Beryllia (BeO) ceramic.

Flashover and Sparkover Experiments.

The voltage at which a discharge will occur between two flat electrodes in contact with the surface of a solid dielectric is called the flashover voltage. At atmospheric pressure a flashover will occur when the electrical stress in the gap between the electrodes exceeds a critical value. The magnitude of this critical stress depends primarily on the electric strength of the surrounding medium. The voltage at which the critical stress will be reached depends on the geometry of the specimen/electrode system and the dielectric constant of the specimen. In general, flashover voltage varies inversely with dielectric constant at the lower frequencies, as shown in a previous study[4].

At the low pressures encountered in space applications, the mean free path of residual gas molecules is so much greater than normal electrode (hardware) spacings that ionization processes no longer govern the breakdown phenomena. Therefore, flashover voltage would be expected to depend on factors other than the electric strength of the surrounding medium and the dielectric constant of the specimen.

Preliminary experiments were conducted using the specimen shown in Figure 1, which had been used in previous experiments at atmospheric pressures. Using a 0.060" gap between the flat circular electrodes, the flashover behavior in vacuum was erratic. With polyethylene, for example, the 60 cps values ranged from 2.2 to 12.0 KV-rms. At atmospheric pressure the same material yielded values from 2.5 to 4.6 KV-rms.

4

A series of uniform field sparkover measurements, using silver coated spherical lenses as electrodes, showed that the microscopic roughness of the electrodes dominated the breakdown process when the measurements were made in vacuum. Direct-voltage measurements with roughened electrodes showed that the surface condition of the anode did not influence the sparkover voltage, but roughness of the cathode caused a significant decrease in sparkover voltage. The best electrodes that could be made in the laboratory still yielded a considerable spread in results. The presence of dust particles under the metallic coating caused irregularities that influenced emission from the cathode.

Similar results were obtained when flashover voltage was measured for a gap formed by depositing circular patterns of evaporated silver or aluminum on a flat specimen. The average value could be increased by making the specimen surface smoother before the electrodes were deposited. This resulted in smoother electrodes, thereby influencing field emission.

In spite of the spread in results, a step-by-step testing procedure showed that x-ray irradiation had no immediate effect on flashover voltage. Detailed data can be found in the cited references.

A-C Losses.

With most materials, dielectric constant and dissipation factor decrease during vacuum exposure. This improvement in loss properties is associated with the removal of moisture and other volatile products. The largest changes occur during the early stages of exposure and the magnitude of the changes depends upon the specimen temperature and the previous environmental history of the specimen. Corresponding increases in ϵ' and $\tan\delta$ are observed during recovery at room condition. The observed changes are greatest at low frequency and are not significant at frequencies in the r-f range. This same

frequency effect is commonly observed in moisture absorption experiments at atmospheric pressure.

The introduction of x-ray irradiation causes only minor changes in the loss properties of most of the materials that have been investigated. The most striking effects are those exhibited by the tetrafluoroethylene resins TFE-6 and TFE-7. Large increases in ϵ' and $\tan\delta$ were observed at frequencies up to 1 kc during irradiation. The results obtained on TFE-6 during irradiation in vacuum and in air are summarized in Figures 2 and 3.

The specimens that were irradiated in vacuum exhibited a maximum value of $\tan\delta$ at an absorbed dose of about 2.5 megarads. A maximum was not observed when the specimens were irradiated in air. The recovery data of Figure 3 shows a marked difference in the recovery characteristics on the vacuum-irradiated and air-irradiated specimens. $\tan\delta$ decreased during the 30-day recovery period for the specimens irradiated in air. The rate of decay decreased during the recovery period ($\tan\delta$ plotted on a logarithm scale), but there was a continuous decay. The specimens irradiated in vacuum showed a sudden decrease in $\tan\delta$ when the irradiation was discontinued, followed by a constant value of $\tan\delta$ during a 5-day recovery period in vacuum. However, when the pressure in the chamber was increased to one atmosphere, a sudden increase in $\tan\delta$ was observed. After a period of somewhat erratic behavior, $\tan\delta$ then remained constant for the remainder of the 30-day recovery period. It should be noted that the sudden increase in $\tan\delta$ occurs whether the cell is filled with dry nitrogen or with air. Repeated experiments with different lots of TFE-6 and TFE-7 produced the same effects.

Attempts to explain these results on the basis of known radiation effects on the structure of the polymers were not successful. Since the surrounding medium had such a significant effect on the observed behavior, an experiment was conducted to determine the effect of

diffusion on induced loss. A 30-mil specimen and a 125-mil specimen were machined from the same 1/2 inch block of TFE-7. A second 30-mil specimen was taken from a sheet of 30-mil skived film, which was also made of TFE-7. Dielectric constant and tanδ measurements were made over the frequency range of 100 cps to 100 kc. The 100 cps tanδ data are summarized in Figure 4.

The inclusion of the 30-mil film proved to be fortuitous because it behaved in a manner that was totally unexpected, and indicated that the processing of the resin plays an important role in radiation effects. The two machined samples followed the same general pattern that had previously been observed with TFE-6 and TFE-7 specimens. The skived film, on the other hand, showed an entirely different behavior, as shown in Figure 4. Its tanδ did not rapidly increase to the high values exhibited by the machined specimens. Rather, it exhibited a slow increase in tanδ during the entire exposure period (480 hours, 12.3 megarads). During the latter part of the exposure period, the increasing tanδ of the film was considerably higher than the decreasing tanδ of the machined specimens.

The recovery data, shown in Figure 5, also indicates a marked difference in behavior between the two types of specimens. The film, which had never reached a peak value of tanδ during irradiation, exhibited a steady decrease in tanδ during the 20-day recovery period in high-vacuum. The machined specimens, however, showed a more rapid decrease in tanδ followed by a period of little change. The 30-mil machined specimen did exhibit a more rapid decay in tanδ than the 125-mil specimen, and this may well be the most significant effect of the reduced thickness.

When the cell was filled with dry (oil pumped) nitrogen, a sudden increase in tanδ was observed for all three specimens. This effect had been observed in all previous experiments with the TFE polymers. The effect was somewhat moderated in the case of the

skived film, but the pattern of behavior was essentially the same.

Corresponding changes in dielectric constant were observed and they are shown in Figures 6 and 7.

The effects are greatly moderated at 1 kc, where the maximum value of tanδ during exposure was 0.0018 for the 30-mil machined specimen, and 0.020 for the 125-mil machined specimen.

It was suggested by the manufacturer that the primary difference between the machined specimens and the skived films is associated with the sintering process. The film is skived from a large diameter cylinder after the sintering process is completed. Therefore, a specimen taken from the outer portion of the cylinder would have been exposed to air during sintering, while a specimen taken from the inner portion of the solid cylinder would have been protected from the atmosphere. There was no way of determining the location from which the specimen used in this experiment had been taken, but another experiment provided data that confirms the suggestion that the presence of oxygen during sintering influences the observed radiation effects.

Two types of TFE-7 specimens supplied by E.I. Du Pont de Nemours and Company, Inc. were used in this phase of the investigation. They are identified as follows:

A-2 Sintered in air, 380°C, 2 hours.

N-2 Sintered in nitrogen, 380°C, 2 hours.

A-16 Sintered in air, 380°C, 16 hours.

N-16 Sintered in nitrogen, 380°C, 16 hours.

The results obtained at 100 cps are shown in Figures 8 and 9. In Figure 8, the specimen sintered for 2 hours in nitrogen exhibited a behavior similar to that of the 30-mil skived film, while the specimen sintered for 2 hours in air showed effects similar to those that had been observed for all other TFE specimens.

The tanδ recovery data (Figure 9) showed the same pattern of behavior that had been previously observed. The recovery period in high-vacuum was extended to 55 days, but no large changes occurred during the latter part of this period. Again, tanδ increased when the cell was filled with dry nitrogen.

The effects were greatly moderated at 1 kc. This same frequency effect has been observed in all of the experiments with the TFE polymers.

The only other material that is reported to show effects similar to the TFE resins is a composition of methyl styrene with a small amount of dimethyl siloxane additive. These results were reported by Pendergast and Hoffman[5]. Specimens of similar composition were obtained from the Delaware Research and Development Corporation, Wilmington, Delaware. During x-ray irradiation for 338 hours in high-vacuum (6 megarads), the dielectric constant of C-1147 remained at a value of 2.55 and the highest value of tanδ measured at 100 cps was 0.0005. No changes occurred when the radiation was removed.

Since the effects reported by Pendergast and Hoffman were not evident under the experimental conditions of this investigation, no correlation could be made with the behavior of the TFE resins.

The difference in behavior caused by the presence of oxygen during the sintering process suggests that end-groups play an important role in the induced loss mechanism. This is supported by the fact that the drastic effects of irradiation were absent in the case of a batch of TFE sheet stock that was stored in the laboratory for several years. Of course, differences in impurities could also influence the induced losses, and the older material could differ from the present resins in this respect.

Because the induced losses decrease so rapidly with increasing frequency, it would appear that a conduction mechanism is responsible

for the observed behavior. However, the induced d-c conductivities of the TFE resins are comparable to those observed with other polymers that do not exhibit induced a-c losses. It has been suggested that the charge transport mechanism is ionic and that the ions produced by the irradiation do not have complete freedom of motion in the presence of an electric field because of the polycrystalline nature of the TFE structure. Evidence of such a restricted motion has been obtained in a qualitative experiment which showed that tanδ decreased with increasing voltage. Such behavior, known as the Garton effect[6], is observed in composite materials where the motion of ions is restricted by barriers.

It should be noted that the FEP copolymers did not exhibit induced a-c losses. There was no evidence that ions were produced by the irradiation, so the difference in behavior cannot be attributed to the lack of crystallinity in the FEP material. It may be that ions are produced, but are free to recombine or become attached at a point on the chain where a bond has been broken by the irradiation. However, this remains to be proven.

The recovery data cannot be fully explained and it is not possible to present a detailed discussion of this behavior in this brief report.

The reason for discussing the exposure experiments in detail is that they demonstrate the importance of conducting electrical measurements during irradiation, rather than before and after. They further illustrate the danger of drawing general conclusions about the behavior of a class of materials based on the observed behavior of a single sample. This is certainly demonstrated by the data of Figure 4 which shows that after a dose of 2.5 megarads the 30-mil skived film had a tanδ of 0.0005, while the 30-mil machined specimen had a tanδ of 0.05 - two decades higher. Furthermore, during the period when tanδ was increasing with one type of specimen, it was decreasing with the other type.

An important parameter that has not been investigated in this program is temperature. Such experiments are planned and will be conducted as time and funds permit. The combined effects of vacuum, irradiation and temperature must be determined experimentally. Extrapolations, particularly at cryogenic temperatures, are not justified on the basis of known effects. This is demonstrated by the work described by Mathes in another paper presented at this symposium.

Induced Conductivity.

X-ray induced d-c conductivity has been investigated in this program. Details will not be given here, but it should be noted that the observed behavior has proven to be dependent on temperature in a way that would not be predicted on the basis of the accepted explanations of induced conductivity in polymers. The behavior, based on conduction by free electrons in the presence of traps, is discussed by Snyder in another paper presented at this symposium. The instantaneous effects of irradiation follow the relationships described in that paper, but prolonged exposure to irradiation and vacuum produce effects that are not readily predicted by the transient behavior. As soon as a material is exposed to the environmental stresses of interest in space applications its structure begins to change and the effects that these changes can have on conductivity must be determined experimentally.

Conclusions.

The effects of space environment on the properties of electrical insulating materials will become a subject of increasing importance as larger vehicles with longer missions become realities. Insulation life, as determined by electrical and mechanical criteria, will become a major design consideration. This symposium has demonstrated the need for detailed investigation of the many factors that contribute to

space environmental effects. Reluctant reference was made to the performance characteristics of insulating systems in a space environment, a subject that has not even been approached in the laboratory.

The present program at the Dielectrics Laboratory includes further investigation of induced conductivity at elevated temperatures; a study of the effects of temperature on irradiation induced a-c losses; and an investigation of the high-frequency behavior of materials at high electrical stresses during vacuum exposure. No low temperature experiments are planned at the present time.

Acknowledgements.

The authors are indebted to the E.I. Du Pont de Nemours Company for the cooperation extended by various members of the Plastics Department and the Experimental Station in the investigation of the effects of x-ray irradiation on tetrafluoroethylene polymers.

References.

1. Dielectrics for Satellites and Space Vehicles, Final Report of Contract DA-36-039-SC-78321, March 1, 1959 - February 28, 1962. The Johns Hopkins University, Dielectrics Laboratory, Baltimore, Maryland.

2. Dielectrics for Satellites and Space Vehicles, Final Report of Contract DA-36-039-SC-89147, March 1, 1962 - March 31, 1963. The Johns Hopkins University, Dielectrics Laboratory, Baltimore, Maryland.

3. "Surface Failure of Electrical Insulating Materials in a Space Environment", L. J. Frisco and A. M. Muhlbaum. Proceedings of the 1962 Electronic Components Conference, Washington, D. C., pp. 166-171 (1962).

4. "The Flashover Strength of Solid Dielectrics", L. J. Frisco and J. J. Chapman. Power App. and Systems, No. 23, pp. 77-83 (1956).

5. "Tensile, Impact and Dielectric Properties of Irradiated Polymers", H. E. Pendergast and A. S. Hoffman. AIEE Conf. Paper 61-391, presented at AIEE Winter General Meeting, January 29 - February 3, 1961.

6. "Dielectric Loss in Thin Films of Insulating Liquids", C. G. Garton. J. Inst. Elect. Eng., 88, II, 103-120 (1941).

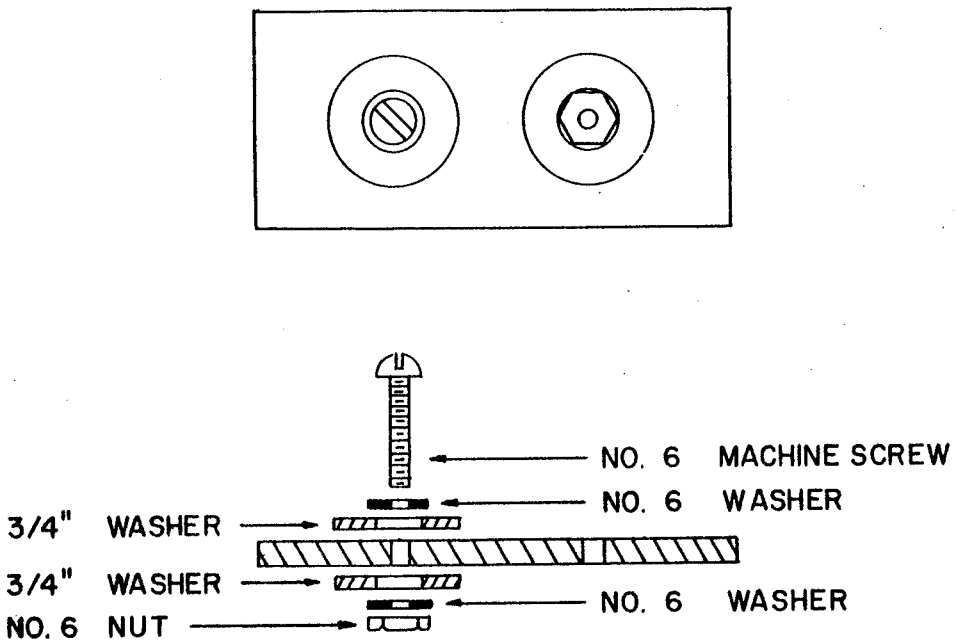

Figure 1. Flashover sample.

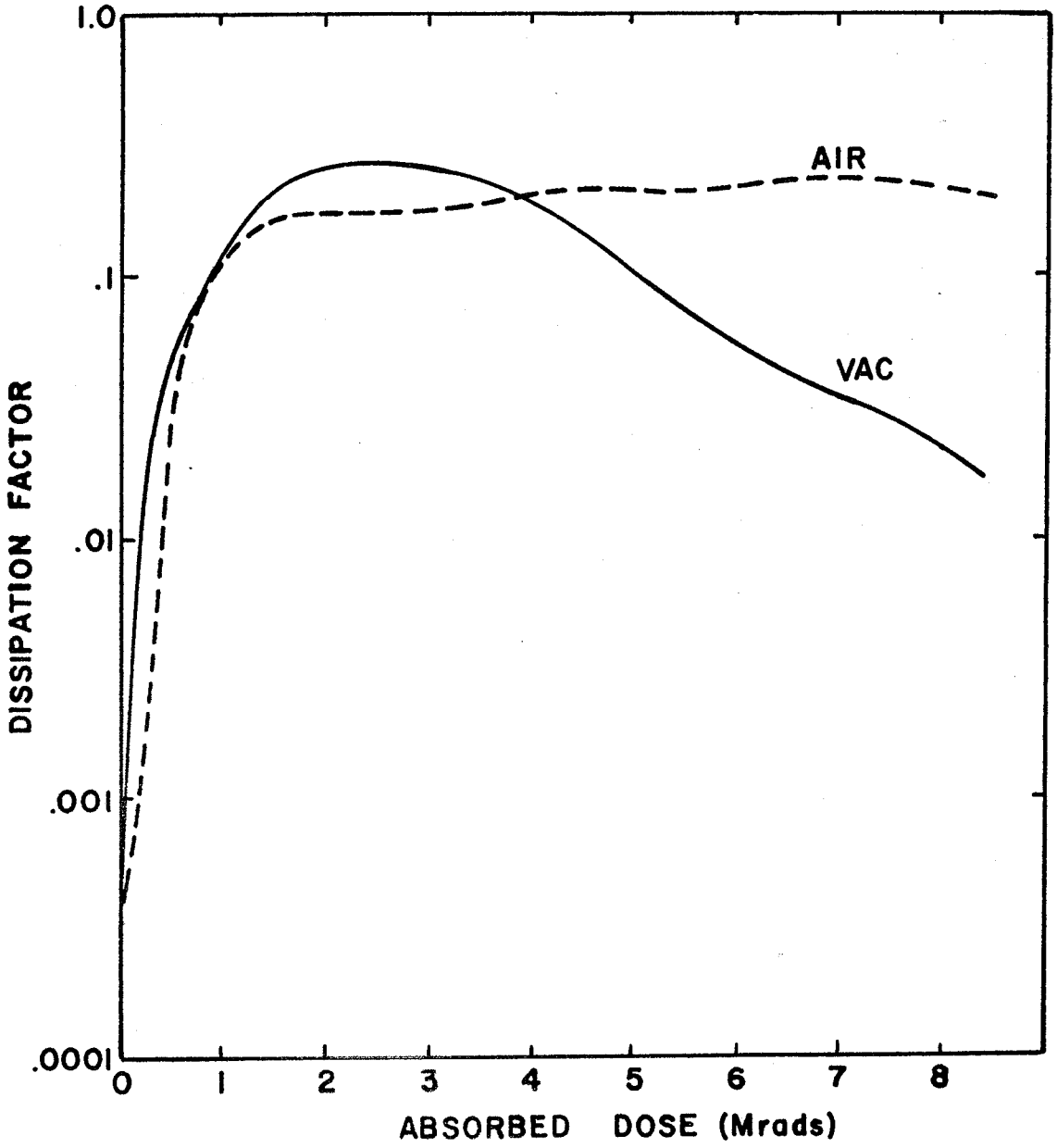

Figure 2. Effect of x-ray irradiation on TFE-6.

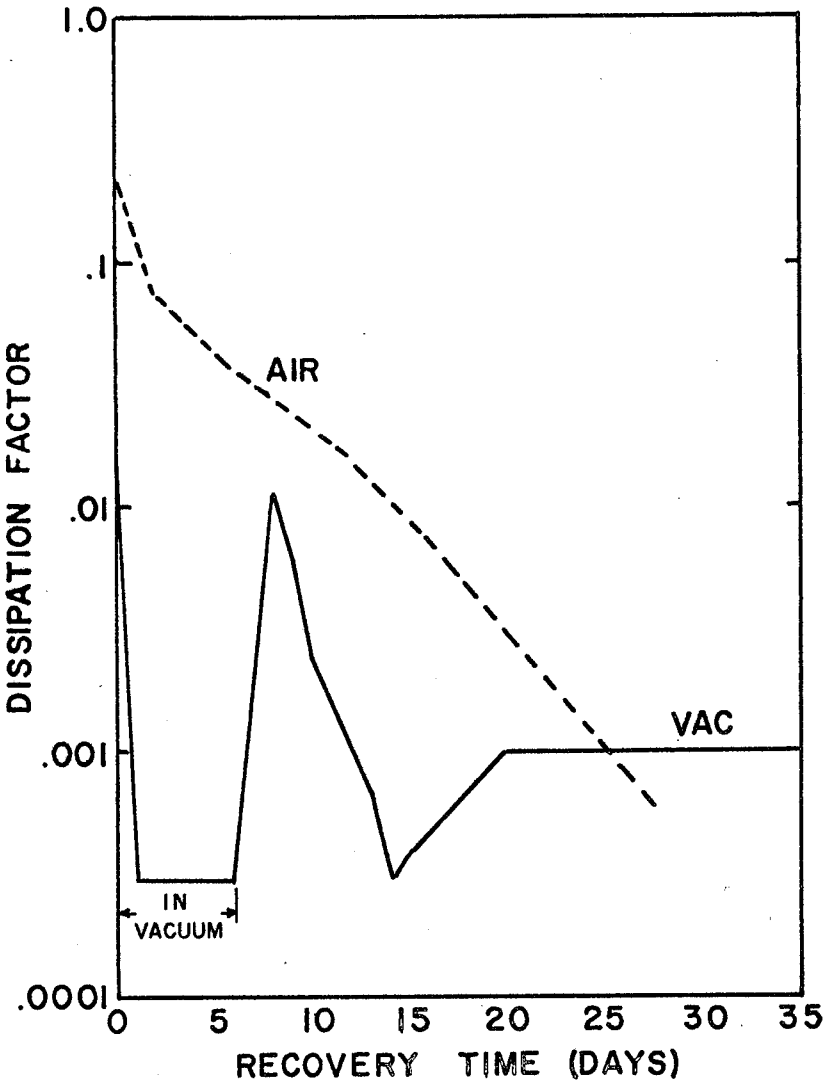

Figure 3. Recovery characteristics of TFE-6 specimens after x-ray irradiation as shown in Figure 2.

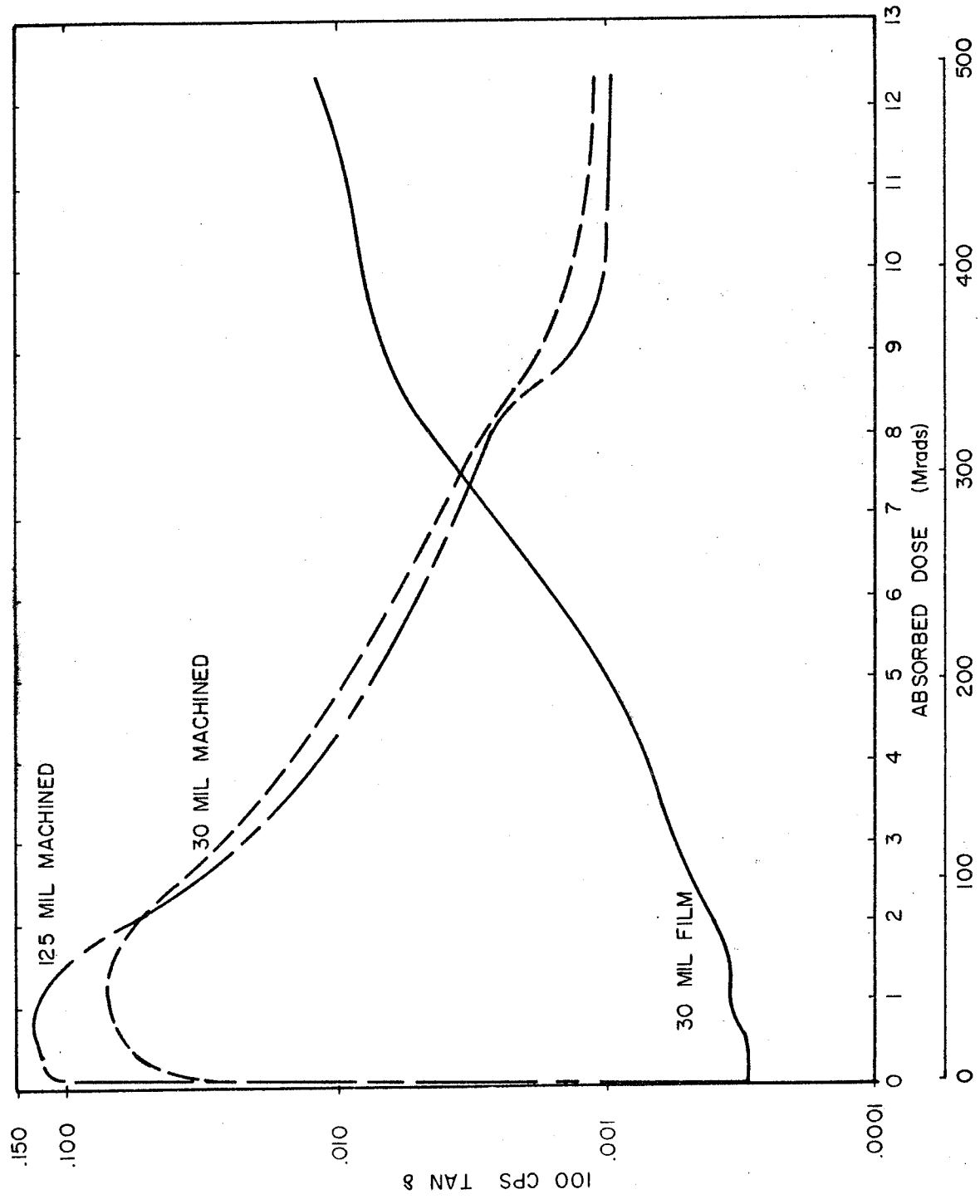

Figure 4. Effect of absorbed dose on 100 cps tanδ of TFE-7; 30-mil machined and 125-mil machined specimens from 1/2" thick block, 30-mil film skived from large diameter cylinder.

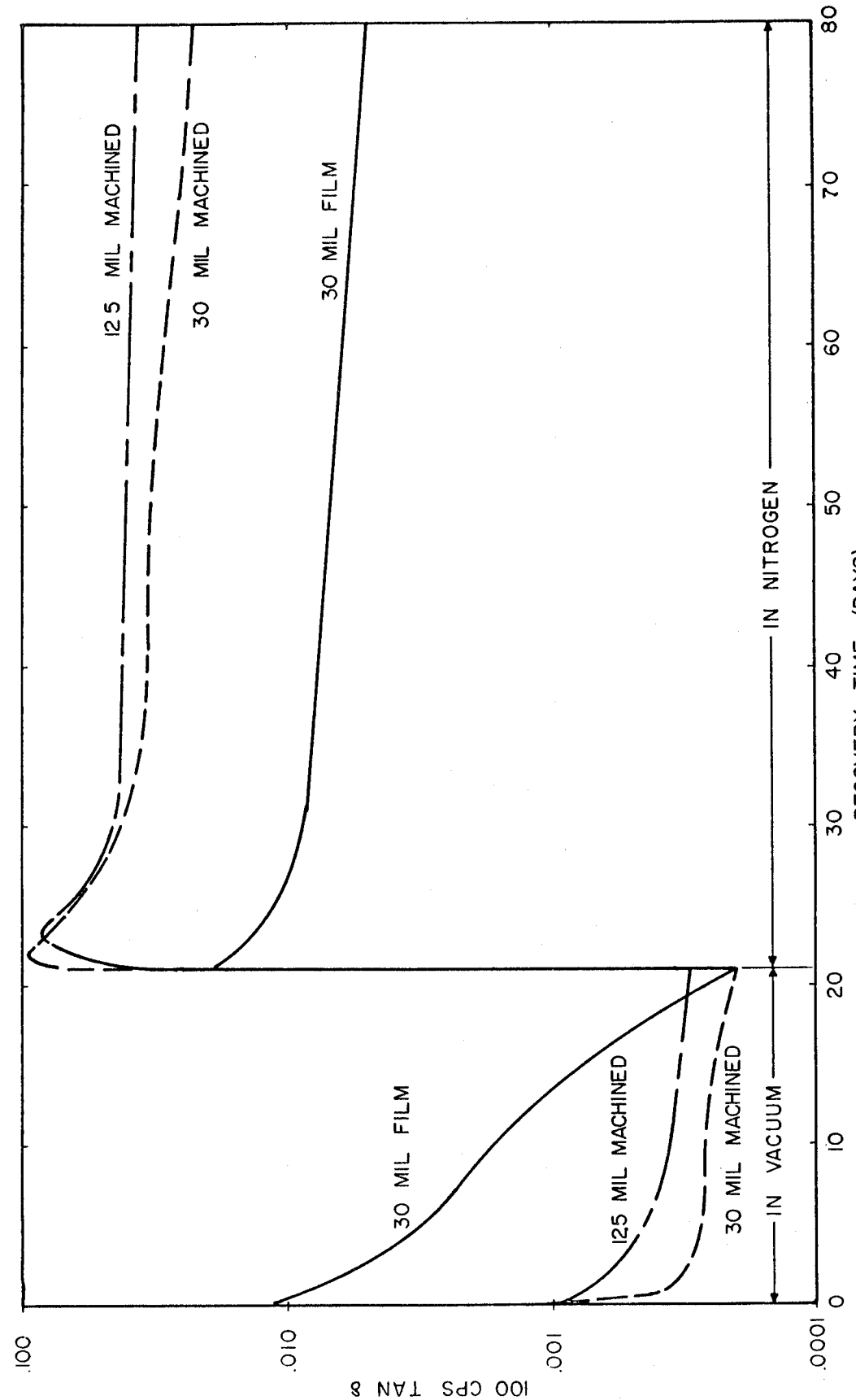

Figure 5. 100 cps tanδ recovery characteristics of TFE-7 after exposure shown in Figure 4.

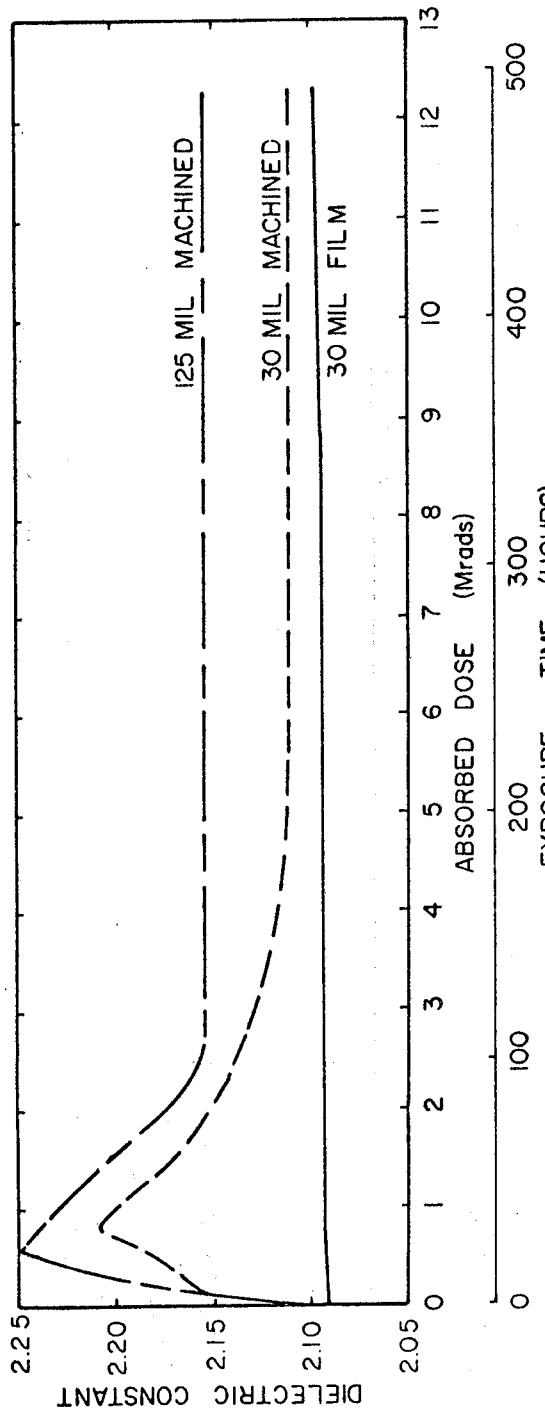

Figure 6. Effect of absorbed dose on 100 cps dielectric constant of TFE-7; 30-mil and 125-mil machined specimens from 1/2" thick block, 30-mil film skived from large cylinder.

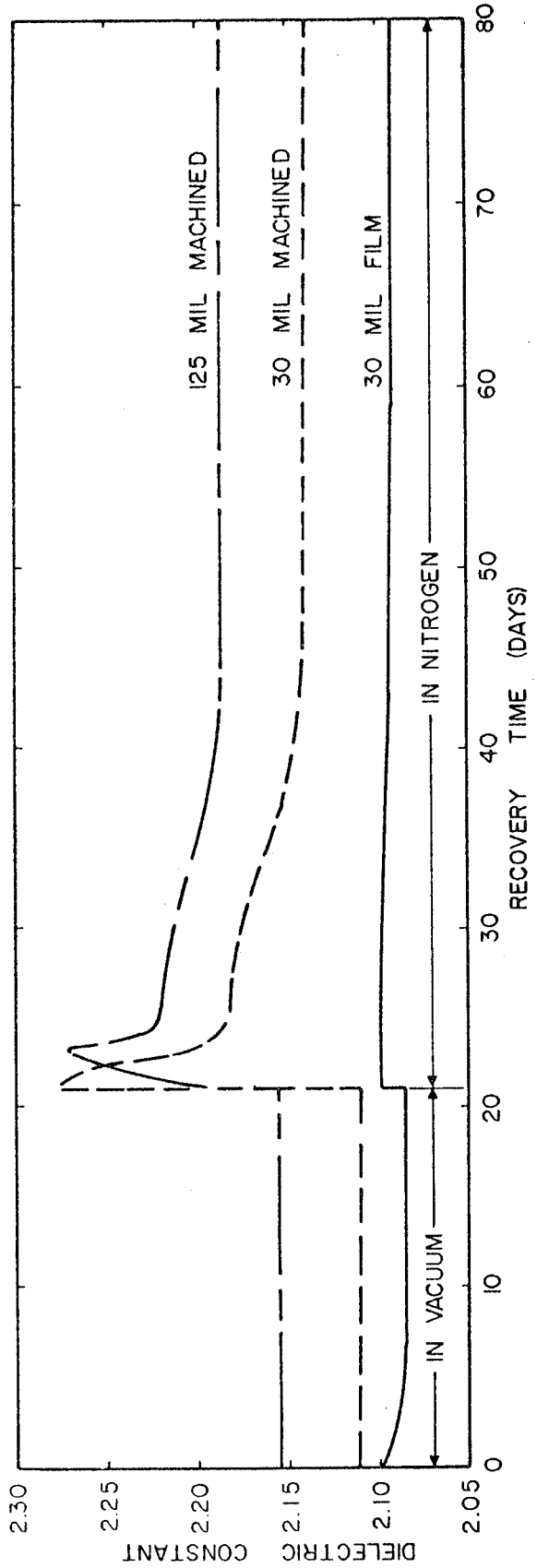

Figure 7. 100 cps dielectric constant recovery characteristics after exposure shown in Figure 6.

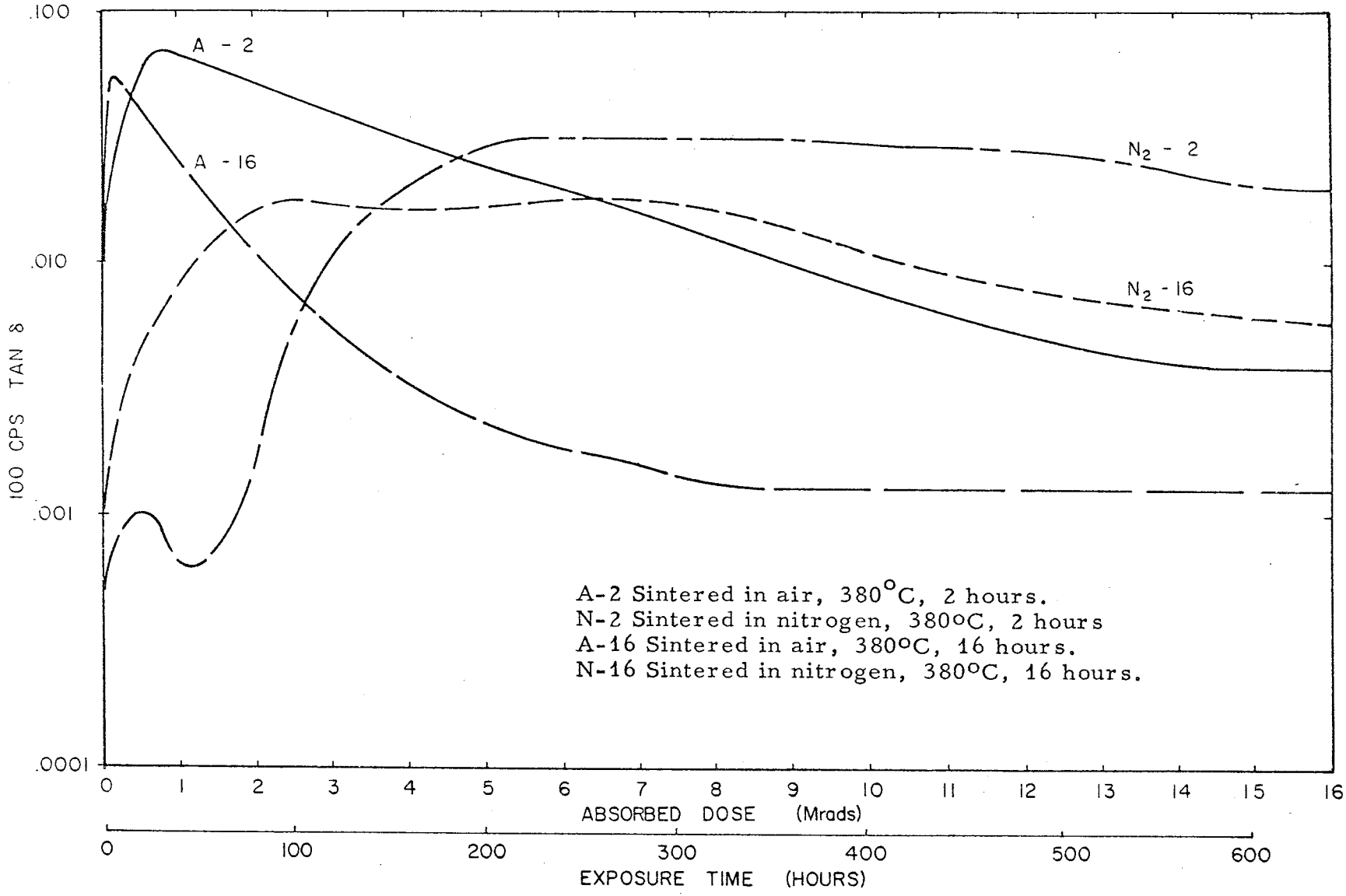

Figure 8. Effect of sintering conditions on x-ray induced tanδ of TFE-7 at 100 cps.

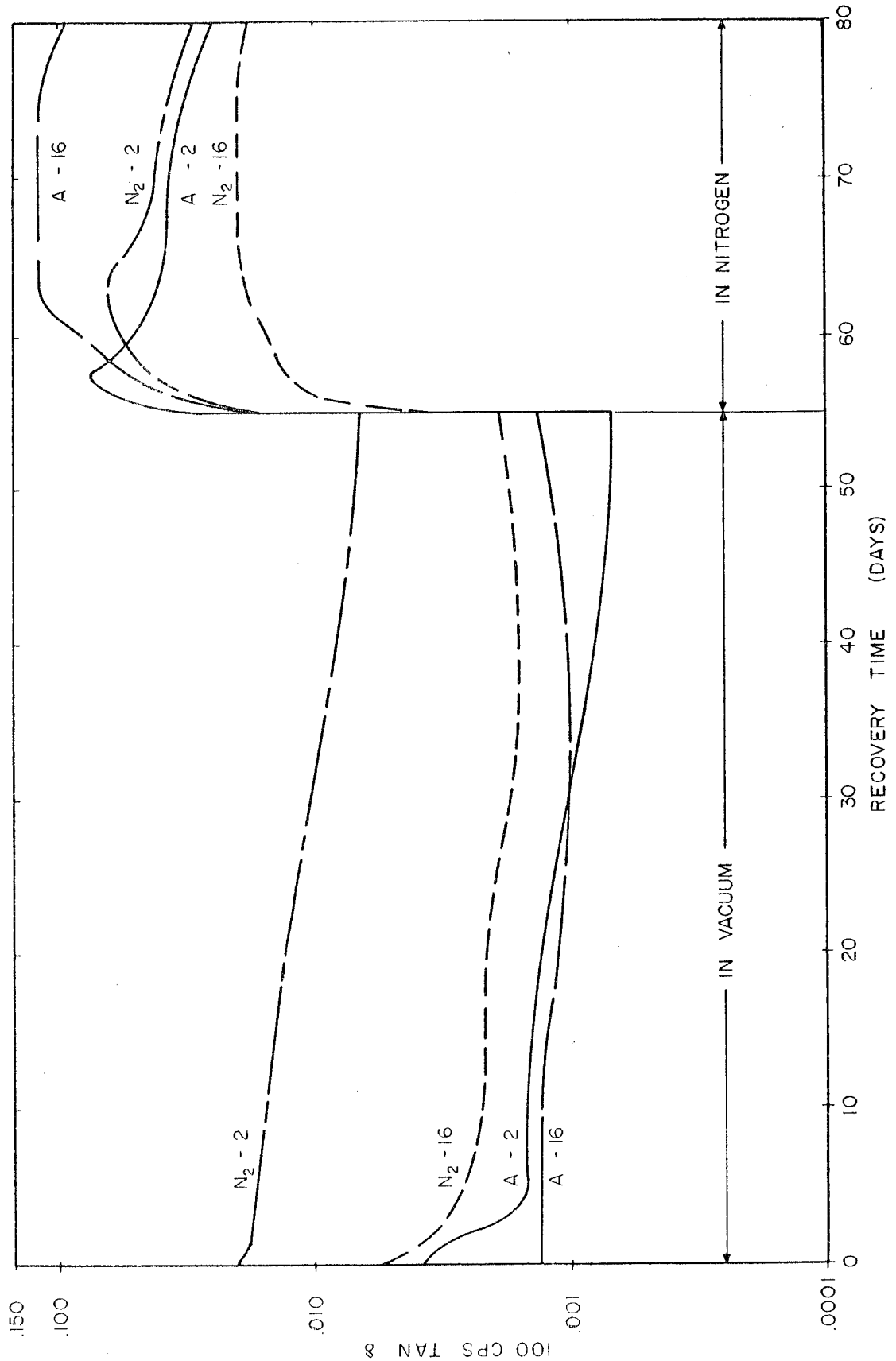

Figure 9. Effect of sintering on 100 cps tanδ recovery characteristics of TFE-7 after exposure shown in Figure 8.

A Brief Summary

of

Space Nuclear Radiations and Effects

Westinghouse Symposium on
"Dielectrics in Space"

June 25-26, 1963

Compiled by

K. H. Sun

Radiation and Nucleonics Laboratory
Westinghouse Research Laboratories
Pittsburgh 35, Pennsylvania

Space Nuclear Radiations

I. Galactic Cosmic Rays - Mostly Protons

II. Solar-Flare Particles - Mostly Protons

III. Earth Trapped Radiations

A. Van Allen Belt - Mostly Protons and Electrons

B. Artificial Belt - Mostly Electrons and γ-Rays

IV. "Impact" Radiations

(For future spaceship traveling close to the speed of light)

K. H. Sun
Westinghouse

I. Galactic Cosmic Rays

Flux ~ 2.1 $cm^{-2} sec^{-1}$

Energy Density ~ 1 ev cm^{-3} (Interplanetary)

Composition (outside atm.):

Particles	%
Protons	85
α-Particles	12.6
Z = 3-5	0.3
Z = 6-9	0.8
Z > 10	0.3
Electrons, etc.	1

Energy Spectrum (see next page)

Average Dose: 0.1 - 1 r/week

Highest Localized Dose: 10^4 r/Particle (in a fiber 10μ diameter and a few mm long)

References:

A. W. Wolfendale, Cosmic Rays, 1963
T. Foelsche, AIEE Conf. Paper 61-1143, 1961

I. Galactic Cosmic Rays

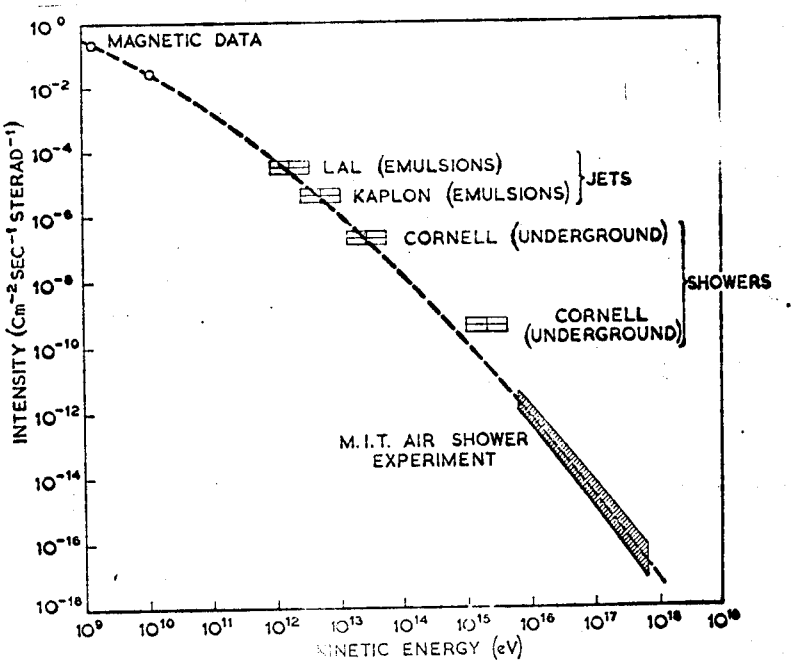

Integral Spectrum of Galactic Cosmic Rays

(Wolfendale, Cosmic Rays, p. 90)

II. Solar Flare Particles

Energy Spectrum

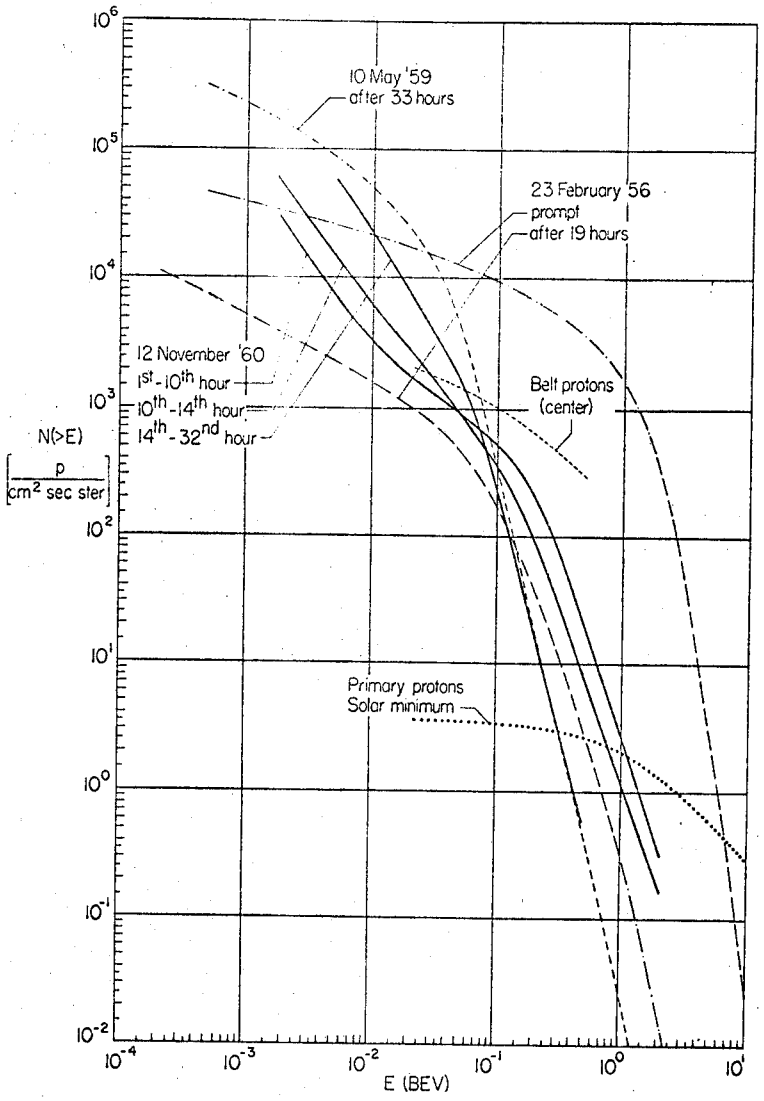

T. Foelsche, AIEE Conference Paper 61-1143, 1961

II. Solar Flare Particles

Dose Rate vs Absorber Thickness

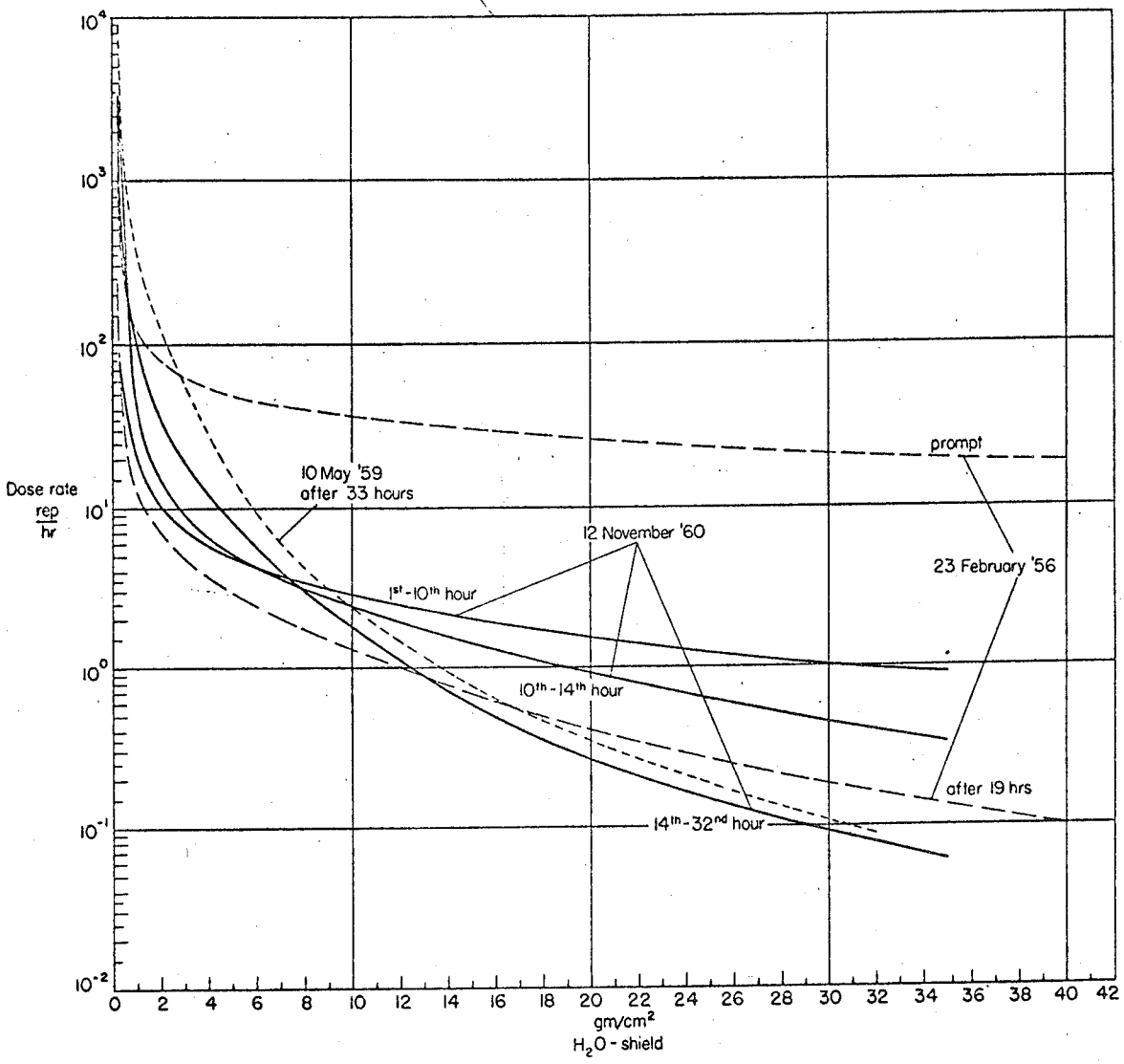

T. Foelsche, AIEE Conference Paper 61-1143, 1961

II. Solar Flare Particles

Dose per Flare vs Absorber Thickness

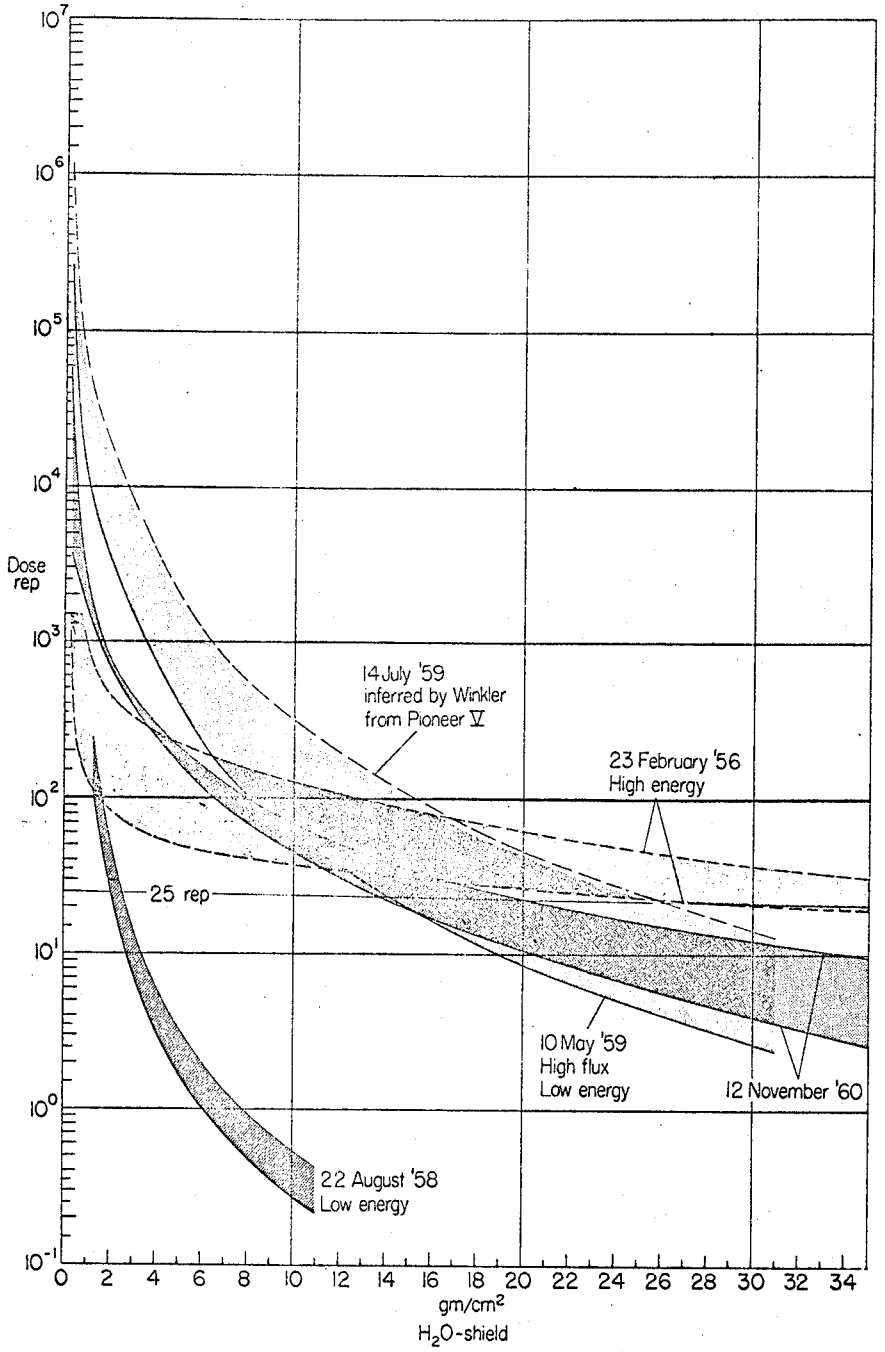

T. Foelsche, AIEE Conference Paper 61-1143, 1961

III. Earth Trapped Radiations

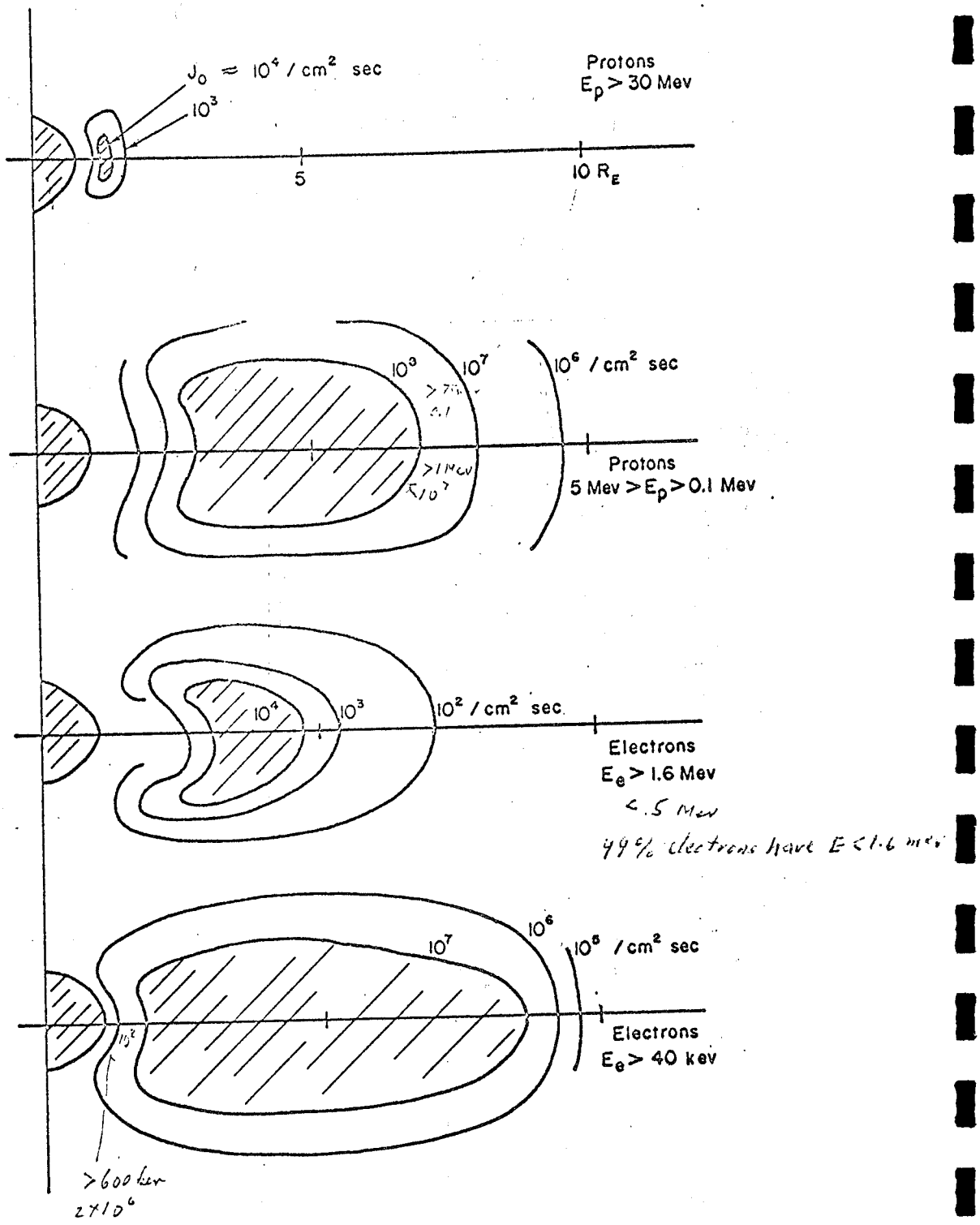

Van Allen Belts

Some Sample Structure Functions

NAS/NRC 1079, p. 7-17

III. Earth Trapped Radiations

Artificial Belt

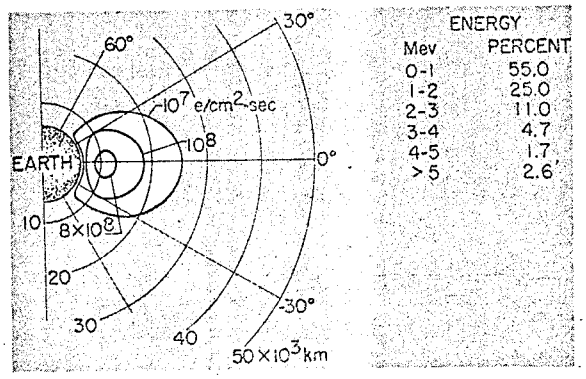

Flux Contours of Artificial Electron Belt (NASA SP-11, Vol. II, p. 443

ESTIMATED RADIATION EXPOSURE IN SPACE

I. Galactic cosmic radiation

	Gross ionization dosage	Heavy primary hits	
		Without shield	20 g/cm^2 of H_2O
During solar activity years	0.45 to 1.0 rem/week 25 to 50 rem/year	6/cm^2/day	2/cm^3/day

II. Belt radiation

Particles	Belt	Energy, MeV	Flux $cm^{-2}sec^{-1}$	Dose megarad yr^{-1}	Penetration Thickness in Material of Unit Density cm
Proton	Outer	0.1	10^8	24,000	0.002
	Inner	30	10^4	0.15	1.0
Electron	Inner	0.1	10^8	350	0.015
	"Inner" (artif.)	1.0	10^9	120	0.4

III. Solar cosmic radiation

	Inside spherical shields, neglecting self-shielding	
	2 g/cm^2 of H_2O	25 g/cm^2 of H_2O
Low energy, extreme flux May, July 1959	2,500 to 15,000* rep	6 to 25 rep
Medium energy, extreme flux November 1960	600 to 800 rep	6 to 19 rep
High energy, high flux February 1956	80 to 400* rep	25 to 50* rep

*These values are extrapolated and highly uncertain.

T. Foelsche, AIEE Conference Paper 61-1143

K. H. Sun, Unpublished

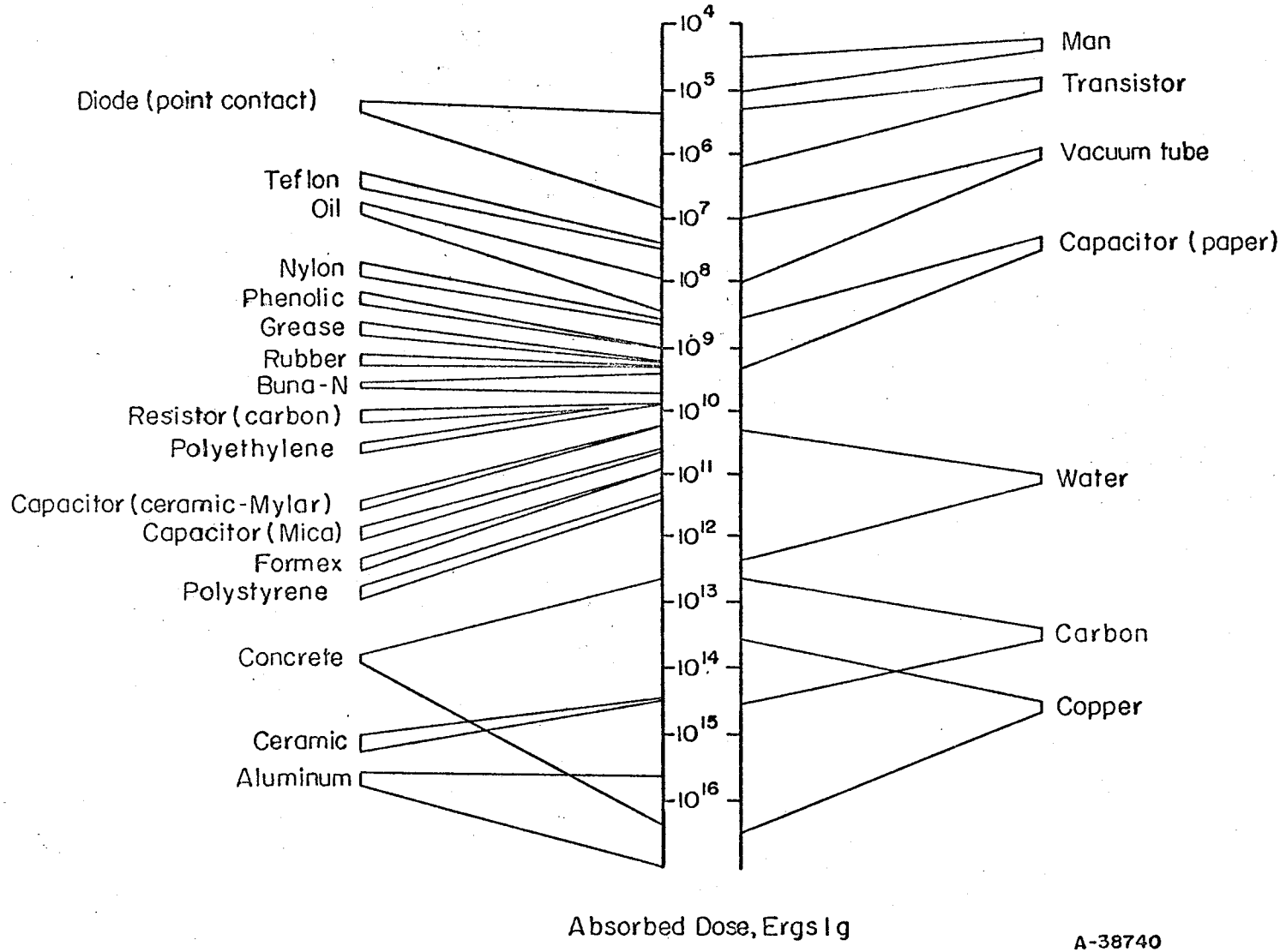

FUNCTIONAL RADIATION DOSE THRESHOLD

Taken from Reference 29.
REIC Memo 21, 1961

HIGH ENERGY ELECTRON IRRADIATION OF PLASTICS FOR COMMUNICATIONS SATELLITES

by

J. V. Pascale, D. B. Herrmann, R. J. Miner
Bell Telephone Laboratories, Incorporated
Murray Hill, New Jersey

ABSTRACT

The effect of ionizing radiation on the mechanical and electrical properties of 45 plastics being studied for possible use in communications satellites is described. The maximum total Van de Graaff electron flux is 5.8×10^{16} electrons/cm^2, which is equivalent to about 18 years in the Van Allen radiation belt.

Types of plastics evaluated include polyethylenes, polypropylenes, styrene polymers, polyamides and others.

Mechanical properties determined are indentation hardness, stiffness in flexure, tensile strength and elongation.

Electrical properties determined are dielectric constant, dissipation factor, and d-c insulation resistance.

Of the materials investigated the styrene polymers are the most resistant to radiation. Plastics showing severe degradation are the acrylics, cellulosics and fluorocarbon polymers.

Also in Modern Plastics 41(2):239-49, 244-49, 248-53, 374, 378 Oct. '63

HIGH ENERGY ELECTRON IRRADIATION OF PLASTICS FOR COMMUNICATIONS SATELLITES

by

J. V. Pascale, D. B. Herrmann, R. J. Miner
Bell Telephone Laboratories, Incorporated
Murray Hill, New Jersey

Introduction

The use of plastics in communications satellites has greatly stimulated interest in the effect of high energy ionizing radiation on these materials. The Telstar orbits traverse the inner Van Allen radiation belt up to an apogee of 3500 miles for Telstar I and 6700 miles for Telstar II. Plastic materials used as electrical insulation, in components, or as structural parts in a satellite must be those with the longest functional lifetime in this especially severe environment. After all, ocean cables are accessible for repair, but satellites are not, at least at present.

To obtain information on what happens to their mechanical and electrical properties 45 plastics (Table 1) were exposed to a one million electron volt beam from a Van de Graaff accelerator, to a maximum flux of 5.8×10^{16} electrons/cm^2, or 1800 megarads. This is equivalent to the radiation that would be received during about 18 years of orbiting in the inner belt.

Recent calculations by Brown and Gabbe[1] of the Bell Telephone Laboratories based on Telstar I satellite data indicate that the peak flux encountered in its orbit was approximately 8×10^8 electrons/cm^2 sec, above 200 Kev near the equator and at altitudes between 1200 and 2500 miles. This flux is considerably higher than reported by Van Allen and others.[2,3,4] However, because the orbit spends only about 20% of its time in this region and because of decay of the peak flux with time, the average flux in the Telstar orbit over a period of several months is approximately 10^8 electrons/cm^2 sec above 200 Kev.

Experimental

A turntable device, shown schematically in Fig. 1, was used as the mounting rack for the irradiation of ten test specimens. Each of five aluminum frames contained a test specimen 2-1/2" x 2-1/2" x 1/16" for dielectric studies, and each of the other five contained ten test strips 2-1/2" x 1/4" x 1/16" of the same material for the determination of mechanical properties subsequent to irradiation. Precooled nitrogen was allowed to flow into the turntable device to simulate a space environment free of oxygen. Built into the base of the table was a cooling coil. An average temperature of about 60°C was maintained for the

specimens. The turntable contained a removable heavy aluminum cover with a sector-shaped opening on the top. The opening was placed directly beneath the extension window (aluminum, 2 mils thick) of the Van de Graaff accelerator during the irradiations. A 5-mil thick aluminum scattering foil covered the opening midway between the 4 inches separating the extension window and the mounted rotating specimens.

This irradiation procedure followed preliminary dosimetry measurements simulating the identical geometrical arrangement using a Faraday cage (a total electron absorber) with a 1.25 cm^2 defining aperture. The Van de Graaff accelerator was operated at 200 μamp and 1 Mev; the Faraday cage measured the incident radiation passing through the aluminum window and the additional scattering foil.

The total time to irradiate each series of 10 specimens to a 5.8×10^{16} electrons/cm^2 flux when operating the Van de Graaff at 200 μamp beam current was 7 hours and 40 minutes.

The irradiated materials were stored in a nitrogen filled desiccator for 3 days prior to testing. Studies of high density polyethylene indicate that this period of time was adequate to allow almost complete decay of free radical concentration. (Electron spin resonance measurements show

that at least 98% of the immediate post-irradiation free radical concentration had decayed in 24 hours.) Then, specimens were conditioned according to Procedure A of ASTM Designation D618, Conditioning Plastics and Electrical Insulating Materials for Testing. Both irradiated and unirradiated materials were treated identically, and the mechanical properties measured at the standard laboratory atmosphere (23 ± 2°C and 50 ± 5% R.H.) of ASTM D618.

1. Mechanical Testing Procedures

   (a) Indentation Hardness - The familiar ASTM D1706-61 Rockwell Hardness Test could not be employed because the softer materials were below the range of the testing equipment and the test specimens were too small. It was therefore necessary to utilize a Shore Durometer in obtaining approximate indentation hardness values.

   (b) Stiffness in Flexure - The Tinius Olsen Stiffness Tester was employed in accordance with ASTM method D747, Stiffness in Flexure of Plastics, to obtain relevant information. This method was suitable for examining the various plastics over a wide range of flexibility.

   (c) Tensile Strength and Elongation - Although the test strips (2-1/2" x 2-1/2" x 1/16") did not conform

to ASTM specifications, useful comparative data were obtained using a bench model Instron with a jaw separation of one inch, and crosshead speed was varied to suit each material.

2. Electrical Testing Procedures

The liquid displacement method, ASTM D1531-61, was followed as given, except for the size of the specimens, the use of center plates of different thicknesses to conform to the wide differences in thickness of the specimens and the use of Dow Corning 200 (one centistoke) fluid (dimethyl-polysiloxane) as the standard liquid dielectric in place of benzene because some of the plastics are soluble or partly soluble in the latter.

The dielectric constant and dissipation factor were determined at two test frequencies: one kilocycle per second with a Bell Telephone Laboratories capacitance-conductance bridge and one megacycle per second with a Boonton Radio Corporation 260-A Q-meter using ultrahigh Q coils (500 to 600). The temperature range of the fluid during the measurements was 23.9 to 25.4°C.

The d-c insulation resistance was determined with a General Radio 1230-A d-c amplifier and electrometer, at 100 volts and at the ASTM D618 standard laboratory atmosphere

with the same test specimens clamped between metal electrodes two inches in diameter. The electrification time was two minutes.

Discussion of Results

The gross physical changes that occurred in the 45 plastics are shown in Fig. 2. Those that disintegrated when an attempt was made to test them include the acrylics, acetal resins, fluorocarbon polymers, cellulosics and polyethylene terephthalate. Many others broke into several pieces. A few materials expanded due to trapped gases, among these were polymethyl methacrylates, styrene-acrylic copolymer, rubber modified acrylic plastic and chlorinated polyether.

Most of the materials were darkened in varying degrees by the irradiation and many showed modifications in color associated with chemical changes. The change in color of irradiated polymers is often due to the formation of conjugated double bonds. However, the diallylphthalates, phenolplastics, epoxy-molding compound and black-pigmented polyethylene, which were dark to begin with, showed only minimal color changes. An interesting finding was that many of the disintegrated materials, which were light in color initially, remained light even after the irradiation.

Table 2 lists the plastics that were so seriously degraded by the irradiation that they could not be tested. The materials are listed with corresponding code numbers and electron fluxes given the specimens prior to their removal from the turntable.

1. Mechanical Properties

Table 3 contains data on the Shore D (Durometer) hardness (indentation) of the specimens before and after irradiation. Each value is an average of up to 5 determinations.

A low density polyethylene, 3, shows no change, but the same base polymer containing carbon black shows an increase of 17%. Another low density polyethylene, 5, but with a melt index 10 times that of 3, increases by 40%, an indication of effective crosslinking. The polypropylenes, on the other hand, have sizable decreases, softening about 25%, a result of molecular scission.

Polystyrene, 1, styrene acrylonitrile copolymer, 25, and styrene divinylbenzene, 31, are highly radiation resistant, showing very little change in hardness. But two copolymers containing butadiene, 20 and 26, increase in hardness. The polyamides also show moderate increases. All of the other plastics tested, except polyurethane, 42,

remain practically unchanged. The polyurethane increases to a greater extent than any of the others, becoming hard and brittle. The polyethylene terephthalates, 41 and 44, were too brittle and glass-like to be tested.

Data on stiffness in flexure, determined with a Tinius Olsen stiffness tester, are given in Table 4. The polyethylenes all show decreases, except the one containing the black pigment, 45. The two higher density polyethylenes, 2 and 4, decrease appreciably. The polypropylenes were too soft to test, again indicating molecular scission. Polystyrene, 1, styrene acrylonitrile copolymer, 25, and styrene divinylbenzene, 31, show little change. However, the two copolymers show considerable increases in stiffness. The polyamides also show large increases, with a very large increase in 11, indicating a predominance of crosslinking over scission. The next four groups, diallyl phthalates, phenolplastics, epoxy molding compound and alkyd resin, all very stiff initially, show small changes. The PVC acetate and polyethylene terephthalate decrease, largely an effect of enbrittlement due to crosslinking. The polyurethane, initially very low, increases almost 200%, correlating with a large change in hardness.

Tensile strength at break values are found in Table 5. Most of the polyethylenes show a decrease; the two that increase are higher density polymers. It should be

noted that all of these materials have low initial tensile values so that the large changes shown appear more significant than they really are. The polypropylenes decrease almost 100%, again showing the effect of scission. The styrene polymers, as radiation resistant as they are in other respects, appear to be adversely affected in tensile strength by radiation. The polyamides show large increases in tensile strength in agreement with the hardness and stiffness changes, all apparently due to crosslinking. The diallyl phthalates are affected differently, one has an increase of over 100%, the other was too brittle to test, as were the polyethylene terephthalates. The polyurethane shows a decrease in tensile strength, again in good agreement with the hardness and stiffness changes.

All of the polyethylenes, polypropylenes, polyamides, PVC acetate, polyethylene terephthalates, polyurethane and even the styrene-butadiene polymers have an almost complete loss of ultimate elongation (Table 6). However, the polystyrene and styrene-acrylonitrile, with low initial values, remain low, with a 50% loss, and styrene divinyl benzene remains practically unchanged. The diallyl phthalates, having low initial values, decrease and increase, respectively.

2. Electrical Properties

The electrical properties put the plastics in a somewhat different relationship than the mechanical properties.

It is evident from Figs. 3 and 4 that the low dielectric constant materials show little or no change when measured at frequencies of one kilocycle and one megacycle per second.

Only two plastics, both styrene based, show no change in dielectric constant: polystyrene, 1, and styrene divinylbenzene, 31. This is in agreement with the findings of Charlesby[5], Bovey[6], Sisman and Bopp[7] and Bradley[8] that polymers containing the benzene ring, particularly those in which it constitutes a high proportion of the molecule and occupies a pendant position, have a very high resistance to ionizing radiation.

Two other styrene plastics, 20 and 26, show increases in dielectric constant of less than 1.5%. However, a styrene-acrylo nitrile copolymer, 25, shows a dielectric constant increase of more than 6% at one kilocycle. Presumably, in cases like this, that part of the molecule in which the benzene rings are not present, or are widely spaced, is more adversely affected by electron irradiation. The higher dielectric constant polyamides and phenolplastics, however, show large decreases at one kilocycle. Indeed, the decrease in dielectric constant of the single stage phenol plastic is remarkable, from over 14 to 7.5, this in spite of the presence of benzene rings in the molecule. These benzene rings, however, are links in the molecular chain, rather than

appendages to it. The effect is not nearly as great at one megacycle. The two stage phenolplastic, 30, does not decrease as much as the single stage material at one kilocycle, but shows the same frequency relationship. The polyamides behave in a similar manner with frequency. The polyurethane is unique in having a larger dielectric constant decrease at one megacycle than at one kilocycle. The polyurethanes have a complex molecular structure, with nitrogen and oxygen atoms as well as carbonyl groups in the chain in addition to carbon. Crosslinking induced by the electron irradiation may reduce the polarity at the higher frequency. All of the other materials exhibit relatively small changes in dielectric constant at both frequencies.

The increases in dissipation factor of the polyethylenes, and polypropylenes at both one kilocycle, Fig. 5, and one megacycle, Fig. 6, are relatively large. However, these materials have such low dissipation factors that even after the substantial increases shown, they are still good electrical insulators.

The polystyrene and styrene divinylbenzene, 1 and 31, are very resistant to radiation, in fact, the dissipation factors actually decrease at one kilocycle and show almost no change at one megacycle. The remaining styrene polymers have higher dissipation factors at both frequencies both before

and after irradiation. The polyamides show an appreciable decrease, especially at one kilocycle.

Although, ions formed on irradiation would ordinarily influence electrical properties, it is necessary to consider that the movement of ions may be severely hindered by extensive crosslinking.

Most of the other materials have high initial dissipation factors, with the phenolplastics the highest of all. The diallyl phthalates and phenolplastics show small decreases at one kilocycle with the former showing little or no change at one megacycle. The two phenolplastics, however, behave quite differently at one megacycle, the single stage showing a 34% decrease and the two stage a large increase of 1300%. The dissipation factor of the polyvinylchloride acetate increases by about the same percent at both frequencies, that of the epoxy molding compound increases at one kilocycle and decreases at one megacycle. The polyethylene terephthalate, polyurethane and polyvinylfluoride all show appreciable increases at one kilocycle, and either a small increase or a small decrease at one megacycle. An interesting finding is that polyurethane shows practically no change in dissipation factor at one megacycle. In view of what happened to the mechanical properties of this material, an appreciable increase in dissipation factor might have been expected.

The materials that show the largest percentage increases in dissipation factor, the polyethylenes, also show the largest decreases in d-c insulation resistance, Fig. 7, with one exception. Electron irradiation of low density polyethylene, 5, for example, brings down its d-c insulation resistance at least two and one-half orders of magnitude. The same property of intermediate density polyethylene, 6, is reduced three orders. A reduction of at least two orders is shown by polyethylenes 2, 3 and 4. The exception is the black polyethylene, 45, which does not change. This material, however, has an initial insulation resistance at least two orders lower than that of most of the other polyethylenes. In spite of the reductions, the latter are left with insulation resistances higher than those of most of the other plastics, because their initial values are so high, sometimes beyond the upper limit of measurement of the equipment used. The polypropylenes behave differently, number 7 decreasing in insulation resistance to a lesser extent than the polyethylenes; number 8 actually increasing slightly. Polystyrene, 1, unexpectedly decreases more than two orders in insulation resistance but there is no measurable change in the styrene divinylbenzene, 31. Two of the styrene polymers, 20 and 26, show slight increases; the styrene acrylonitrile copolymer, 25, goes down one order.

The three polyamides, starting with a relatively low level of resistance, are all improved by the irradiation by about one order. The diallyl phthalates show little change. The phenol plastics, starting with a low insulation resistance, increase, almost an order for the two-stage and one and a half orders for the single stage. The epoxy molding compound decreases by one order and the PVC acetate by two. Polyethylene terephthalate increases slightly. Polyurethane, starting lower than all the other materials, drops still lower. Polyvinylfluoride remains the same.

Summary and Conclusions

All of the plastic materials investigated were affected to some extent by electron irradiation, which in most cases comprised a maximum total electron flux of 5.8×10^{16} electrons/cm^2 and an accelerated dose rate. The acrylics, cellulosics, fluorocarbon polymers, acetal resins, and polycarbonate were so adversely affected physically, even before many had been subjected to the maximum flux, that neither their mechanical nor electrical properties could be determined. The predominantly observed effects in those materials which were tested mechanically and electrically were embrittlement with a corresponding decrease in elongation, an increased dissipation factor and a lowered d-c insulation resistance. The styrene polymers were the most

resistant to radiation, styrene divinylbenzene outstandingly so. Therefore this class of materials is the most acceptable for communications satellites.

ACKNOWLEDGEMENTS

The authors appreciate the helpful assistance and suggestions of V. T. Wallder, D. W. McCall, W. L. Brown, and R. Salovey of the Bell Telephone Laboratories.

REFERENCES

1. Brown, W. L. and Gabbe, J. D., Jl Geophysical Research, 68, 607, (1963).

2. Van Allen, J. A., Jl. Geophysical Research 64, 1683, (1959).

3. Vernov, S. N., Chudakov, A. E., Gorchakov, E. V., Logachev, J. L., and Vakulov, P. V., Planetary and Space Science 1, 86, (1959).

4. Holly, F. E., Jl. Geophysical Research 65, 771, (1960).

5. Charlesby, A., "Atomic Radiation and Polymers", Pergamon Press, New York (1960).

6. Bovey, F. A., "The Effects of Ionizing Radiation on Natural and Synthetic High Polymers", Interscience Publishers, New York (1958).

7. Sisman, O. and Bopp, D. C., ORNL-928 (June 29, 1951).

8. Bradley, A., Plastic Design and Processing, pp. 18-24, Nov., 1961.

TABLE I

Code No.	Material	Remarks
1	Polystyrene	General purpose
2	Polyethylene	d. = .95 natural
3	Polyethylene	d. = .92 melt index 0.2
4	Polyethylene	d. = .96 natural
5	Polyethylene	d. = .92 melt index 2, natural
6	Polyethylene	d. = .947 natural
7	Polypropylene	Low ash
8	Polypropylene	High ash
9	Polyamide	Type 66
10	Polyamide	Type 610
11	Polyamide	Type 6
12	Polymethyl methacrylate	Cast
13	Acetal Resin	Copolymer
14	Acetal Resin	Homopolymer
15	Polytetrafluoroethylene	Fluorocarbon resin
16	Polyfluoroethylenepropylene	Copolymer
17	Polychlorotrifluoroethylene	Homopolymer
18	Polyvinyl chloride	DOP plasticized
19	Polyvinylidene fluoride	Homopolymer
20	Styrene-butadiene	High impact styrene
21	Allyl carbonate	Cast
22	Polyvinyl chloride	Rigid
23	Polymethyl methacrylate	Molding grade
24	Rubber modified acrylic plastic	Molding grade
25	Styrene-acrylonitrile copolymer	
26	Acrylonitrile-butadiene-styrene	Natural
27	Diallyl phthalate	Glass filled black
28	Diallyl phthalate	Orlon filled green
29	Phenolplastic	Single stage mineral, flock black
30	Phenolplastic	2 stage asbestos black
31	Styrene-divinylbenzene	Cross-linked polystyrene
32	Epoxy molding compound	Mineral filled black
33	Alkyd molding compound	Glass filled gray
34	Styrene acrylic copolymer	
35	Cellulose acetate	.010" thick, clear
36	Cellulose propionate	Clear
37	Cellulose butyrate	Clear
38	Chlorinated polyether	Natural
39	Polycarbonate	Clear
40	Polyvinyl chloride acetate	.015" thick, clear
41	Polyethylene terephthalate	Weather stabilized, 0.005" thick
42	Polyurethane	Elastomer
43	Polyvinyl fluoride	400 gage, 0.004" thick
44	Polyethylene terephthalate	Regular, 0.005" thick
45	Polyethylene	2.6% carbon black, melt index 0.2

d = density

TABLE 2

CODE NO.	MATERIALS	TOTAL FLUX (10^{16} ELECTRONS PER CM^2)
12	POLYMETHYL METHACRYLATE	1.22
13	ACETAL RESIN	1.22
14	ACETAL RESIN	1.22
15	POLYTETRAFLUOROETHYLENE	1.22
16	POLYFLUOROETHYLENEPROPYLENE	3.67
17	POLYCHLOROTRIFLUOROETHYLENE	3.67
18	POLYVINYL CHLORIDE	3.67
19	POLYVINYLIDENE FLUORIDE	3.67
21	ALLYL CARBONATE PLASTIC	4.10
22	POLYVINYL CHLORIDE	4.10
23	POLYMETHYL METHACRYLATE	4.10
24	RUBBER MODIFIED ACRYLIC PLASTIC	5.80
34	STYRENE ACRYLIC COPOLYMER	2.90
35	CELLULOSE ACETATE	5.80
36	CELLULOSE PROPIONATE	4.10
37	CELLULOSE BUTYRATE	4.10
38	CHLORINATED POLYETHER	2.90
39	POLYCARBONATE	5.80
43	POLYVINYL FLUORIDE	5.80

TABLE 3

SHORE HARDNESS

	CODE NO.	INITIAL	IRRADIATED	% CHANGE
POLYETHYLENES	2	67	64	-4
	3	55	55	0
	4	71	69	-3
	5	50	70	+40
	6	68	62	-9
	45	53	62	+17
POLYPROPYLENES	7	100	74	-26
	8	100	73	-27
STYRENE POLYMERS	1	87	86	-1
	20	73	86	+18
	25	87	87	0
	26	78	88	+13
	31	86	88	+2
POLYAMIDES	9	79	86	+9
	10	77	83	+8
	11	74	86	+16
DIALLYL-PHTHALATES	27	92	95	+3
	28	91	93	+2
PHENOL PLASTICS	29	92	93	+1
	30	93	94	+1
EPOXY	32	91	93	+2
ALKYD	33	94	95	+1
PVC ACETATE	40	78	76	-3
POLYETHYLENE TEREPHTHALATES	41	81	NA	
	44	84	NA	
POLYURETHANE	42	43	72	+67

TABLE 4

STIFFNESS IN FLEXURE (PSI X 10^3)

	CODE NO.	INITIAL	IRRADIATED	% CHANGE
POLYETHYLENES	2	102	38	−63
	3	26	18	−31
	4	158	67	−58
	5	25	21	−16
	6	109	87	−20
	45	26.6	29.3	+10
POLYPROPYLENES	7	155	NA	
	8	110	NA	
STYRENE POLYMERS	1	335	291	−13
	20	146	291	+99
	25	405	384	− 5
	26	258	365	+49
	31	323	321	0
POLYAMIDES	9	156	241	+54
	10	138	210	+52
	11	107	310	+181
DIALLYL-PHTHALATES	27	889	885	0
	28	516	535	+ 4
PHENOL PLASTICS	29	758	727	− 4
	30	1369	1266	− 8
EPOXY	32	592	614	+ 4
ALKYD	33	1201	1206	0
PVC ACETATE	40	437	308	−30
POLYETHYLENE TEREPHTHALATES	41	979	814	−17
	44	1033	686	−34
POLYURETHANE	42	7.0	19.3	+176

TABLE 5

TENSILE STRENGTH AT BREAK (PSI X 10^3)

	CODE NO.	INITIAL	IRRADIATED	% CHANGE
POLYETHYLENES	2	3.0	1.7	-43
	3	2.0	1.1	-45
	4	3.8	4.1	+ 8
	5	1.4	1.0	-29
	6	1.9	2.1	+11
	45	2.3	1.2	-48
POLYPROPYLENES	7	2.6	0.1	-96
	8	3.0	0.2	-93
STYRENE POLYMERS	1	8.0	4.0	-50
	20	1.7	1.1	-35
	25	8.7	5.7	-34
	26	4.3	1.8	-58
	31	7.5	8.6	+15
POLYAMIDES	9	6.5	11.7	+80
	10	6.3	9.4	+49
	11	5.7	11.8	+107
DIALLYL-PHTHALATES	27	5.2	NA	
	28	4.5	9.2	+104
PHENOL PLASTICS	29	4.3	4.6	+ 7
	30	4.2	5.8	+38
EPOXY	32	3.6	3.9	+ 8
ALKYD	33	5.2	6.8	+31
PVC ACETATE	40	7.0	7.3	+ 4
POLYETHYLENE TEREPHTHALATES	41	22.5	NA	
	44	22.4	NA	
POLYURETHANE	42	6.8	2.8	-59

TABLE 6

ULTIMATE ELONGATION (PER CENT)

	CODE NO.	INITIAL	IRRADIATED	% CHANGE
POLYETHYLENES	2	665	10	-98
	3	797	8	-99
	4	1365	14	-99
	5	1110	9	-99
	6	430	13	-97
	45	1125	9	-99
POLYPROPYLENES	7	330	43	-87
	8	1470	59	-96
STYRENE POLYMERS	1	4.2	2.3	-45
	20	25	2	-92
	25	5.5	2.9	-47
	26	24	1.6	-93
	31	6.5	6.9	+6
POLYAMIDES	9	616	33	-95
	10	100	23	-77
	11	520	43	-92
DIALLYL-PHTHALATES	27	2	NA	
	28	2.3	4.5	+96
PHENOL PLASTICS	29	1.7	1.7	0
	30	1.3	1.7	+31
EPOXY	32	1.8	1.7	-6
ALKYD	33	2	1.8	-10
PVC ACETATE	40	98	11	-89
POLYETHYLENE TEREPHTHALATES	41	103	NA	
	44	100	NA	
POLYURETHANE	42	1135	13	-99

FIG. 1

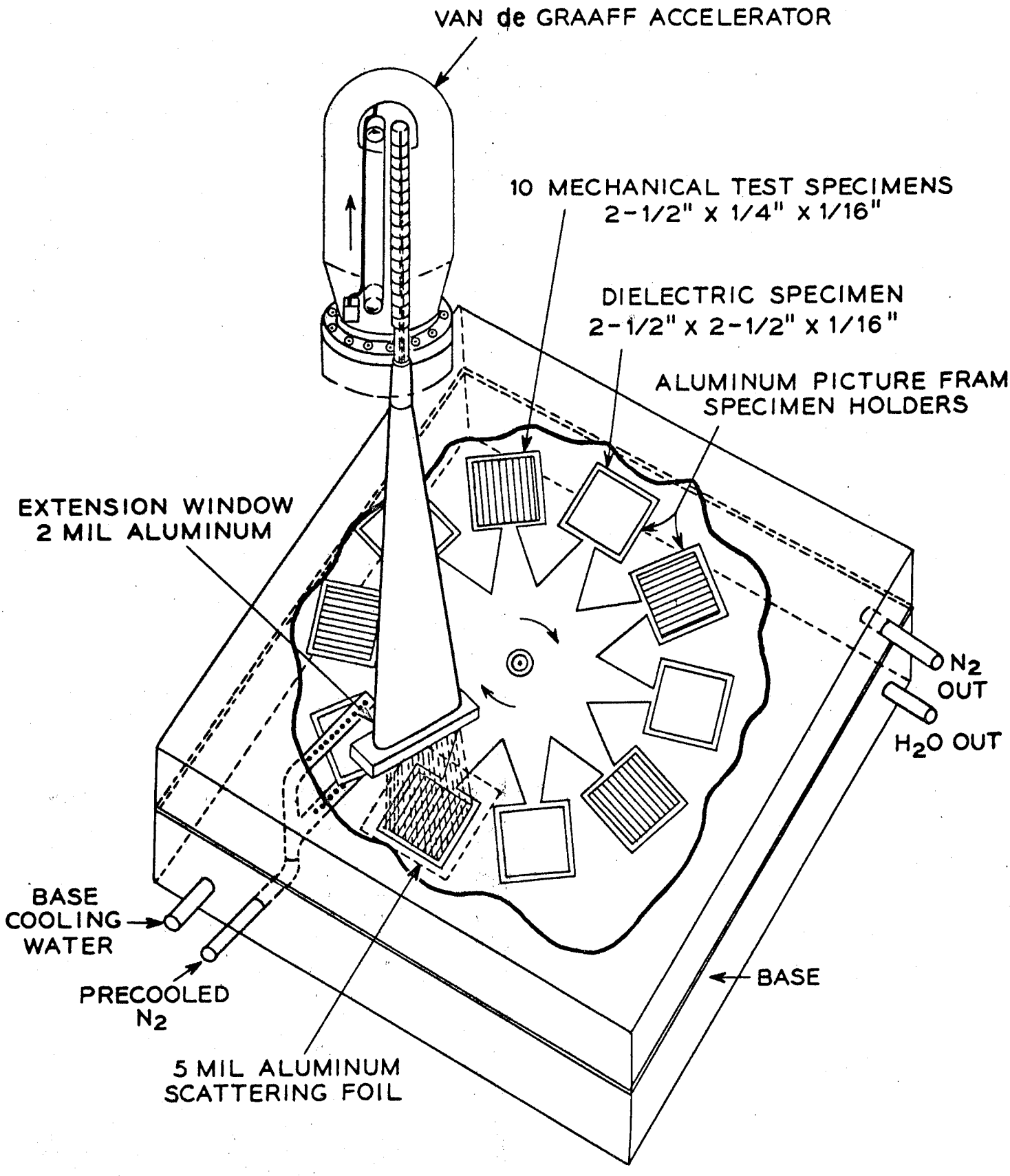
VAN de GRAAFF ACCELERATOR
10 MECHANICAL TEST SPECIMENS
2-1/2" x 1/4" x 1/16"
DIELECTRIC SPECIMEN
2-1/2" x 2-1/2" x 1/16"
ALUMINUM PICTURE FRAME
SPECIMEN HOLDERS
EXTENSION WINDOW
2 MIL ALUMINUM
N_2
OUT
H_2O OUT
BASE
COOLING
WATER
PRECOOLED
N_2
BASE
5 MIL ALUMINUM
SCATTERING FOIL

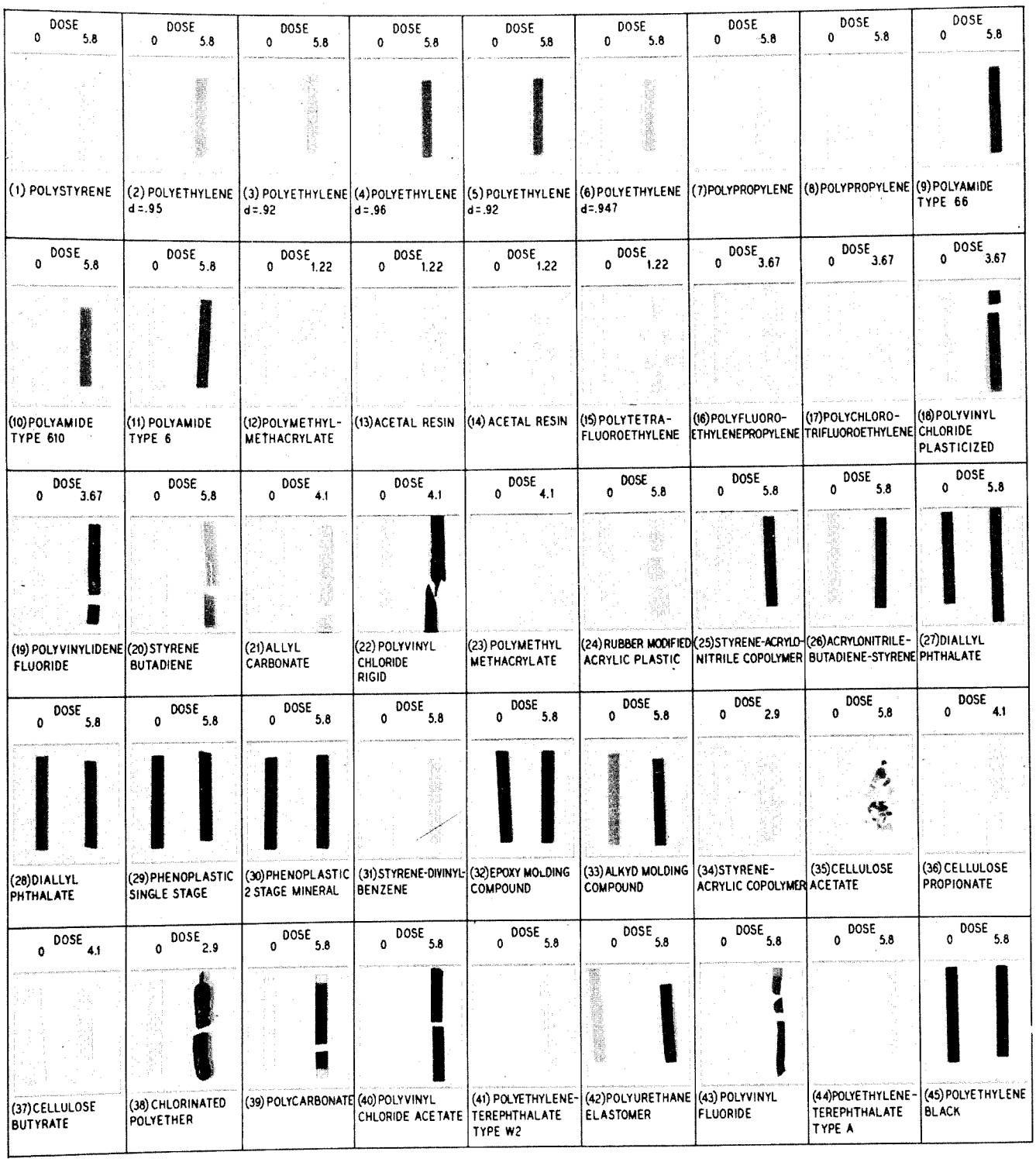

DOSE = $\times 10^{16}$ ELECTRONS/SQ. CM.

Figure 2

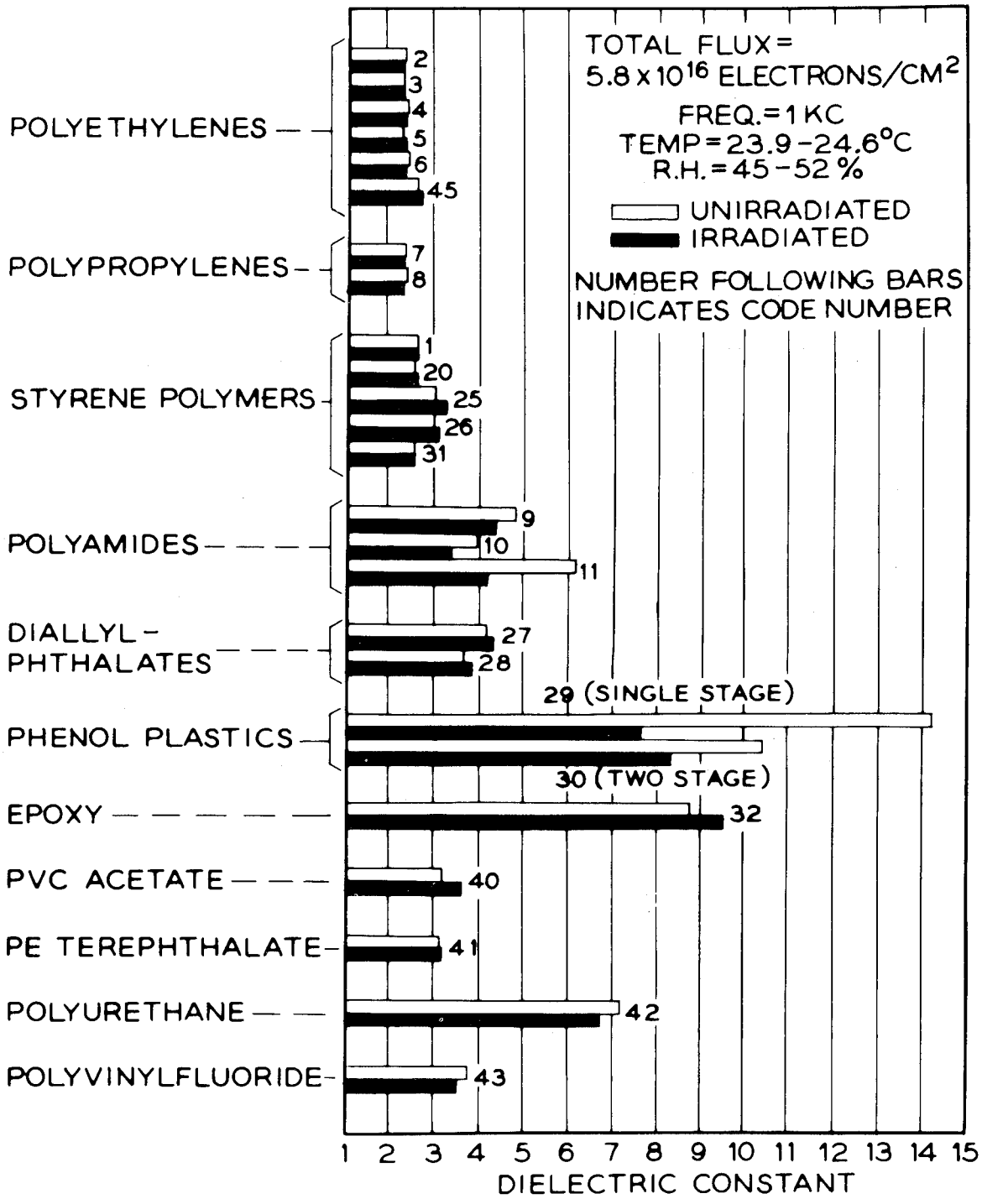
TOTAL FLUX=
5.8 x 10^16 ELECTRONS/CM^2
FREQ.=1 KC
TEMP=23.9-24.6°C
R.H.=45-52 %
UNIRRADIATED
IRRADIATED
NUMBER FOLLOWING BARS
INDICATES CODE NUMBER
POLYETHYLENES
POLYPROPYLENES
STYRENE POLYMERS
POLYAMIDES
DIALLYL-
PHTHALATES
PHENOL PLASTICS
EPOXY
PVC ACETATE
PE TEREPHTHALATE
POLYURETHANE
POLYVINYLFLUORIDE
2
3
4
5
6
45
7
8
1
20
25
26
31
9
10
11
27
28
29 (SINGLE STAGE)
30 (TWO STAGE)
32
40
41
42
43
1 2 3 4 5 6 7 8 9 10 11 12 13 14 15
DIELECTRIC CONSTANT

Figure 3

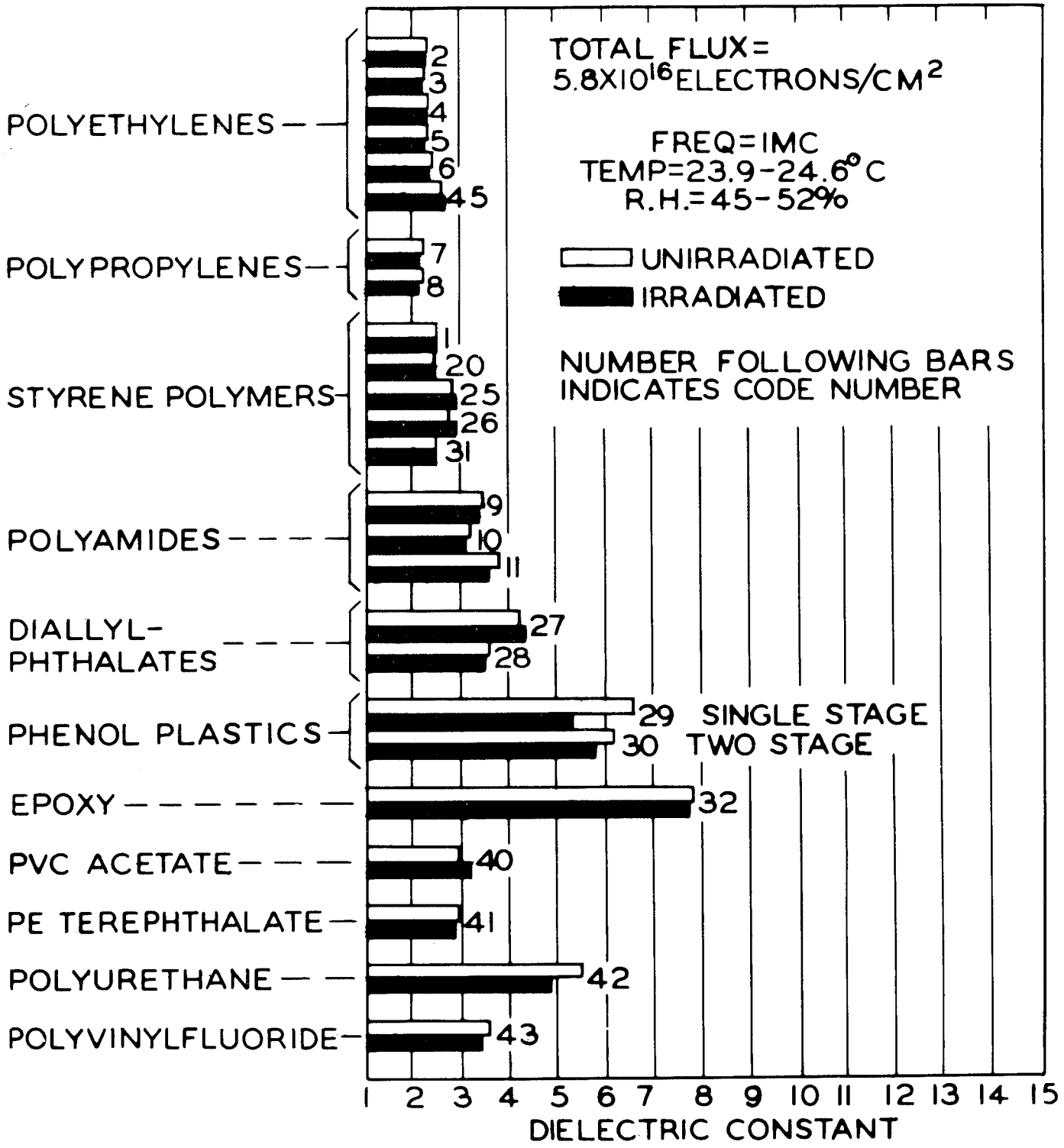
TOTAL FLUX=
5.8X10^16 ELECTRONS/CM^2
FREQ=IMC
TEMP=23.9-24.6°C
R.H.=45-52%
UNIRRADIATED
IRRADIATED
NUMBER FOLLOWING BARS
INDICATES CODE NUMBER
POLYETHYLENES
POLYPROPYLENES
STYRENE POLYMERS
POLYAMIDES
DIALLYL-
PHTHALATES
PHENOL PLASTICS
EPOXY
PVC ACETATE
PE TEREPHTHALATE
POLYURETHANE
POLYVINYLFLUORIDE
2
3
4
5
6
45
7
8
1
20
25
26
31
9
10
11
27
28
29 SINGLE STAGE
30 TWO STAGE
32
40
41
42
43
1 2 3 4 5 6 7 8 9 10 11 12 13 14 15
DIELECTRIC CONSTANT

Figure 4

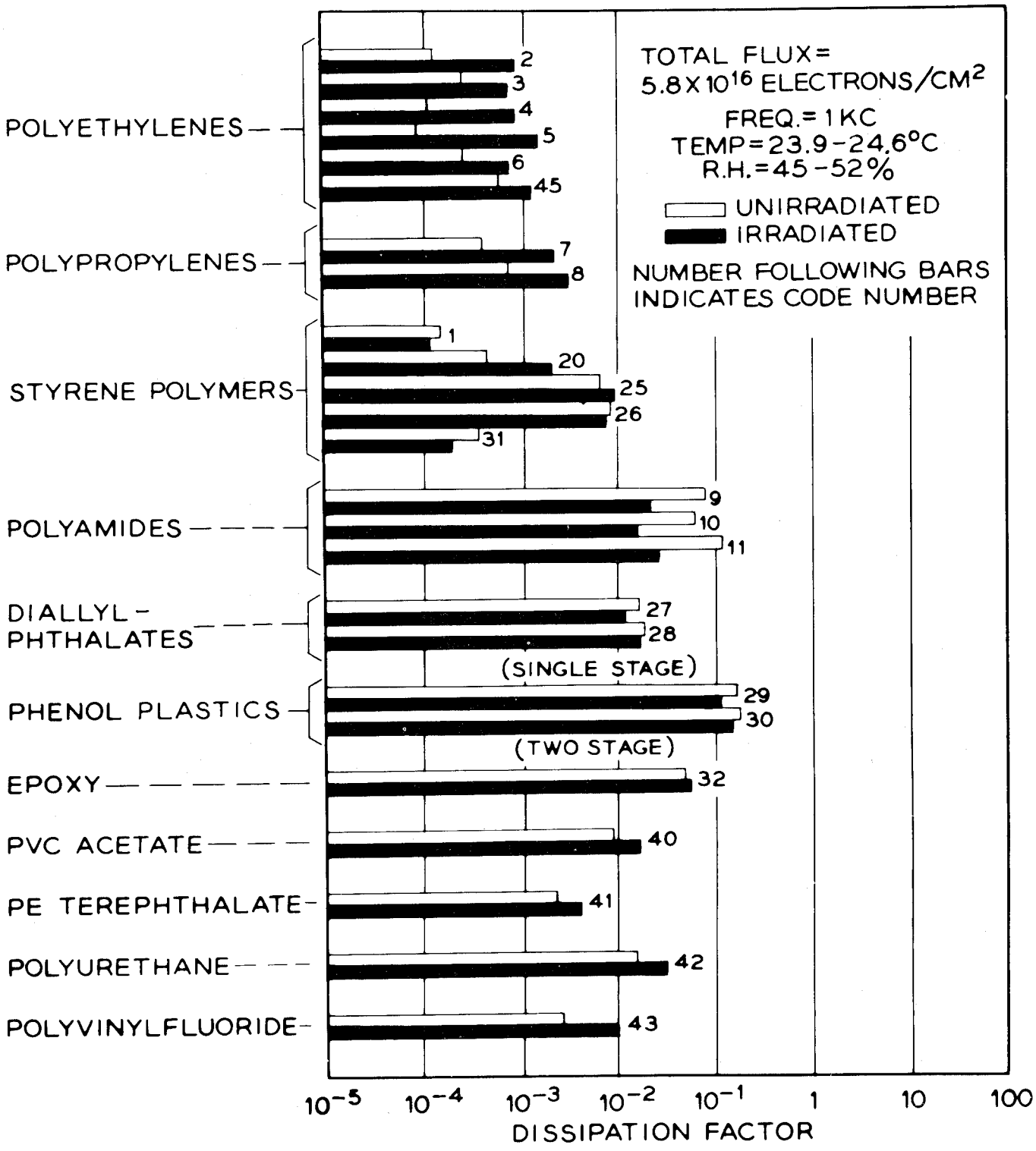
TOTAL FLUX=
5.8X10^16 ELECTRONS/CM^2
FREQ.=1KC
TEMP=23.9-24.6°C
R.H.=45-52%
UNIRRADIATED
IRRADIATED
NUMBER FOLLOWING BARS
INDICATES CODE NUMBER
POLYETHYLENES
POLYPROPYLENES
STYRENE POLYMERS
POLYAMIDES
DIALLYL-
PHTHALATES
(SINGLE STAGE)
PHENOL PLASTICS
(TWO STAGE)
EPOXY
PVC ACETATE
PE TEREPHTHALATE
POLYURETHANE
POLYVINYLFLUORIDE
2
3
4
5
6
45
7
8
1
20
25
26
31
9
10
11
27
28
29
30
32
40
41
42
43
10^-5
10^-4
10^-3
10^-2
10^-1
1
10
100
DISSIPATION FACTOR

Figure 5

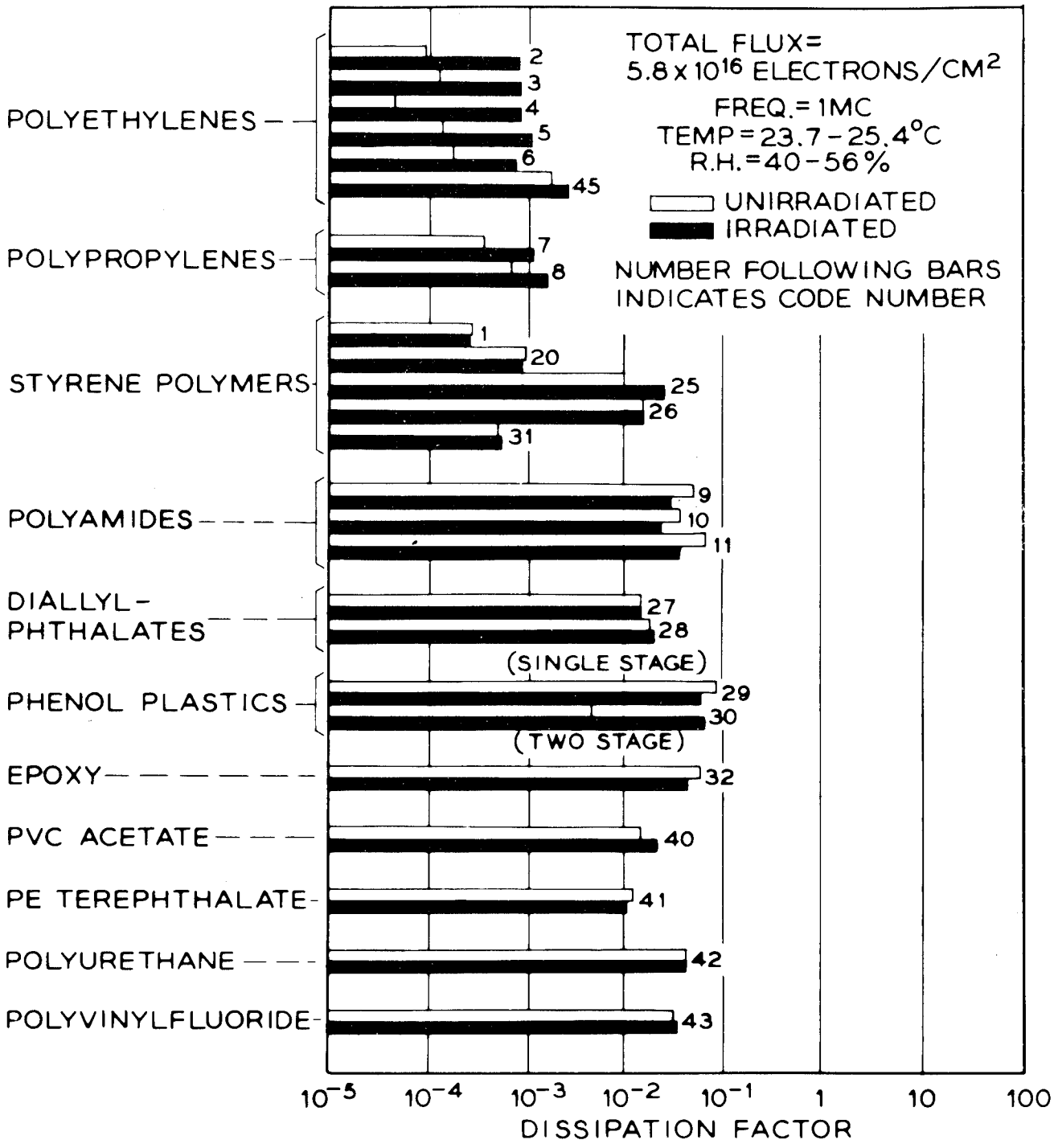
TOTAL FLUX=
5.8 x 10^16 ELECTRONS/CM^2
FREQ.= 1MC
TEMP = 23.7 - 25.4°C
R.H. = 40 - 56 %
UNIRRADIATED
IRRADIATED
NUMBER FOLLOWING BARS
INDICATES CODE NUMBER
POLYETHYLENES
POLYPROPYLENES
STYRENE POLYMERS
POLYAMIDES
DIALLYL-
PHTHALATES
(SINGLE STAGE)
PHENOL PLASTICS
(TWO STAGE)
EPOXY
PVC ACETATE
PE TEREPHTHALATE
POLYURETHANE
POLYVINYLFLUORIDE
2
3
4
5
6
45
7
8
1
20
25
26
31
9
10
11
27
28
29
30
32
40
41
42
43
10^-5
10^-4
10^-3
10^-2
10^-1
1
10
100
DISSIPATION FACTOR

Figure 6

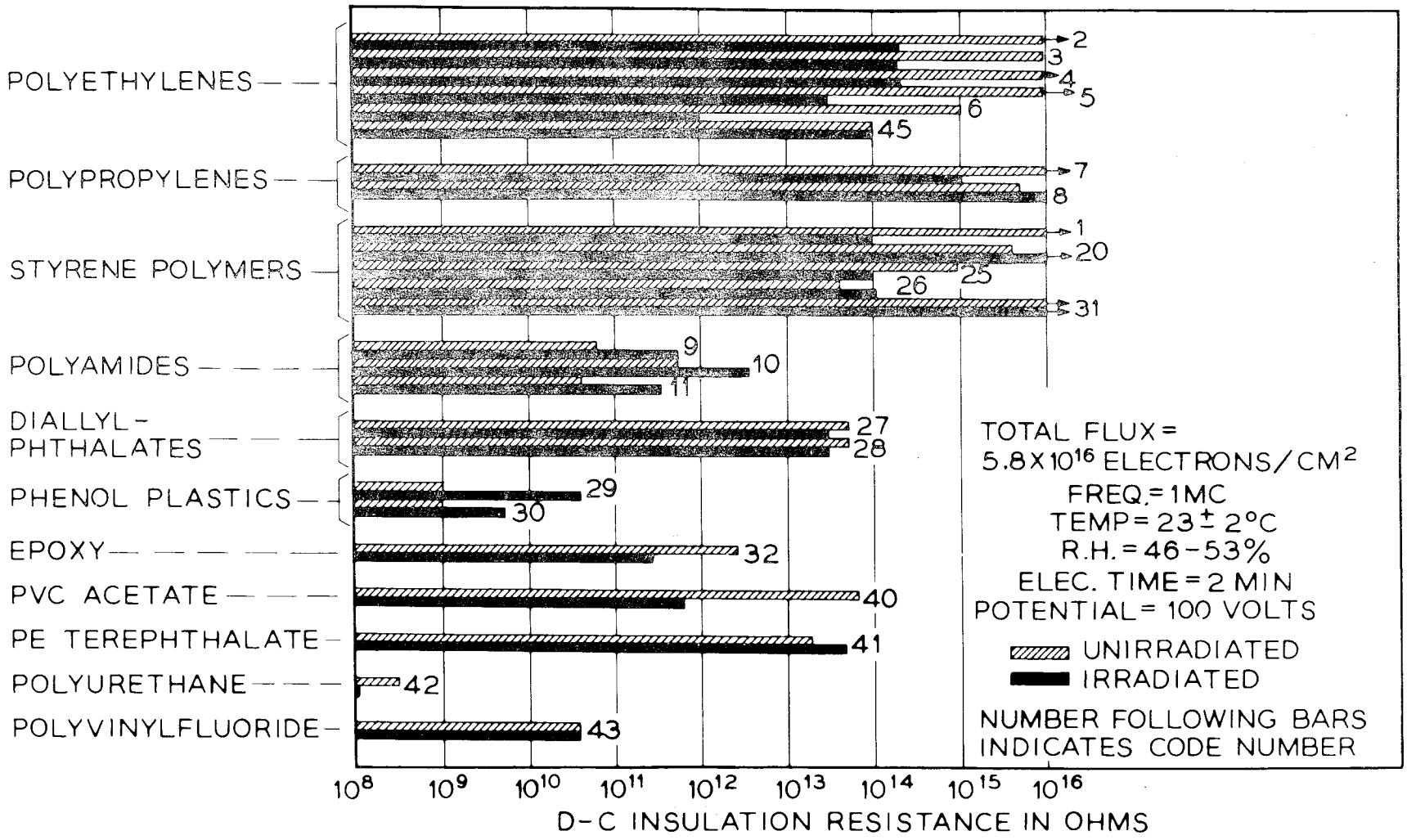

Figure 7

CLM 27725

RADIATION INDUCED CONDUCTIVITY IN DIELECTRIC MATERIALS

by

A. W. Snyder
Sandia Corporation
Albuquerque, New Mexico

The paper presented by Dr. Snyder was not made available for this booklet. However, the data and information in his paper relating to induced conductivity at various levels of gamma and neutron radiation flux are all contained in the following published papers:

1. Gamma Ray Induced Conductivity in Insulating Materials - S. E. Harrison, F. N. Coppage, A. W. Snyder - Paper No. CPA 63-5156 IEEE (Electronuclear Conference, Richland, Washington, May 1, 1963).

2. Neutron Effectiveness in Producing Photoconductivity in Organic Insulating Materials - F. N. Coppage, A. W. Snyder, F. C. Peterson - Paper: SCR 670* (Sandia Corporation Report).

3. Gamma Ray Photoconductivity Decay in Organic Dielectric Materials - S. E. Harrison - Paper: SCR 671* (Sandia Corporation Report).

Dr. Snyder indicated in his paper the levels of induced conductivity to be expected from the radiation fluxes present in outer space, particularly in the Van Allen belts. Those flux levels are indicated by the summary of Dr. Sun contained in this booklet.

---

*Available through the AEC Technical Information Service.

THE EFFECTS OF HIGH ENERGY RADIATION ON THE POLARIZATION CURRENTS IN SOME GLASSES

R. A. Weeks and E. Lell[1]

Solid State Division, Oak Ridge National Laboratory*
Oak Ridge, Tennessee

Insulators which have been electrostatically charged have been observed to discharge, leaving in the insulator visible tracks along which the discharge took place.[2] The electrostatic charging can be induced on the surface or in the bulk of an insulator by electron or gamma-ray irradiation.[3,4] Since these discharges have been observed in some glasses and not in others, there is some interest in the process by which charge and energy, supplied during irradiation, were stored in such insulators. Glasses with a high ($\sim 10^{19}$ ohm-cm) and some with low ($\sim 10^{17}$ ohm-cm) intrinsic resistivity exhibit the discharge effect when irradiated with electrons. Since the discharge effect involves electrical processes, it seemed reasonable to investigate the D. C. electrical properties of the glasses of interest. The available data[2,5,6] on the effect indicated that the decay time for its disappearance was quite long, and thus our interest was directed to a study of the low-frequency and dc conductivity of several glasses.

In Figure 1 the loss tangent (ac conductivity) of a lead silicate glass is shown as a function of frequency and time after electron irradiation.

---

* Oak Ridge National Laboratory is operated by Union Carbide Corporation for the United States Atomic Energy Commission.

There are two features of these measurements that should be noted: (1) there is maximum in the loss tangent at some frequency below 50 cps, and (2) at least the high-frequency tail of this maximum disappears in a time of the order of 24 hr. It has also been observed that two glasses, exhibiting the discharge effect, also show the greatest increase in the loss tangent at 50 cps. Since this increase disappears in 24 hr, and the discharge effect can be observed after a time $\gg$ 200 hr, the two phenomena are probably not directly related.

The polarization, P, is defined as the electric dipole moment per unit volume and is given by the relation

$$P = D - \epsilon_o E \tag{1}$$

where D is the displacement field, E is the laboratory field, and ϵ_o is the dielectric constant. The current for a constant laboratory field is $J = \partial D/\partial t$ and from Eq. (1), $-J = \partial P/\partial t$.

The polarization P' at a microscopic point in the material being polarized can also be written

$$P' = N \alpha E' \tag{2}$$

where N is the number of polarizable units, α is the polarizability, and E' is the local field acting on the polarizable units. Thus, the current due to these units is

$$J' = \frac{\partial}{\partial t} (N \alpha E') \, . \tag{3}$$

The polarizing entities have been represented by only one term in Eq. (3), but in a real material, it is certainly probable that several such terms may be required. Therefore, a better approximation would be to write the polarizability term as a summation, e.g., $\alpha = \sum N_i \alpha_i$.

One of the terms in this summation originates from space charge effects. The space charge term is due to an accumulation of charges at the electrodes, and also at internal surfaces. With respect to the glasses the experimental results shown in Figure 2 and other results indicate that there is probably no electrode space charge term. Considering the known properties of glass, it also appears reasonable to eliminate a space charge term on internal surfaces. With the elimination of the space charge terms, only the dipole and orientation terms are left, and Equation (3) can be written

$$J' = \left(E + E'(t)\right) \frac{\partial}{\partial t}\left[\sum_{i=1}^{n} N_i \alpha_i\right] + \left[\sum_{i=1}^{n} N_i \alpha_i\right] \frac{\partial E'(t)}{\partial t} \quad . \qquad (4)$$

The relation between the observed current and the current at a microscopic point must now be considered, and there are several experimental facts, which have a bearing on this problem. These experimental results are: (1) The observed currents are proportional to applied voltage for voltages > 3900 V cm^{-1} or for duration of applied voltages for times ≥ 120 minutes. (2) The observed polarization currents and final conductivity (at times > 30 hours) are inversely proportional to the thickness of specimen. (3) The principle of superposition is obeyed. On the basis of these facts, it is assumed that the observed current and the sum of microscopic currents are identical, i.e., $J = J'$.

An analysis of the decay of the current through the specimens, the polarization current, showed that it could be reasonably fitted to a function of the form

$$i = \sum_{i=1}^{K} a_i e^{-t/\tau_i} + bi_o,$$

where a_i is a constant appropriate to the characteristic time τ_i, b is a constant for a particular glass, and i_o is the current observed after a time long compared with the longest τ_i and is presumed to be the intrinsic conductivity. In Figure 3 a decay curve is shown of a lead silicate glass which had been given a Co^{60} gamma-ray dose of 10^6 r. An analysis of the curve gave four characteristic times. The numbers in parentheses are the values of the a_i's which are the intercepts at t = 0.

In Table I the τ_i's found by this analysis are shown for two specimens subjected to gamma-ray irradiation and measured at about 25°C and at two higher temperatures. The average values of the τ_i's are given for the unirradiated and irradiated conditions and the rms deviation calculated. At the elevated temperatures the τ_i's exhibit a decrease that is larger than this rms deviation.

Although the τ_i's showed only small changes with these treatments, the a_i's and the intrinsic conductivity bi_o exhibited larger variations.

The experimental observations, which have been reported, have been fitted to a sum of exponential terms. The number of such terms required to fit the data are four plus a constant term, and the characteristic times of these four terms are not altered by irradiation. These four terms may be related to the dipole and orientation polarizability terms. Although it is not possible from these data to distinguish the terms, the summation terms in Eq. (4) may be reduced to four terms. Since these data showed that only the strengths of the terms were altered by irradiation, and that the polarizability terms, as defined by the characteristic times, were constant, Eq. (4) becomes

$$J = \left[E + E'(t)\right] \left\{ \alpha_1 \frac{\partial N_1}{\partial t} + \alpha_2 \frac{\partial N_2}{\partial t} + \alpha_3 \frac{\partial N_3}{\partial t} + \alpha_4 \frac{\partial N_4}{\partial t} \right\} \quad (5)$$

This equation has an implied assumption in it, i.e. $\frac{\partial E'(t)}{\partial t}$ is small relative to the $\frac{\partial Ni}{\partial t}$ terms.

It has been noted that the polarization currents observed in the lead of the ohmic character of the polarization current is shown in Figure 2. In these measurements the polarization currents were obtained as a function of voltage. A given voltage was applied for a period of ~125 minutes, and the specimen was then depolarized completely before the next voltage was applied. The data points were obtained for varying periods of time after the application of the voltage. For the shorter periods of time (10 minutes and 20 minutes) the current is not a linear function of voltage below ~4000 V cm^{-1}. At 120 minutes after application of the voltage the current is approximately proportional to voltage for both of the glasses shown in Figure 2. Although not shown, observations on a pure silica glass have indicated a linear relation between current and voltage from 10 minutes to 120 minutes. It is evident that above 4000 V cm^{-1} the polarization current is proportional to the applied voltage in the glasses which have been investigated.

The strengths of the four polarization processes were observed to vary with γ-ray dose. This effect is shown in Figures 4 and 5. In Figure 4 the polarization currents at two times after application of a voltage (3900 V cm^{-1}) are shown as a function of Co^{60} γ-ray dose. The peak in the enhancement of the strength of the polarization current by irradiation is clearly evident in both curves. There are differences between the two curves, which indicate that those processes with large characteristic times are primarily effected by the irradiation. This is evident in the ratio

between the peak value and initial value for the 10 minutes curve (~3) and that for 120 minutes curve (~5.6) and also in the ratios of peak value to the value at maximum dose (1.3 for the 10 minutes curve and 1.7 for the 120 minutes curve). There are also some differences in the shapes of the curves.

In Figure 5 the polarization currents as a function of duration of applied voltage are shown for various Co^{60} γ-ray doses. The odd numbered curves were obtained 24 hours after irradiation and the even numbered curves were measured immediately after irradiation. A comparison of curve XIII and XV with curve VII shows that the largest changes in the polarization occur in those processes with the longest characteristic times.

The even-numbered curves in Figure 5, taken immediately after irradiation, show that there is an enhancement of the polarization, which disappears in 24 hours. This enhancement is apparently independent of γ-ray dose for doses greater than 10 minutes. It may also be independent of dose for those of shorter duration, but experimental evidence is lacking. An investigation of the decay of this short lifetime enhancement has indicated that at least two processes may be involved.

Discussion

Taylor has shown[7] that the increase in the loss tangent at low frequencies (Figure 1, curve for the unexposed case) is due to a distribution of relaxation times for sodium ion diffusion. The increase that we observed after irradiation may have been due to the same mechanism. The increase in the loss tangent resulting from irradiation could be caused by a change in this distribution. However, Taylor's results showed that there was no change in the distribution with heating, and our τ_i's derived from the dc

measurements showed very little, if any, change with irradiation. It would be questionable on the basis of these results to relate the increase in loss tangent to a change in the distribution of relaxation times for ion diffusion. It is possible that irradiation displaces ions from deep traps and that while they are removed from the traps they can contribute to the ion diffusion and are observed as an increase in the loss tangent. Over a period of time these ions would be retrapped, thereby producing the observed decay in the irradiation-enchanced loss tangent. Since the irradiation can also generate electrons and holes, these can alter the ionization states of such traps, and a fraction of the ions released by the irradiation would not be retrapped.

The hypothesis that the time-dependent decay of the current through the specimen can be expressed as a sum of exponentials in time is based on the following facts:

1. The principle of superposition is obeyed. The observed decay curves can be resolved into linear sections which extend over one or more decades of current. The τ_i's for several measurements under a variety of conditions have an rms deviation that is less than $\pm$ 9% for τ_2 and less than $\pm$ 6% for the other three τ's. These rms deviations indicate a reasonable agreement between the hypothesis of superposition and the observed curve. Other functions have not been analyzed, and it is possible that with four adjustable parameters a different function could be found which would fit the observed curve.

2. Ohm's law is apparently applicable for the conditions of our experiment.

3. The final conductivity over a limited range of temperatures. This deviation could result from two independent processes.

4. The polarization currents found in other experiments on glasses[7,8] and in other materials[9,10] exhibit an exponential time dependence. The

fundamental assumption in these experiments is that there is a periodic array of potential wells in which charge carriers are trapped. In the absence of a field, these charge carriers and the associated charges of the structure creating the potential wells have a net dipole moment of zero. The application of an electric field changes the relative depth of the wells along the field direction, and these are perferentially filled by charge-carrier diffusion. The intrinsic conductivity of the glasses is due to such a process.[7,9,11] Another process closely related to this one and which exhibits an exponential dependence on time is the reorientation of dipoles already present in the system. In this case neither charge component of the dipole diffuses away from the other, and there are several orientations possible, with each separated by a potential barrier. The τ's that we have found may be the relaxation of such a process.

One apparent contradiction between the experimental results and this hypothesis is that a thermal activation energy of $\sim$1 ev should be observed. In the temperature range over which measurements have been made (Table I), the τ's appear to be temperature independent as compared with the intrinsic conductivity. The polarization process characterized by the τ's may not be thermally activated in the temperature range which we have investigated.

Summary

The data do not support a space-charge hypothesis. There is agreement with the hypothesis that the polarization effects occur in the bulk of the glass.

The bulk polarization processes which have long, approximately temperature-independent relaxation times may furnish a mechanism by which charge and energy are stored. There does appear to be a correlation between large values of the τ's and the discharge effect.

REFERENCES

1. Guest scientist from Bausch and Lomb, Inc., Rochester, New York.
2. S. Whitehead, Dielectric Breakdown of Solids, p. 170, Oxford University Press, London, 1951.
3. B. Gross and P. V. Murphy, Nukleonik 2, 279 (1960).
4. Cover Picture of J. Appl. Phys. 32, (1961).
5. V. Cullen, in Proc. Hot Lab. Equip. Conf., 7th, Cleveland, 1959.
6. R. C. Hudson and R. A. Weeks, Solid State Div. Ann. Progr. Rept. August 31, 1961, ORNL-3213, p. 89.
7. H. Taylor, Trans. Faraday Soc. 52, 873 (1956).
8. R. J. Charles, J. Appl. Phys. 32, 1115 (1961).
9. R. W. Dreyfus, Phys. Rev. 121, 1675 (1961).
10. J. R. Freeman et al., Rev. Mod. Phys. 33, 553 (1961).
11. R. J. Maurer, Phys. Rev. 59, 691 (1941).

FIGURE CAPTIONS

Figure 1 Loss Tangent of a Lead Silicate Glass at Various Times After an Electron Irradiation with 1.5 μa of 1.5-Mev Electrons for 5 minutes. The temperature during irradiation was ~30°C and during measurement was 23°C.

Figure 2 Polarization Current Resolved into Four Processes, Each with a Characteristic Time. The specimen had been exposed to 10^6 r of Co^{60} gamma rays prior to the measurement. (The constant term bi_0 was first subtracted, leaving the linear portion labeled as τ_4, which was then subtracted from the remainder, giving the linear portion labeled τ_3, etc.).

Figure 3 The Polarization Current in a Lead Silicate Glass is Given as a Function of Voltage for Various Times after Application of the Polarizing Voltage. Before each increase in the voltage the specimen was depolarized by shorting the electrodes.

Figure 4 The Polarization Current in a Lead Silicate Glass at Various Times after Application of the Polarizing Voltage is Shown as a Function of Co^{60} γ-ray Dose. The specimen was depolarized between each irradiation.

Figure 5 The Polarization Current in a Lead Silicate Glass is Given for a Period of 120 minutes as a Function of Co^{60} γ-ray Dose. The even numbered curves were recorded immediately after irradiation and the odd numbered curves were recorded 24 hours later. The specimen was depolarized after each measurement.

Table I The DC Polarization Relaxation Times of a Lead Silicate Glass

Treatment	τ_1	τ_2	τ_3	τ_4
Specimen III (unexposed)	3.1	13.8	62	366
One week		14.0[a]	62[a]	334[a]
Turned[b]	3.1	14.5	62	336
10^5 r Co^{60}	2.5	14.0	65	360
2×10^5 r	2.8	13.8	68	375
5×10^5 r	3.0	17.0	66	380
1×10^6 r	3.0	15.0	65.5	375
Specimen IV				
5×10^5 r Co^{60}	3.0	16.5	64	395
1×10^6 r	3.0	16.0	62.5	390
Average value	2.94 ± 0.20[c]	15.0 ± 1.4[c]	64.2 ± 2.0[c]	368 ± 20[c]
Specimen IV (unexposed)				
43°C	2.3	12.2	57.5	345
68°C	2.2	12.2	51.0	330

[a]Specimen III was removed from the specimen mount and stored in a dry atmosphere for one week. The recorder was not turned on soon enough to record τ_1.

[b]Specimen III was removed and then reinserted in about 10 minutes, reversed with respect to the applied voltage.

[c]The error is the rms deviation from the average value.

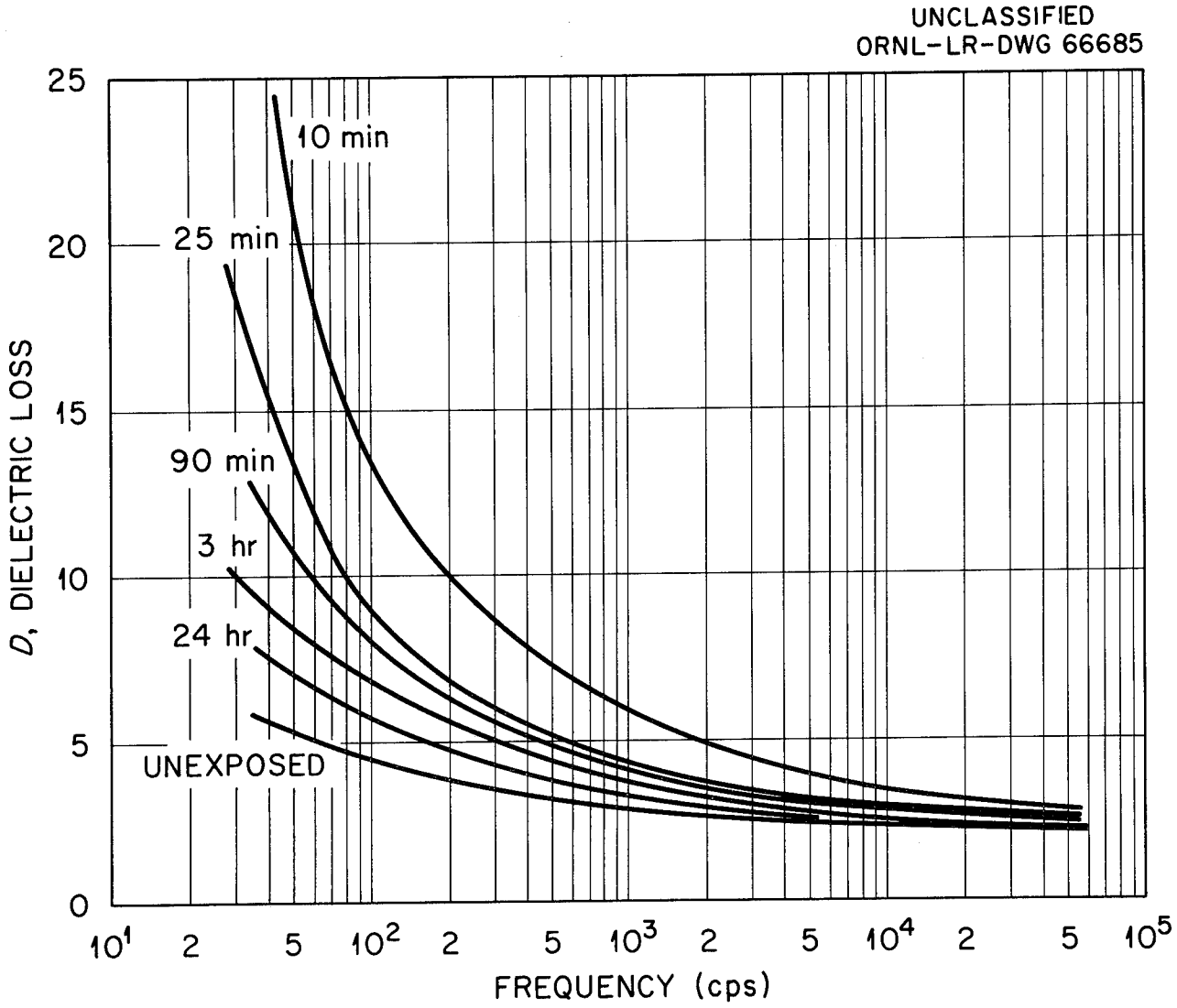

Electron Irradiation of Lead Silicate Glass.

Fig. 1

CLM 27861

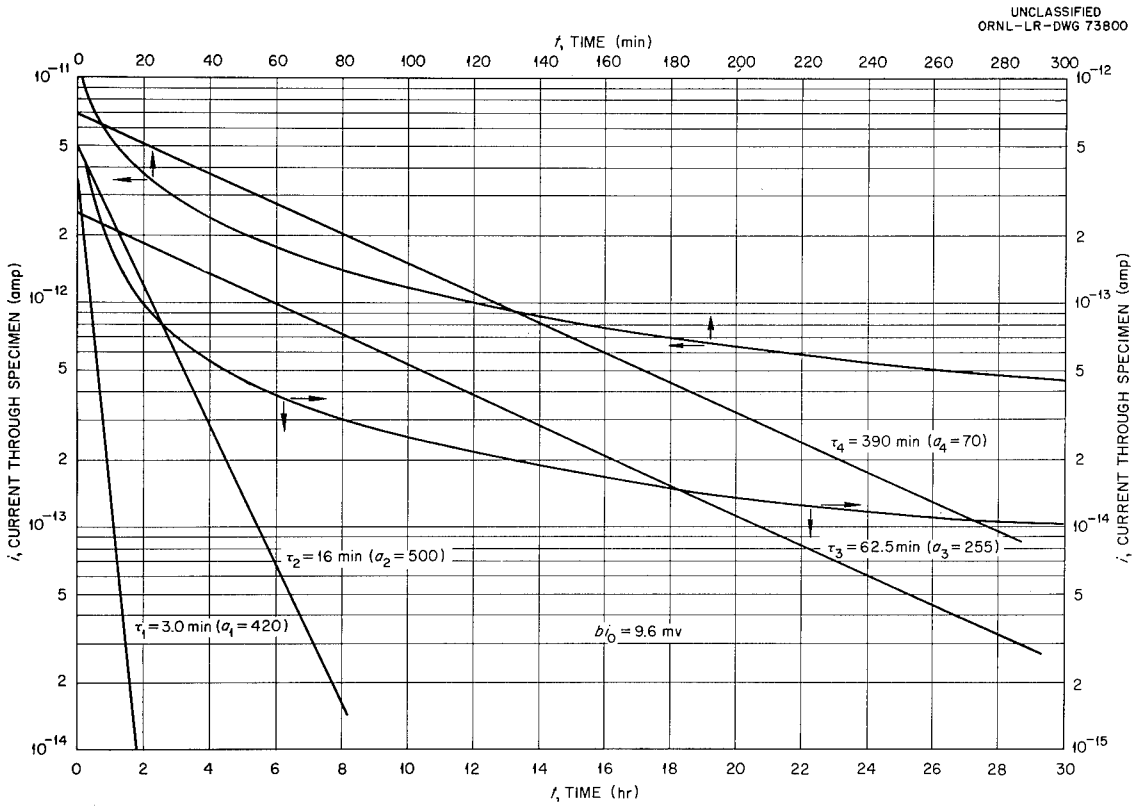
UNCLASSIFIED
ORNL-LR-DWG 73800
t, TIME (min)
0 20 40 60 80 100 120 140 160 180 200 220 240 260 280 300
i, CURRENT THROUGH SPECIMEN (amp)
10⁻¹¹ 5 2 10⁻¹² 5 2 10⁻¹³ 5 2 10⁻¹⁴
10⁻¹² 5 2 10⁻¹³ 5 2 10⁻¹⁴ 5 2 10⁻¹⁵
τ4 = 390 min (a4 = 70)
τ3 = 62.5 min (a3 = 255)
τ2 = 16 min (a2 = 500)
τ1 = 3.0 min (a1 = 420)
bi0 = 9.6 mv
0 2 4 6 8 10 12 14 16 18 20 22 24 26 28 30
t, TIME (hr)

Fig. 2

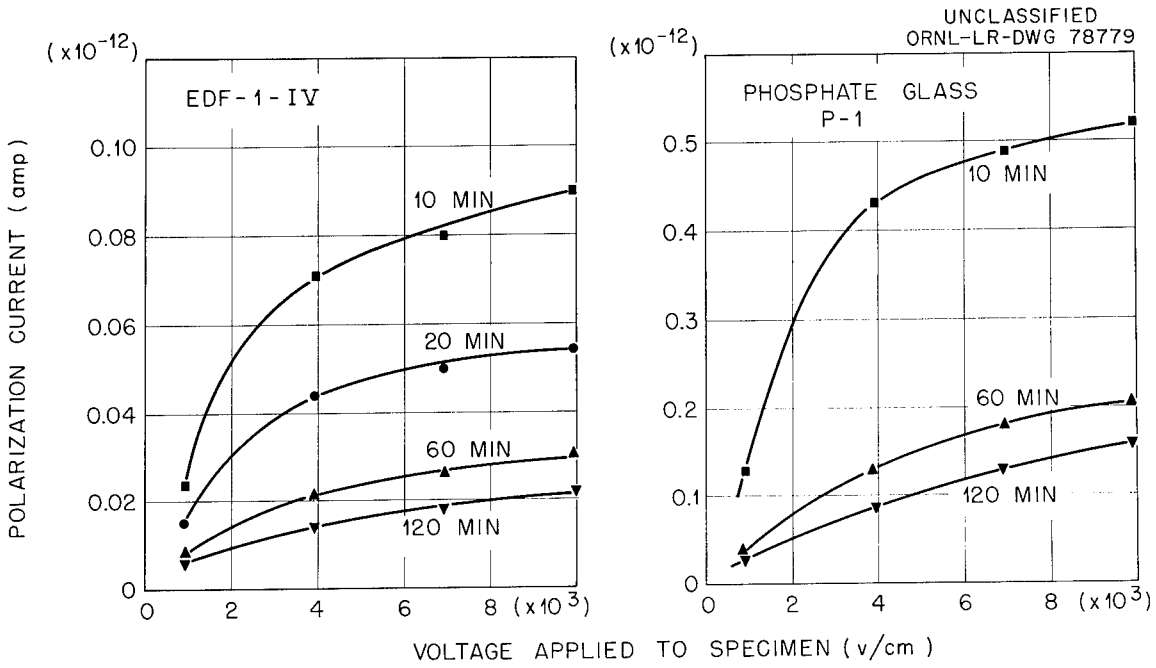

Polarization Current vs Applied Voltage.

Fig. 3

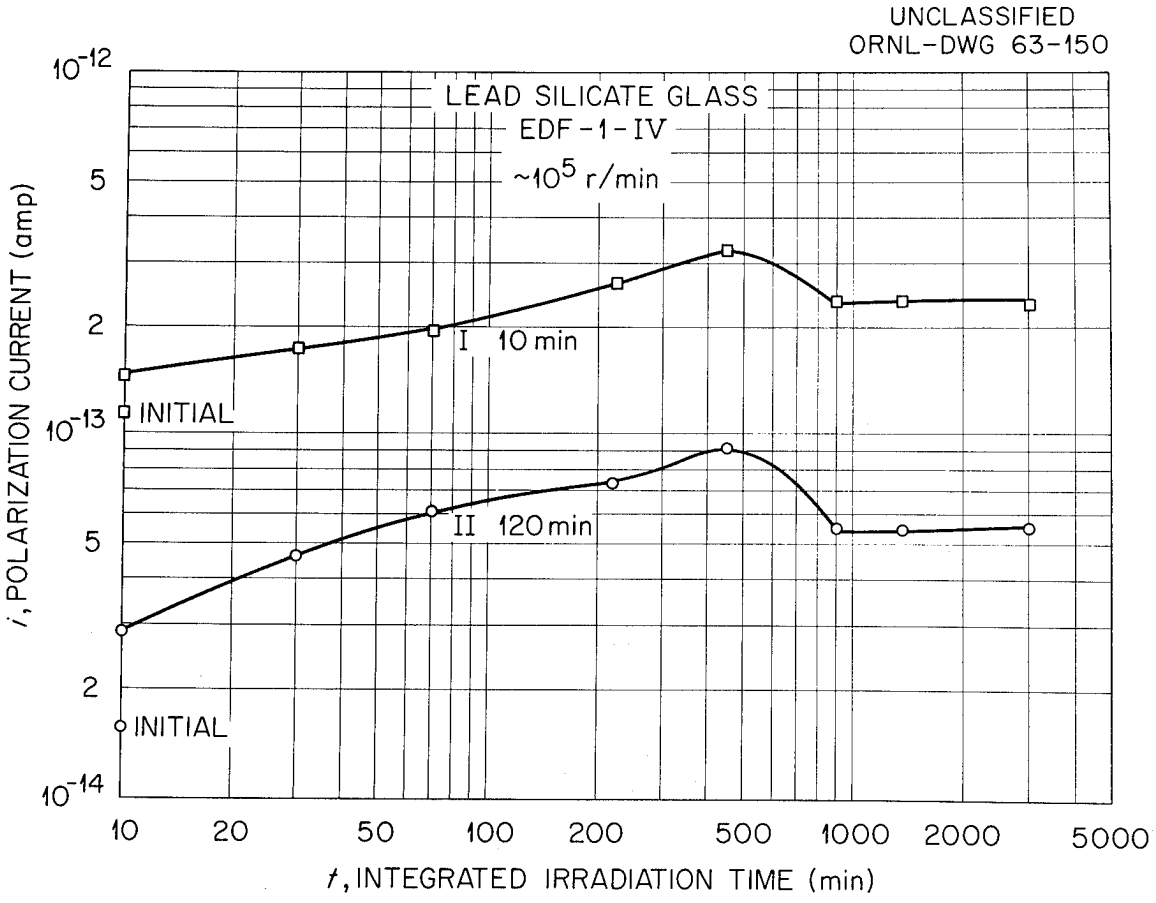

Fig. 4

CLM 27859

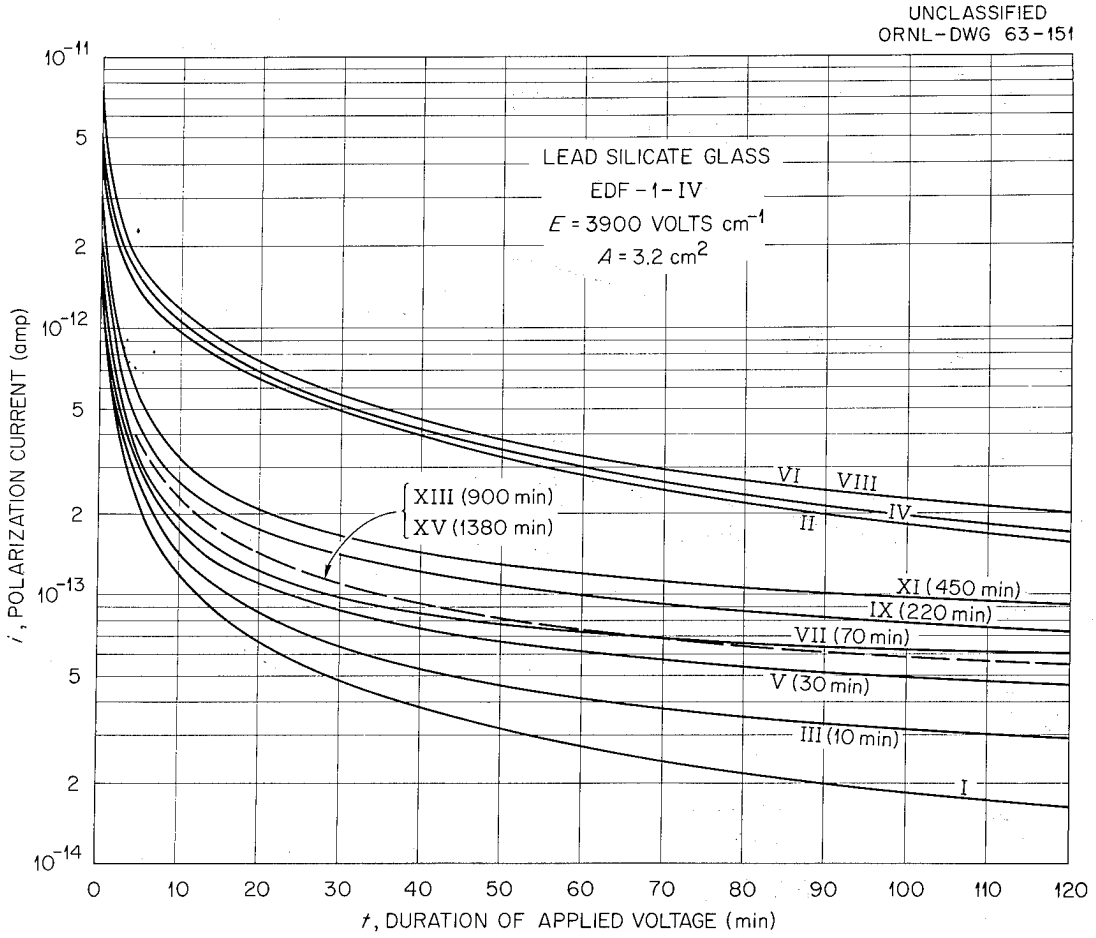
UNCLASSIFIED
ORNL-DWG 63-151
LEAD SILICATE GLASS
EDF-1-IV
E = 3900 VOLTS cm⁻¹
A = 3.2 cm²
VI
VIII
IV
II
XIII (900 min)
XV (1380 min)
XI (450 min)
IX (220 min)
VII (70 min)
V (30 min)
III (10 min)
I
i, POLARIZATION CURRENT (amp)
t, DURATION OF APPLIED VOLTAGE (min)
10⁻¹¹
5
2
10⁻¹²
5
2
10⁻¹³
5
2
10⁻¹⁴
0
10
20
30
40
50
60
70
80
90
100
110
120

Fig. 5

SPACE SIMULATION AND ITS EFFECTS ON MATERIALS

DIELECTRICS IN SPACE

SYMPOSIUM

WESTINGHOUSE RESEARCH LABORATORY

JUNE 25 - 26, 1963

G. R. BLAIR

HUGHES AIRCRAFT COMPANY

CULVER CITY, CALIFORNIA

INTRODUCTION

There are several areas of space study in which the Hughes Aircraft Company is deeply involved. It is not possible to encompass all the areas, and disciplines in one brief paper. Consequently, only four areas will be discussed. These are:

1) Thermal control surfaces
2) Elastomers
3) Optical materials

DISCUSSION

A very large portion of the HAC effort is devoted to the study of passive thermal control surfaces. These surfaces are characterized by two parameters, α_s and ϵ_{in}. Various parts of a space vehicle are exposed to the solar energy, in a greater or lesser extent, depending upon orbit, and axis orientation. If the vehicle is in the ecliptic plane, it will be alternately illuminated by the sun and eclipsed by the earth's shadow. Certain orbits make it possible for the vehicle to be exposed continuously to the solar rays. If the vehicle is spinning (spin stabilized) or fixed in its orientation, the surface will be completely exposed or one side will be continuously in shadow. The type of thermal control surface to be applied to the vehicle will be determined by the orientation. Thus, in a spin stabilized vehicle the α_s is as important as the ϵ_{in}. In a fixed vehicle, one side will require α_s data, and the shadow side will require only ϵ_{in} data. The range of values of α_s and/or ϵ_{in} will be determined by the function. For instance, the portion of the liquid hydrogen tank oriented toward the sun must reflect as much of the solar energy as possible. This requires a very low α_s .

To understand the terms α_s and ϵ_{in} the energy exchange must be considered. The fraction of the solar energy absorbed by a real body, in relation to an ideal black body is termed the solar absorptance and given the symbol α_s. This term is generally considered to cover the wavelength region 0.20μ to 2.7μ although the region of interest may be shifted to any preferred range. The region generally considered includes about 80% of the solar spectrum, which is the major radiative heat load imposed on space vehicles.

Two typical thermal control surface may appear equally white to the eye and have relatively low solar absorptances. However, one may have a lower α_s than the other because of a lower absorption in the ultraviolet region, or in the infrared region. Two such materials are exemplified by ZnO and HAC inorganic pigment. The ZnO has a very steep absorption edge (about 100% absorption) at about 3800Å, while the HAC pigment absorbs only 25% at the same wavelength.

The infrared emittance, ϵ_{in}, is defined as the ratio of energy emitted by by a real body to that of an ideal black body at the same temperature and in the same wavelength interval. The wavelength interval is generally taken as 1.5μ to 27μ, defined by the equipment limitations rather than for theoretical reasons. Some companies measure out to 35-40μ. A very useful, but fictitious, relation

is found in α_s/ϵ_{in} ratio. As it stands the ratio is thermodynamically meaningless, but it serves a useful practical purpose. The ratio could still be used, and yet be thermodynamically correct, if the α_s were written $\alpha_{0.2-2.7\mu}$ and the ϵ_{in} written as $\epsilon_{1.5-27\mu}$ By convention, among those active in the field of thermal control, the α_s and ϵ_{in} are used with the understanding of their true meaning. In essence, the α_s/ϵ_{in} ratio is a figure of merit, describing how well a surface acts as an energy tranducer, absorbing at one wavelength and emitting at some other. The values of α_s and ϵ_{in} are generally integrated from spectral data.

Even though the α_s/ϵ_{in} ratio may indicate a designers dream, the values are without use, if the surface alters by a change in absorptance. The change in α_s is brought about by absorption of the solar energy resulting in bond rupture, lattice displacement, color center formation, etc. It has been reasonably well established that the major degradation is brought about by the ultraviolet energy in the region of 2000Å to 4000Å. The damaging wavelength is dependent upon the selectivity of the material being irradiated and is controlled by the absorption edge. It becomes most important, therefore, to determine for each material, considered as a thermal control surface, the absorption edge. Once this parameter has been established, the intensity of the ultraviolet used may be correctly determined.

A complicating factor in laboratory simulation is the bleaching effect. This may occur simultaneously with the degradation of the surface. This merely complicates space simulation tests, and again, depends upon the material degraded, and the mechanism of degradation.

For the purposes of thermal control degradation studies, we may plot the region 2000-4000Å of the Johnson curve with the spectrum, in the same region, for a BH-6 high pressure mercury arc. The plot is shown in Fig. 1 (slide 1), a serious mismatch is at once obvious. In this curve, the two energies are plotted for five fold intensity. The solar curve is at five times the Johnson curve, and the mercury spectrum is also that obtained by the so called five times intensity. The usual practice is to integrate the BH-6 energy over the 2000Å-4000Å region. This is not a correct procedure. The intensity factor must be related to the material as noted earlier.

During the operation of the BH-6 a decrease in energy output is noted. Fig. 2 (slide 2) shows the energy drop as a function of time. This drop occurs for the region 2000Å-4000Å. It is to be noted that after 190 hours the energy drops nearly 50%. It has been determined by HAC that most of this drop occurs in the region below 3100Å. HAC has now begun continuous monitoring of lamp output with a grating monochromotor. By using a combination of filters, and the monochromator, it has been determined that the HAC inorganic thermal control is completely unaffected by radiation above 3150Å.

To conduct space radiation tests, thermal control specimens are prepared as 7/8" discs. A single sample is placed in the vacuum chamber shown in Fig. 3 (slide 3) which is pumped down with a gas sorption pump, sealed off, baked out at 250°F for 24 hours. At the end of this time, the pressure has been reduced to 1 x 10^{-8} torr prior to irradiation. At the end of the test, the pressure is almost invariably in the high 10^{-9} torr range. A desorption of gases occurs during the irradiation, caused by the photons and a temperature rise in the sample. Four samples are irradiated at one time. One such irradiation set-up is shown in Fig. 4 (slide 4). While these four samples are being irradiated, several more are being prepared and evacuated. These chambers are being used to study the photo-thermal effect. Other chambers may be thermally controlled anywhere in the region from liquid nitrogen to +500°F., the actual temperature being dictated by the temperature predicted for that coating on the space craft. The intensity of irradiation is controlled by moving the samples toward or away from the BH-6 lamp. After the samples have been irradiated, they are removed from the chamber, and examined for their spectral characteristics. This examination is carried out on the Gier-Dunkle integrating sphere and heated hohlraum. The equipment is shown in Fig. 5 (slide 5), the two units give near normal spectral data. The raw data is fed to a 7090 IBM machine for convenience in calculating the integrated total normal values. In addition to the near normal data, this equipment is used to obtain angular data out to 70° incidence angle.

The extent of degradation for a few representative surfaces is shown in Fig. 6 (slide 6). The comparison is made to HAC inorganic white (far left) after 1000 SEH (solar equivalent hours), a TiO_2 pigmented epoxy after 500 SEH, a TiO_2 pigmented acrylic paint after 250 SEH not shown is an antimony trioxide paint made for OSO-II. Its degradation after 100 SEH is equivalent to that of the acrylic. The OSO-II paint was designed to degrade by HAC for the OSO-II satellite. This paint is being flown with a sample of TiO_2-epoxy for obtaining correlation data between laboratory and actual space conditions.

The space activities at HAC are not confined to research on thermal control surfaces. Many other materials are examined for their compatibility with the space environment. In many cases, it is sufficient to run degradation studies (particularly where temperature is the only desired variable) at 10^{-6} torr. At this pressure, the gas molecules have a very long mean free path. The evaporated materials are removed from the sample vicinity by liquid nitrogen cold walls or traps. A very common material used for space vehicle applications is silicone rubber. Fig. 7 (slide 7) illustrates the effect of vacuum and elevated temperature on sample weight for only one silicone rubber. A not so often considered parameter is hardness after vacuum treatment. Fig. 8 (slide 8) illustrates the effect upon Shore A hardness after the vacuum treatment. In these experiments the volatile materials were removed by liquid nitrogen traps.

Fig. 9 (slide 9) is a view of a test on an experimental potting material for a traveling wave tube. The material is a urethane base loaded for high thermal conductance. This test has been running for two months, during which time water was continually evolved and trapped in liquid nitrogen.

It is not generally thought that optical parts may be considered as space materials. Infrared radiometers employ materials which are sensitive to vacuum and ultraviolet light. One such material is KRS-5. This material is a mixed single crystal of thallium iodide and bromide. At times during an orbit, infrared radiometers are directed toward the sun. After having "looked" at the sun, the instrument fails to operate. HAC has investigated the effect of high temperature and ultraviolet light upon KRS-5. Fig. 10 (slide 10) shows the change in transmission of KRS-5 after 48 hours at one solar intensity during irradiation at 2×10^{-8} torr. Fortunately, this degradation may be mitigated by appropriate optical means which do not allow the KRS-5 to view the sun directly.

In addition to being subjected to U.V. damage, the KRS-5 may sublime quite readily. Fig. 11 (slide 11) shows a sample of KRS-5 which has been heated to 130°C in a vacuum of 1×10^{-8} torr. At a temperature of about 230°C, the KRS-5, at 10^{-5} torr, loses 80% of its weight by sublimation. It is quite obvious that optical parts must be protected from large temperature increases. Fig. 12 shows the comparison during test of KRS-5 and CsI at 10^{-8} torr and 130°C.

Everything which has been discussed makes one think that only problems exist with materials in space. This is not quite the case, since the good materials are not very spectacular during test. There are many good space materials which have not been mentioned in this report. One good use of temperature and solar absorptance is shown in Fig. 13 (slide 13). This material is a foam-in-space plastic. At atmospheric pressure and room temperature, the tablets are stable, in fact stable enough to "iron" into a cloth substrate. In vacuum, and under solar irradiation, the pellet foams to form a mass which is continuous and structurally rigid.

SPECTRUM OF BH-6 LAMP
SUPERPOSED OVER SOLAR SPECTRUM

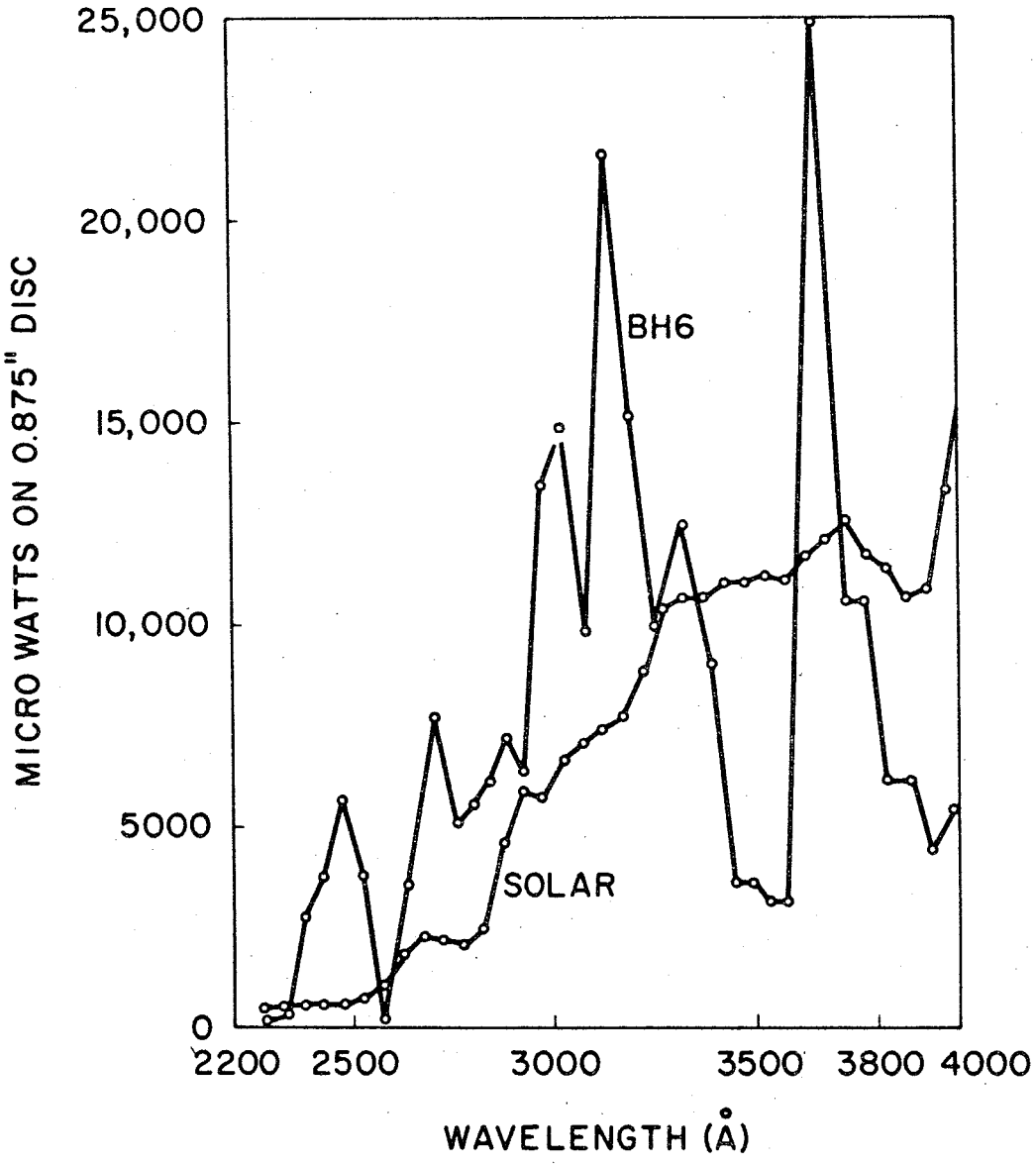

Figure 1

Figure 2

DECREASE OF ULTRAVIOLET RADIATION (<3100 Å) OF A BH6 MERCURY ARC VS OPERATING TIME

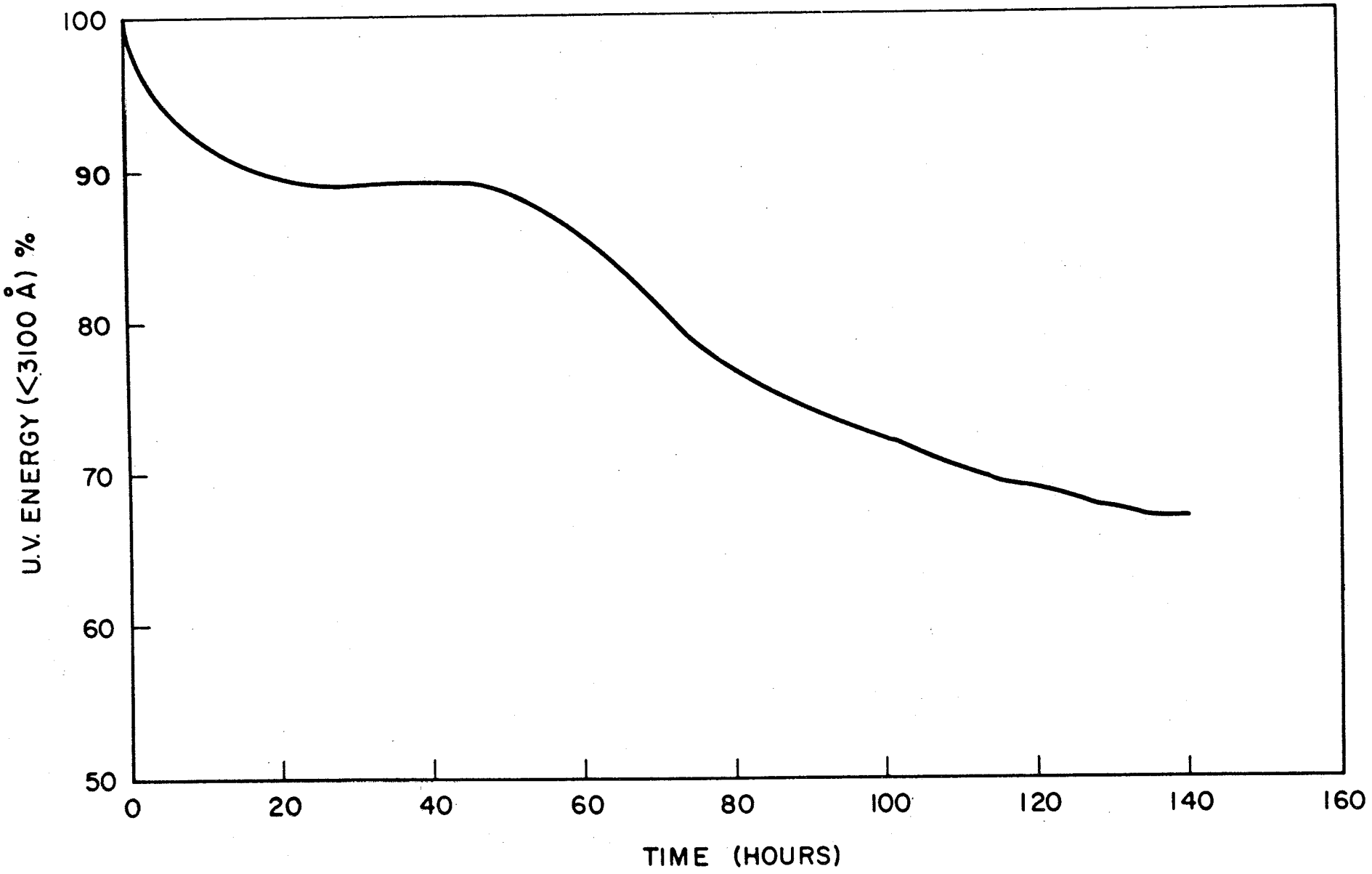

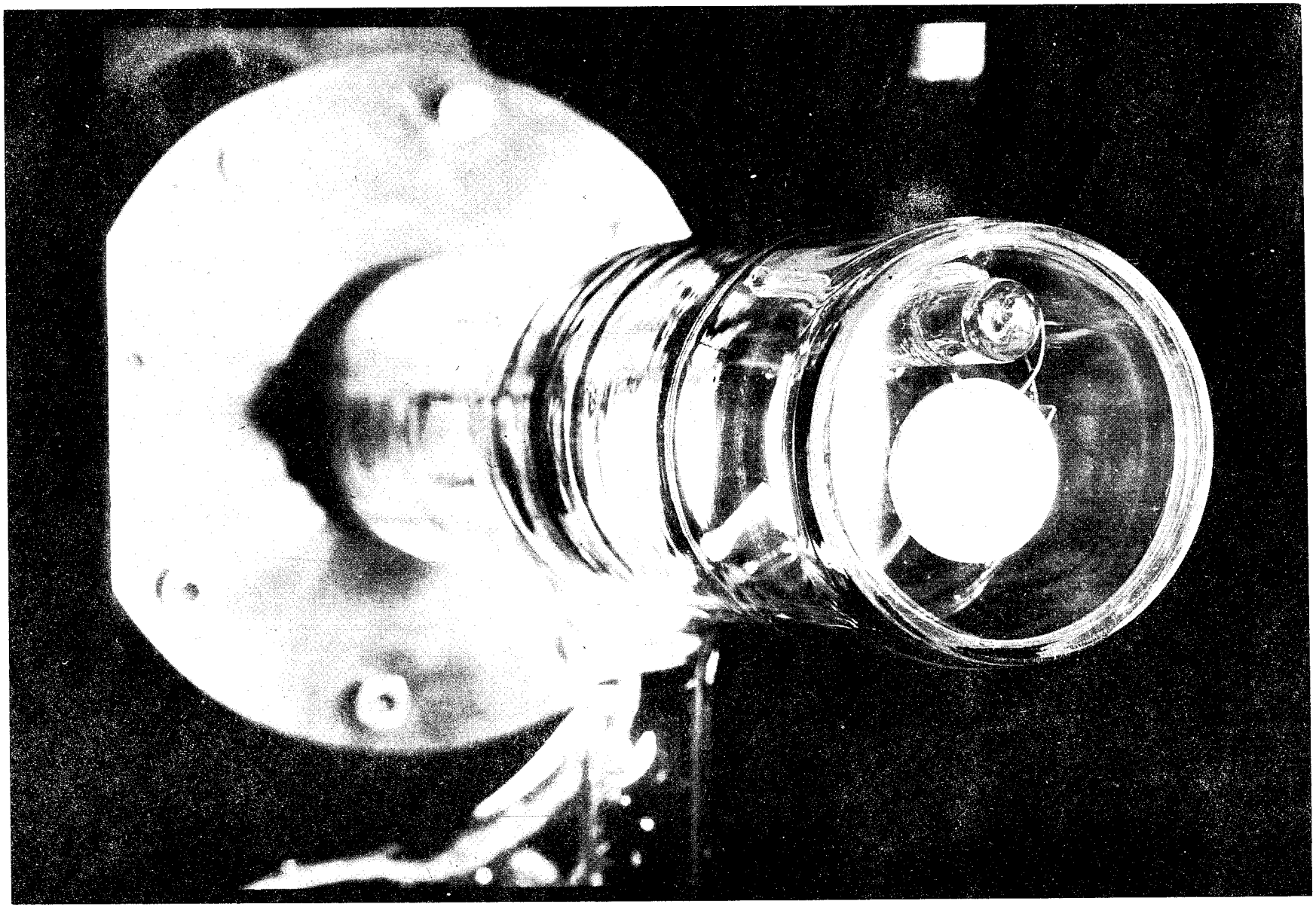

Figure 3

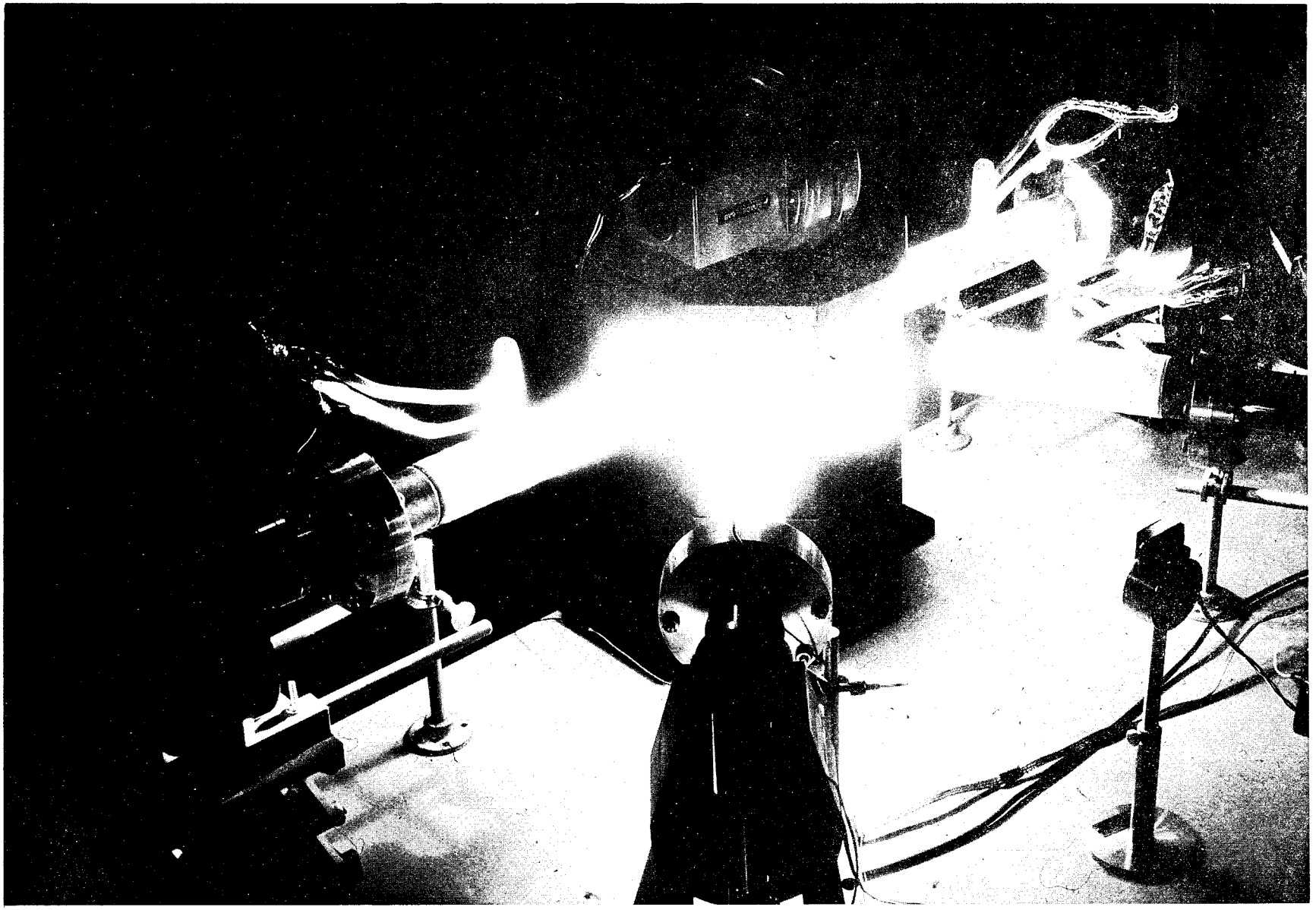

Figure 4

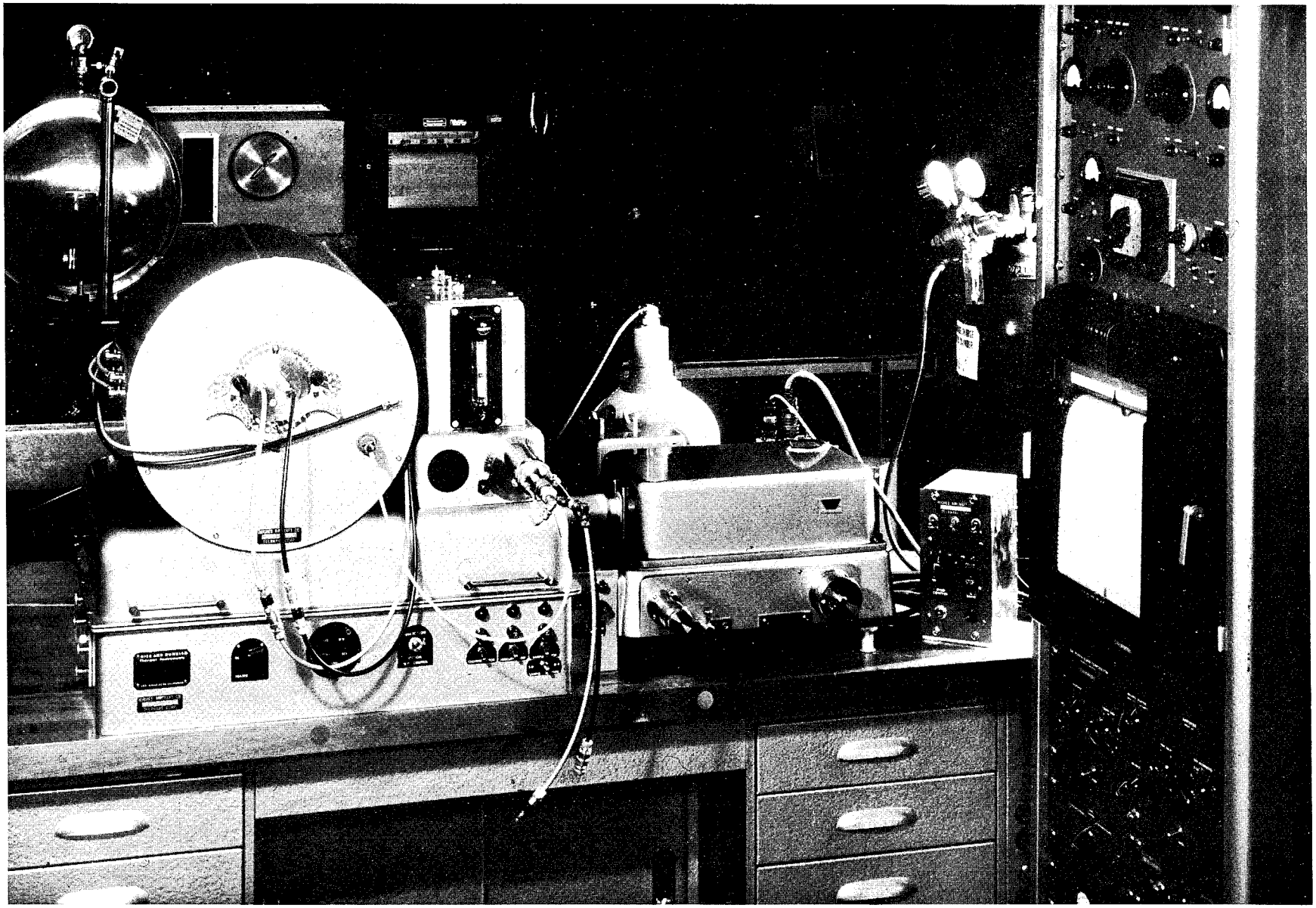

Figure 5

Figure 6a

SURFACE	α BEFORE	α AFTER	EXPOSURE (HRS)
HAC WHITE	0.19	0.23	960
$Sb_2 O_3$	0.20	0.33	240
TiO_2 Epoxy	0.23	0.35	240
TEFLON TYPE A	0.25	0.25	240
TYPE C	0.25	0.30	240
ANODIZED Al	0.25	0.27	240
ALUMINIZED TEFLON FEP, TYPE C	0.16	0.33	240

2nd SURFACE

Figure 6b

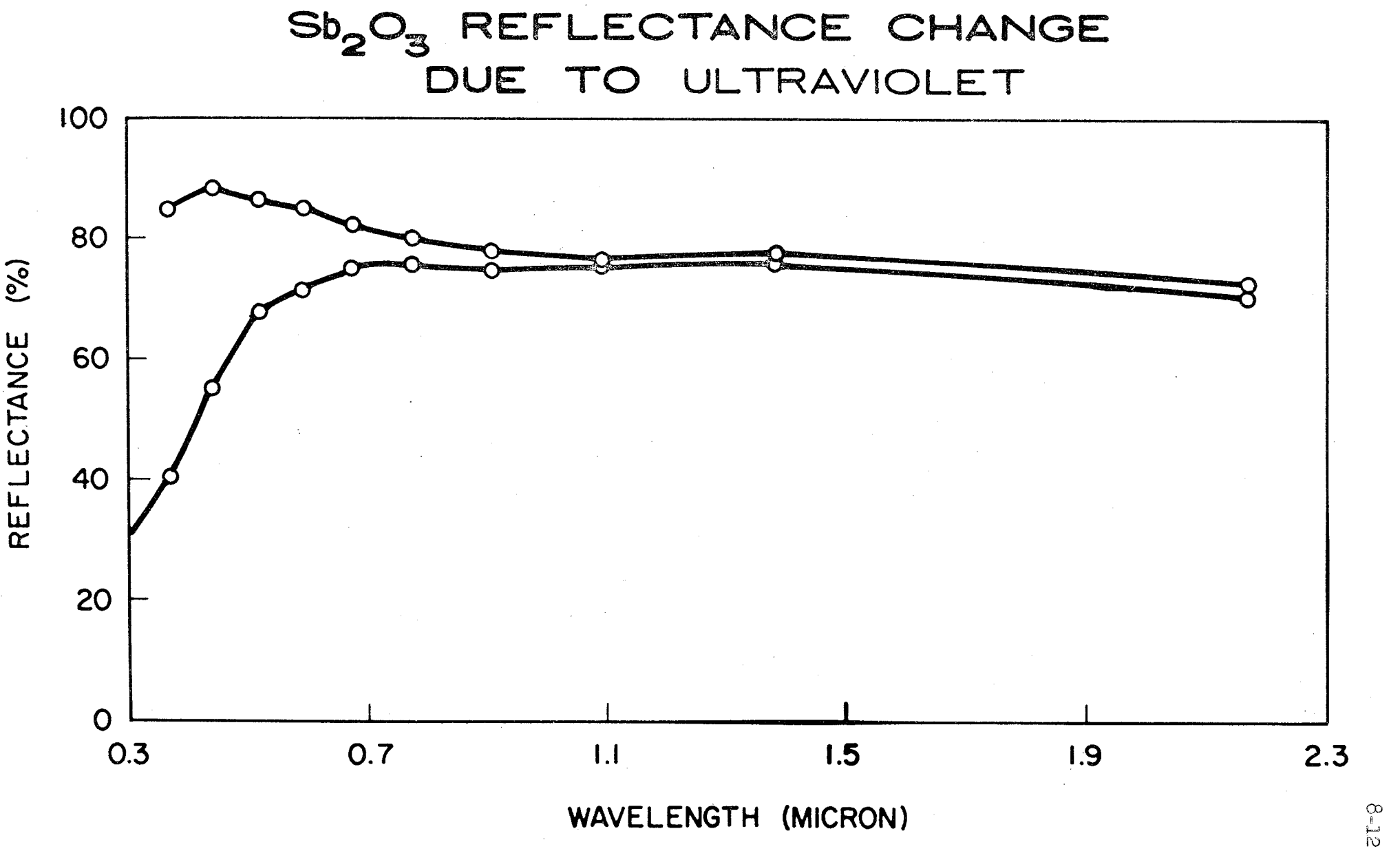
Sb_2O_3 REFLECTANCE CHANGE
DUE TO ULTRAVIOLET
REFLECTANCE (%)
100
80
60
40
20
0
0.3
0.7
1.1
1.5
1.9
2.3
WAVELENGTH (MICRON)

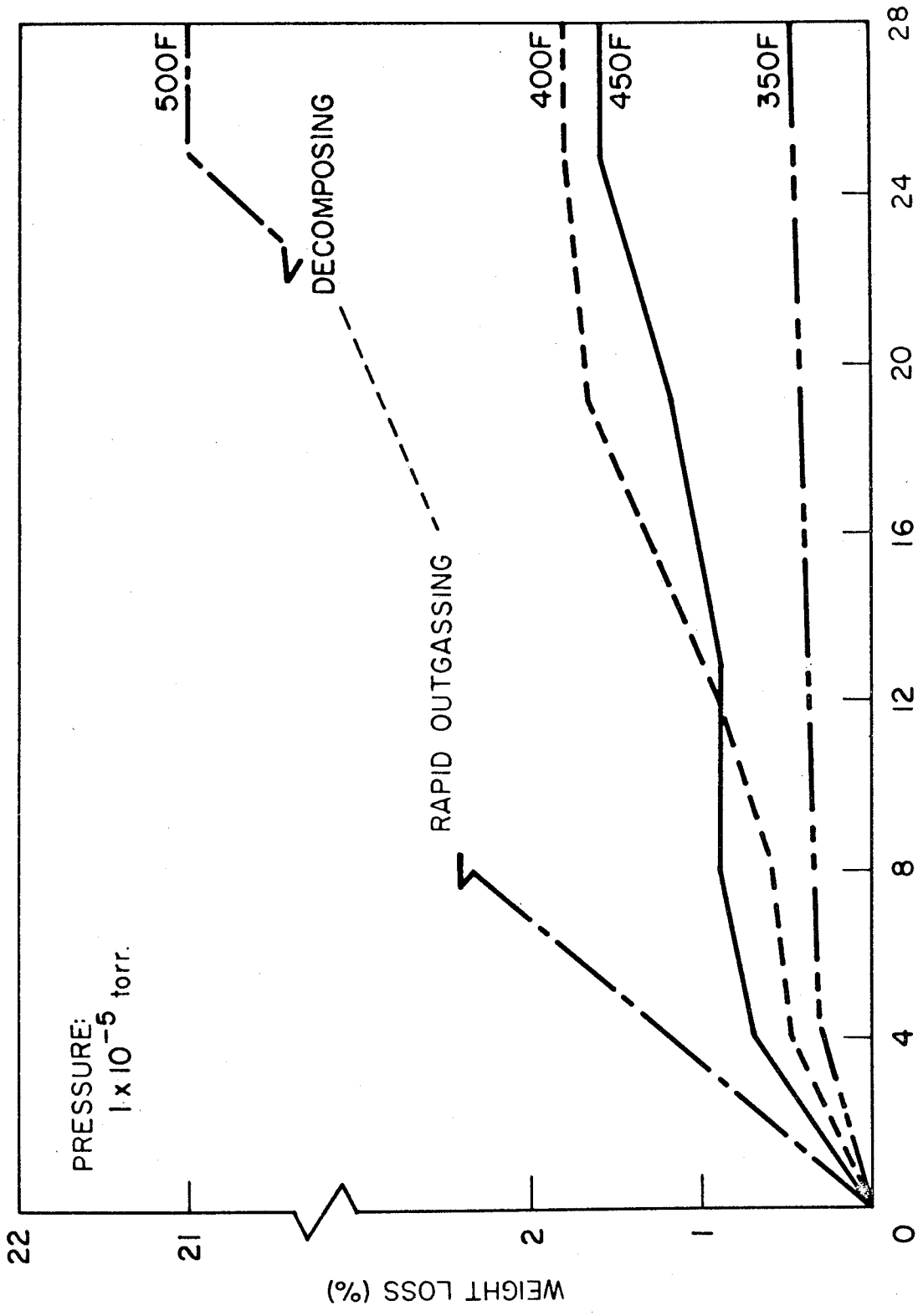
WEIGHT LOSS OF SILICONE RUBBER
AMS 3604
PRESSURE:
1 x 10⁻⁵ torr.
500F
DECOMPOSING
400F
450F
350F
RAPID OUTGASSING
WEIGHT LOSS (%)
22
21
2
1
0
4
8
12
16
20
24
28
VACUUM EXPOSURE TIME (DAYS)

Figure 7

SHORE "A" HARDNESS OF SILICONE RUBBER

AMS 3604

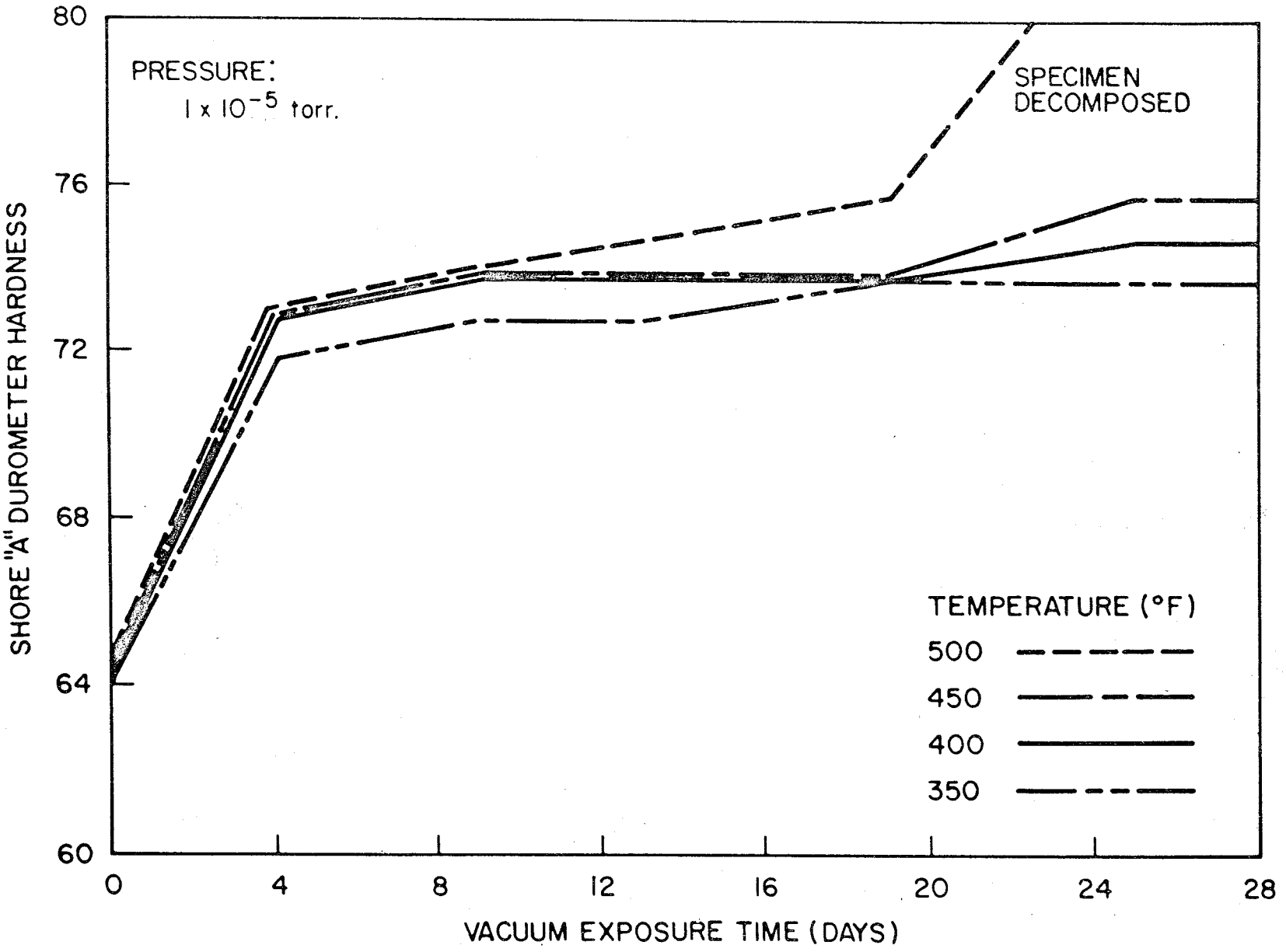

Figure 8

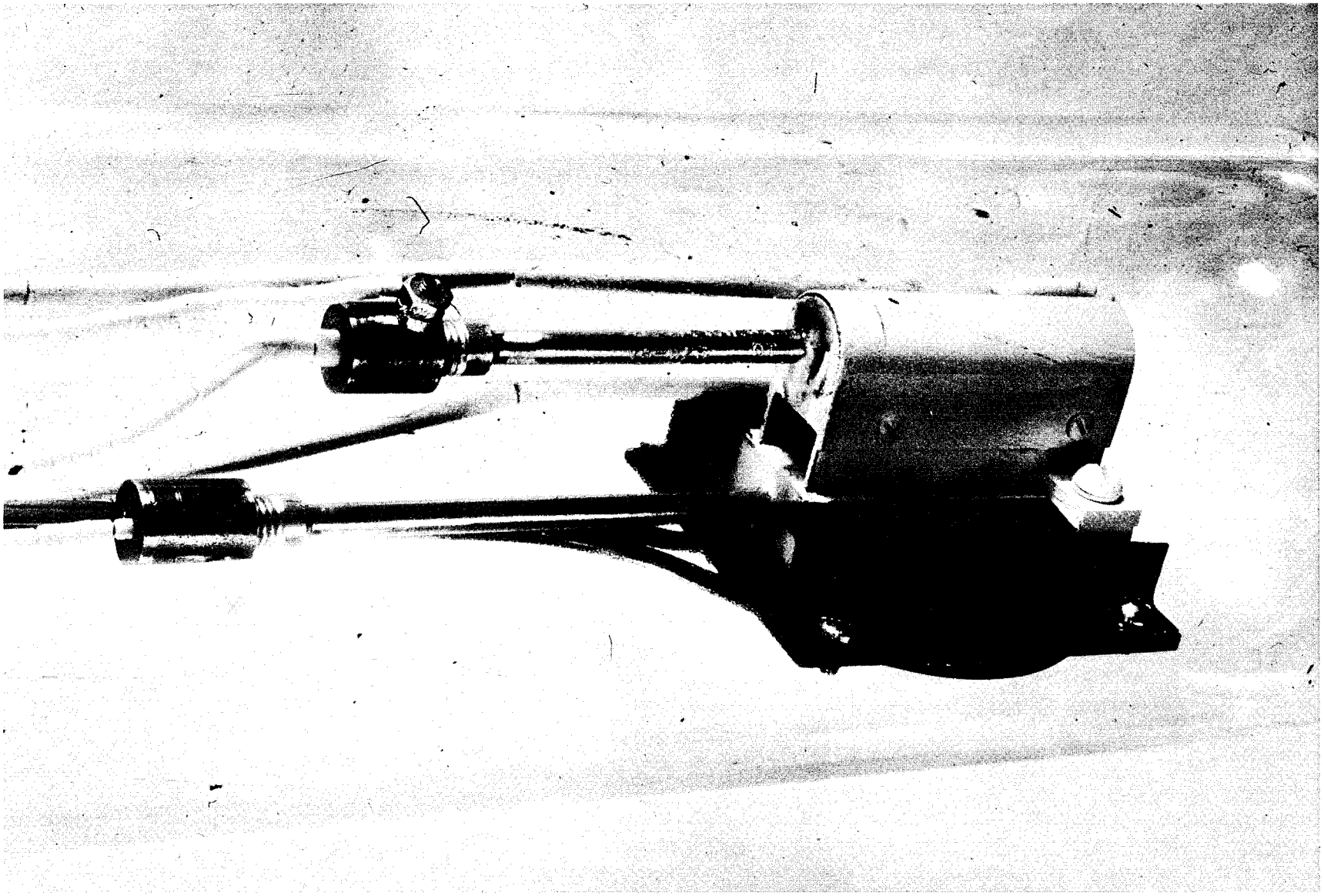

Figure 9

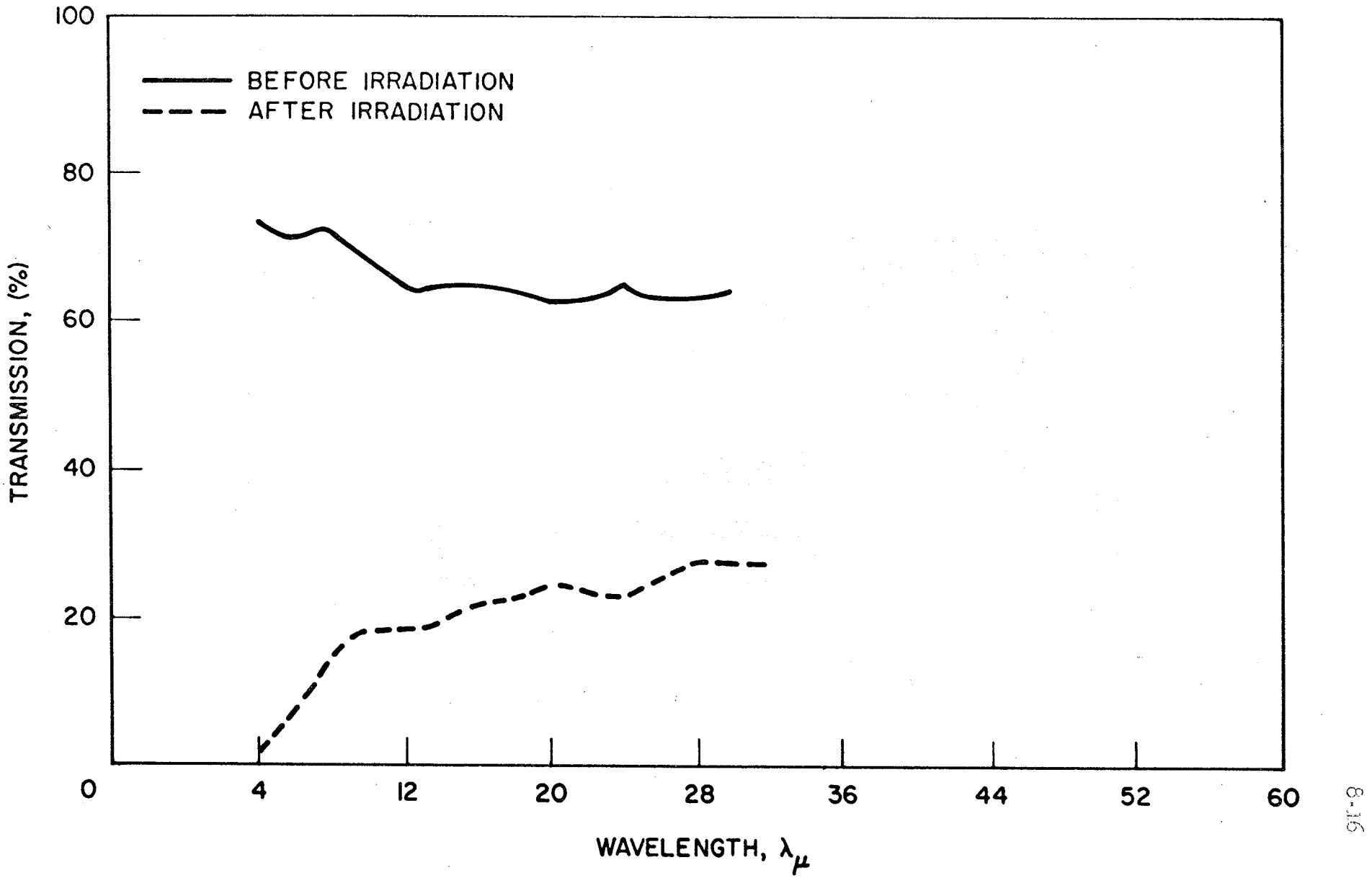
KRS-5 IRRADIATION BY U.V.
50 SOLOR EQUIVALENT HOURS 3x10^-8 TORR, 80°C
BEFORE IRRADIATION
AFTER IRRADIATION
TRANSMISSION, (%)
100
80
60
40
20
0
4
12
20
28
36
44
52
60
WAVELENGTH, λμ

Figure 10

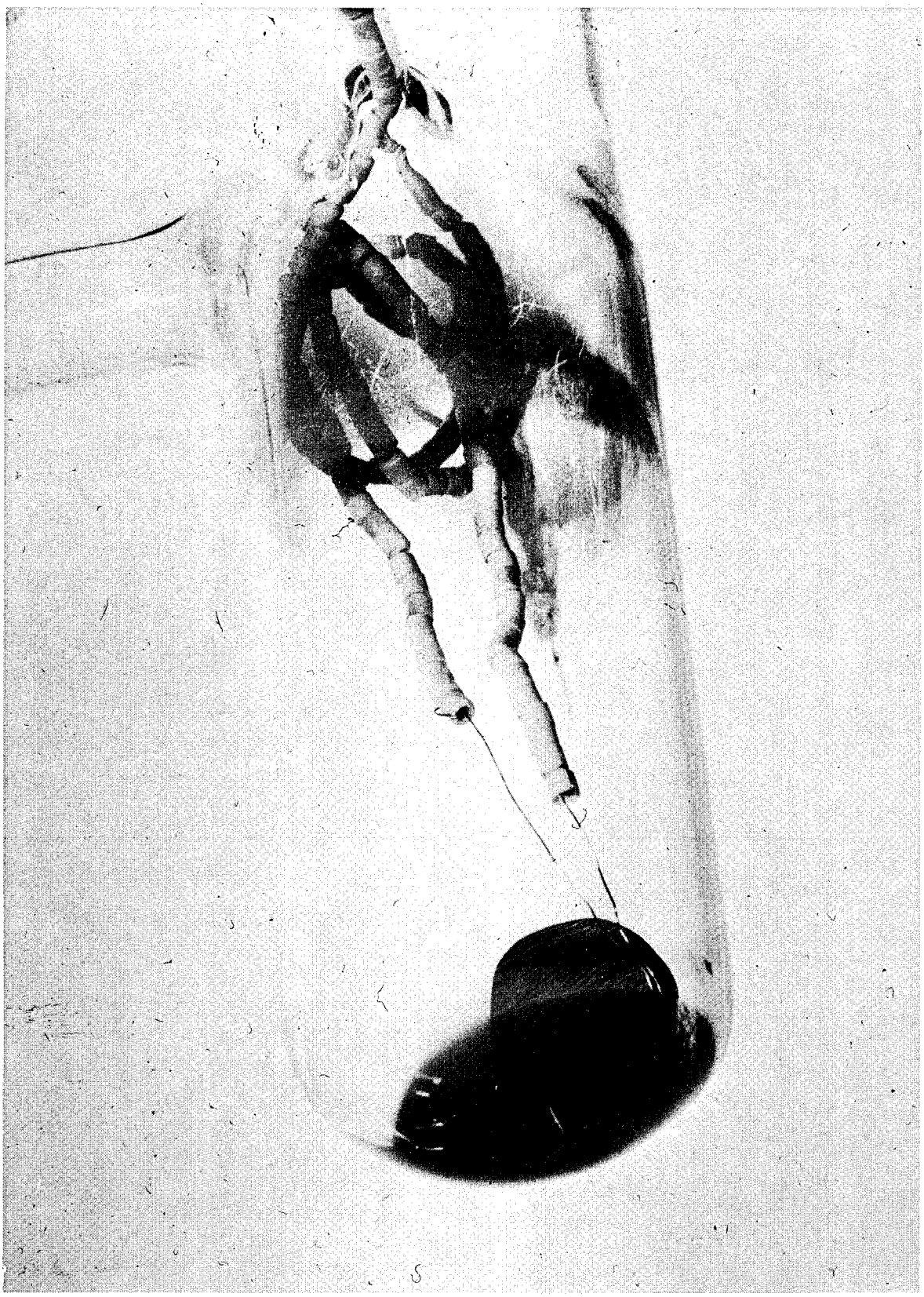

Figure 11

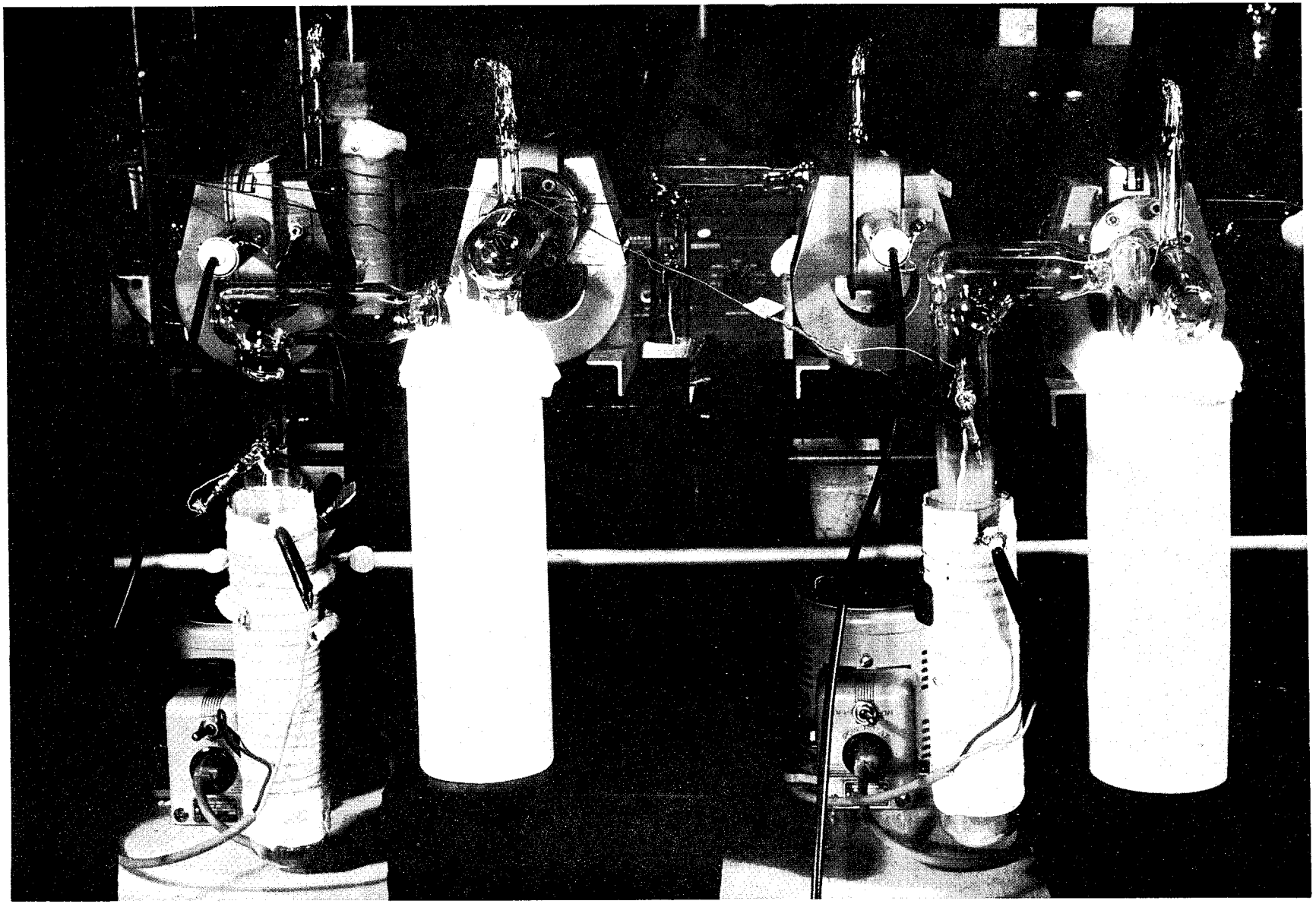

Figure 12

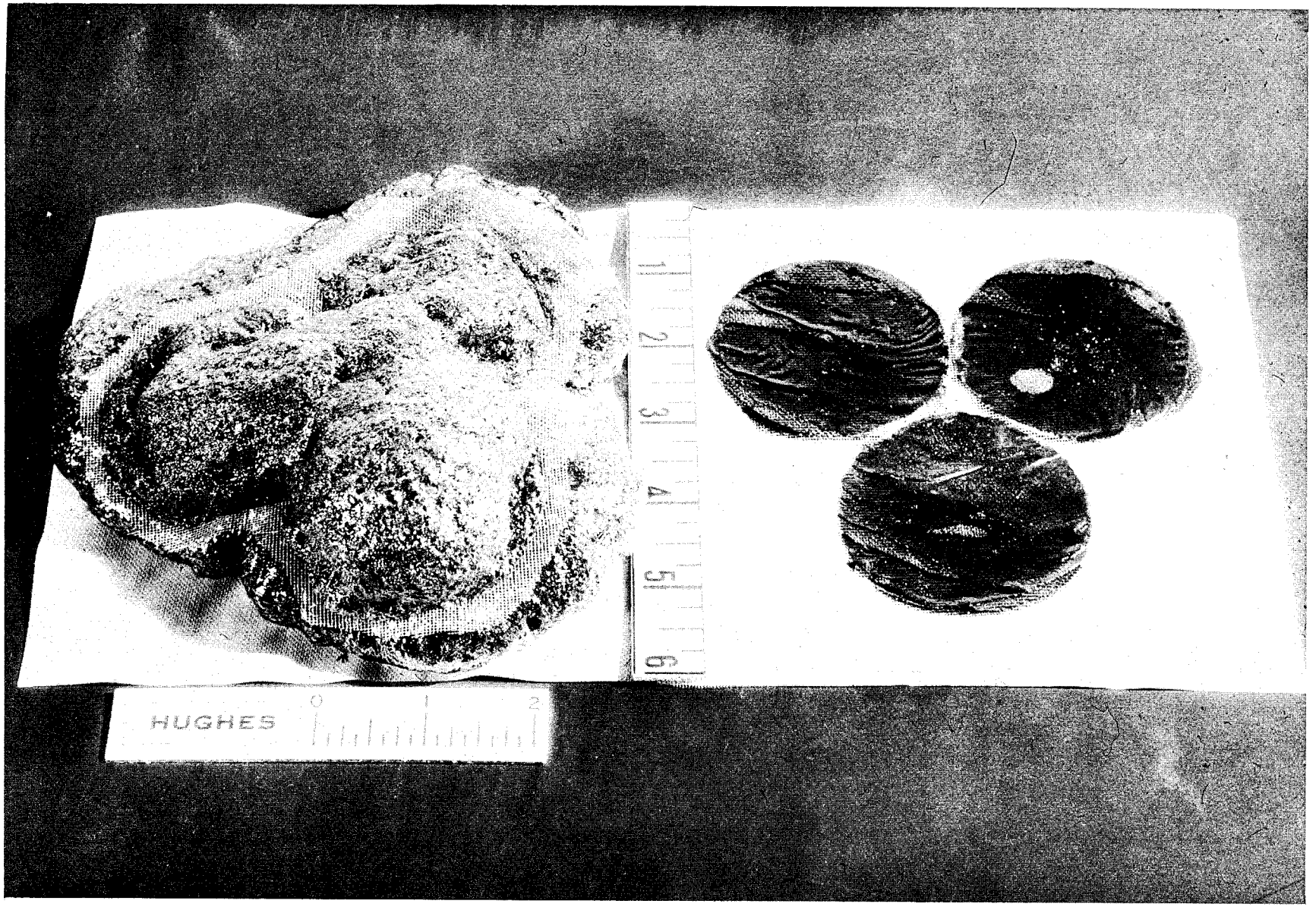

Figure 13

Failure Mechanisms in Dielectrics Under Space Conditions and Techniques for Their Investigation in the Laboratory. S. M. Skinner, W. J. Lytle, J. W. Merck, Westinghouse Air Arm Division

A. Types of Failure Mechanisms in Space Flight

I. Introduction

Mechanisms which cause failures in dielectrics under space conditions include all those which might commonly be met in the laboratory or in normal use, together with additional mechanisms attributable to unusual conditions which may be anticipated in space. Since effects of high energy radiation have been treated both in the literature and in an early session of this meeting, mechanisms related directly to high energy radiation in space will not be considered below.* Other effects which may be important in the space environment include: for the exterior or the unencapsulated interior, the effects of space vacuum, the effects of micrometeorite impact and fluctuating temperatures and magnetic fields; for an enclosed capsule such as the living space of an astronaut, temperature fluctuations, the effects of internal frictional contact between materials, and the accumulation within the enclosed environment of trace amounts (or more)** of gaseous products too expensive to remove by atmospheric treatment.

II. Vacuum

From the point of view of failure mechanisms, a vacuum should not be regarded as something magic or highly catastrophic; it is a region in which, because of low pressure, the rate of certain reverse kinetic process, such as gaseous surface bombardment or the supply of atoms participating in one direction of diffusion or chemical reaction has been brought to nearly zero; a pressure of 10^{-5} tor will already have reduced the latter to nearly zero, and therefore for measurement of chemical reactions or of many volume effects, and of diffusion controlled changes, pressures of 10^{-6} or 10^{-7} torr should be quite sufficient. Surfaces may require pressures to be reduced to 10^{-12} or 10^{-13} torr, and bombardment, in order that final traces of monolayers be removed and they remain degassed for finite measurement times. Therefore, investigation of surface properties which depend sensitively upon the presence of fractional or whole monolayers of adsorbed materials must provide such conditions. Since many desired properties are not this sensitive, and since suitable conclusions may often be drawn from experiments at the higher pressures, provided sufficient care is taken to assure identical specimen history for consecutive specimens,

---

* For the present purposes, specific environmental conditions during launching and passage through the various atmospheric layers including the ionosphere, will be omitted.

** The effect on extensive flights may be analogous to the stuffiness of an unaired room. Vapors may condense and gases may be adsorbed on solid surfaces. Astronaut Gordon Cooper had to use manual control for reentry because of a "single electric short in the auto-pilot", caused by moisture which had condensed in the cabin.

much useful data on failure mechanisms can be obtained without providing super-complex and expensive laboratory facilities. Electrical properties of a surface or interface composition and structure, and valid experimental results at any pressure can only be attained by use of the stringent precautions characteristic of surface chemistry. For normal use inside the capsule, high vacuum measurements are likely to contribute little direct information; however, for operation in the vacuum of space, such measurements should be made and suitably interpreted; considerable evicence points to the fact that the electrical properties of dielectric surfaces show greater variations from point to neighboring point, as very clean surfaces become cleaner.

III. Mechanical Damage

Any mechanical damage such as internal cracks or major fracture or even distortion will, and any chemical change of the surface or volume of a dielectric may, cause sufficient change in its electrical behavior so that it may be regarded as a failure mechanism. It is necessary therefore to examine the way in which electrical properties depend upon mechanical stressing or impact, and upon mechanical damage, from accumulations or dislocations, or phase changes, to fractures or microfractures.

IV. Loss of Volatiles

An especially important mechanism which affects dielectrics under conditions of low pressure, is the loss of volatiles or adsorbed gases. If such volatiles are lost at a slow rate, the final effect includes change in tensile and deformation characteristics, differences in resistance to impact or fatigue, and changes in the nature of the statistical contributions to the entropy term in the response to various types of deformation. It has recently been shown that removal of low molecular weight components from polyethylene[1] before using it as a metal adhesive increases greatly the strength of the adhesive specimens made with it. By ref. 2,[2] it must be presumed that the presence or absence of low molecular weight fractions in a plastic affect greatly the degree to which it wets surfaces at normal or enhanced temperatures, and therefore, will affect both adhesion and the friction experienced by any moving object coming into contact with it.

Similarly, if volatile components of the adsorbed film on dielectrics are removed, major effects on friction and adhesion may be expected. Savage's experiments[3] showed that the decrease in partial pressure of H_2O vapor adsorbed by graphite brushes at upper altitudes caused seizing between brush and commutator of the motors tested.

Since adsorbed layers may differ on different portions of the surface, and since the removal of volatiles may not be uniform throughout a solid because of different structure and different mobilities at different regions in the material, localized differences of chemical composition may be found. Whereas the original surface presumably was close to thermodynamic equilibrium, the depleted volume and surface may be far from such equilibrium; the result may be a metastable situation in which equilibrium (in the absence of triggering through impact or temperature rise, etc.) may not be achieved for long periods of time.

If, on the other hand (as in the interaction of high energy radiation with the internal volume of the material), the volatiles accumulate more rapidly than they can diffuse or otherwise reach the surface, internal pressures build up which can cause cracking, voids, or even more extensive damage such as microexplosion. This can be seen (but has not always been recognized) in samples subjected to radiation at rates that are too great, in order to achieve a total radiation dose in a conveniently small total experimental time. From the point of view of practical use, the most dangerous situation is probably that in which extensive minor (not evident unless painstakingly looked for) damage has been done, rather than that in which visually obvious damage is done. The analog of loss of volatiles in space is well known in the field of plastics: over a period of time, even at normal conditions, the uncompensated partial pressure of plasticizers and low molecular weight fractions causes continued loss of these components, causing the material to change from flexible to brittle, and to lose its impact resistance, as well as to change the nature of its mechanical response to deformation.* This, in extended flights in space, may be the cause of harmful mechanical failures, as well as of undesired changes in electrical characteristics. There is some indication that long-term effects of such loss may differ in quality or magnitude of effect from those observed in the early and middle stages of the loss. This is not a matter which can fully be investigated by accelerated test techniques, since the acceleration must be by temperature change which may activate other types of mechanism as well. Accordingly, structural members, nose cones, dielectric supports or bearings, etc. intended for external use in the craft should be given laboratory examination over extensive periods of time.

V. Migration Between Surface and Interior

A number of experimental results have shown that the surface of a solid polymer is not a smooth, passive interface, an inert assemblage of atoms vibrating slightly and periodically creating or annulling vacancies and interstitials. Instead it appears to be a region possessing greater kinetic disturbance than expected from the surrounding environment. Material which deposits on a polymer surface may shortly be found under the surface because of transmitted motions of the giant molecules, the penetration into the interior occurring more rapidly than in dielectrics such as ceramics, mica, etc., at the same temperature.

VI. Micrometeorites

Micrometeoric impact should differ little from impact of similar particles in the laboratory, and, except for long term effects, can be studied relatively easily.

VII. Magnetic Fields

Intense or fluctuating fields offer little damage except to magnetic materials, unshielded plasmas, or heavy current flows. Their effects should be investigated primarily, for items such as magnetic recorders or memories, or when the field is so large that the mechanical Maxwell ($\propto B^2$) forces become large.

---

* See Section BII, below.

VIII. Temperature

The effects of temperature change include the usual ones concerned with unequal expansions and resulting mechanical fractures, or binding of close tolerance designs; suitable design can avoid these. Other temperature effects include loss or gain of adhesion, variations in deformation potentials in materials, thermoelectric effects, evaporation and volatilization, freezing and its associated contraction or expansion, and various temperature-dependent changes in charge carrier density, dislocation density, dielectric constant and loss factor, etc.

IX. Accumulation of Trace Elements Inside the Capsule

Within the capsule, the accumulation of traces of gases which diffuse out of materials, or result from bodily processes or mechanical operations, and then later condense or are adsorbed on free surfaces within the capsule, may affect bearings, electrical components and solid state devices,* and switches and remote control relays. Since friction between surfaces depends upon the nature of the surface, this is especially vulnerable to surface contamination by such vapors. Breaking strengths of metal wires or glass fibers have been shown to be dpendent upon the gas or liquid in which they are immersed.

X. Charge Transfer

A major effect of any contact between materials is the charge transfer which is initiated. Thus contact electrification arises from the physical motions which must be performed by the astronaut, and from any periodic, random, or moving contact between materials. Charge deposition may also occur from the effects of high-energy radiation or strong fields which activate electron emission. Such electrical effects are difficult to measure, because they usually appear to be so random that the measurements are not easily interpreted. However, they have definite electrical effect[4], which may even create free energy conditions favorable to the onset of localized chemical reactions. If dielectrics are too insulating, such charges may persist for days or even years[5], and subject the astronaut to working in an environment of random electrical fields, and possible internal discharges; certainly causing preferential deposition of charged particles existing in the internal atmosphere.

XI. Other Effects

A number of other more subtle effects can occur, not all of which can presently be recognized. These include quantum effects, long-term effects of mechanical stress, electrical Maxwell forces, UV-activated photochemical processes especially in heterogeneous materials, and others, as well as combinations of these, especially combinations of anisotropic effects. The field requires detailed investigation by methods which will recognize both the known and the newer or more unusual effects.

---

* It is easy to show by placing a transistor with, say, oxide-coated (passivated) surface on a curve tracer, that finite quantities of organic liquids on the passivated surface alter the performance of the transistor. With sophisticated apparatus, this "field-effect" may be shown for nonvisible condensed or adsorbed films.

XII. Measurement of Failure Effects

The usual electrical measurements which are made on dielectrics are: surface and/or volume resistivity, breakdown field intensity, and the frequency dependent dielectric constant and loss factor or dissipation factor. Since a number of physical and chemical mechanisms contribute to the measured value of each of these, it may, however, be quite meaningless to take resistivity measurements or dissipation factor or loss factor measurements on a number of samples of different materials at only one temperature, and one or two frequencies, such as 1 kc/sec or 1 Mc/sec. With sophisticated measurements, such as relatively thorough study of the dependence of these constants upon temperature, frequency, and chemical environment, much information may be obtained.[6] More such measurements must be made to extract the information which they present.

Othere methods which may be used include X-ray examination by various techniques, a number of optical examination methods including the use of polarized light, magnetic measurements including the Mössbauer magnetic resonance approach where applicable and the effects of surface adsorption upon the density of unpaired electrons, electron beam methods[7], annihilation of positrons within the material, and others. With most dielectrics, there may be too small a free charge density to permit a number of measurements used in semiconductor technology to be made effectively, as, for example, Hall effect measurements. Therefore it becomes necessary to look into other types of measurements which will demonstrate the electrical properties of dielectrics sensitively and with precision. Certain of these will be described in what follows, each being illustrated with sample results obtained from them. All of these are unconventional, and were essentially new at the time of their first use except as stated; they have each been shown to yield precise information if suitable care is taken in sample preparation and measurement techniques.

B. Unconventional Experimental Measurements, Useful for Examination of Failure Mechanisms

I. The Effect of Electrical Fields (without electrode contact) Upon the Tensile Properties of a Dielectric

ASTM-type samples of commercial uncharged dielectrics were subjected to standard tensile tests, both without and with strong d.c. electric fields (applied without electrode contact) traversing them perpendicular to the direction of extension. In some cases, there was little effect, in others, a noticeable effect.[8] Figure 1 shows the relation between ultimate elongation and tensile strength for extension of a glass reinforced polyester 1) in zero field, and 2) with a voltage of 6000 V between the electrodes, (which represents a nominal field of 7.5 kV/cm or actual field within the material of somewhat over 2 kV/cm). Since the effect is probably in part a surface one, the field values may be less important than the overall applied voltage. Nevertheless, the effect shows that what is regarded as an inert, non-reacting dielectric may show mechanical properties that change as the space-craft enters regions of high electrical fields. More important, however, is the fact that the fundamental mechanisms underlying the behavior of dielectrics can be investigated in this manner.

II. Impact and Fatigue Behavior of Plastic Materials

By an apparatus which delivers blows of predetermined magnitude to a dielectric sample, and which measures simultaneously the successive rebounds, and

the electrical charge on the sample at which the impact head look just before and just after impact (or at any minute fraction of the impact cycle), C. C. Lee[9] has shown that the fatigue resistance of the materials which he examined can be divided into three main types:

1. The Impact Resistance Index decreases until it reaches a stable level. Apparently the material is not broken but internal bonds are broken. Typical material: - glass reinforced polyester.
2. Impact Resistance Index increases at first, then reaches a maximum or plateau, and when cracking occurs, there is visible break and sudden drop in the impact resistnace index. Typical material: poly(vinyl chloride).
3. Impact Resistance Index increases to a plateau. At the breaking point the impact resistance index increases instead of decreasing. Typical material: heterogeneous filled plastics, such as acrylonitrile rubber with poly(vinyl chloride, the copolymer being filled with various platelet or powder fillers.

This conclusion could not have been drawn from the mechanical responses alone. The electrical charges result from contact charging and dielectric distortion during the impact, and represent another type of electrical effect which accompanies mechanical effects but is usually not measured.

III. Charge Transfer During Repetitive Contact[10]

Figure 2 shows an apparatus in which a dielectric specimen is repetitively contacted by a metal probe. The electrometer measures the amount of charge transferred between the two at each successive contact. Such contact charging depends sensitively upon the chemical nature of the contacting materials and, therefore for a given probe, upon the composition, structure, and degree of surface contamination of the dielectric. Figures 3 and 4 show typical charge vs. number of contacts curves; these obey quite accurately the condenser charging equation, and if the original slope of these curves is plotted as a function of composition of the dielectric, curves such as shown in Figure 5 are obtained. The method therefore promises to yield considerable information about polymer composition and structure. This method has been used to separate otherwise indistiguishable specimens of a particular dielectric from others of the same dielectric, where minor differences in the fabrication resulting from the processes of different manufacturers were involved. The method is of little value except with dielectrics, since with more conductive materials, the charge transfer occurs wholly during the first contact.

IV. Electrical Effects in Adhesion[11]

Upon the break and separation of the two members of a metal-dielectric-metal adhesive bond, a voltage trace can be obtained from an oscillograph connected across the two separating metal members, no external potential being included in the circuit, Figure 6. By suitable interpretation it is possible both to correlate the total amount of charge transferred and the Maxwell forces from this charge with the breaking strength of the specimen, and by an examination of the structure of the trace to obtain a clue to the sequence of events occurring during break. Figure 7 shows a set of traces resulting from break of identically prepared specimens, the stronger ones being on the right, and the weaker ones on the left. Each break in the curve corresponds to a catastrophic occurrence; if the break is an upward deflection, part of the adhesive and the charge bound on it have repidly been torn away, whereas, if it is downward, either a part of the

adherend has been torn out or a part of the adhesive has rebounded towards the other adherend. The interpretation of such photographs is an art acquired without major difficulty after a few experiments, and the experimenters mentioned in footnote 12 were able to interpret such traces in considerable detail of physical mechanisms and events occurring during the microseconds of break. By performing similar experiments in progressively increasing vacuum in a sylphon specimen container, Trivisonno was able to show that the total charge accompanying break increased with decrease of pressure, measuring as well a number of other details about the break.

V. The Use of Luminescent Powders for Surface Charge Mapping[13]

In the course of the work described in the last section, Kern, Trivisonno, and Gaynor, each used a technique first used by Woodland and Ziegler namely, charge mapping by means of a mixture of luminescent powders. The method is described in reference 8a; it consists of dry mixing two luminescent powders of different colors, which normally assume opposite charges in the equilibrium state, till the mass as a whole is uncharged, and storing them in a desiccator. If the mixture is blown through a dust atomizer at the surface to be investigated, the separate particles deposit preferentially upon charges opposite to their own, and the distribution of electrical charge upon the surface is mapped in color when the surface is illuminated by UV light. The color slide shown at the conference showed such a distribution, and showed the way in which negative charge concentrates around craters where portions of the surface of the dielectric have been torn out. The mapping exhibits the whole distribution of charge over the surface at the instant the powder was applied, with resolving power limited by the size of powder particles used. After the powder is applied further changes in charge distribution do not take place as they would in the absence of powder, and therefore if a kinetic process is being studied, successive stages of the process must be exhibited on a series of successive specimens.

VI. Frictional Contact: Stick-slip and Charge Transfer[14]

Figure 8 shows an apparatus constructed so that a specimen may be moved under an insulated probe, and the instantaneous load and drag of the probe be indicated on a recorder or oscillograph. Simultaneously the instantaneous charge transfer to the probe may also be indicated by connecting it to the input of an oscilloscope. Figure 9 shows a typical trace from the passage of the probe over p-type silicon specimen which received n-doping in a bull's-eye pattern. The lower photograph shows a cross-section of the diameter of the bull's-eye specimen after the measurement was made, and the sample was then angle-lapped and stained. The upper photo shows, to the same scale, the response of the probe made before the angle-lapping and staining. Here, the upper trace is the drag trace, and the lower one measures the charge transfer. The degree of sensitivity of the charge transfer trace to material composition is evident, down even to minute changes in chemical (alloy) nature of the surface. This sensitivity is also indicated in Figure 10. Here, over an oxide masking of the silicon surface there was spattered a single drop of water, and the wafer was immediately placed in the diffusion furnace; at a temperature of 1200°C, presumably the water flashed away instantaneously. After diffusion the oxide was etched away, and a frictional pass was made over the wafer. The results are shown in the upper traces, and to the same scale in the lower photograph are shown the effects of the water droplet (through the oxide), which were brought out, after the trace was taken, by staining.

With this apparatus, additional information as to the nature of adhesional contact between the probe and the sample can be secured by obtaining a periodic stick-slip phenomenon and looking at the period of the stick-slip in terms of other measured experimental parameters.

VII. Photovoltaic Effects[15]

A number of these have been investigated. In the interests of the time and space and space available, only Figure 11 will be shown here, namely the degree to which the photovoltaic response depends upon the pressure applied to the probe. This can be used to examine the nature of the interrelation between electrical and mechanical effects in a dielectric. By a somewhat different technique, the photovoltaic response has been used to examine the oxidation or passivating processes on a germanium surface, with the possibly surprising but definite result that different oxidation processes are simultaneously taking place at neighboring regions of the surface, and that therefore the electrical properties of contiguous regions of the surface vary in different functional manners during the time from a clean surface to a completely oxidized surface.

VIII. Mechanical Flexure: Self-healing Cracks[16]

By making suitable electrical contact to a dendrite without external voltage in the circuit, characteristic patterns were obtained upon flexure of the sample. The ones after one hour's flexure could be microscopically correlated with the appearance of new cracks in the material or with extensions of old ones. Because similar peaks occurred at less than one hour, a search was made, and it was experimentally verified that they also corresponded to cracks, but that these cracks were self-healing upon release of stress, in the sense of the self-healing cracks in glass observed by Finkel and Kutkin[17].

IX. Electrical Hysteresis Curves in Plastics[18]

The experiments just described were prompted by an earlier set of flexure experiments performed by Kern et al. In these, plastic samples were flexed with electrodes placed so as to observe the charge on the surface resulting from the distortion. It was confirmed that the charges did not result from flexure of the electrodes, and capacitance changes were negligible. By plotting the charge against the distortion, on an X-Y recorder, it was found that a hysteresis loop resulted, the charge on the return portion of the distortion cycle being parallel and similar in shape to, but at a lower or higher magnitude than that during the flexing portion of the cycle. The earlier apparatus is shown in Figure 12, and some typical results in Figures 13 and 14. The shape does not change with repeated flexures, except that a noncatastrophic type of fatigue shows itself in the decrease in the area of the hysteresis loop. Because of this and several other minor factors, it is possible to examine the mechanical and dielectric properties of the materials under changing environmental conditions, and identifying rapidly the occurrence of any major change in the material resulting from environmental or other parameters applied to the material.

C. Conclusion:

The types of failure mechanisms and effects which may be expected in dielectrics under space conditions have been considered phenomenonologically,

and from these have been drawn conclusions as to what types of measurements should be undertaken to study the mechanisms. A number of unconventional experimental techniques have been described, which are related to electrical effects which: a) may demonstrate the subtle processes going on in dielectrics under space conditions, or b) may be used as investigative tools in the examination of dielectrics to replace those which cannot suitably be performed because of insufficient charge density or current flow. This by no means exhausts the list of possible electrical phenomena which, alone or in conjunction with other phenomena, can be utilized to examine and draw conclusions as to what happens to dielectrics in space, or under other conditions. Although expensive laboratory facilities are not needed for these methods of investigation, a tremendous amount of care in processing and experimental technique, and in the manner of interpretation is necessary. In most cases, it will be necessary for the experimenter to make his own materials, such as plastics or ceramics, by reproducible methods, rather than relying upon commercial sources. Minute attention to cleanliness, reproducible processing steps, and details of measuring techniques are required, and the processes cannot be trusted routinely to uninspired technicians. If the requirements just discussed, however, are satisfied, a wealth of significant data can be obtained which sheds additional light on the electrical behavior of dielectrics under various environmental conditions, and therefore permits recognition of mechanisms which are responsible for failures in the dielectrics under space conditions.

References

1. Bikerman, J. J. (apparently unpublished). Analogous work of his is Bikerman, J. J. and Marshall, D. W., J. App. Polymer Sci. 7, 1031 (1963).

2. Shapiro, L. and Schonhorn, H. Am. Chem. Soc. Los Angeles Meeting, 1963. The same factors determine adhesion, and the spreading of films on solids, and therefore adhesion is directly related to surface tension and wetting.

3. Van Brunt, C. and Savage, R. H., Gen. Elec. Review, 47, 16 (July, 1944); 47, 28 (Aug., 1944). Savage, R. H., ibid, 48, 13 (Oct., 1945). Sims, R. H., Proc. Inst. Elect. Engrs. II, 101, 217 (1954).

4. Skinner, S. M. and Dzimianski, J. W., Final Report, Study of Failure Mechanisms, Technical Documentary Report No. RADC-TDR-63-30, Dec., 1962. Sec. 4.13, Transistor Failure by Surface Charging. Also ref. 5 and others below.

5. Skinner, S. M., Gaynor, J and Sohl, G. W., The Electrostatic Component of Adhesion. WADC Technical Report 56-158, Aug., 1956. See also ref. 13b.

6. As evidenced by numerous publications in J. Phys. Chem., J. Am. Chem. Soc., and J. Chem. Phys. Comprehensive discussions are in:
Cole, R. H., Dielectric Polarization and Loss, Annual Review of Physical Chemistry, Vol. 11, 1960, pp. 149-68. Annual Reviews, Inc. Palo Alto, Calif.
Smyth, C. P., Dielectric Behavior and Structure, McGraw-Hill Book Co., Inc., New York City, 1959.

7. Angello, S. J. 2nd Interim Engineering Report, Material Processing and Phenomena Investigation for Functional Electronic Blocks. 1 Jan - 6 Mar., 1963. ETL, ASD, Contract No. AF33(657)-9897, Wright Air Development Center, US Air Force.

8. Skinner, S. M. and Kern, E. L., The Effect of an Applied Electrical Field on the Mechanical Response of Solid Polymeric Materials. Manufacturing Chemists Association Report No. MCA-2, Dec., 1959.

9. Lee, C. C., Rovatti, W. S., Bobalek, E. G., and Skinner, S. M. To be published.

10. Skinner, S. M. and Kern, E. L., The Nature of the Frictional Stick-slip Phenomenon and of the Kinetics of Contact Charging of Polymer Surfaces. Final Report, Office of Ordnance Research, Project No. 1090, Feb., 1959.

11. a. Ref. 5 above.
    b. Skinner, S. M., Kern, E. L., and Park, K. M., Effects of Space Charge in Polymeric Materials on Mechanical and Adhesive Properties. Wright Air Development Center, Technical Report, No. 58-9, Jan., 1958.
    c. Skinner, S. M. and Gaynor, J. Plastics Technology, 1, 626 (1955).
    d. Trivisonno, N. M., Thesis, Case Institute of Technology, 1959.

12. Gaynor, J., Sohl, G. W., Trivisonno, N. M., Kern, E. L., Liu, P. All at Case Institute of Technology at the time of their work.

13. a. Hull, H. H., J. App. Phys., 20, 1157-9 (1949) (nonluminescent powders).
b. Woodland, P. C. and Ziegler, E. E., Modern Plastics, 28, 95 (May 1951).
c. Reference 4. Also, Automatic Control, Vol. 18, 34-35, May, 1963.

14. Reference 10.

15. Reference 4, Section 4.5, 4.6, 4.7.

16. Reference 4, Section 4.11.

17. Finkel, V. M. and Kutkin, I. A., Dokl. Akad. Nauk SSSR, Vol. 143, No. 1, pages 90-91, March 1, 1962.

18. Kern, E. L. and Skinner, S. M., J. App. Polymer Sci., Vol. 6, 404-421 (1962).

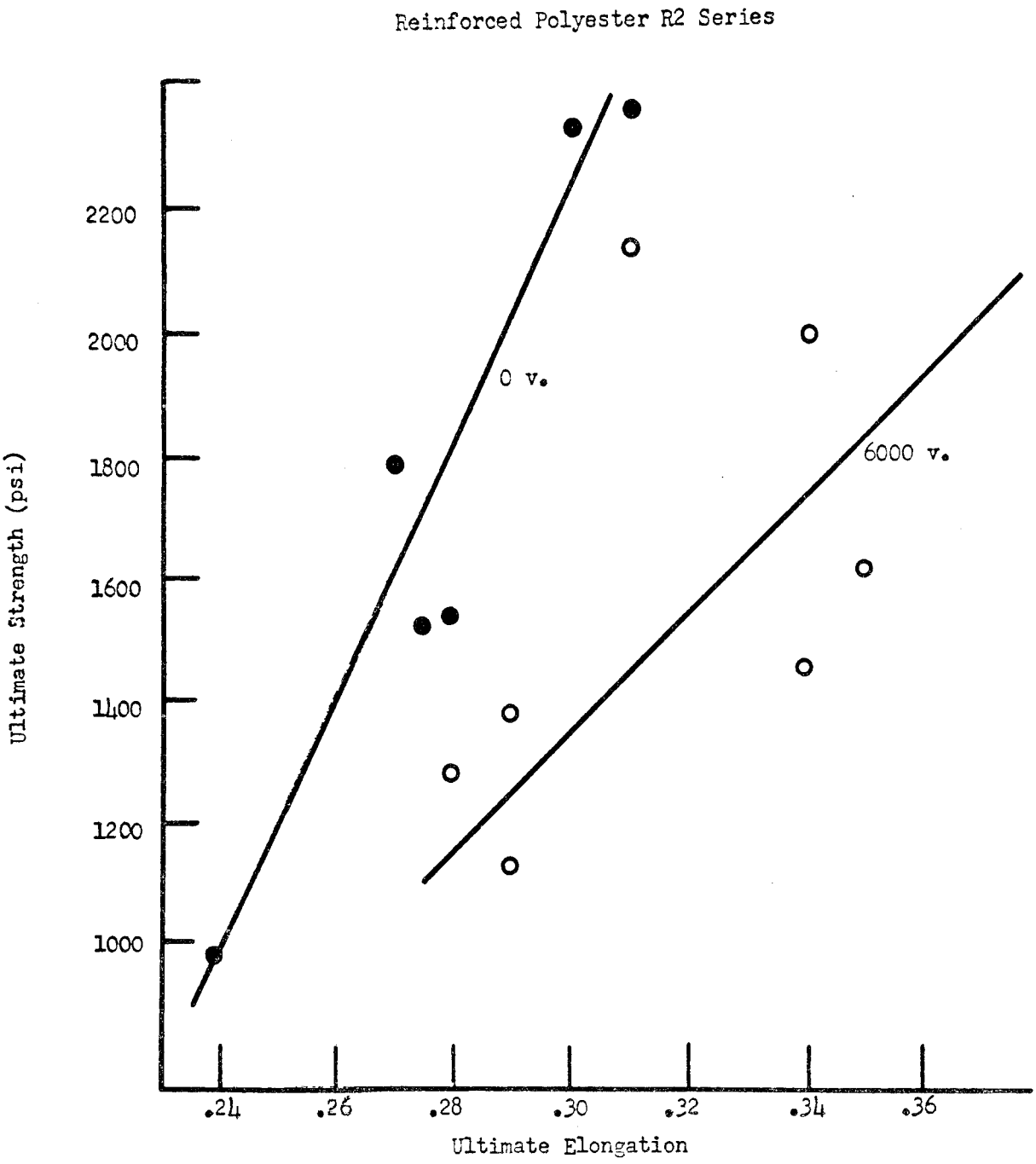

Figure 1. Effect of Electric Field Upon Tensile Properties: Glass Reinforced Polyester.

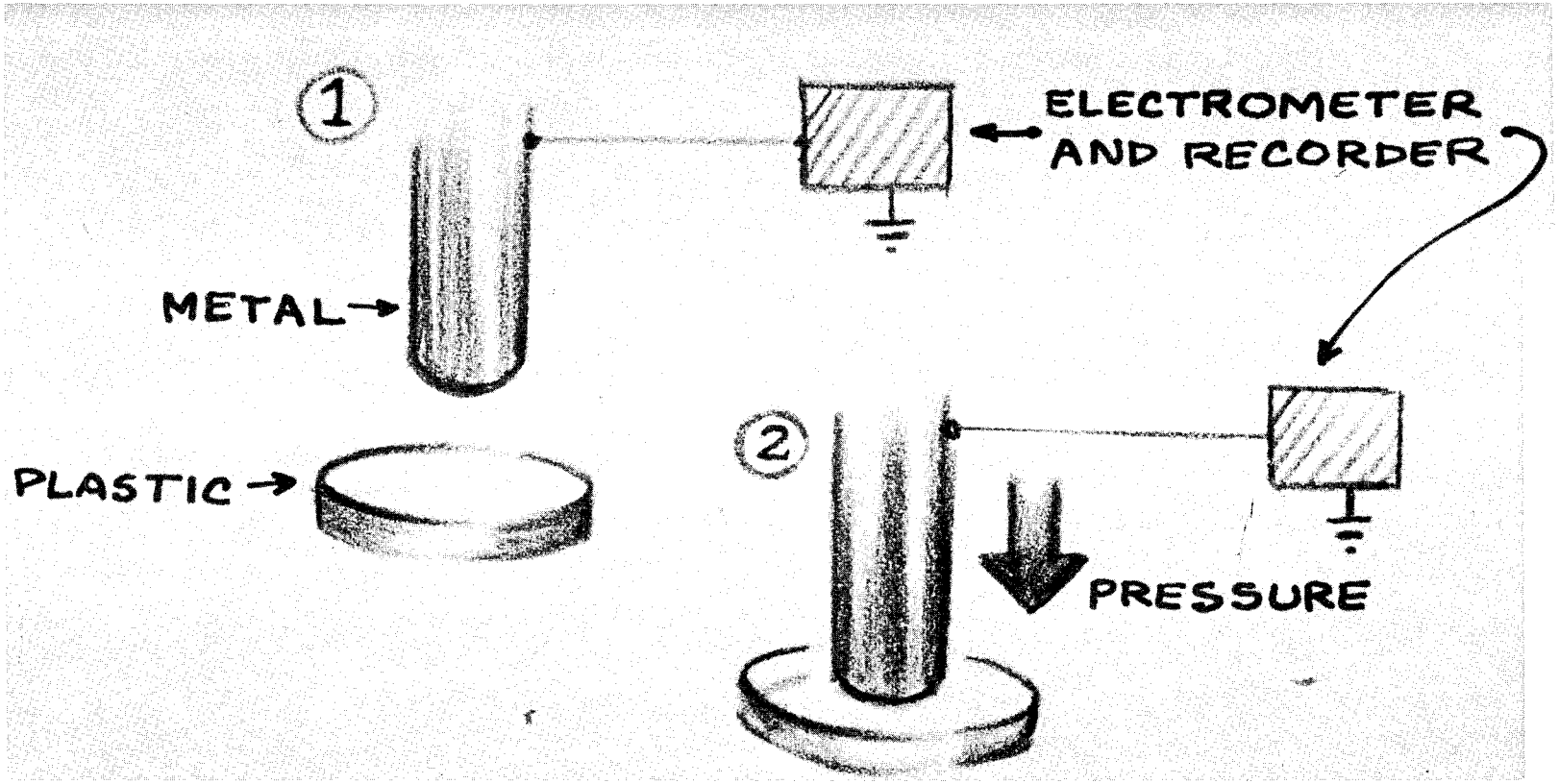

Figure 2. Repetitive Contact Apparatus: Mechanical Drive.

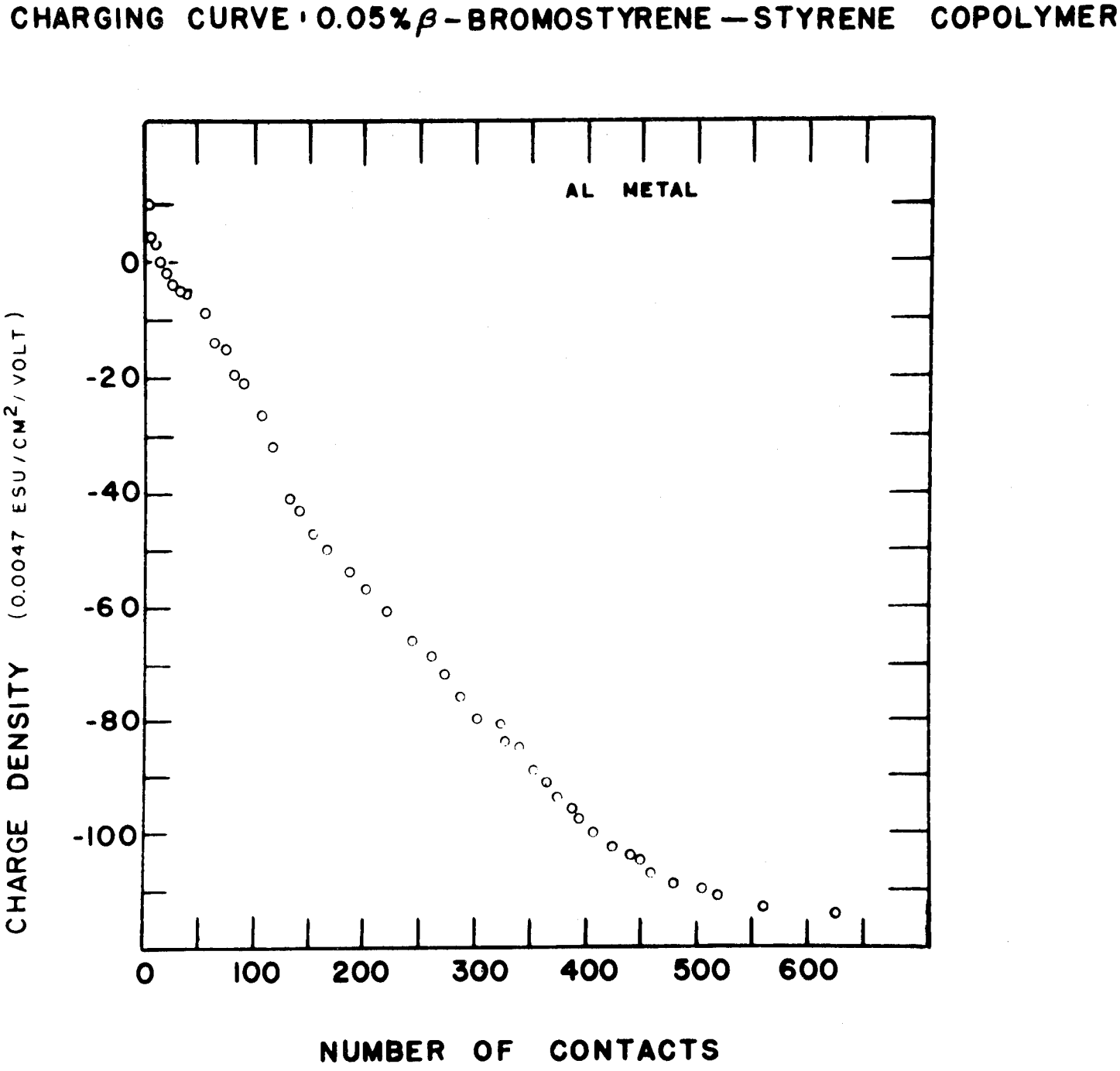

Figure 3. Charge Transfer vs. Number of Contacts: PMMA - Aluminum electrode.

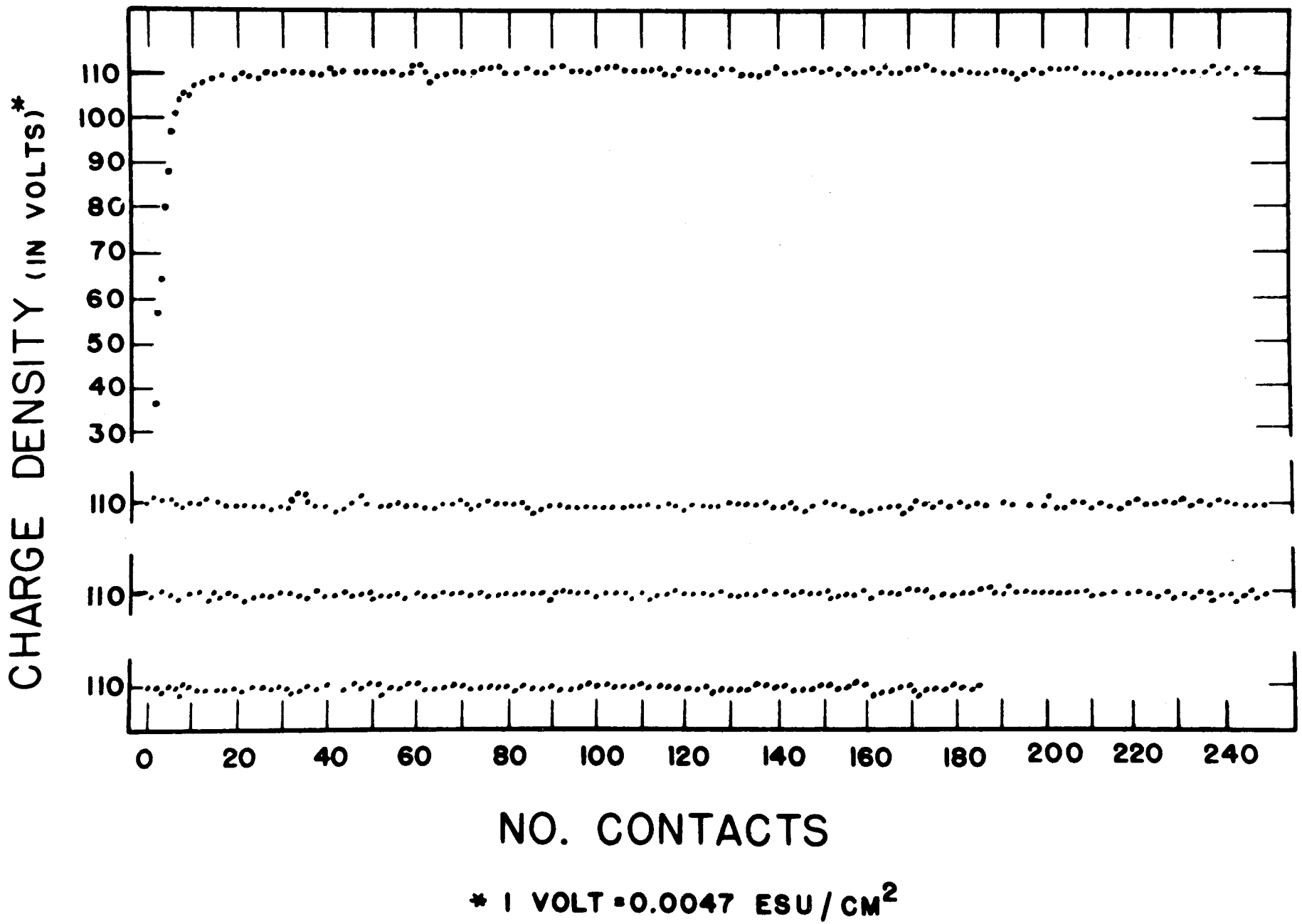

CLM 27817

Figure 4. Charge Transfer vs. Number of Contacts: Bromostyrene-styrene Copolymer Al-electrode.

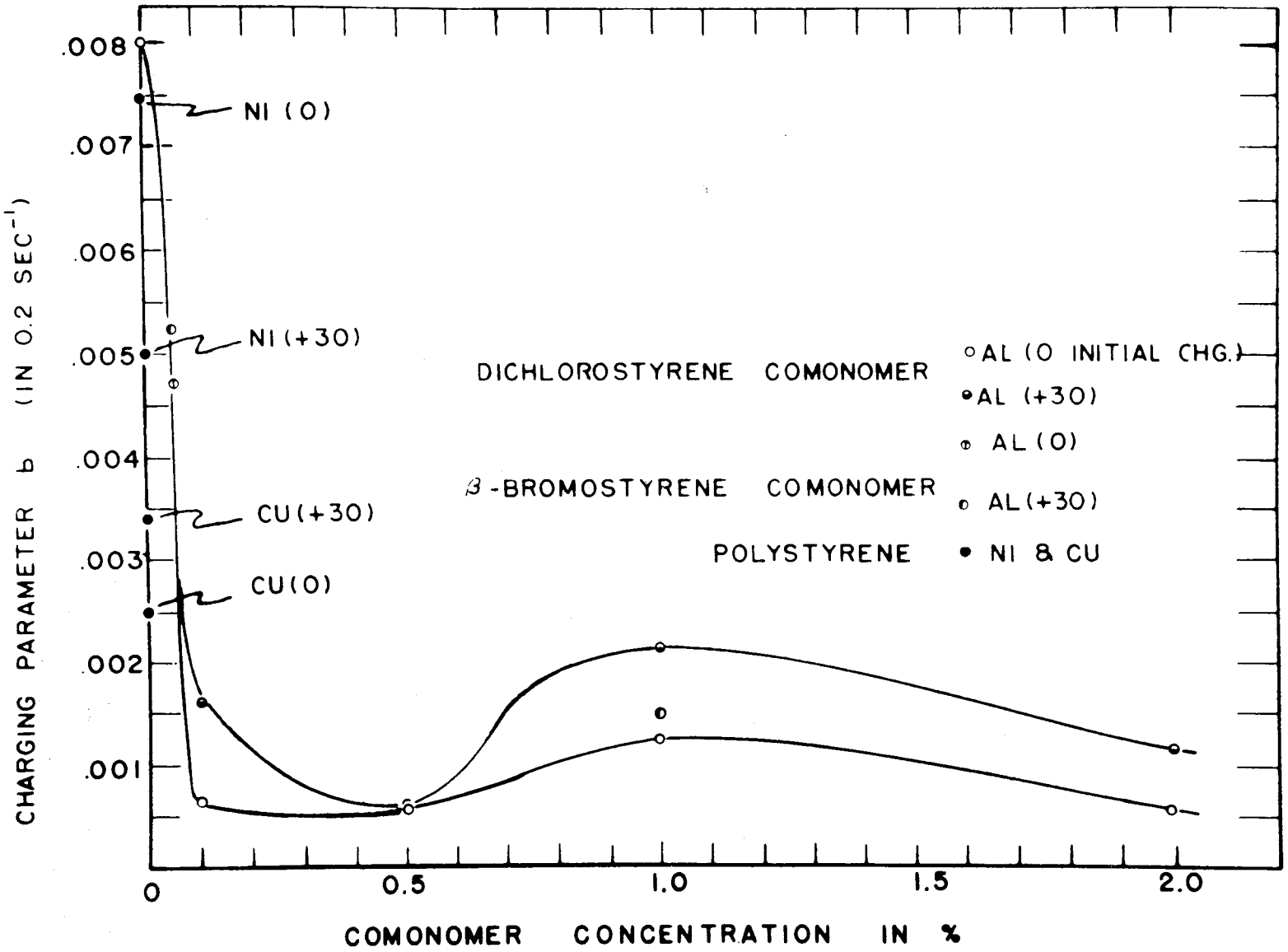

Figure 5. Dependence of Charge Transfer Parameter Upon Chemical Nature of Material.

CLM 27818

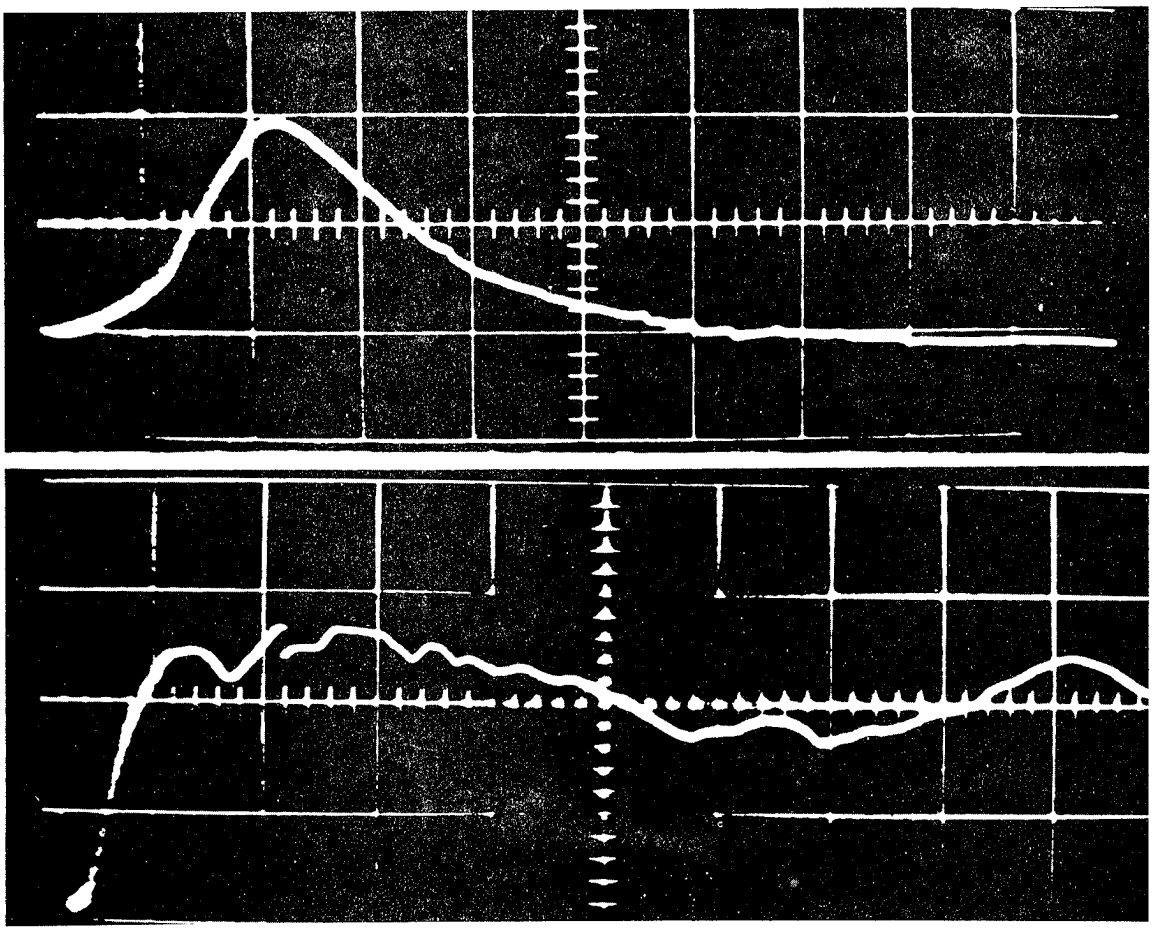

Figure 6. Measurement of Electrical Potentials in Adhesive Break.

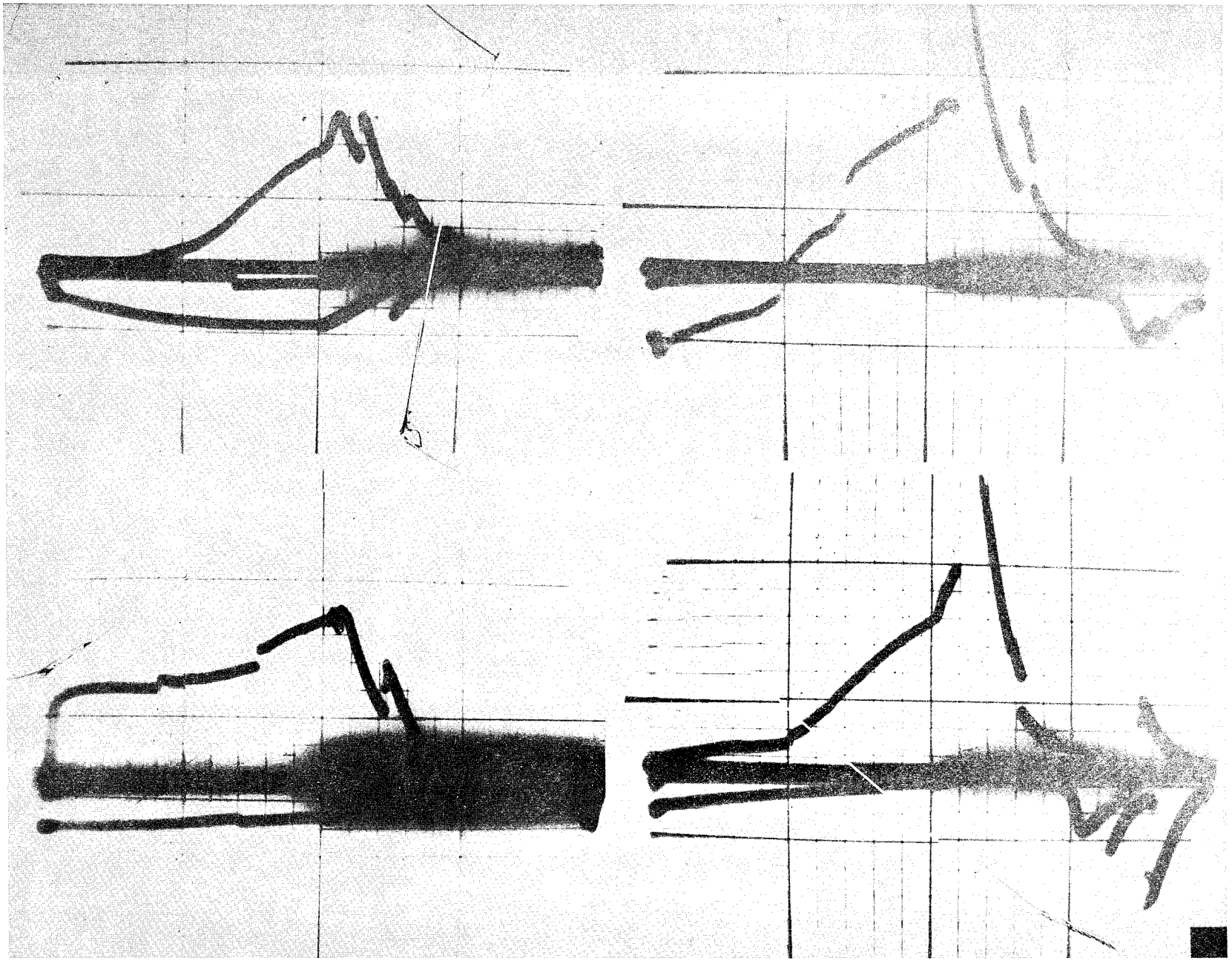

Figure 7. Observed Potentials at Break of Adhesive Bond.

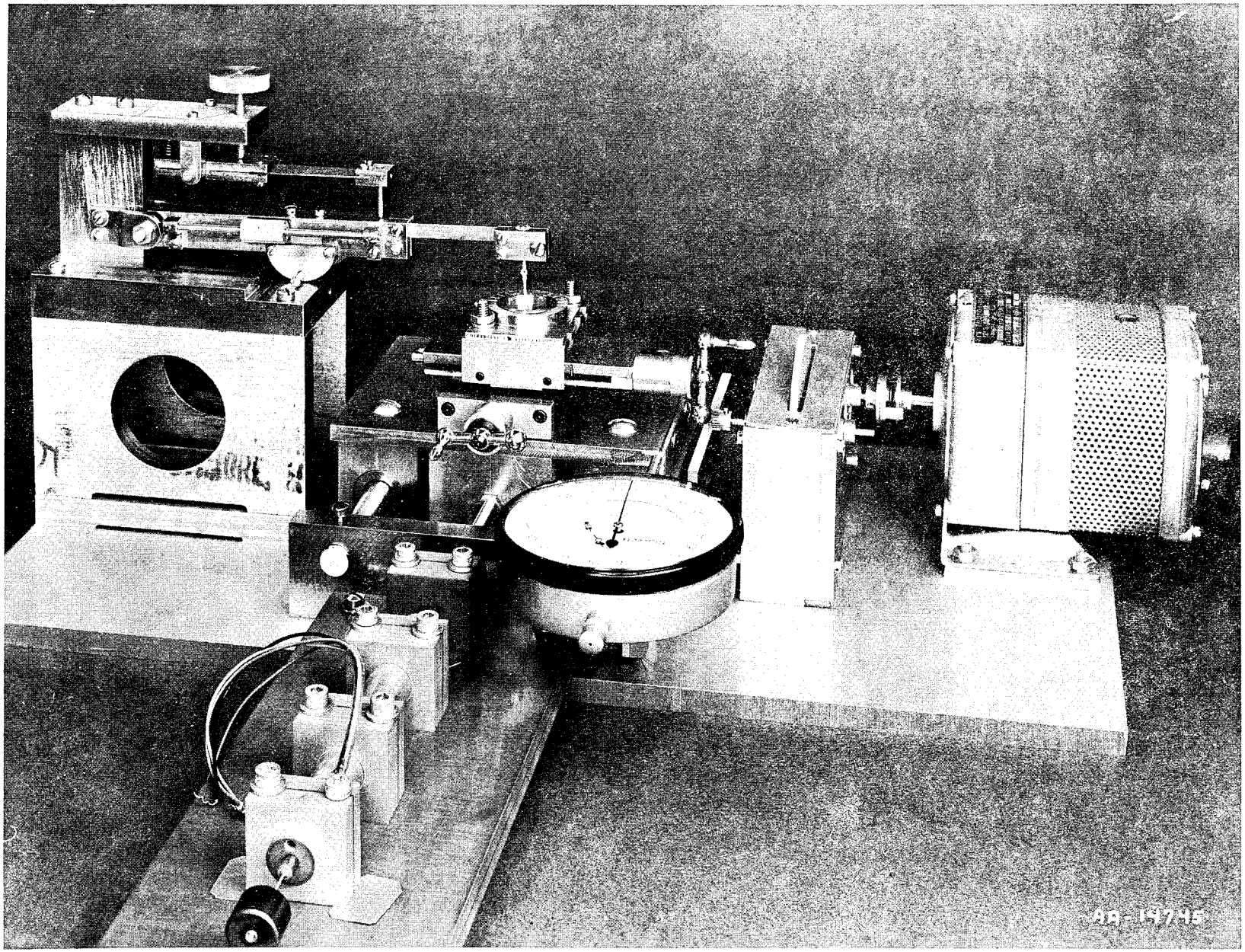

Figure 8. Electro-frictional Contact Apparatus.

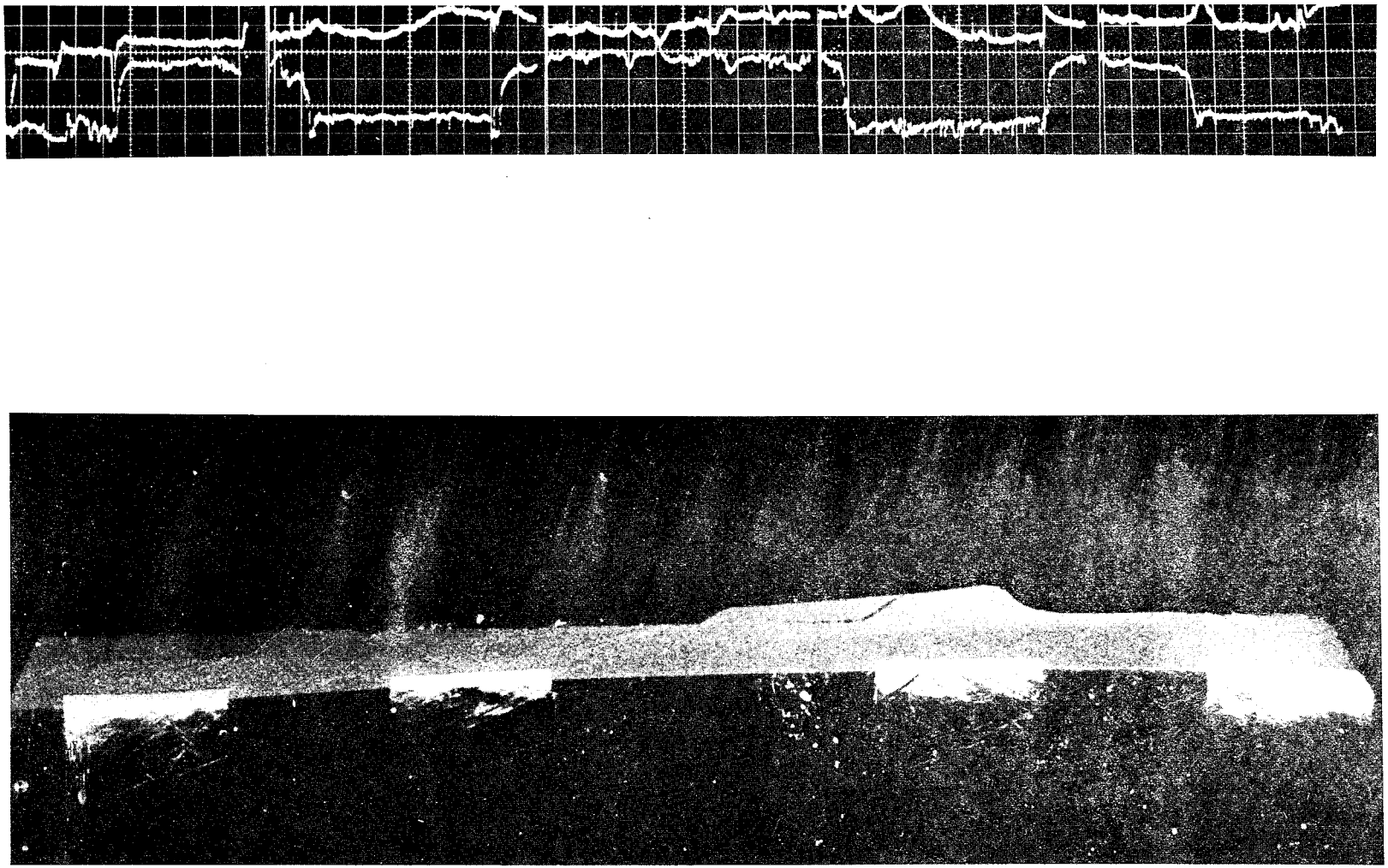

Figure 9. Electrical and Frictional Response to Change of Surface Composition.

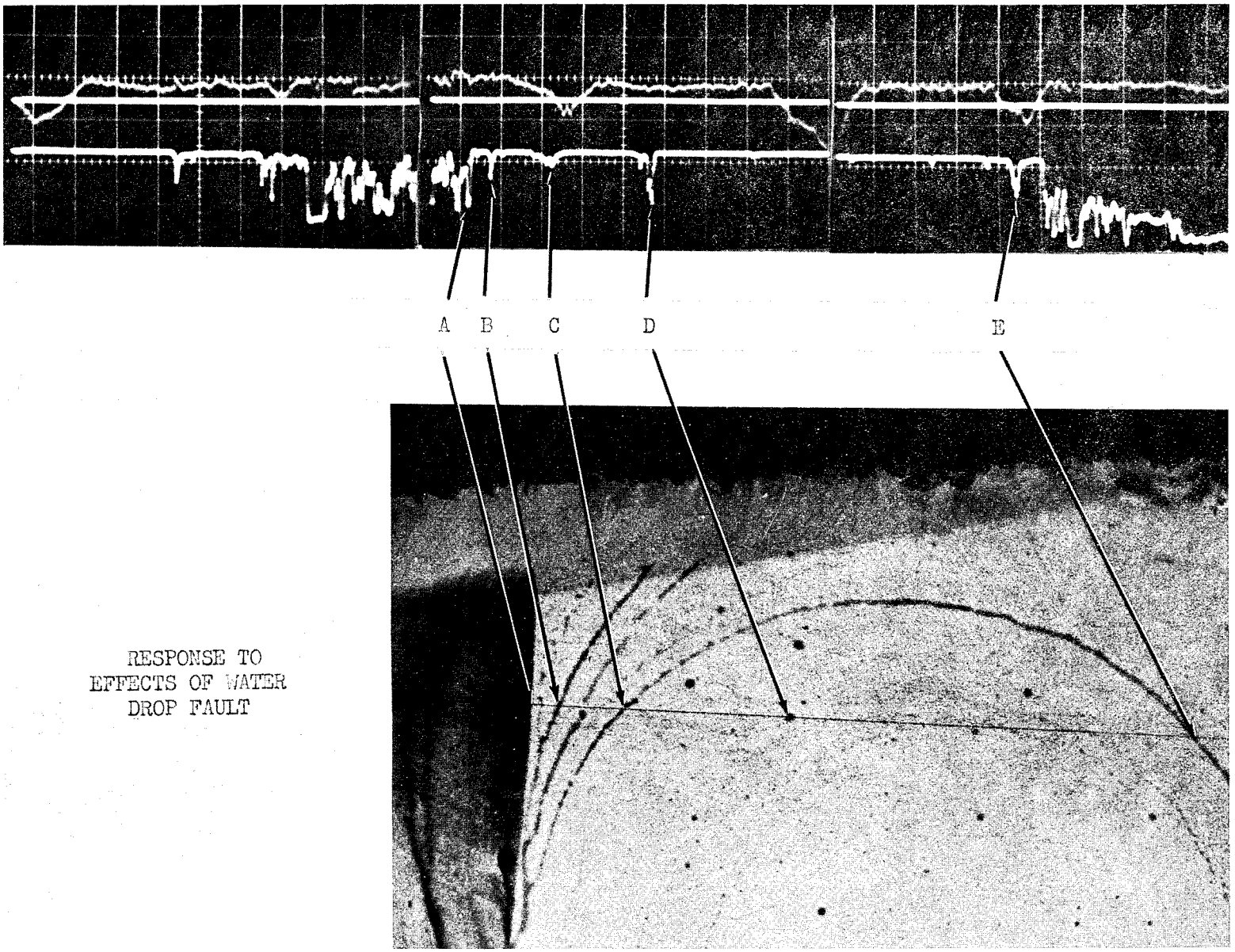

Figure 10. Electrical Contact Response to Damage from Water Drop on Silicon Wafer.

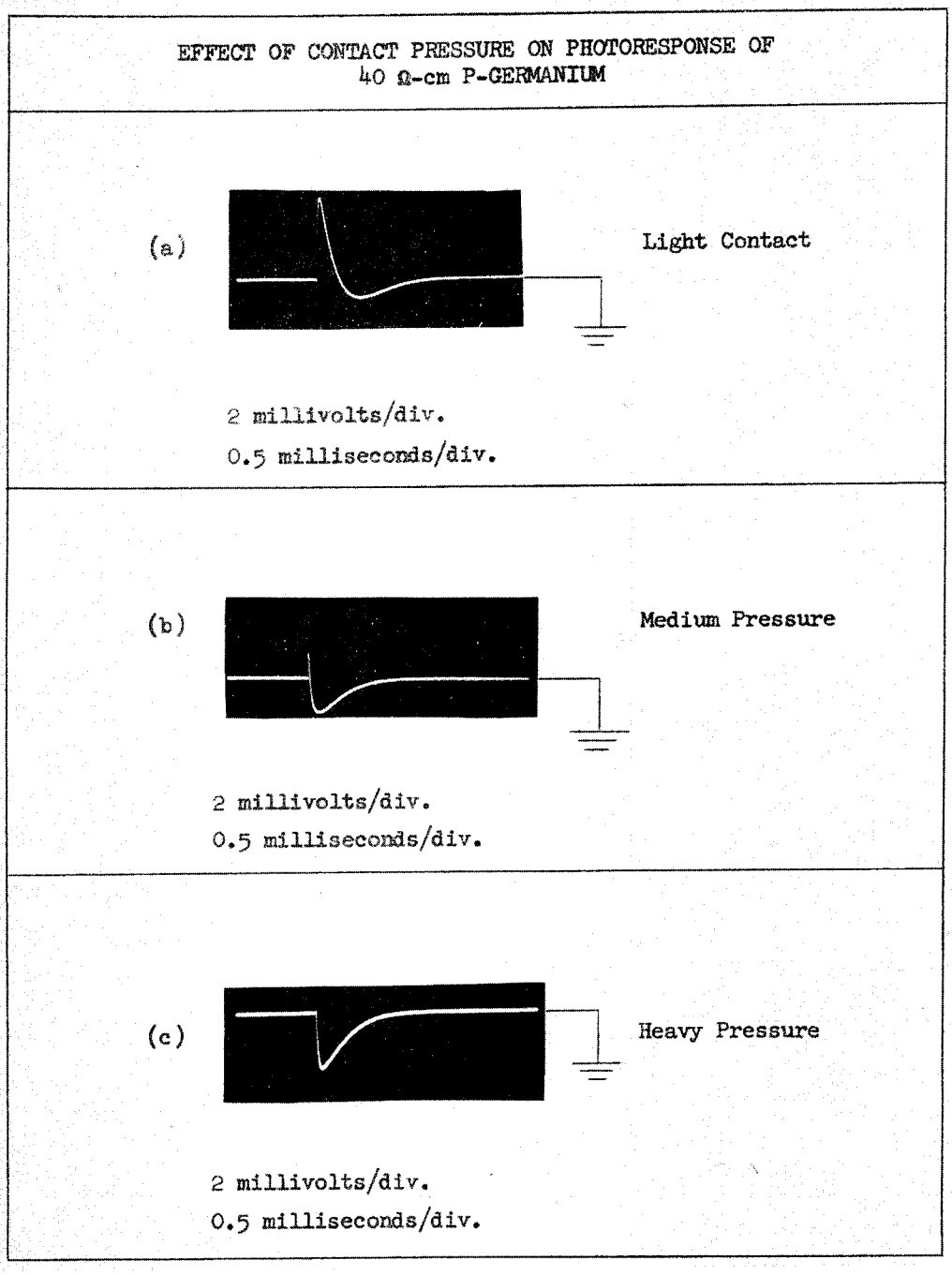

Figure 11. Dependence of Photovoltaic Response Upon Pressure: 40 ohm cm P-germanium.

ELECTROMECHANICAL HYSTERESIS MEASUREMENTS

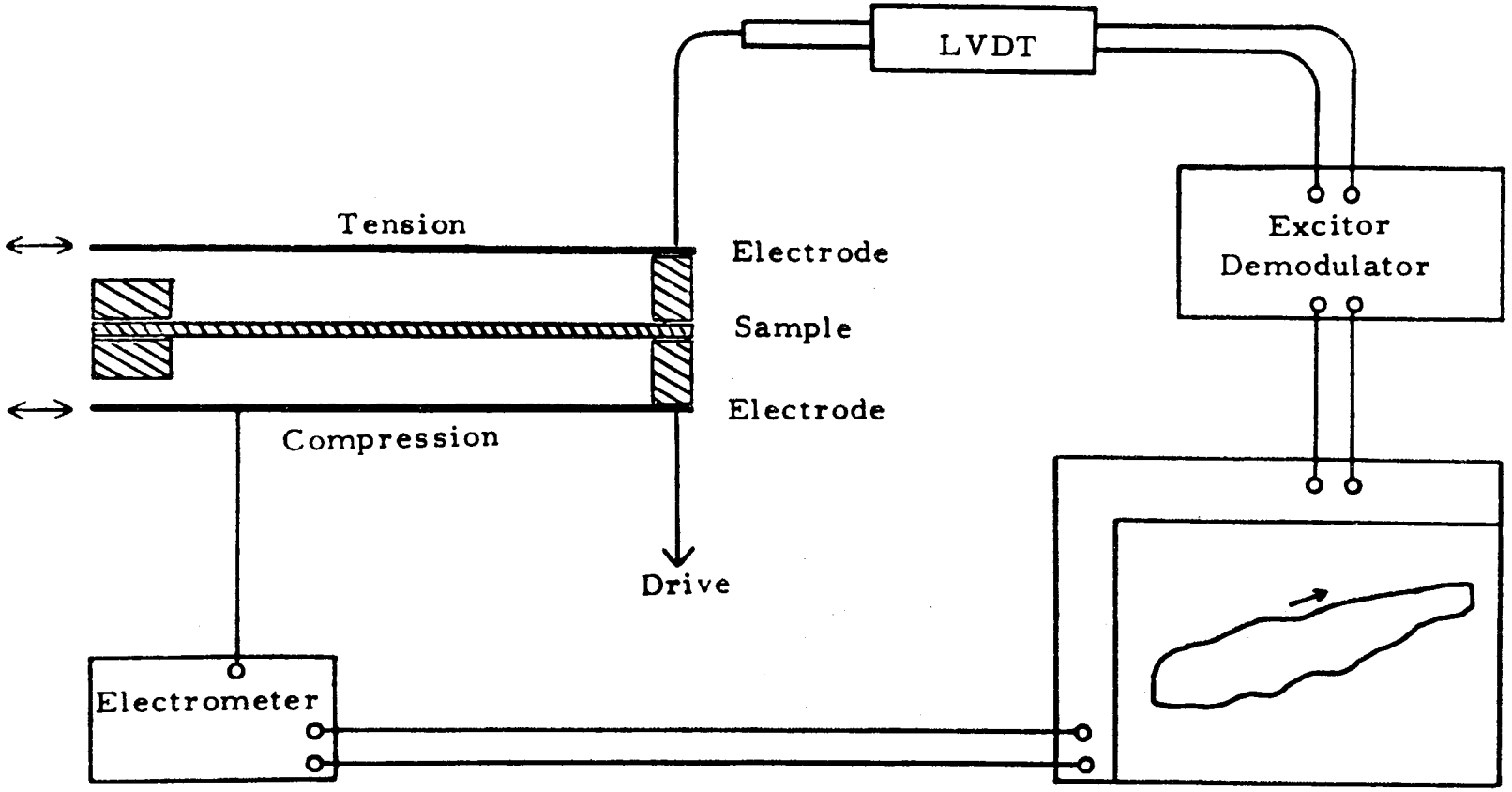

Charge-strain hysteresis apparatus.

Figure 12. Dielectric Charge Hysteresis Apparatus.

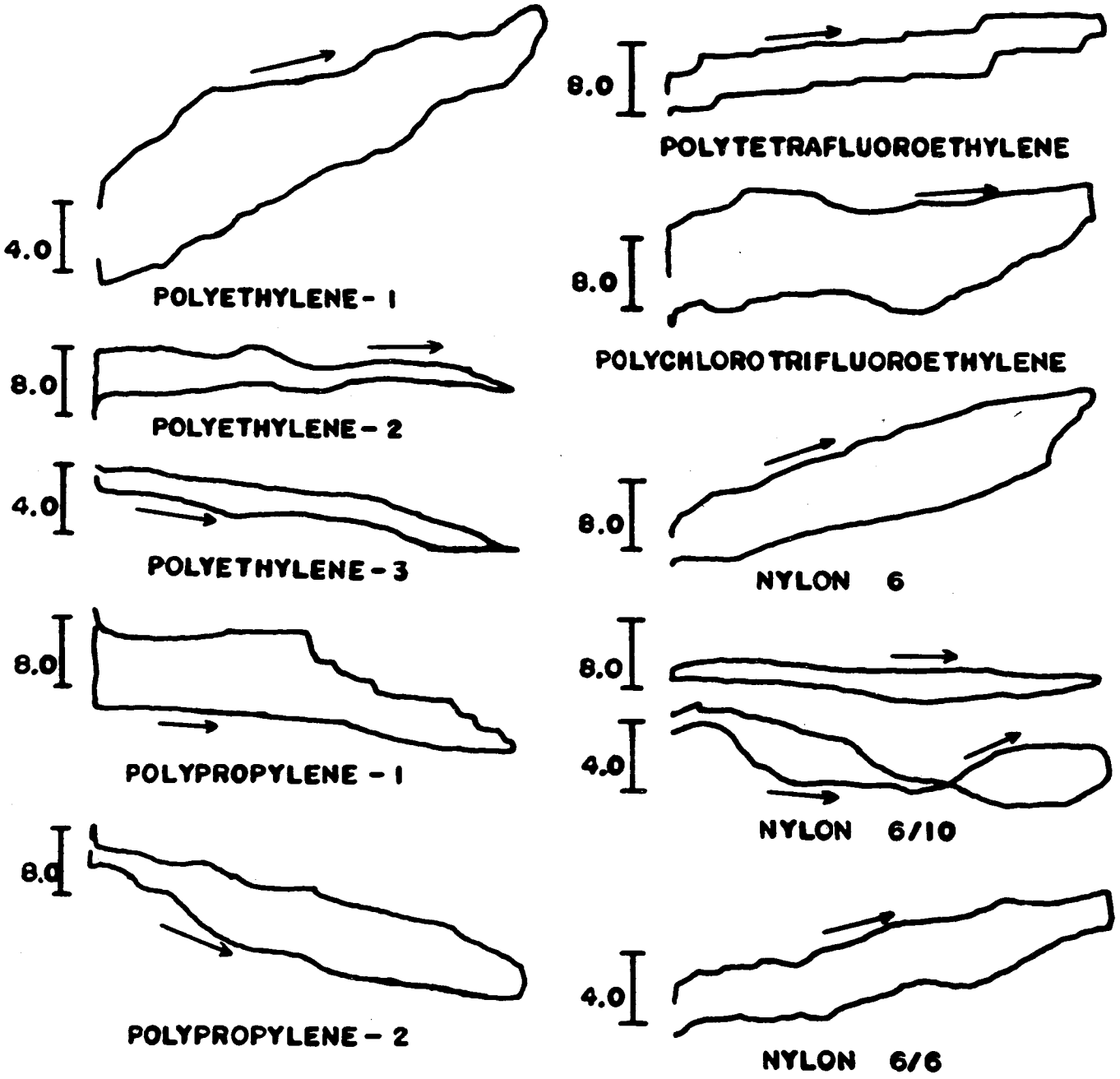

CLM 27826

Figure 13. Hysteresis Curves for Solid Polymers.

ELECTROMECHANICAL HYSTERESIS MEASUREMENTS

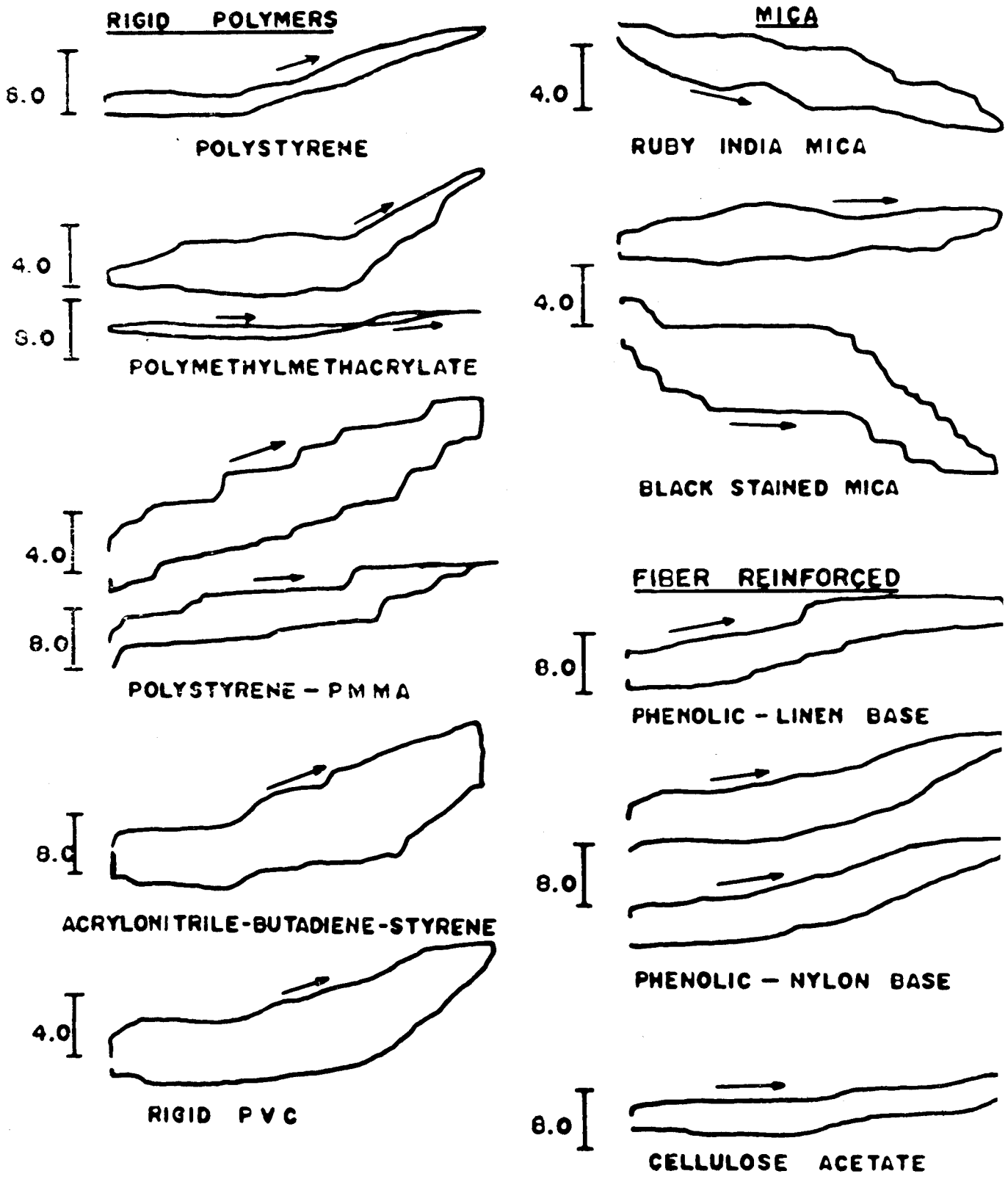

Figure 14. Hysteresis Curves for Solid Polymers.

PROPERTIES OF DIELECTRICS
at
CRYOGENIC TEMPERATURES

K.N. Mathes
Advanced Technology Laboratories
General Electric Company
Schenectady, N.Y.

INTRODUCTION

For many years the phenomenon of superconductivity has sparked fundamental interest in the properties of metals at cryogenic temperatures (-196 C and lower). Little interest has been exhibited in nonmetallic materials until space age requirements resulted in a consideration of such problems. The properties of dielectrics at cryogenic temperatures appear to be important in three respects:

1. To permit performance of electrical devices in space applications requiring cold temperatures, such as in cryogenic liquid fuels or on the dark side of the moon.

2. To permit design of electrical devices utilizing special characteristics available at cryogenic temperatures.

3. To provide fundamental information important to scientific understanding of dielectrics.

This paper reports some initial results in these three respects.

PROPERTIES OF DIELECTRICS AT LOW TEMPERATURES

Physical Properties

In many applications insulating materials fail physically before they fail electrically. At cold temperatures dielectric materials are generally quite strong but also quite brittle (low elongation to break). The thermal contraction of insulation from room to low temperatures is large compared to that of metals as shown in Fig. 1. Consequently, insulated structures containing metallic components, such as potted coils, are subject to considerable differential contraction as they cool. The problem is accentuated with rapid cooling since many materials exhibit poor thermal conductivity at very low temperatures.

The combination of thermal contraction and brittleness at low temperatures can lead to mechanical failure. Any movement at low

temperatures may lead to failure -- thus shock and vibration are important. The ability of magnet wire and small cable insulation to move at low temperatures has been evaluated with repeated mandrel flexibility tests in liquid helium. Typical results are shown in Fig. 2. The best insulation, an aromatic, polyamide (DuPont ML*), can be flexed over a 1/8" mandrel without failure. Extruded polytetrafluoroethylene (DuPont TFE Teflon*) is the best extruded covering. It is apparent that materials differ widely in their ability to be flexed at cryogenic temperatures.

Information is available, also, which indicates that flexibility is dependent among other factors, on molecular weight. Very sensitive indications of curing, thermal degradation and hydrolytic molecular scission have been obtained with flexibility measurements at cryogenic temperatures.

Electrical Properties

The voltage breakdown of wire insulations has been investigated also. Typical results are shown in Fig. 3 for ML enamel and glass fiber insulations in air at room temperature, in liquid nitrogen, in liquid helium and in vacuum at liquid helium temperature (4.2 K). It should be remembered that ML provides a continuous film and glass fiber only a spacing. Liquid nitrogen and liquid helium impregnate the glass fiber. As expected, a high breakdown is obtained with glass fiber, but in liquid helium it is very low. The results of breakdown tests on the cryogenic liquids themselves (Fig. 4) provide an answer. Liquid helium itself has a very low breakdown voltage. Many other extremely interesting and unexpected breakdown results have been obtained but time does not permit presentation here.

The DC resistivity of most dielectrics is very high at cryogenic temperatures. Typical results for a polar liquid are shown in Fig. 4. As temperature is decreased, resistivity rapidly increases to such high values that they cannot be measured. The DC resistivity of some materials, such as certain ceramic titanates, can be measured even at liquid helium temperature but polarization effects are very marked.

* A copyrighted name of the DuPont Co., Wilmington, Delaware.

The AC characteristics of most dielectrics can be measured at cryogenic temperatures although results for some materials like Teflon are at the limits of sensitivity for dissipation factor. Typical results for a polar liquid are shown in Figs. 5 and 6. The characteristic sharp decrease in both dielectric constant and dissipation factor at the freezing point of about -50C is apparent. At the lower temperatures the results are largely independent of frequency. However, frequency dependency of dissipation factor even at liquid helium temperature (-269 C) is noted for some materials such as barium, titanate, ceramic and polyvinyl-fluoride film (DuPont Tedlar*) as shown in Figs. 7 and 8. The frequency dependency of dissipation factor indicates that dielectric absorption is not completely "frozen out" even at -269 C (4.2K). Additional measurements as a function of temperature(shown in Figs. 9 and 10 for barium titanate ceramic) indicate room and liquid helium temperature.

The AC properties of dielectrics at cryogenic temperatures are fascinating. Volger of Phillips in Eindhoven, Holland, has shown that absorption peaks in quartz at very low temperatures can be both produced and erased with strong irradiation. Interesting changes in the exceedingly low values of dissipation factor with frequency have been observed for liquid nitrogen, hydrogen and helium, even though helium, in particular, would be expected to be completely non-polar.

The peculiar electrical properties of helium have been demonstrated further by Careri in Rome. He has found that ion mobility in super fluid helium increases as temperature decreases. The field for interesting theoretical investigation of dielectrics at cryogenic temperatures seems limitless.

CONCLUSIONS

While some theoretical dielectric investigations have been made with cryogenic liquids, the dielectric understanding of most non-metallic materials at very low temperatures is still quite limited. Studies to date indicate that evaluation at cryogenic temperatures can lead to fundamental new understanding of the characteristics of

polymers and other dielectrics. Engineering information on the properties of insulating materials at very cold temperatures is also just starting to become available. Without question, the needs of the space age will accelerate the development of both scientific and engineering understanding with dielectrics at cryogenic temperatures.

July 30, 1963

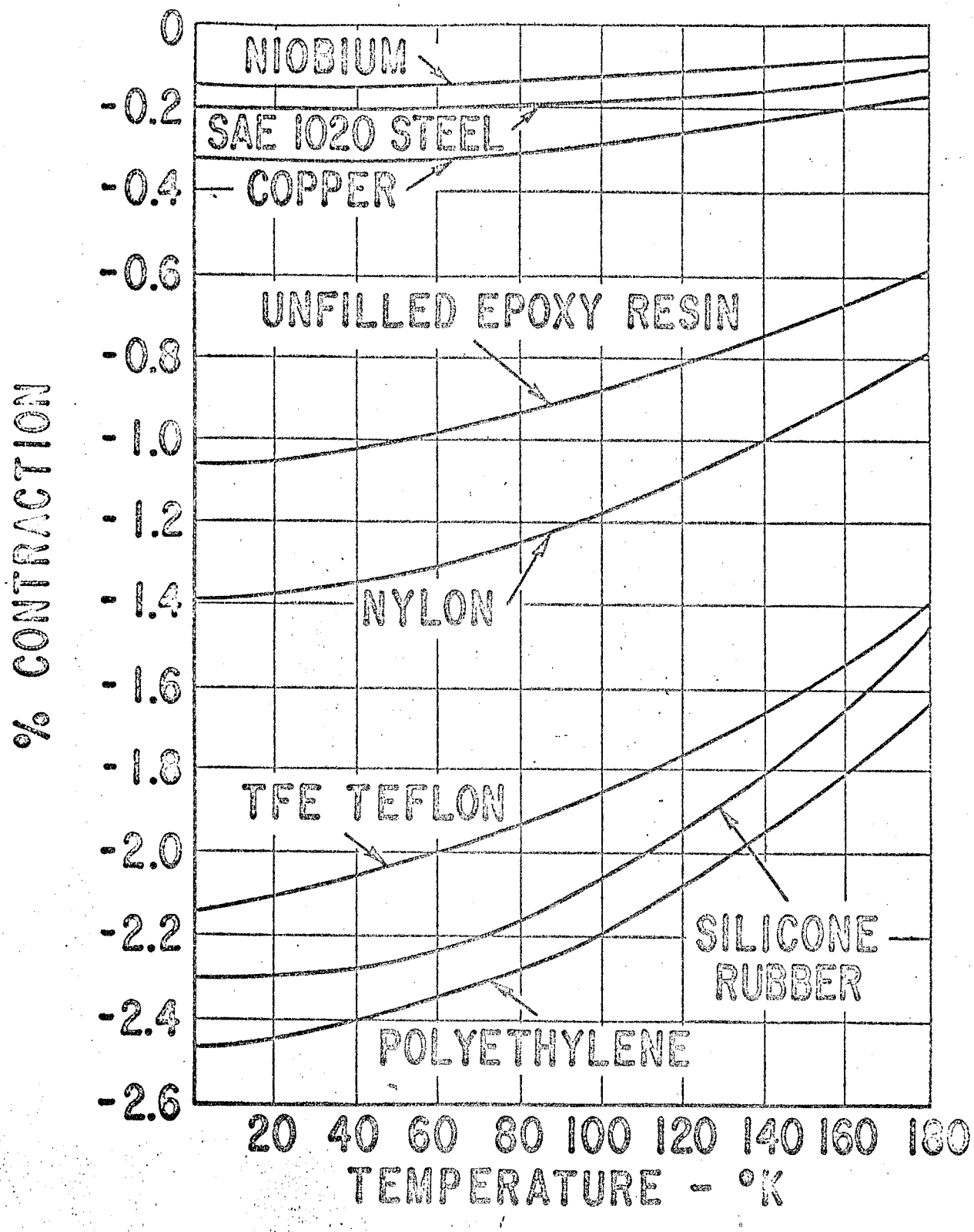

Fig. 1. Thermal Contraction with Decrease in Temperature Selected Insulating Materials and Metals

MANDREL FLEXIBILITY IN LIQUID He

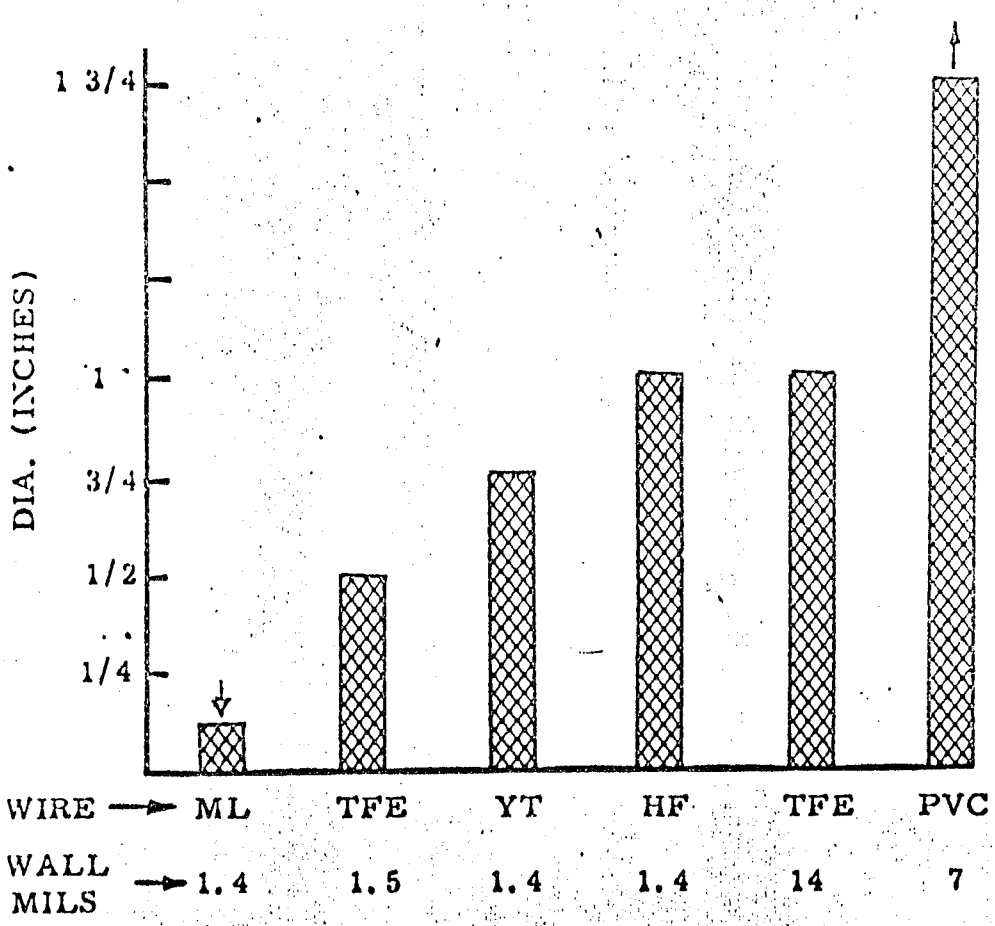

Fig. 2. Mandrel Diameter to Cause Failure of Magnet Wire Insulation in Liquid Helium

ML - DuPont Polyimide
TFE - DuPont Teflon
YT - Polyester Enamel
PVC - Plasticized Polyvinyl Chloride

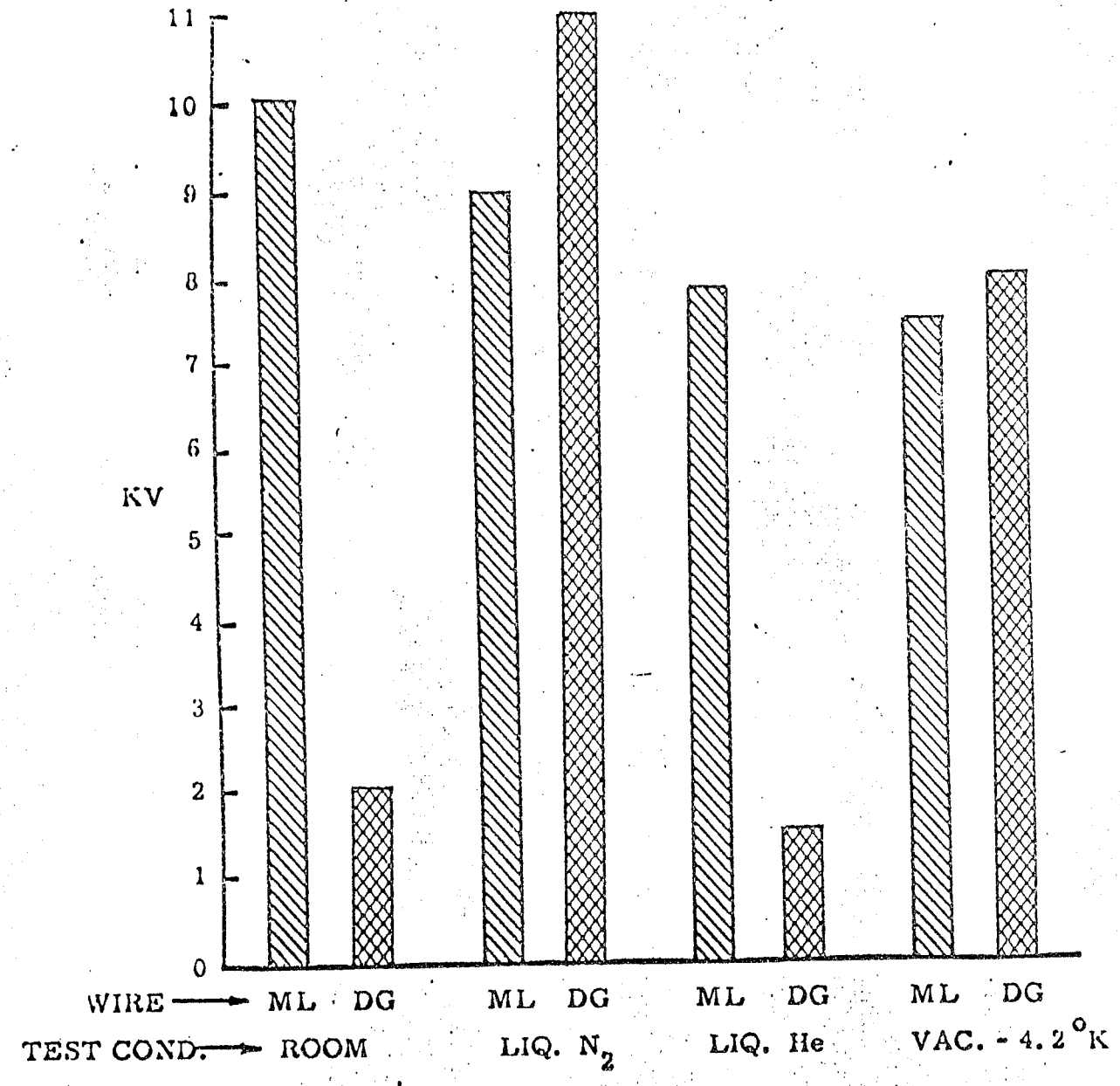

Fig. 3. Voltage Breakdown of Magnet Wire Insulation.

ML - DuPont Polyimide
DG - Polyimide Impregnated Double Glass

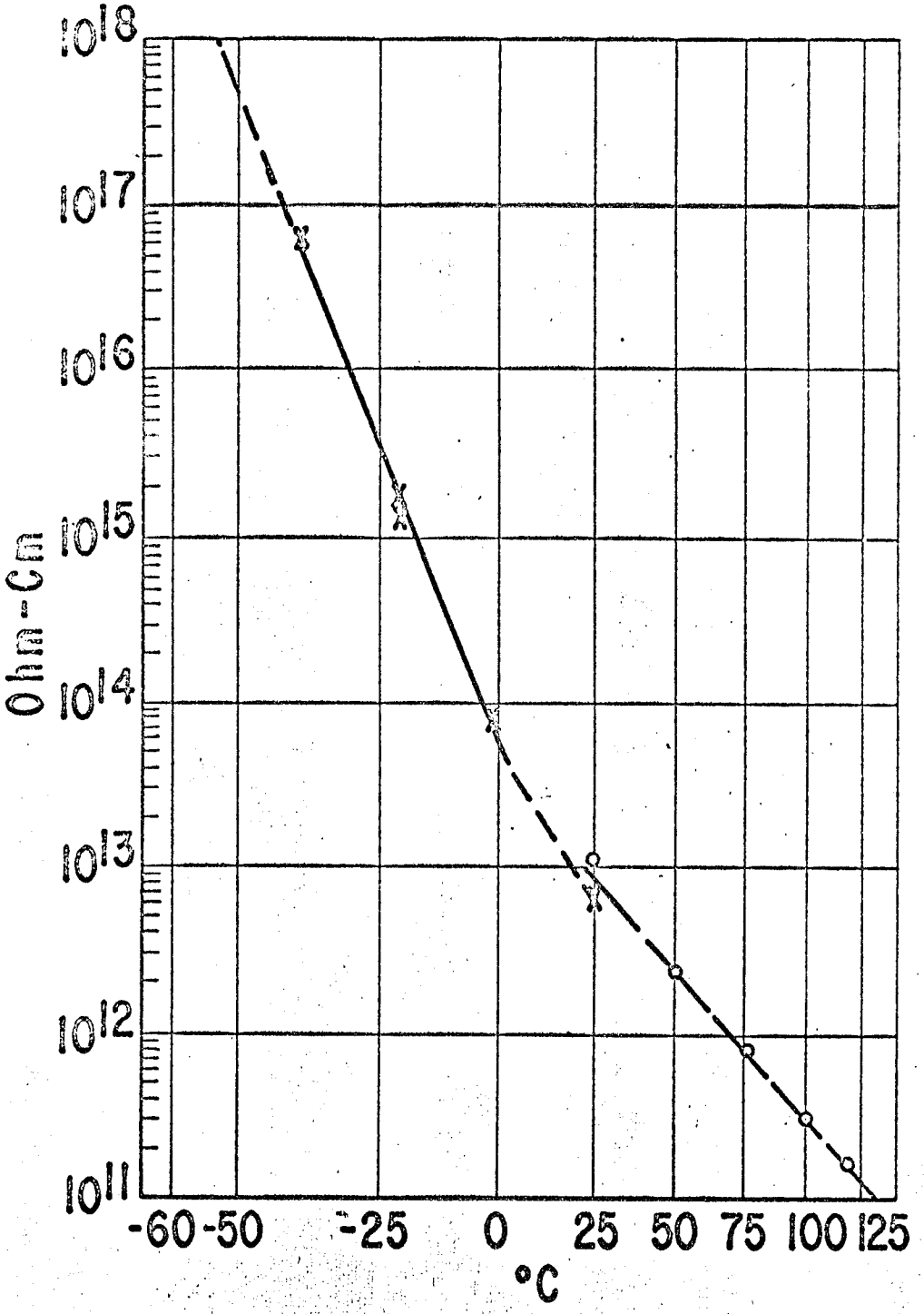

Fig. 4. Resistivity of a Polar Liquid Dielectric vs. Temperature

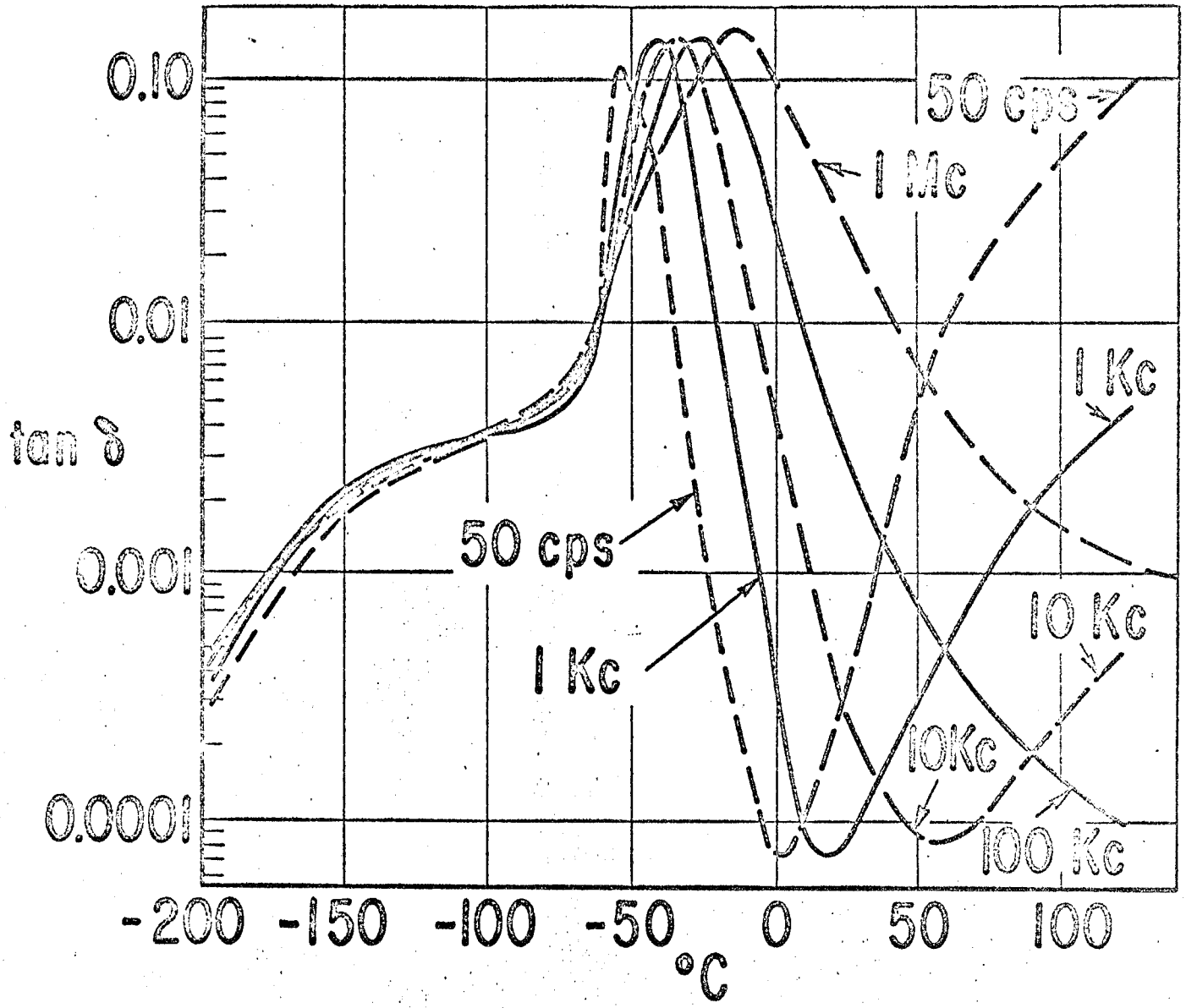

Fig. 5. Dissipation Factor, tan δ vs. Temperature at Several Frequencies for a Polar Liquid Dielectric

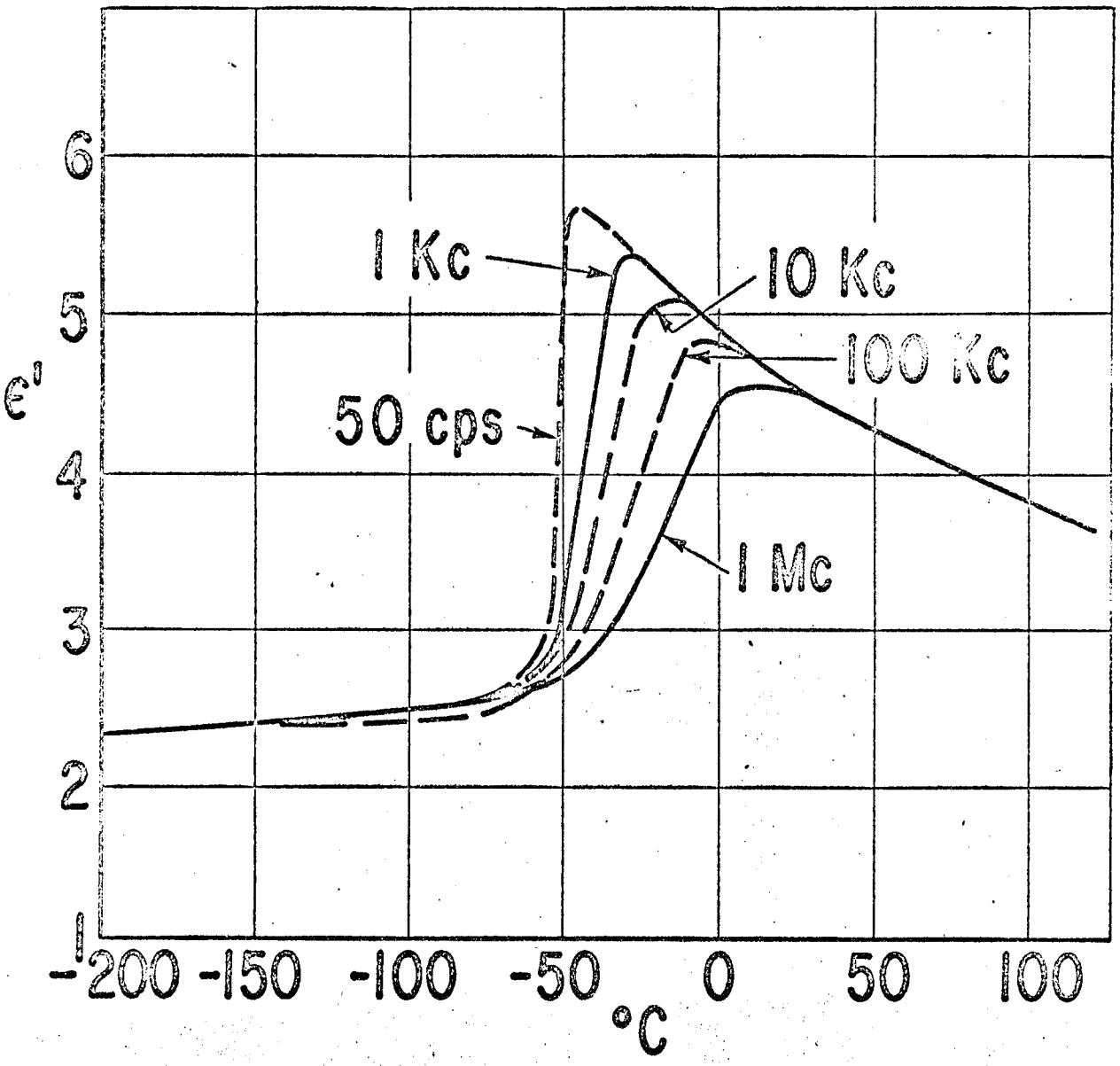

Fig. 6. Dielectric Constant, ε', vs. Temperature at Several Frequencies for a Polar Liquid Dielectric

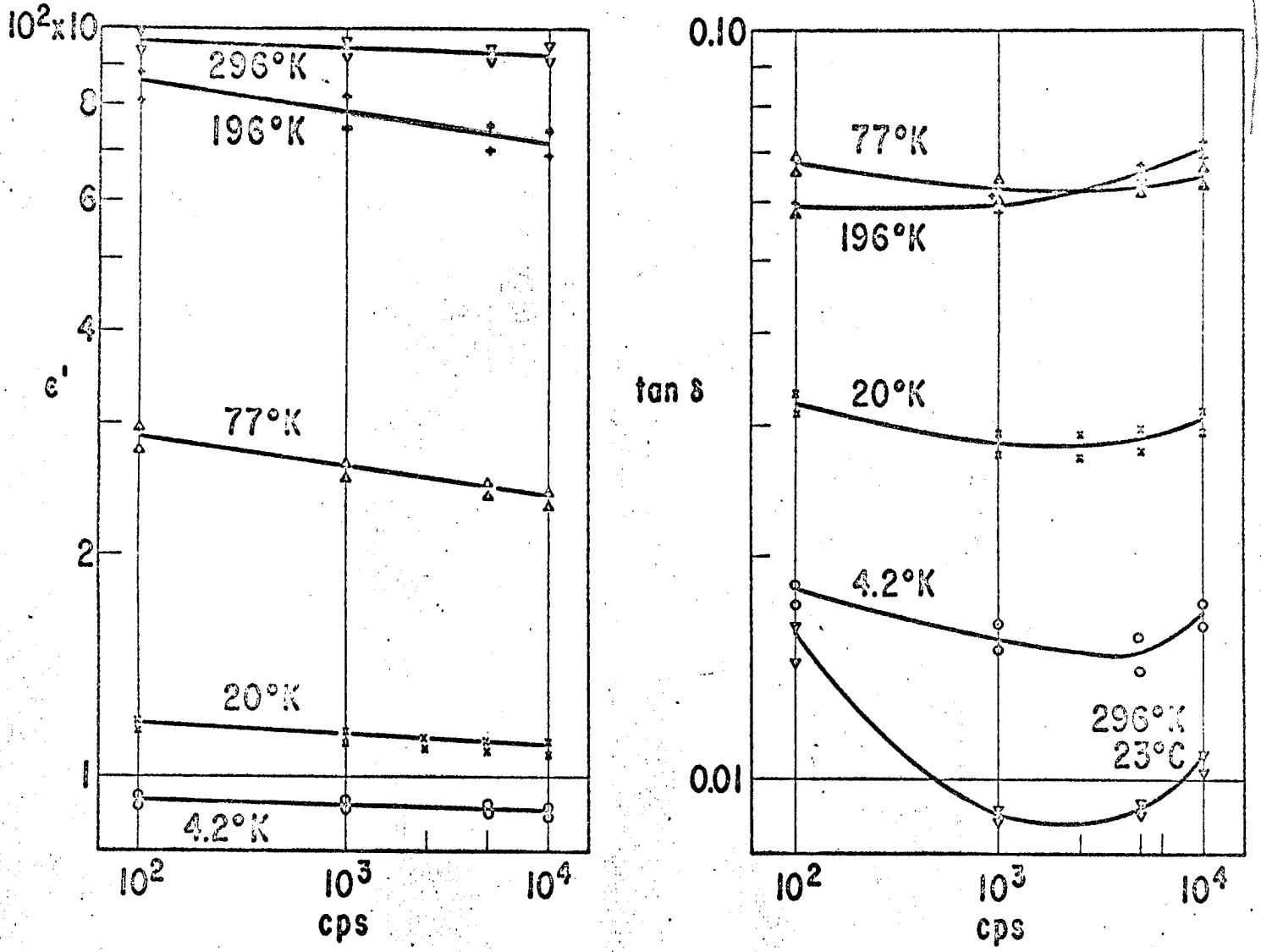

Fig. 7. Dissipation Factor, tan δ, and Dielectric Constant, ε', of DuPont Tedlar vs. Frequency at 296, 77 and 4.2°K

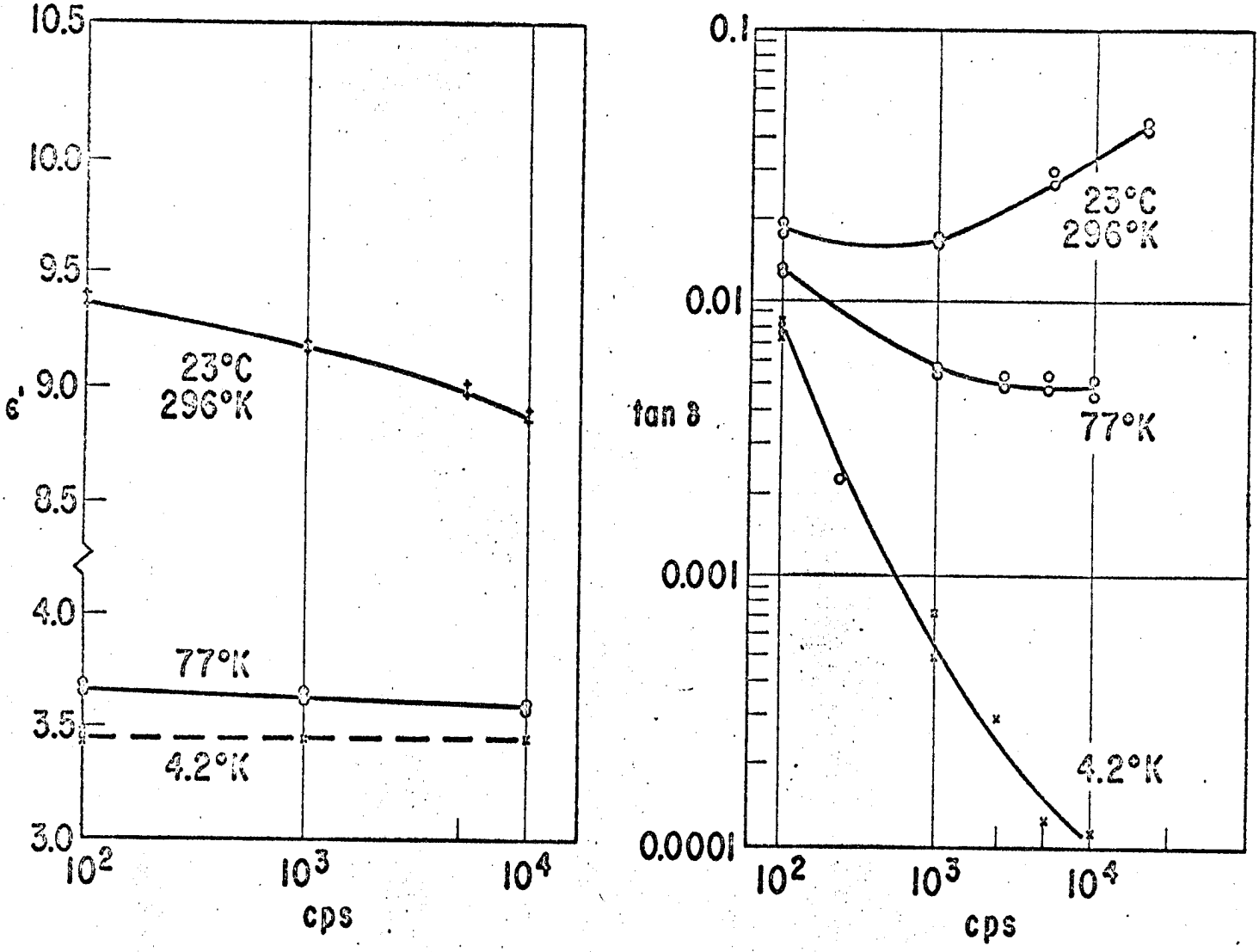

Fig. 8. Dissipation Factor, tan δ, and dielectric constant, ε', for Barium Titanate vs. Frequency at 296, 77, 23 and 4.2°K

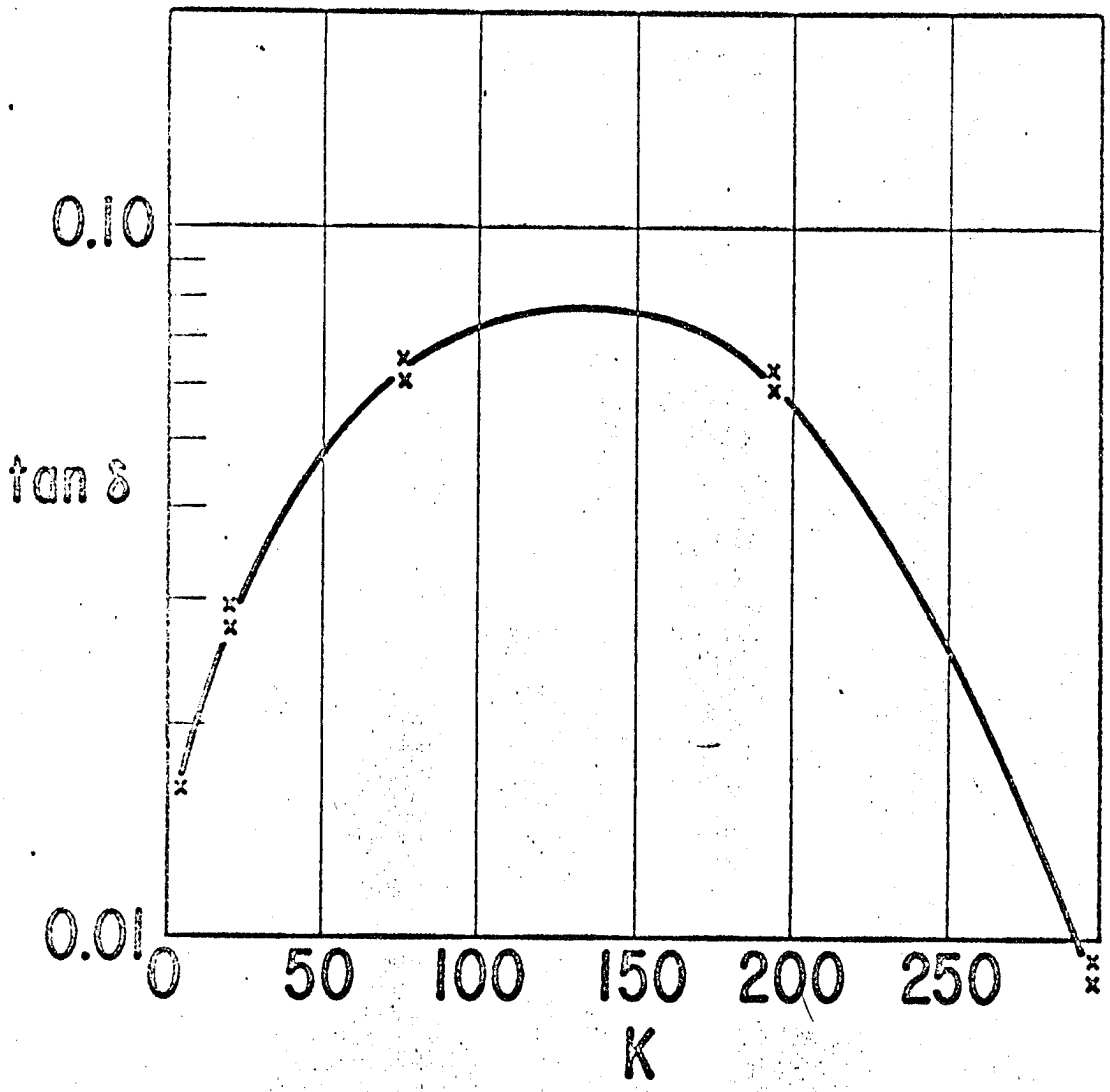

Fig. 9. Dissipation Factor, at 1000 cps vs. Temperature for Barium Titanate Ceramic

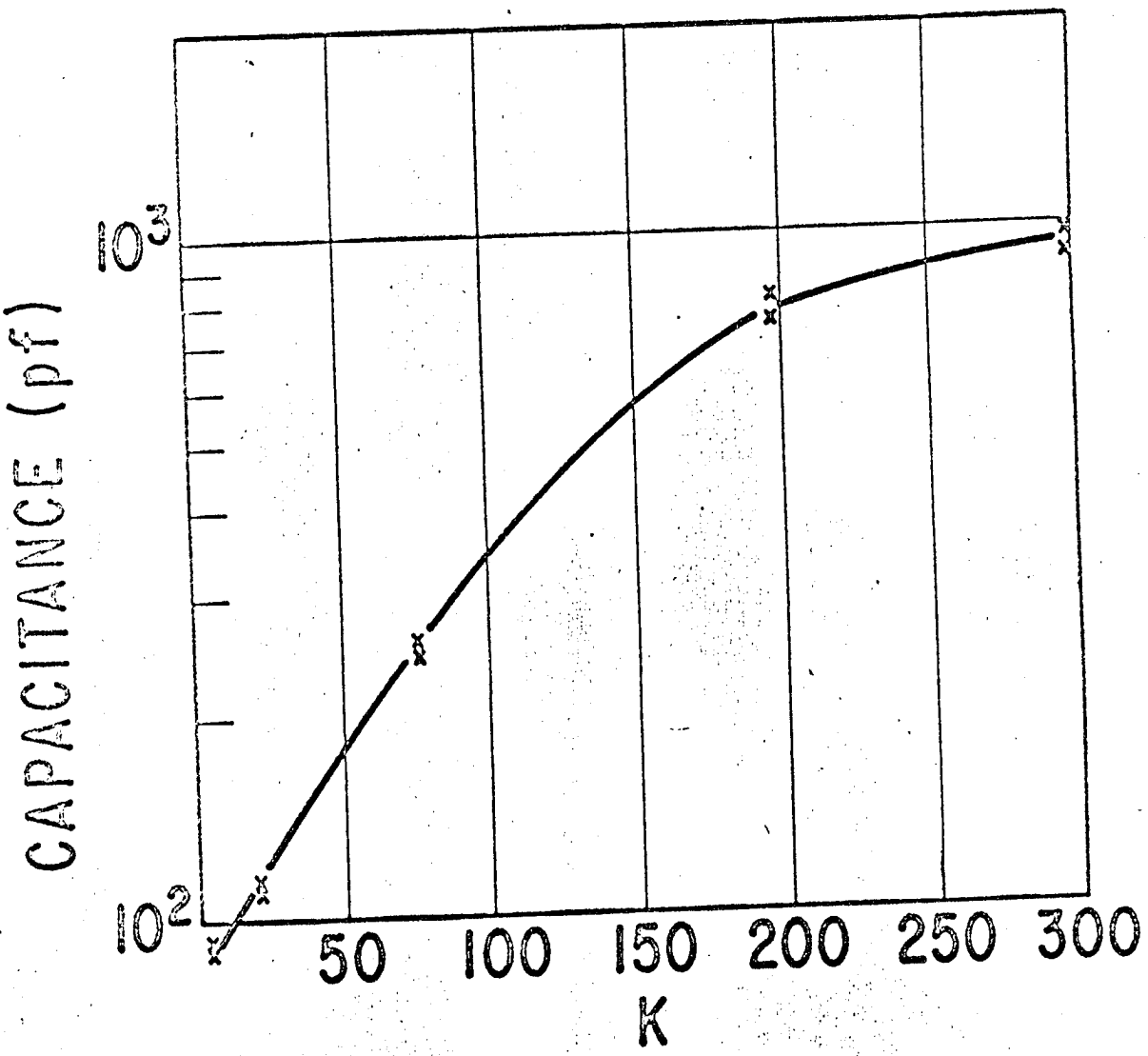

Fig. 10. Capacitance of Barium Titanate at 1000 cps vs. Temperature

THERMAL BEHAVIOR OF NEWER TYPES OF HIGH STABILITY POLYMERS

G. R. Sprengling
Westinghouse Research Laboratories
Pittsburgh 35, Pennsylvania

There has been a quiet revolution in high temperature polymeric dielectrics in the last few years. New materials have appeared which not only raise the temperature limit to which such dielectrics are useful but also broaden the scope of application and use properties. This paper presents data on a few such materials and some factors important for their creation and use as dielectrics.

It has been calculated on theoretical grounds that it should be possible to create organic polymers with acceptably low degradation rates up to around 500°C. If this is so, then it is evident that even the present generation of high temperature polymers does not approach the theoretical limit. Concerning pure thermal stability we can say that there appears to be little direct correlation between this property and the textbook values for the energy of the bonds involved in polymers now available. The problem here is perhaps not so much finding higher energy bonds to link a polymer as it is avoiding degradation mechanisms that do not involve the textbook bond energy but instead a much lower one. But even polymers that have approximately the same thermal degradation rate as measured by, for example, one of the weight loss methods often show widely different thermal lives as dielectrics. Evidently other factors beside thermal stability alone are involved and may indeed be crucial for dielectric performance on earth and in space.

Examination of an actual thermal degradation curve for a typical high temperature resin (Figure 1) casts more light on the effective behavior of such polymers. Degradation in vacuum of a sample in form of a film of less than 0.001 inch thickness was followed by means of a recording microbalance. The results differ from many other degradation curves in that the sample was thin enough so that diffusion of volatile degradation products to the sample surface was at no time the rate limiting step and also because the weight changes are not clouded by absorption of water or other atmospheric components during transfer from an oven to a balance.

The material tested to get the curve in Figure 1 was a sample of a well-known high temperature phenolic resin. Its overall behavior is typical of a class of polymers with potential for thermal stability. Without going into the finer details, it is useful to note two gross aspects of its behavior. As is apparent from the curve, there is an initial very rapid loss in weight. This initial volatile loss often does not show up in degradation studies by other methods but is nevertheless real and typical of the behavior especially of all normal condensation polymers that we have

studied. For different polymers in this class the weight loss in the first 10 minutes under these conditions may vary from 5% to 40%. The samples were in all cases given a full cure before testing on a curing schedule recommended for each resin. The amount lost from a given polymer varies rather little with the test temperature in the range 350°-500°C or the ambient pressure. About the nature of the substances lost during this initial period, our work has shown us two general facts: Condensation reactions continue in many polymers long after the polymer is ostensibly completely cured, and small volatile molecules are evolved as a by-product. The bulk of the volatile material, however, is low molecular weight polymer, which is generally unavoidably still present in completely cured, cross-linked condensation polymers, as the theory of such condensations tells us.

The gross effect of such volatiles loss is, of course, volume shrinkage of the polymer. This may have both desirable and undesirable results. In itself the volatiles loss does not affect the structure or stability of the backbone network of the polymer. The volatile molecules lost never were a part of this network. But if the polymer has a stiff, cross-linked network structure the volume shrinkage resulting on such loss will lead to internal stresses and crazing or fissuring of the bulk polymer. Electric strength, one of the chief properties demanded of any dielectric, is not an intrinsic property of such polymers in the range of conditions normally used but rather a defect state property. Micro-fissures, therefore, lead to serious loss in electric strength. Such fissuring also offers a path for rapid ingress of air oxygen and thus may cause an apparent large decrease in thermal stability in air. On the other hand, there is a growing body of evidence in support of a theory promulgated by Professor F. J. McGarry at M.I.T. to the effect that the chief effective bond in a resin-glass aggregate containing glass fibers is a frictional one. Here volume shrinkage of the polymer matrix may lead to increased frictional forces and higher mechanical strength, at least up to the point where the tensile strength of the polymer is exceeded.

After the initial volatiles loss it is characteristic of polymers with good potential for thermal stability to stabilize at a low and, as far as we can see from curves like Figure 1, a nearly constant rate of weight loss. Such stabilization is not true of all polymers. For example, a good many epoxy resins we have tested have shown a curve continuing at a relatively high rate to essentially 100% weight loss. The volatile fragments into which the samples tested broke down were of rather high molecular weight--on the order of 1000 or more--and diffuse through bulk polymer so slowly that in thicker samples the rate of weight loss is dependent on the diffusion rate. Degradation in such polymers shows up as a softening as they are plasticized by their own, retained degradation products.

In many thermally stable polymers the instantaneous rate of weight loss does not actually become constant, as we can see in the plot of Figure 2. Considering the data this way it is apparent that in the period following the initial loss of volatiles the instantaneous degradation rate decreases rapidly to very low values over a very narrow span of conversions. In the experiment shown we were unable to follow the rate to yet lower values since

we had reached the sensitivity limit of the balance used to measure the weight loss. Obviously, the rate must level off somewhere below the curve shown. This drop in rate is the opposite of what one might expect in a polymer degrading by a random break mechanism. In such a polymer the probability for formation of a volatile molecule by degradation is a function of the number of polymer molecule ends, which increases with conversion. One would thus expect an increasing rate. In some polymers a rate decreasing with increasing conversion is explained by degradation taking place preferentially at specific weak spots in the chain, which are progressively eliminated as the degradation proceeds. However, in a large class of polymers of present interest for their thermal stability, analysis shows that the passage through this region of rapid rate decrease is accomplished by increasing aromaticity of the polymer. Most generally stated, the polymer goes through a stage of fused aromatic rings which could be a step toward the formation of graphite. However, the end products at any stage of degradation here considered may be jet black but are of high electrical resistivity; they are not graphite.

One thing more has not been covered in Figure 1. Toward the end of the experiment when a very low if not steady rate of degradation in vacuum had been attained, air was admitted to the system. The change in the rate slope is apparent. The change in degradation rate on thus going from vacuum (or inert atmosphere) to air is shown for several types of polymers in Figure 3. It is evident from this that in the usual terrestrial environment oxidative degradation completely overshadows straight thermal degradation. Conversely, in space we may expect many polymers to exhibit better thermal stability by several orders of magnitude than in air. This improvement may be expected to be in inverse ratio to the oxygen partial pressure of the environment.

The facets of polymer degradation that we have been talking about seem to us to contain at least some of the factors that prevent present polymeric dielectrics from reaching in practice the thermal performance that they appear in theory to be capable of. On this basis we can formulate a number of requirements to be met by a polymer dielectric designed for optimum thermal stability:

1) Such a polymer should have a structure that permits no low energy degradation mechanisms. This is simply to say that thermal stability should be relatively good to begin with or the other factors involved in prolonging its dielectric life will not become operative.

2) The ideal polymer should have a highly aromatic structure to begin with or at least a structure capable of aromatization with the minimum molecular change. The thermally very stable form such a polymer reaches after the preliminary stages of degradation does not, of course, have the same molecular structure as the original polymer. The final stable structure may nevertheless be just as useful as dielectric as the original one provided the changes involved in going from the one to the other are not destructive. The process might then best be considered a final step in polymer cure.

3) Either the amount of volatile material initially present in such a polymer or at least the destructive effects of its loss must be minimized. There are several possible means of accomplishing this. For example, only long molecules can be left in the B-stage of the polymer which is converted into a dielectric member through final cure. This leads to highly viscous solutions in the form in which the polymer is applied. Or, the polymer can be given inherent creep, which will allow it to use this mechanism for relieving internal stresses engendered by the volume change ensuing on initial volatiles loss. Other mechanisms are possible. It should be remembered that the outgassing or removal of these volatile fractions from a polymer dielectric is final; the resultant product can be as stable as a high vacuum oil.

4) As few reactive groups as possible should be left in the final polymer in order to minimize oxidative degradation. Since reactive groups of much the same nature are often needed for the formation of the polymer in the first place this may not be easy to do. An alternative solution possible in at least some dielectric members is to diffusion limit the rate of oxygen entry and thus the oxidative degradation rate.

Attacking the problem of a space dielectric in this manner brings with it several corollary advantages: Relatively high resistance to radiation and corona discharges, due to high aromaticity of the polymer; low electric loss and high electric strength, due to lack of functional groups or defects in structure; low outgassing, due to removal of initial volatiles; and in general much superior performance in space relative to that on earth.

We have at the Westinghouse Research Laboratories attempted to prove out some of the ideas expressed above by creating a number of new families of polymers intended for use as dielectrics in various forms. Of course, not all of the principles discussed can be applied to any one polymer. Individual factors in the behavior as discussed above may assume dominating importance depending on the aggregate in which the polymer is combined and the demands of the end use intended. The materials designated by the letter "D" in the following figures are resins in the Doryl family of polymers based on diphenyl oxide, recently introduced commercially by Westinghouse. Materials designated by "E" contain another thermally stable polymer which is still in the laboratory stage at present. The "AI" refers to one member of the family of aromatic-imide resins as developed by Westinghouse. All materials shown were manufactured and tested in the same manner to insure comparability of data.

Even in dielectric members mechanical strength is often required. Figure 4 shows the thermal aging behavior in air of a number of new and older polymers in form of glass cloth laminates. Here the behavior of the well-known high temperature phenolic and the standard silicone laminate shown represent extreme behavior types. The silicone has lower initial volatiles loss and is also able to relieve internal stresses by creep. It never reaches very high at-temperature strength but maintains its properties for a very long time. As we saw in Figures 1 and 2, the phenolic resin is

characterized by relatively high initial volatiles loss and is also a rigid resin. It reaches very high at-temperature strength but degrades rapidly due both to its molecular structure and to fissuring caused by increasing internal stresses. Heretofore there have really been no materials available intermediate in behavior between these two extremes. This gap we have attempted to fill. Only a few compositions are shown of the many variants available. Each also is intended to optimize some factor in processing or behavior in use other than mechanical strength. For example, the lowest D-polymer on the graph is outstanding for electric strength, low electric loss, and punchability. The next higher D-polymer line is for a laminate made by bag molding with only 15 lbs. pressure, a technique often necessary for the forming of large or complicated dielectric structures but usually leading to serious loss in thermal life. The highest D-polymer line shows another type of pressure laminate intended for high mechanical strength at temperatures with still very good electrical properties. The AI-polymer shown is only one of a class yielding the highest known maintained mechanical strength together with excellent electrical properties wherever the processing necessary for its manufacture allow its application. The aging temperature for this curve was 15°C higher than for the other materials shown. The E-polymer shown belongs to still another class of resins about which we do not yet know as much as about the others. It was included to show that a variety of polymer systems with different polymer chain units and different bonds can all be made to exceed the thermal performance we have been accustomed to expect in organic polymers.

Application of the factors discussed in the beginning of this paper to dielectrics is shown more directly in Figure 5, which shows thermal stability of composite dielectrics as measured by an electrical criterion. Here the absolute degradation rate in vacuum of the AI-resin shown is approximately on a par with the silicone used, whereas the D-resin actually has a somewhat faster degradation rate. However, the manufacture and processing of these two resins was such as to minimize initial volatiles evolution and create a tight structure with a low rate of oxygen ingress. In addition, the AI-resin is able to relieve internal stresses by creep. Therefore internal fissuring of the resin and loss of electric strength are minimized. The results are easily visible. That oxidation was still the chief mode of degradation is shown by the last line in the figure showing life in a nitrogen atmosphere. A similar greatly extended life might be expected in the vacua of space.

Both the D-resin and AI-resin shown have a highly aromatic structure. As expected, they both also have superior corona resistance relative to other polymers and are unaffected in all properties so far tested by radiation to 10^9 rad. Lacking rotating polar groups, both resins show low electrical loss factors at from 60 to 10^{10} cycles not only at room temperature but also at elevated temperatures, as shown in Figure 6.

In sum, it would seem that organic polymer dielectrics are capable now of far higher thermal performance than once thought possible. Such performance is not necessarily confined to a few unique polymers. The properties of the new thermally stable dielectrics are particularly adaptable to the

space environment, in which their life is greatly extended relative to other possible dielectric materials. However, it is also true that all such organic polymers are thermodynamically unstable at their use temperatures. There is a point in the temperature scale at which inorganic dielectrics must take over. Inorganic materials may have the advantage of being already in their highest oxidation state as prepared and of having a thermal stability not dependent on the strength of covalent bonds. It is usual here to speak of inorganic polymers but if the goal is to mimic the structure of an organic polymer using "inorganic" atoms there, truly useful inorganic polymers seem still to be a thing of the future. However, it is not necessary to carry over the structures and techniques of organic polymer chemistry into the inorganic field. Workable dielectrics in this area already exist.

To close this presentation with a look into the future, Figure 7 presents thermal life data on the same scale as the previous figures for an inorganic laminate developed at the Westinghouse Research Laboratories. Variants of this inorganic system are also used for motor insulation and the like, the performance of which is reported elsewhere in this Symposium.

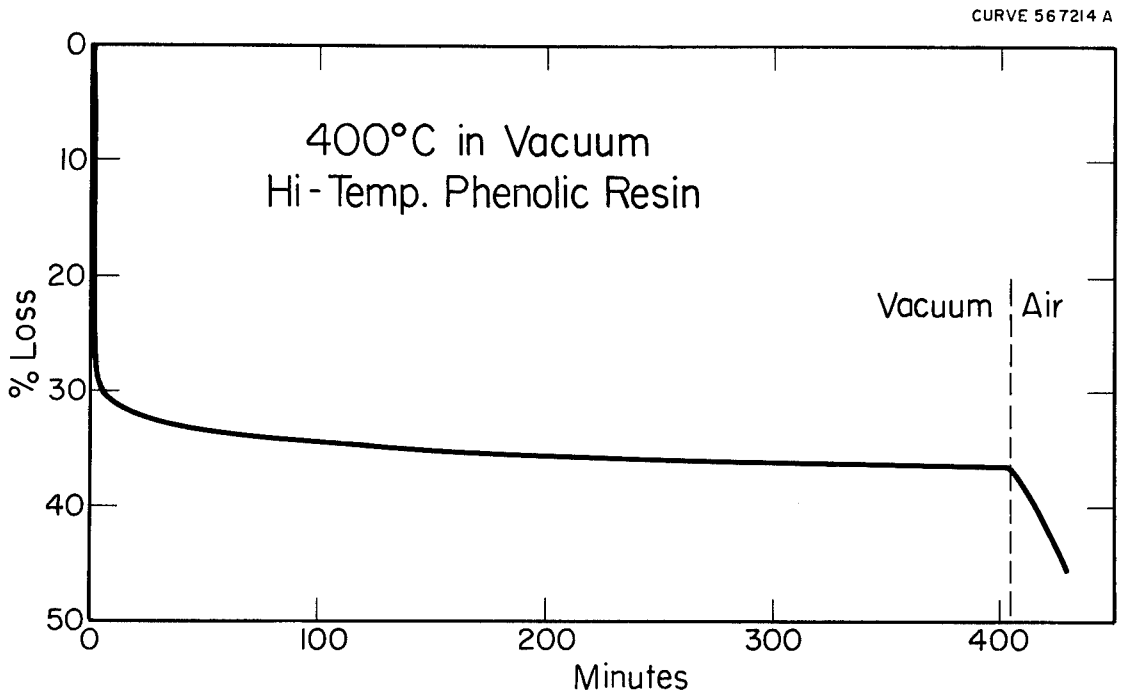
CURVE 567214 A
400°C in Vacuum
Hi-Temp. Phenolic Resin
Vacuum
Air
% Loss
0
10
20
30
40
50
0
100
200
300
400
Minutes

Figure 1

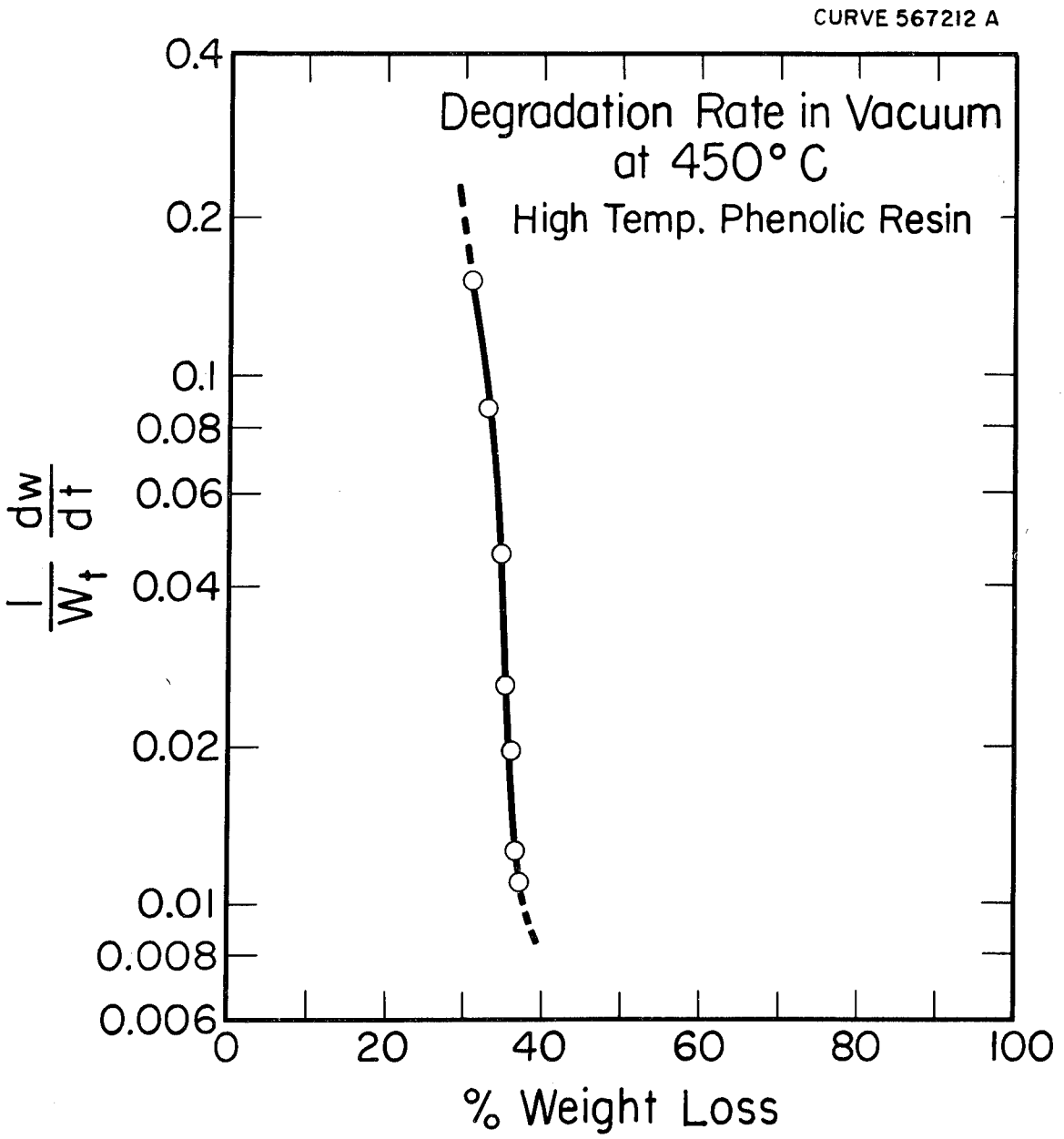
CURVE 567212 A
Degradation Rate in Vacuum
at 450° C
High Temp. Phenolic Resin
0.4
0.2
0.1
0.08
0.06
0.04
0.02
0.01
0.008
0.006
$-\frac{1}{W_t}\frac{dw}{dt}$
0
20
40
60
80
100
% Weight Loss

Figure 2

DWG. 626A615

Degradation Rates in Air and Vacuum

	air rate/vacuum rate
Phenolics	100 - 250
Silicones	10 - 25
PTFE, etc.	~1

Figure 3

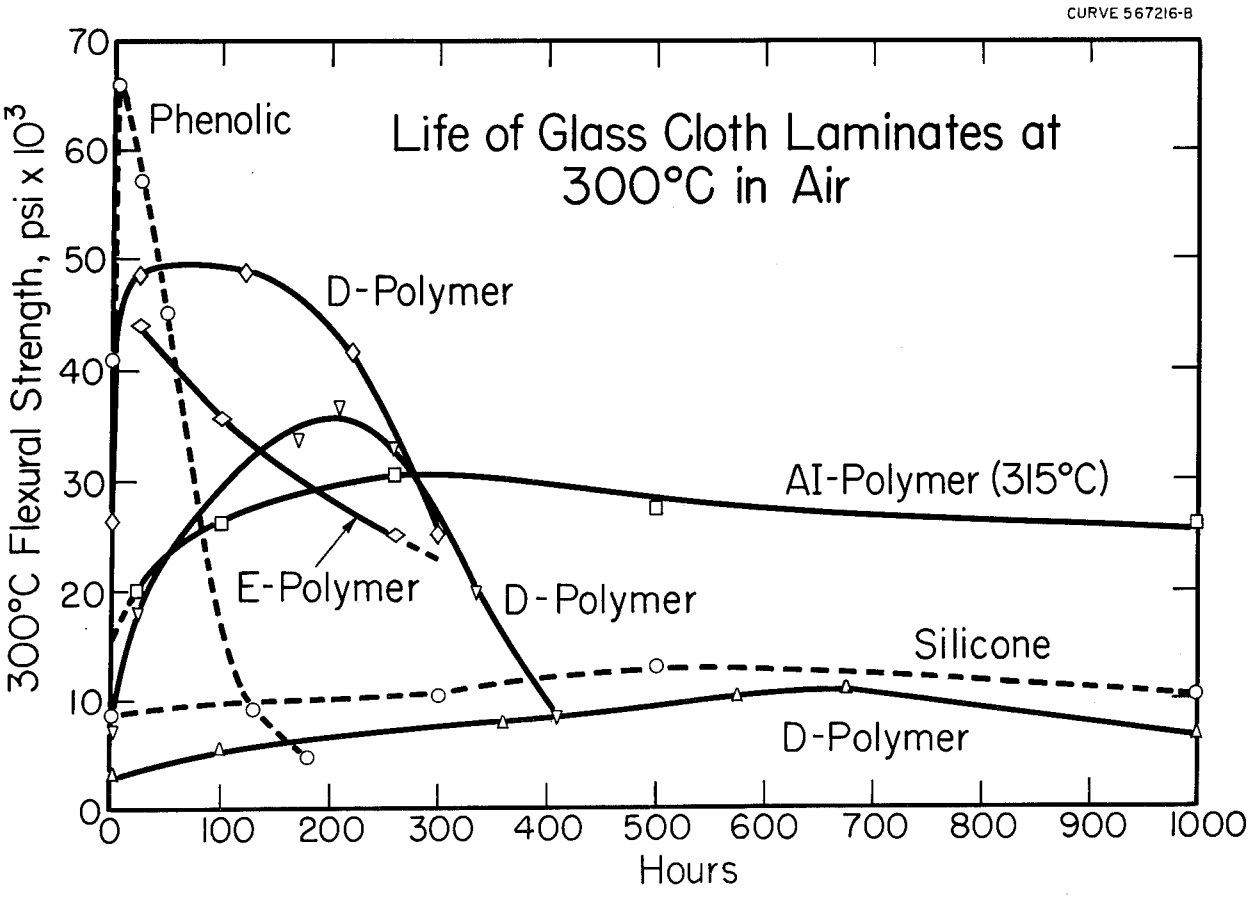
CURVE 567216-B
Life of Glass Cloth Laminates at 300°C in Air
300°C Flexural Strength, psi x 10^3
Hours
Phenolic
D-Polymer
AI-Polymer (315°C)
E-Polymer
D-Polymer
Silicone
D-Polymer
0
10
20
30
40
50
60
70
0
100
200
300
400
500
600
700
800
900
1000

Figure 4

DWG. 626A616

Dielectric Life of Glass Cloth Based Tubes at 300 °C

Endpoint: 200 V/mil electric strength

	Life in Air, hours	Initial Electric Strength (av. V/mil on 1/16 in.)
Silicone	50	320
D-resin	650	900
AI-resin	1000	900
	Life in N_2	
D-resin	>> 3000	900

Figure 5

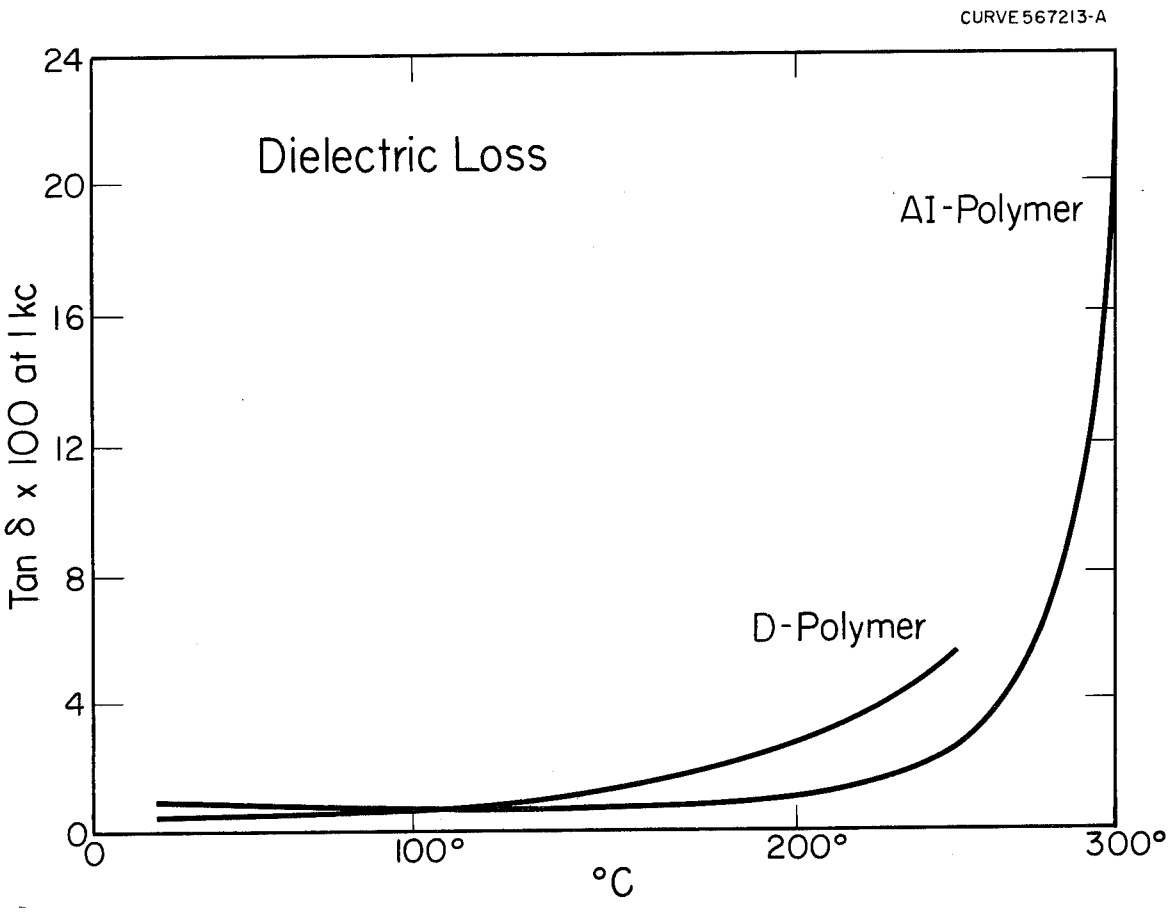
CURVE 567213-A
Dielectric Loss
AI-Polymer
D-Polymer
Tan δ x 100 at 1 kc
24
20
16
12
8
4
0
0
100°
200°
300°
°C

Figure 6

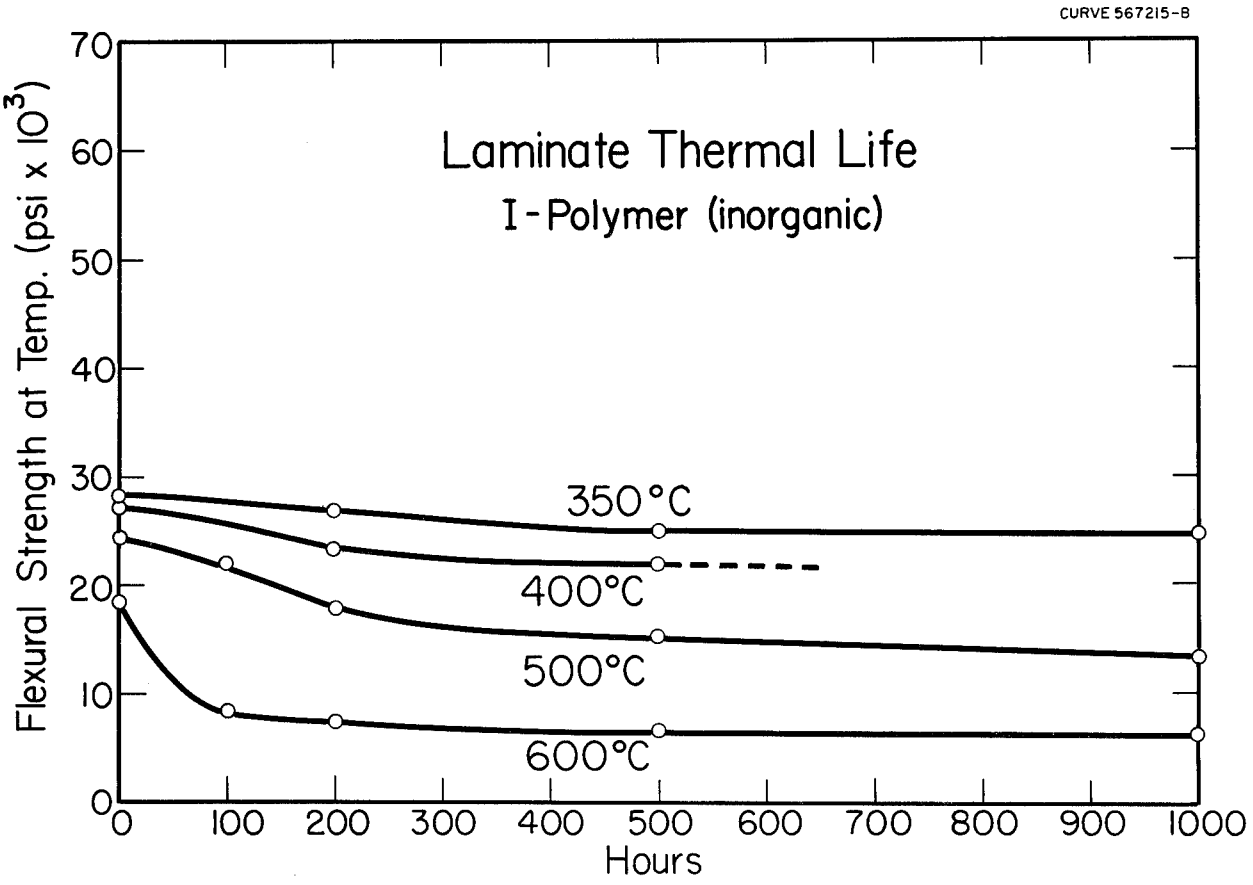
CURVE 567215-B
Laminate Thermal Life
I-Polymer (inorganic)
Flexural Strength at Temp. (psi x 10^3)
70
60
50
40
30
20
10
0
350°C
400°C
500°C
600°C
0
100
200
300
400
500
600
700
800
900
1000
Hours

Figure 7

ANALYSIS OF SOLAR ENERGY CONVERSION USING THIN DIELECTRIC FILMS

By Benjamin H. Beam*

National Aeronautics and Space Adminstration
Ames Research Center
Moffett Field, Calif.

Generation of electrical power in space is a very important aspect of space flight. Many of the problems of the exploration and utilization of space would be so much simpler if more power were available in the vehicles. Increased power generally requires increased weight, however, and weight is sharply limited by the capability of the launching rockets. Different energy conversion schemes are thus considered good or bad primarily on the basis of power-to-weight ratio, with other characteristic features of a particular system of less importance except to the extent that they affect the power-to-weight ratio.

The most casual review of the literature reveals a wide variety of energy conversion systems being actively considered and developed now. There are several major and distinct categories for solar energy conversion systems alone ranging through photovoltaic, thermoelectric, thermionic, magnetofluiddynamic, and turboelectric. Dielectric energy conversion does not fit well into any of these established categories, and, in fact, has not been widely regarded as a promising power supply. Curiously, however, a number of analyses of dielectric systems have been presented, and the conclusions have been generally favorable with regard to power-to-weight ratio. These analyses include a number of papers by S. R. Hoh starting in 1959,[1] a paper by myself in 1960, NASA TN D-336,[2] and an analysis by J. D. Childress in 1962.[3]

The purpose of this paper is to pursue the analysis of dielectric energy conversion to a point where a reasonable accounting can be made of the power output, losses, and items of weight in space power systems of this type. Equations are developed for performance in terms of dielectric properties, and your close attention to the details of this development is invited. The results are then applied to a comparison with solar cells for a typical space vehicle payload.

The principle of energy conversion in a dielectric is described in Figure 1. A variable capacitor is characterized by two different values of capacitance C_1 and C_2. Closing of the switch S_1 permits charging of the initial capacitance C_1 to a voltage V_1 and a charge $q = C_1V_1$. Opening the switch S_1 isolates the capacitor electrically so that in changing the capacitance from C_1 to C_2 its charge remains constant and its voltage undergoes a change from V_1 to V_2. The change in capacitance is assumed to be caused by a temperature change in the

*Chief, Measurements Research Branch

dielectric. The switch S_2 can now be closed and the charge completely removed through a load resistor assumed capable of absorbing all the energy usefully, reducing the capacitor voltage to zero. The cycle is then completed by restoring the capacitor from C_2 to its original value C_1. If switching and circuit losses are neglected and this idealized procedure is repeated f times per second, the power developed is the difference between that supplied by the battery and delivered to the load.

$$P = \frac{1}{2} fC_2V_2^2 \left(1 - \frac{C_2}{C_1}\right)$$

Note that this net power is realized only when the initial and final charge on the capacitor is zero.

This simplified circuit is helpful in describing principles but not very satisfying for critical analysis because of the neglect of power losses in the circuit which may be important. In Figure 2 a more practical circuit is shown. Note first that the battery connection is now such that charge drawn from the battery V_b in charging the capacitor is later restored on discharging the capacitor, so that the net drain on the battery is only that due to capacitor leakage. The capacitor leakage resistance is shown as R_l in parallel with $C(T)$. Both are functions of temperature due to heat flow in and out of the dielectric, and may also be functions of voltage stress. Assuming R_l is defined in terms of T and V, one could, in principle, get an average value of V^2/R_l for a cycle and represent this by V_2^2/R_{l_o}, where R_{l_o} is some effective value of R_l. Where only small changes in temperature are involved, and in the applications considered in this paper this will be the case, R_{l_o} is approximately equal to the value of R_l at the mean temperature of the dielectric.

Switching is considered to be accomplished by the silicon-controlled rectifiers SCR_1 and SCR_2. The resistance R is the resistance of the SCR in the forward direction in series with the inductor and circuit resistance. The inductors L are necessary to minimize switching loss, since it is a fact, for example, that closing a switch to charge a condenser containing only a capacitor and battery results in an unrecoverable switching energy loss equal to the energy stored in the capacitor. The inductor permits reduction of the loss during a cycle of charge and discharge by a factor of approximately $(\pi/2)R\sqrt{C_2/L}$ which can be designed to be small for appropriately selected values of R, L, and C_2.

Note also another very important feature which the inductance provides, that is, the complete charge and discharge of the capacitor, resulting in maximum power output for a given capacitance change. During the charging cycle, the voltage on the capacitor rises to nearly

twice V_b as a result of the presence of the inductance. Similarly, if the battery in parallel with the load is selected to have a voltage equal to $V_b[(C_1/C_2)-1]$ then as the capacitor is discharged through SCR_2, the voltage on the capacitor goes completely to zero while a steady output voltage of $V_b[(C_1/C_2)-1]$ is maintained.

The performance of this circuit is summarized in the expression for power:

$$P = \frac{1}{2} fC_2V_2^2 \left(1 - \frac{C_2}{C_1} - \frac{\pi}{2} R\sqrt{\frac{C_2}{L}} - \frac{1}{fR_{l_o}C_2}\right)$$

This circuit model is efficient and will be assumed to apply in the following analysis.

For the cycle considered here, variations in capacitance are accomplished through changes in temperature of the film. At any temperature of the film there is a corresponding value of capacitance as shown in Figure 3. It is now assumed that the temperature varies by some small amount $\tilde{T}$ from an average value T_o, and that the capacitance varies linearly with temperature over this region of interest, so that

$$C = C_o \pm \tilde{C} = C_o (1 \pm \beta\tilde{T})$$

for C/C_o and $\tilde{T}/T_o \ll 1$. On substitution, to the first order in $\tilde{C}/C_o$

$$P = \frac{1}{2} fC_oV_o^2 \left(2\beta\tilde{T} - \frac{\pi}{2} R\sqrt{\frac{C_o}{L}} - \frac{1}{fR_{l_o}C_o}\right)$$

The power per unit area of film can then be calculated, using

$$C_o = \frac{K_oA}{l} ; \qquad E_o = \frac{V_o}{l}$$

$$\frac{P}{A} = \frac{1}{2} K_oE_o^2 \left(2fl\beta\tilde{T} - \frac{\pi}{2} fl R\sqrt{\frac{C_o}{L}} - \frac{l}{R_{l_o}C_o}\right)$$

One can then consider in detail the temperature extremes for the dielectric. The situation being considered is shown in Figure 4. A cylindrical thin film is rotating in space at a rotational frequency f. A heat balance equation can be considered in which the heat input is considered to be entirely due to radiation from the sun. Heat output is through radiation into space from the outer surface according to the fourth power of the surface temperature. One can also show that for thin films there is negligible temperature gradient across the film, and negligible heat conduction along the film compared with that radiated.

The differential equation defining the temperature variations for these conditions is derived in NASA TN D-336, and is shown in Figure 5.

$$\frac{dT}{d\theta} + \eta T^4 = \eta \left(\frac{\alpha}{\epsilon}\right) T_e{}^4 \sin\theta \qquad 0 < \theta < \pi$$

$$\frac{dT}{d\theta} + \eta T^4 = 0 \qquad \pi < \theta < 2\pi$$

where

$$\eta = \frac{\epsilon\sigma}{2\pi f \rho l C_p J}$$

Curves of the variation of temperature with angular position are also shown in the figure. These were obtained by numerical integration on a digital computer. Note that η is a parameter which includes the important physical properties of the film. This includes rotational frequency, f, film density, ρ, film thickness, l, specific heat capacity, C_p, surface emissivity, ϵ, the Joule equivalent, J, and the Stephan-Boltzmann constant, σ. Note also that T_e is the equivalent black-body, subsolar temperature at a given radial distance from the sun. Thus $\sqrt[4]{\alpha/\epsilon}\, T_e$ is merely the equilibrium temperature that a section of the film would achieve with its surface normal to the solar direction.

The dotted sine curve, $\eta = \infty$, represents zero rotational speed for example. In the present analysis attention is directed to the opposite extreme, small values of η representing rapid rotation where the temperature extremes are small. A particularly interesting solution for this case can be derived by assuming that the temperature of the film is some steady T_o with superimposed incremental variation $\tilde{T}(\theta)$. The temperature equation can then be linearized in a manner consistent with the equation for power developed earlier; T can be represented by a Fourier series in θ,

$$T = T_o + \tilde{T}(\theta)$$

$$= T_o + \sum_{n=1}^{\infty} A_n \sin n\theta + \sum_{n=1}^{\infty} B_n \cos n\theta$$

Likewise the right side of the temperature equation can be represented by a Fourier series. The sine term for the heat input due to solar radiation becomes

$$g = \begin{cases} \sin\theta & \text{for } 0 < \theta < \pi \\ 0 & \text{for } \pi < \theta < 2\pi \end{cases}$$

$$= g_o + \sum_{n=1}^{\infty} a_n \sin n\theta + \sum_{n=1}^{\infty} b_n \cos n\theta$$

The temperature equation can be closely approximated for small $\tilde{T}$ by

$$\frac{d\tilde{T}}{d\theta} + \eta T_o^4 + 4\eta T_o^3 \tilde{T} = \eta \left(\frac{\alpha}{\epsilon}\right) T_e^4 g$$

Substituting the Fourier series representation for $\tilde{T}$ and g yields a set of algebraic equations, two for each frequency, containing the unknowns A_n and B_n. One can solve immediately for T_o at any value of η: $T_o = \sqrt[4]{\alpha/\pi\epsilon}\, T_e$ which is the value to which the temperature converges as $\eta \to 0$ in the numerical solution. Likewise, for small η the alternating component of temperature converges very rapidly on the first cosine term in the series.

$$\tilde{T} = B_1 \cos\theta = -\frac{\eta}{2}\left(\frac{\alpha}{\epsilon}\right) T_e^4 \cos\theta \qquad (\text{for } \eta \to 0)$$

This is a gratifyingly simple solution and can be shown to apply over a wide range of η as shown in Figure 6. Here we have compared the precise numerical solutions from NASA TN D-336 with the linearized solution for two different temperature conditions, and the linearized value is shown to apply with reasonable accuracy for values of η less than 10^{-9} per $^{o}K.^{3}$ Acceptance of this linearized value then permits closed solutions for efficiency and performance of energy conversion. Thus the Carnot efficiency becomes

$$\text{Carnot efficiency} = \frac{2B_1}{T_o} = \frac{\epsilon\sigma}{2f\rho l C_p J}\left(\frac{\alpha}{\pi\epsilon}\right)^{3/4} T_e^3 = \pi\eta T_o^3 \ll 1$$

The initial assumption of $\tilde{T}/T_o \ll 1$ is equivalent to assuming low Carnot efficiencies. The power output per unit film area can be derived by inserting $\tilde{T}$ into the equation developed earlier

$$\frac{\text{Power}}{\text{Film area}} = \frac{1}{2} K_o E_o^2 \left(\frac{\beta\alpha\sigma T_e^4}{2\pi\rho C_p J} - \frac{\pi}{2} f l R \sqrt{\frac{C_o}{L}} - \frac{l}{R_{l_o} C_o}\right)$$

Since the incident power per unit area due to solar radiation is σT_e^4 times a shape factor $1/\pi$, the over-all energy conversion efficiency is

$$\text{Over-all efficiency} = \frac{\pi}{2}\frac{K_o E_o^2}{\sigma T_e^4}\left(\frac{\beta\alpha\sigma T_e^4}{2\pi\rho C_p J} - \frac{\pi}{2} f l R \sqrt{\frac{C_o}{L}} - \frac{l}{R_{l_o} C_o}\right)$$

One can also consider the power output per unit weight of the film alone

$$\frac{\text{Power}}{\text{Film weight}} = \frac{1}{2}\frac{K_o E_o^2}{\rho}\left(\frac{\alpha\beta\sigma T_e^4}{2\pi\rho l C_p J} - \frac{\pi}{2} f R \sqrt{\frac{C_o}{L}} - \frac{1}{R_{l_o} C_o}\right)$$

In reviewing these formulas note that the power output and over-all efficiency are dependent on the energy which can be stored in a dielectric $(1/2)K_oE_o^2$, and, in this respect, there is a common interest in developing of dielectrics for other purposes. Note also that the leakage time constant $R\gamma_oC_o$, which is a fundamental property of the dielectric material independent of geometry, should be high so that the latter term in the brackets will be small. The second term in the brackets $(\pi/2)fR\sqrt{C_o/L}$, which also detracts from the power output, can be made arbitrarily small with good circuit design. The most important term in the brackets is the first term. It can be concluded from this that the power output and efficiency are independent of frequency as long as the rotational frequency is high enough that the latter terms in the brackets can be neglected; that is, the product of frequency and change in film temperature is a constant. The influence of the change of capacitance with temperature, film thickness, density, heat capacity, etc., is also clearly shown in the formulas, so that one can consider a wide variety of dielectric materials for possible application here.

In reviewing possible dielectric materials one should note a number of differences between this and more conventional circuit applications. One is that the dielectric strength of insulating films in the vacuum conditions of space will be greatly improved over commerical standard values, as inferred from the data of Inuishi and Powers at M.I.T.[4] Other factors are that the dielectric should be a solid with very low vapor pressure, mechanically strong, and resistant to radiation damage. Ferroelectric materials have been mentioned most frequently for these devices because of high dielectric constant and change of capacitance with temperature. Plastic films may well have superior performance because of higher dielectric strength, and better mechanical and thermal properties in thin films. Studies of comparative performance are now very difficult because of the lack of test data for the conditions of interest.

One can, however, get an appreciation for this type of power unit in comparison with other types by assuming a situation illustrated in Figure 7. Here we have the Thor-Delta launch vehicle with the low-drag payload fairing outline indicated. This vehicle has been used in launching instrumented payloads weighing about 115 pounds. Inside the fairing shown there is a drum shaped volume, the cylindrical surface of which is about 15 square feet in area. We will assume for this comparison that this surface area if completely covered with solar cells on a spinning vehicle would generate about 60 watts of power with a solar panel weight of about 15 pounds. The question is: Are there advantages in going to dielectric energy conversion in this case?

A table of dielectric properties which will be used for a sample calculation is shown in Table I. The dielectric assumed is polyethylene terephthalate, which is a mechanically rugged plastic film now fabricated

in 1/4 mil thickness and having the dielectric properties shown in the table.[5,6] One of the difficulties in assembling a list of this type is that values of dielectric strength, dielectric constant, and leakage factor have not been measured under conditions of high voltage stress, in vacuum, with thermal cycling. The figures shown represent experimental data but not precisely for the conditions considered. These tabulated figures inserted in the previously presented equations yield values of 250 square feet for the film area to obtain 60 watts of power and 0.44 pound for the film weight. The Carnot efficiency is 2.6 percent and the over-all efficiency is 0.63 percent. The film temperature varies $\pm 5^{\circ}$, and η corresponds to 1.6×10^{-10} per $^{\circ}K$.[3] Additional items of weight in circuitry are estimated from Figure 8. The dielectric film is divided into sections, each of which is charged and discharged separately at the appropriate point in the cycle. The batteries have been eliminated in favor of the self-exciting circuit shown in which the two capacitors C store the charge and regulate the d.c. output to the load. Similar circuits are in parallel with the above, being switched through the commutator, so that only two capacitors C and one modest-sized inductor are needed in the auxiliary circuitry of the power system.

The vehicle might look as shown in Figure 9 to almost the same scale as the previous vehicle sketch. Here the film is shown draped around the folding booms inside the Delta fairing. These booms would be extended by centrifugal force and the film held in position by stiffeners and restraining wires after injection into trajectory. The total weight of circuitry, dielectric film, wires, and stiffeners is estimated to be 8 pounds. Other equipment that was inside the vehicle on the other version could be placed on booms. If it is assumed that increases and decreases in weight outside the power subsystem can be traded evenly for no net change, then the vehicle weight has been reduced 7 pounds to a weight of 108 pounds. There are situations in which a saving in weight of this magnitude would be of value in providing additional scientific instrumentation, communication, or trajectory capability.

These calculations are presented to illustrate the possible performance advantages and problems of this type of energy conversion system. There are uses and applications for lighter power systems. The principal unsolved problems now appear to be in understanding dielectric properties for the environment considered.

REFERENCES

1. Hoh, S. R.: Conversion of Thermal to Electrical Energy with Ferroelectric Materials. Proc. of IEEE, vol. 51, no. 5, May 1963, pp. 838-845.

2. Beam, Benjamin H.: An Exploratory Study of Thermoelectrostatic Power Generation for Space Flight Applications. NASA TN D-336, 1960.

3. Childress, J. D.: Application of a Ferroelectric Material in an Energy Conversion Device. Jour. Appl. Phys., vol. 35, no. 5, May 1962.

4. Inuishi, Y., and Powers, D. A.: Electrical Breakdown and Conduction Through Mylar Films. Jour. Appl. Phys., vol. 28, no. 9, Sept. 1957, pp. 1017-1022.

5. Redish, Wilson: The Dielectric Properties of Polyethylene Terephthalate (Terylene). Trans. Faraday Soc., vol. 46, 1950, pp. 459-475.

6. Anon.: Mylar Polyester Film. Bulletin TR-1, E. I. DuPont De Nemours and Co., Inc., Nov. 1959.

TABLE I.- DIELECTRIC PROPERTIES

Type	Polyethylene terephthalate
Dielectric constant, K_o	$3.1 \times 8.83 \times 10^{-14}$ farads/cm
Dielectric strength, E_o	6×10^6 volts/cm
Black-body subsolar temperature, T_e	392° K
Absorptivity, α	1.0
Emissivity, ϵ	0.39
Equilibrium temperature, T_o	373° K (100° C)
Temperature coefficient, β	0.005/°K
Leakage factor, $1/R\ell_o C_o$	0.01/sec
Circuit loss factor, $(\pi/2)R\sqrt{C_o/L}$	0.005
Density, ρ	1.4 gm/cm^3
Specific heat capacity, C_p	0.3 cal/gm-°K
Thickness, ℓ	6.25×10^{-4} cm
Rotational frequency, f	2 cps

ELECTROSTATIC ENERGY CONVERSION

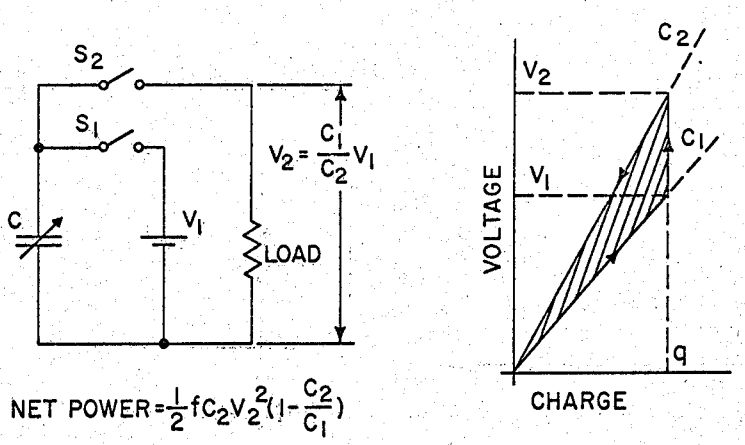

Figure 1.

DIELECTRIC ENERGY CONVERSION CIRCUIT

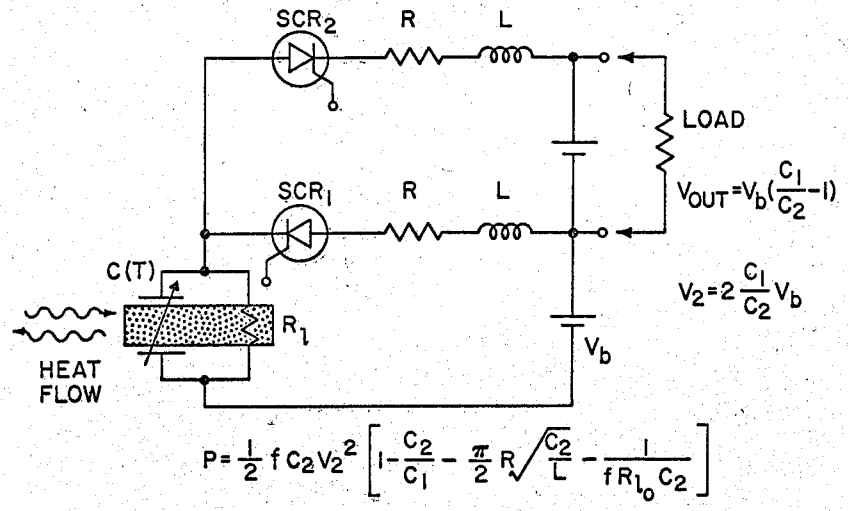

Figure 2.

CAPACITANCE — TEMPERATURE RELATIONS

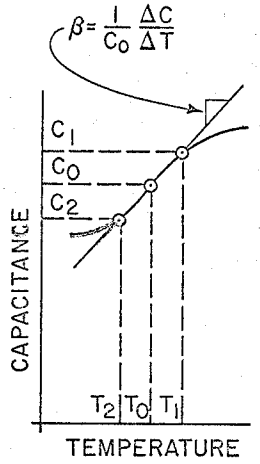

$$C = C_0 \pm \tilde{C} = C_0(1 \pm \beta\tilde{T})$$

$$\frac{\tilde{C}}{C_0} \text{ or } \frac{\tilde{T}}{T_0} \ll 1$$

$$P = \frac{1}{2} f C_0 V_0^2 \left[2\beta\tilde{T} - \frac{\pi}{2} R \sqrt{\frac{C_0}{L}} - \frac{1}{f R_{l_0} C_0} \right]$$

$$C_0 = \frac{\kappa_0 A}{l} \quad ; \quad E_0 = \frac{V_0}{l}$$

$$\frac{P}{A} = \frac{1}{2} \kappa_0 E_0^2 \left[2fl\beta\tilde{T} - \frac{\pi}{2} lfR \sqrt{\frac{C_0}{L}} - \frac{l}{R_{l_0} C_0} \right]$$

Figure 3.

ROTATING CYLINDRICAL CAPACITOR FILM

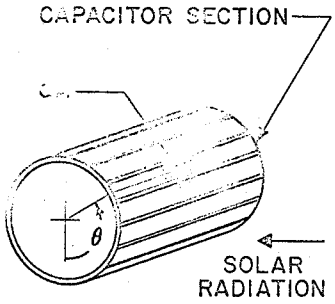

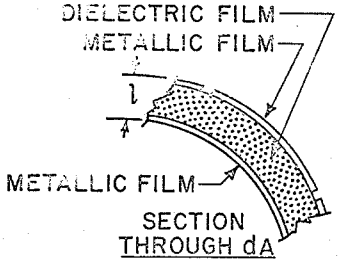

ROTATIONAL FREQ	f
HEAT CAPACITY	C_p
ABSORBTIVITY	α
EMISSIVITY	ϵ
DENSITY	ρ

Figure 4.

TEMPERATURES ON A THIN CYLINDRICAL FILM

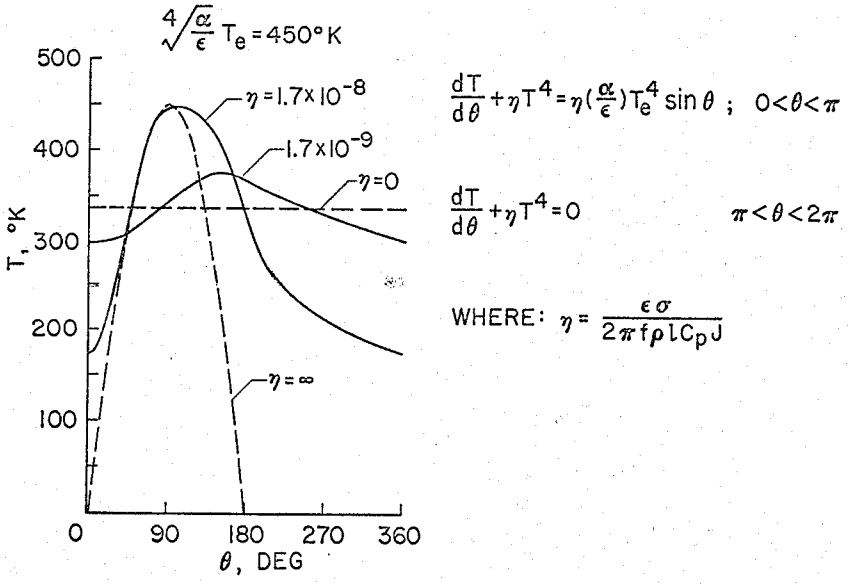

Figure 5.

LINEARIZED AND EXACT SOLUTIONS COMPARED

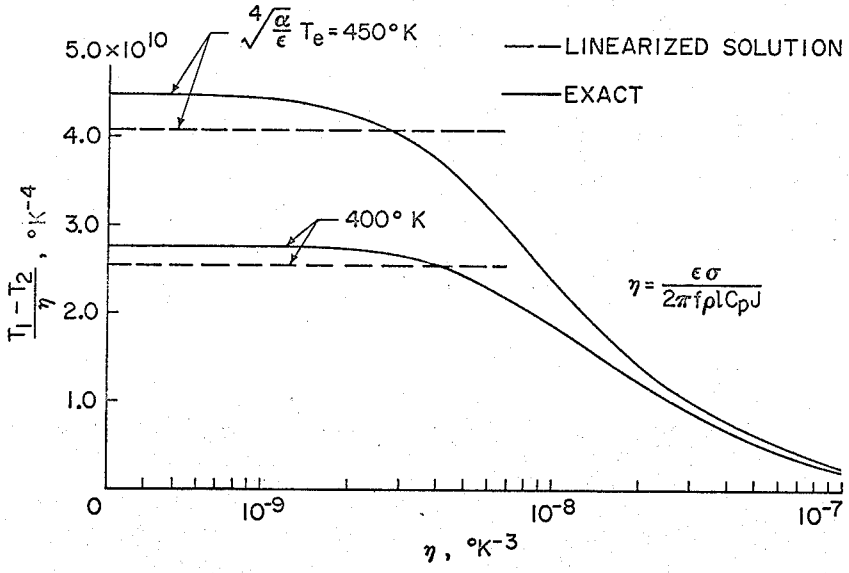

Figure 6.

TYPICAL SOLAR CELL POWER SUPPLY

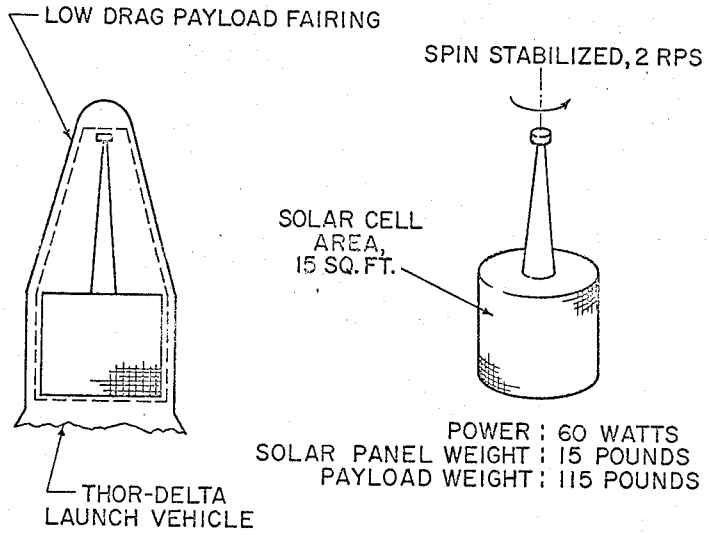

Figure 7.

CIRCUIT SCHEMATIC OF POWER SUPPLY

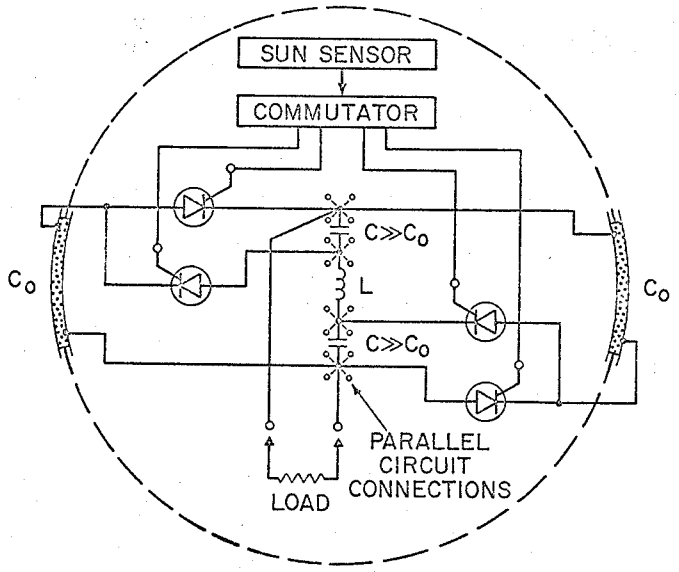

Figure 8.

TYPICAL DIELECTRIC FILM POWER SUPPLY

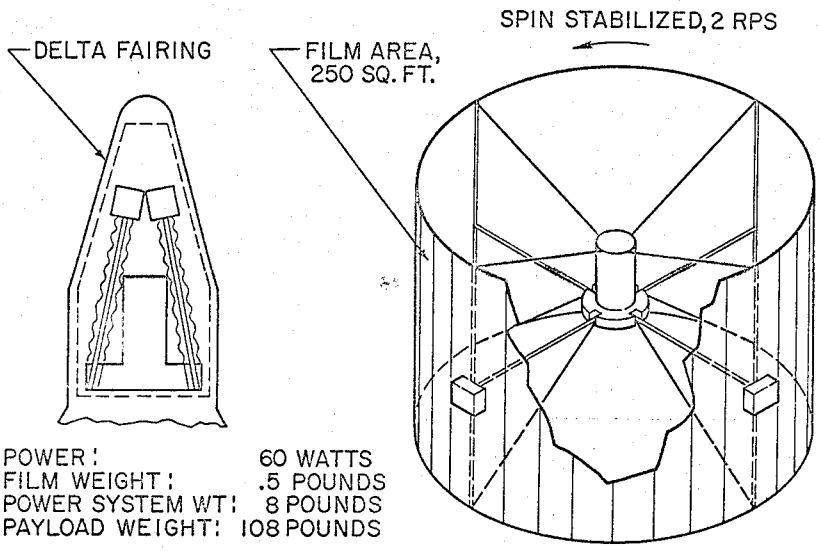

Figure 9.

EVALUATION OF INORGANIC MOTOR INSULATION UNDER SPACE ENVIRONMENT

O. P. Steele, III
Group Leader
Component Development Group
Atomics International
A Division of North American Aviation, Inc.
Canoga Park, California

Symposium on Dielectrics in Space
June 25 and 26, 1963
Westinghouse Research Laboratories, Pittsburgh, Pennsylvania

ABSTRACT

The development of electric power sources for our space program has imposed a whole new set of environmental conditions on dielectrics. This paper deals with tests conducted on an inorganic insulation under simulated high-temperature space conditions and under irradiation. The results appear very promising.

INTRODUCTION

The ever expanding space program with its intricate and long-life mission increases the demand for more electrical power. This demand for power is rapidly exceeding the on-board storage capacity of a space vehicle for electrical energy. As the electrical power requirements increase, it becomes necessary to generate electrical power directly on the satellite, either by solar energy or from high density fuel such as the atom. In the higher power requirements, the complexity, size, and orientation requirements of the solar-electrical conversion system make electrical conversion by nuclear fission the logical choice.

The use of a nuclear-electrical conversion system imposes very strenuous environmental conditions on any dielectric material.

The first of these conditions is high temperature. In nuclear generating systems, as in all systems except those utilizing direct conversion of solar energy to electrical energy in a solar cell, one is dealing with a heat cycle. Because the waste heat from these heat cycles must be dumped by radiation to outer space, weight economy dictates operating at a high temperature. The weight consideration also precludes auxiliary cooling. In a reactor system, the operating temperature of many of the electrical items may exceed 1000°F.

The second environmental condition is the high vacuum of outer space. For a 400-mile orbit, the pressure will be 10^{-9} Torr. In a higher orbit, this pressure may be less than 10^{-13} Torr. These are harder vacuums than it is possible to simulate here on earth.

A third condition for the nuclear system is irradiation. Again, because of the weight consideration and because of the desire for compactness, many of the electrical items, particularly those associated with the reactor control, are required to operate while subjected to the direct reactor neutron and gamma environment. Figure 1 shows a mockup of such a reactor assembly with control actuators mounted directly on the reactor. With the actuators in this position, the dielectric materials are subjected to integrated neutron fluxes of 10^{19} to 10^{20} neutrons per cm^2 over a one-year operating life. In many cases, it is desirable to have even longer life with its associated increase of radiation. The associated gamma dose would be 10^{11} R, or greater, over the one-year period.

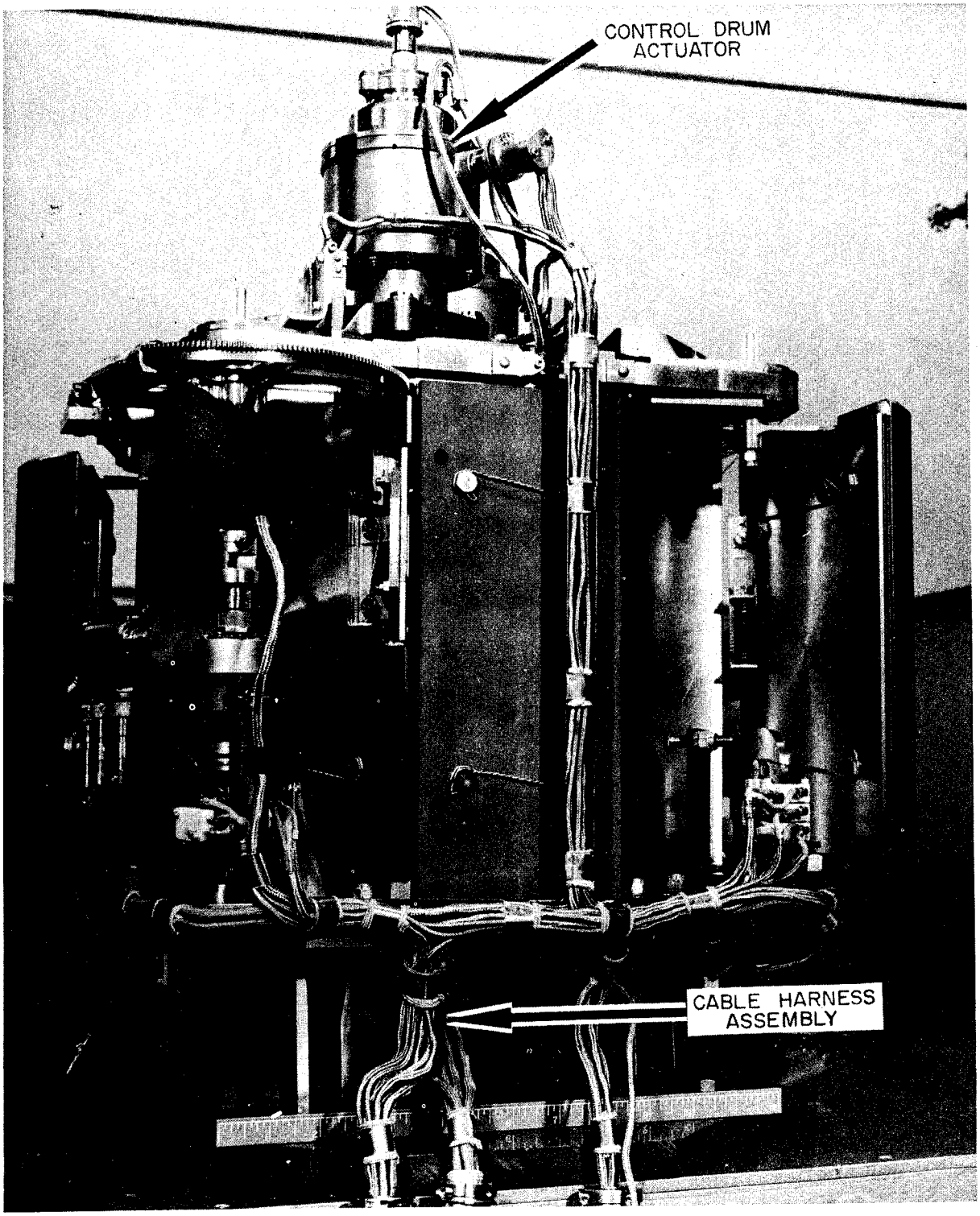

Figure 1. Reactor Assembly

The fourth condition is that of operating lifetime. With the more sophisticated space missions, there is both an economic and project necessity for long-life operation. A one- to two-year life for the electrical equipment is short when compared to industrial 20-year life expectancy. However, it is extremely long when considered for maintenance-free operation under the preceding three environmental conditions.

This paper describes the evaluation of an inorganic insulating system tested under simulated space conditions. Those interested in more details, particularly of the insulating materials and the insulating scheme, can find them in a paper by J. G. Hopp and D. K. McIlvaine of Westinghouse.*

DISCUSSION

The preliminary testing of the inorganic insulation scheme was conducted at Atomics International under vacuum conditions on a standard 400-cycle, 208-volt, 3-phase, 1-horsepower aircraft motor shown in Figure 2. The motor did not represent anything applicable for use as an electrical component for a space power system, but it did represent an item available for test. It cannot be said exactly that this motor was an "off-the-shelf" item as it was still very much of a laboratory curiosity, but at least it was available in a reasonably short time for early evaluation.

The magnetic material used in the motor was laminated high silicone steel, protected against oxidation by a coating of heat-resistant aluminum paint. A rotor squirrel-cage winding was constructed of fine silver with the same silver used to braze the end rings. The slot and phase insulation was a Westinghouse-developed high-temperature laminated mica-glass fabric. The motor had ceramic slot wedges. The stator windings were copper conductors clad with a heat-resistant alloy and insulated with a bonded frit coating. The initial phase connections were welded, and the ends of the windings were welded to solid silver terminals mounted on an inorganic bonded mica-glass composition terminal board. The terminal boards were laced to the winding end extensions with braided glass lacing and were embedded in the potting compound. The potting material is a Westinghouse laboratory-developed material, consisting of a mixture of refractory oxides and glass frits. It was applied to the motor as a

*J. G. Hopp and D. K. McIlvaine, "New Materials for Transformer Rectifier Units, High Temperature Aircraft," A. I. E. E. No. 5983 (1959)

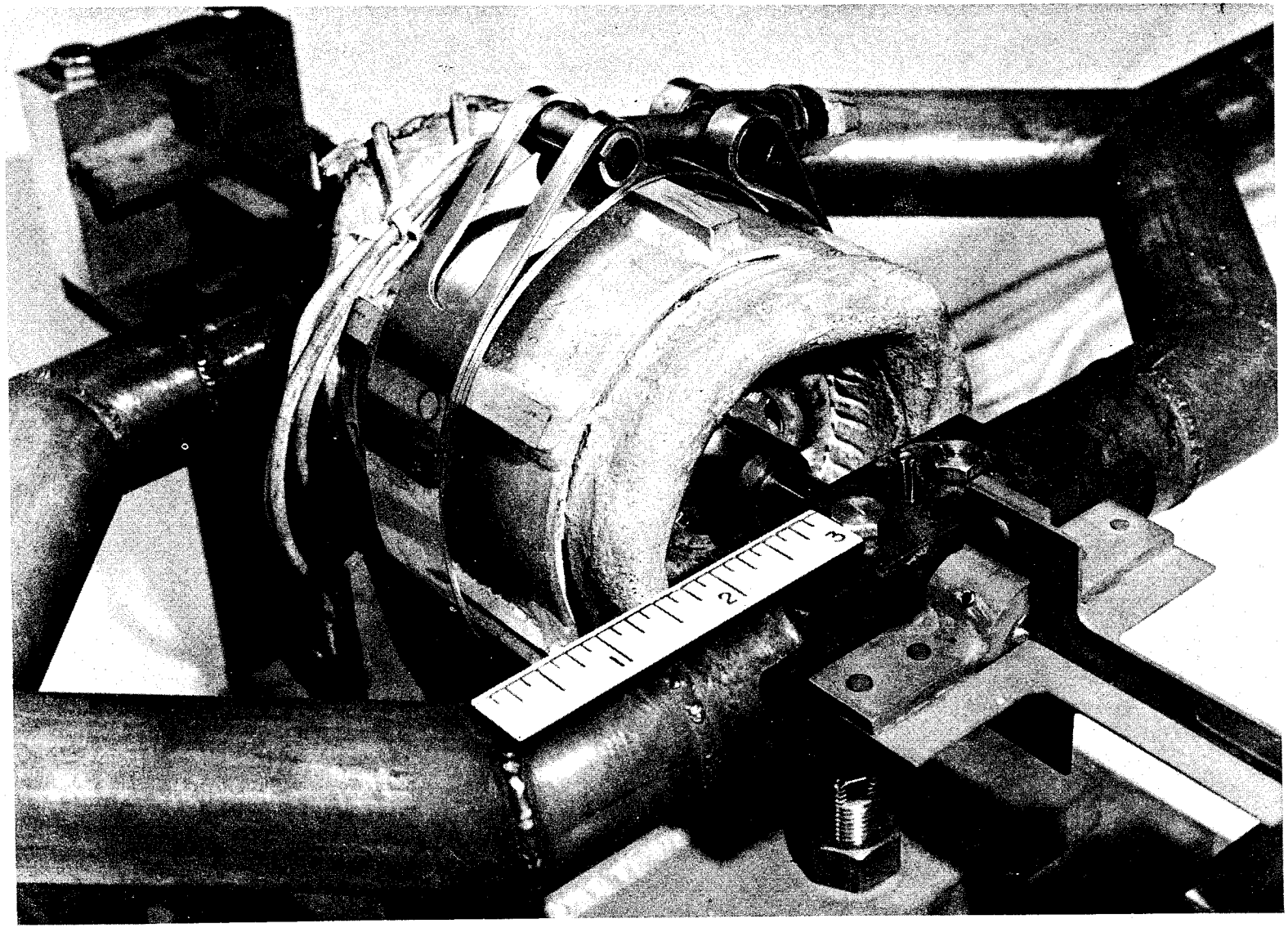

Figure 2. Insulation Test Motor

slurry by vacuum pressure impregnation. The potting over the end-turns portion was shaped and the unit dried and fired. The final firing temperature for the potting material was 600°C.

The motor was tested for 2500 hours at 1000°F in a vacuum of 5×10^{-5} Torr. Figure 3 shows the motor, insulation, and test "jig." The details of the motor tests are covered in another paper by the writer.*

During the 2500-hour test, full voltage was applied to the motor for two seconds once every hour during which time the voltage, current, power, and output torque were recorded. Once every 24 hours the insulation resistance-to-ground was measured with a 250-volt megohm insulation tester. The initial insulation resistance-to-ground on the motor at room temperature was 15 megohms. At 1000°F in vacuums of 5×10^{-5} Torr, the insulation resistance was 1 megohm.

At the completion of 2500 hours, the insulation resistance was still 1 megohm. There was no measurable change in any of the test parameters during the test time other than that normally expected by the initial change from room to operating temperature.

During the test, there was a considerable amount of outgassing of the insulation as detected by the gas load on the vacuum system pumps. After the completion of the test, the cooler regions of the vacuum chamber were coated with a residue which was analyzed and found to be lead and boron. Also, the color of the potted end-turns had changed from their original white or cream color to a pale pink.

Because of the very favorable results obtained in this test, it was decided to procure a number of stators of a size and rating comparable with a space system and in a quantity which would give some evaluation of the manufacturing consistency of the process. Twenty-four stators, as shown in Figure 4, were ordered. Twelve of these stators were wound with the material used in the initial test motor, and the remaining twelve were wound with potting material which had its normal boron replaced with Boron-11. This modification was made in an attempt to minimize the effect on the insulation from nuclear radiation. These units were designed for 28 volts, dc. The stators were made of

*O.P.Steele, III, "The Effect of High Temperature and Outer Space Vacuum on Electrical Equipment," A.I.E.E. No. 61-888 (June 26, 1961)

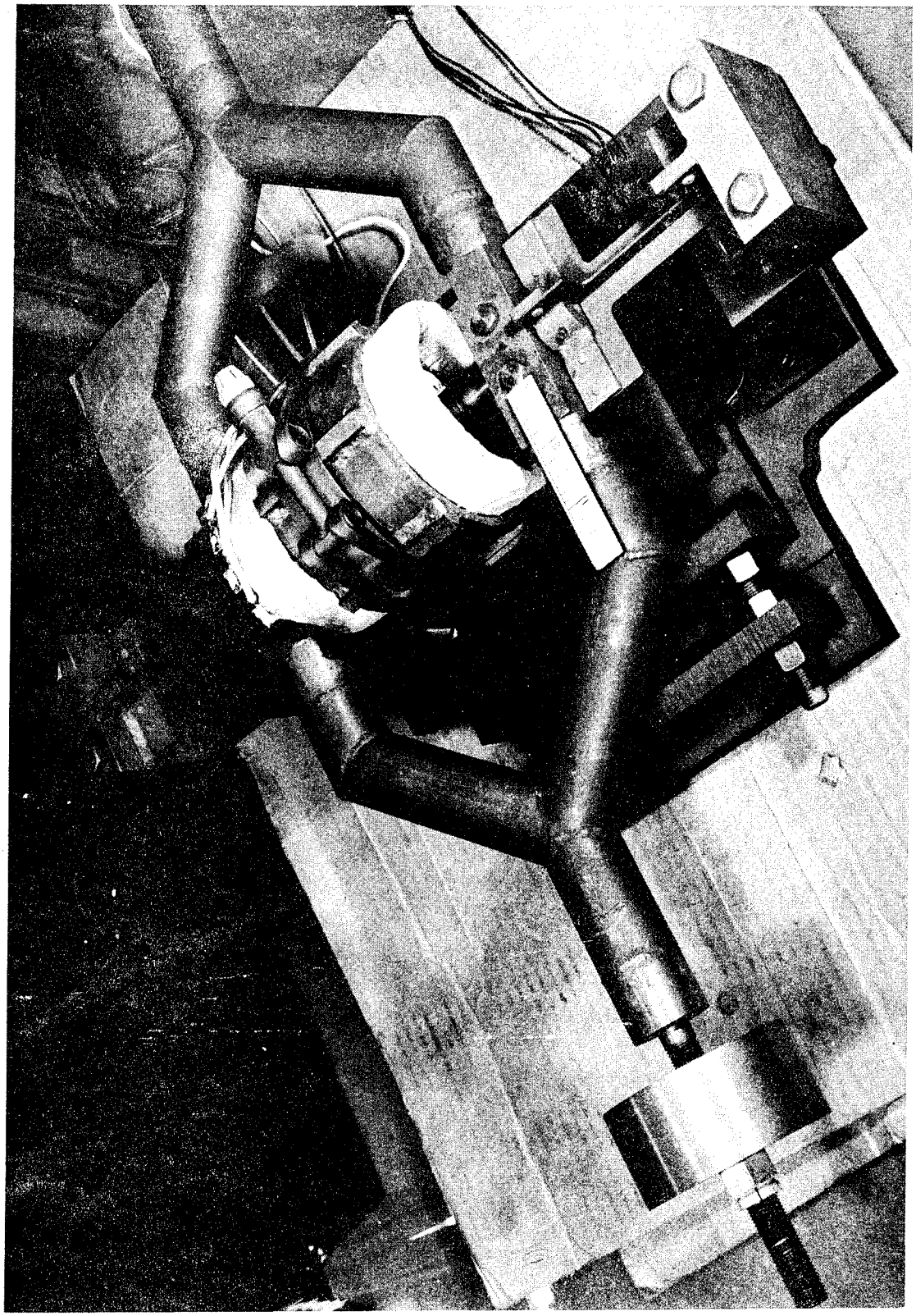

Figure 3. Insulation Test Fixture

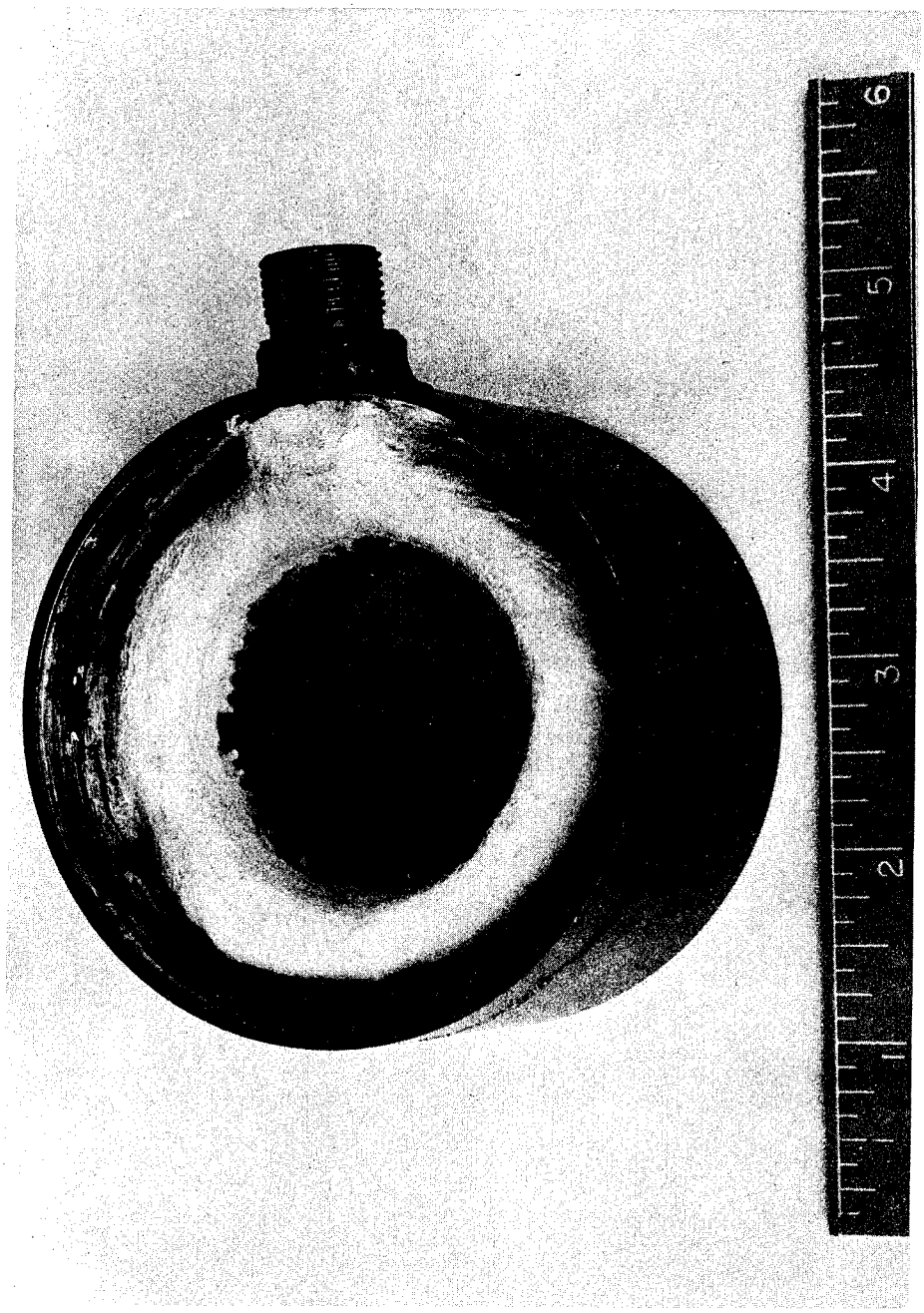

Figure 4. Insulation Test Stator

high silicone iron laminations, which were chrome-plated for oxidation protection. In this design, the coil leads were brought out to a high-temperature connector and welded to the connector pins. The unit used a permanent magnetic rotor. The assembled rotor stator is shown in Figure 5.

From the initial 12 units, two were picked at random for initial evaluation The initial room temperature insulation resistance-to-ground for these two stators, as-received, was 5 and 7 megohms respectively. After subjecting the stators to 50 hours operation at a vacuum of 2×10^{-4} Torr and room temperature, the insulation resistance of these two stators increased to 9,000 and 25,000 megohms, indicating that the insulation is adsorbent and that it had picked up a significant amount of moisture during transit. These stators were given 10 thermal-shock tests, consisting of cycling between 100°F and 800°F, in times varying from 2 to 16 hours. They were then placed in test at 1000°F and vacuum of 5×10^{-5} Torr. Figures 6 and 7 show the motors in the test fixture and the associated vacuum bell jar system in which the tests were performed. A heater surrounding the motor maintained the motor temperature at 1000°F. The test consisted of energizing the motor several times each day and operating it in each direction. Motor torque was measured by the height that the weight was lifted. The scale mounted in front of the unit (Figure 6) shows the length of the torque arm. The insulation resistance-to-ground was measured once each day using a 50-volt potential.

Stator No. 1 had an initial insulation resistance of 646 K ohms at 1000°F and Stator No. 2 (at the same temperature) had an initial insulation resistance of 228 K ohms. However, after approximately 600 hours of testing, each of them reached approximately 40 K ohms. From then on, as can be seen from Figure 8, the insulation resistance vs time was very similar for both stators. The consistency of the manufacturing process is indicated by the closeness with which these two units operated throughout the test. Although the insulation resistance had dropped to 23 K ohms in the first 3000 hours of test, the units were still considered to operate satisfactorily.

An appreciable amount of residue accumulated on the inside of the test chamber, and it was decided to stop the test for examination of the units. After the units were disassembled, a large amount of black residue was found to have collected over the entire inside of the unit housing and over the outside of the stator end turns. Figure 9 shows the difference between the stator before and

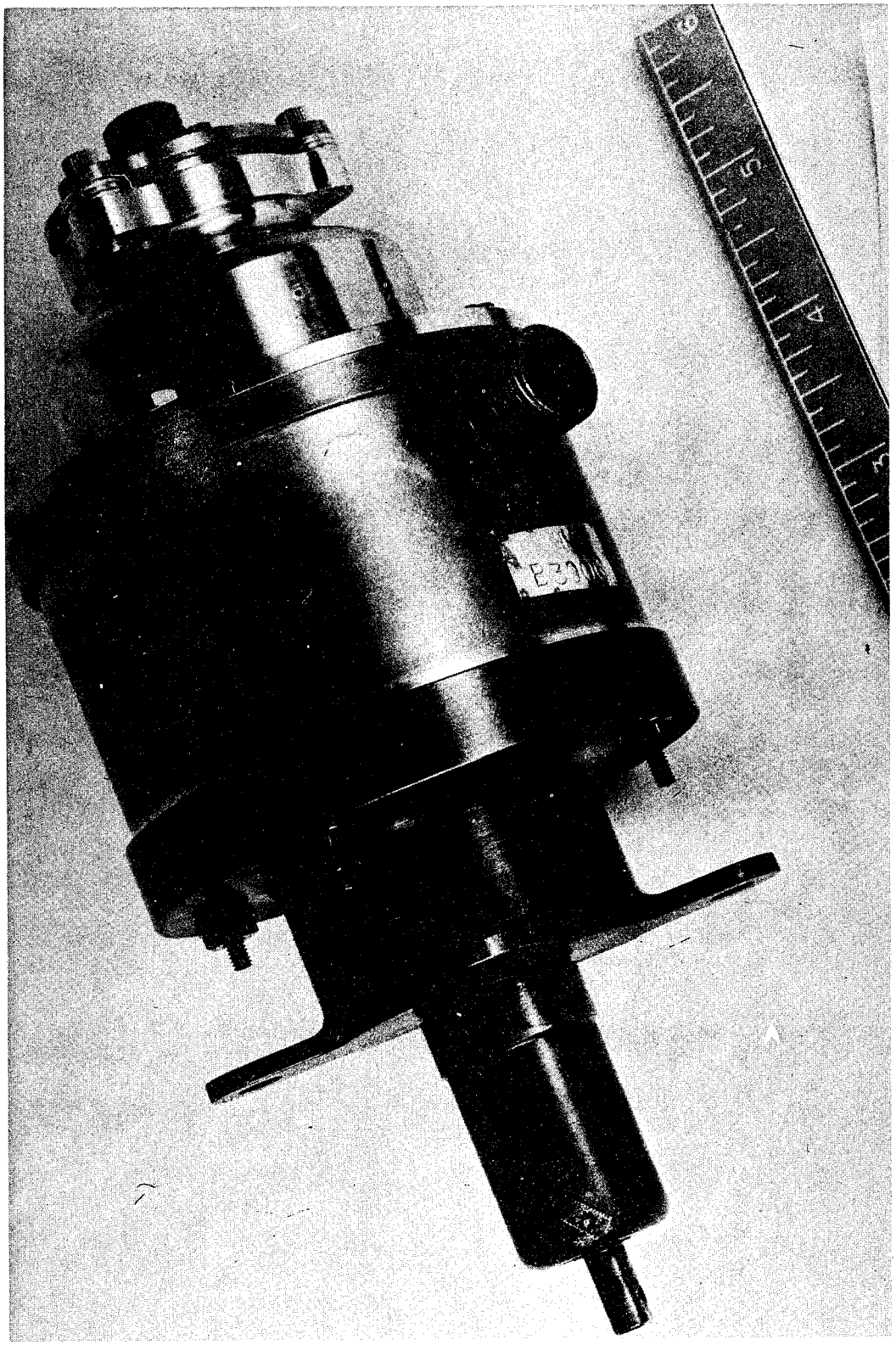

Figure 5. Control Drum Actuator Assembly

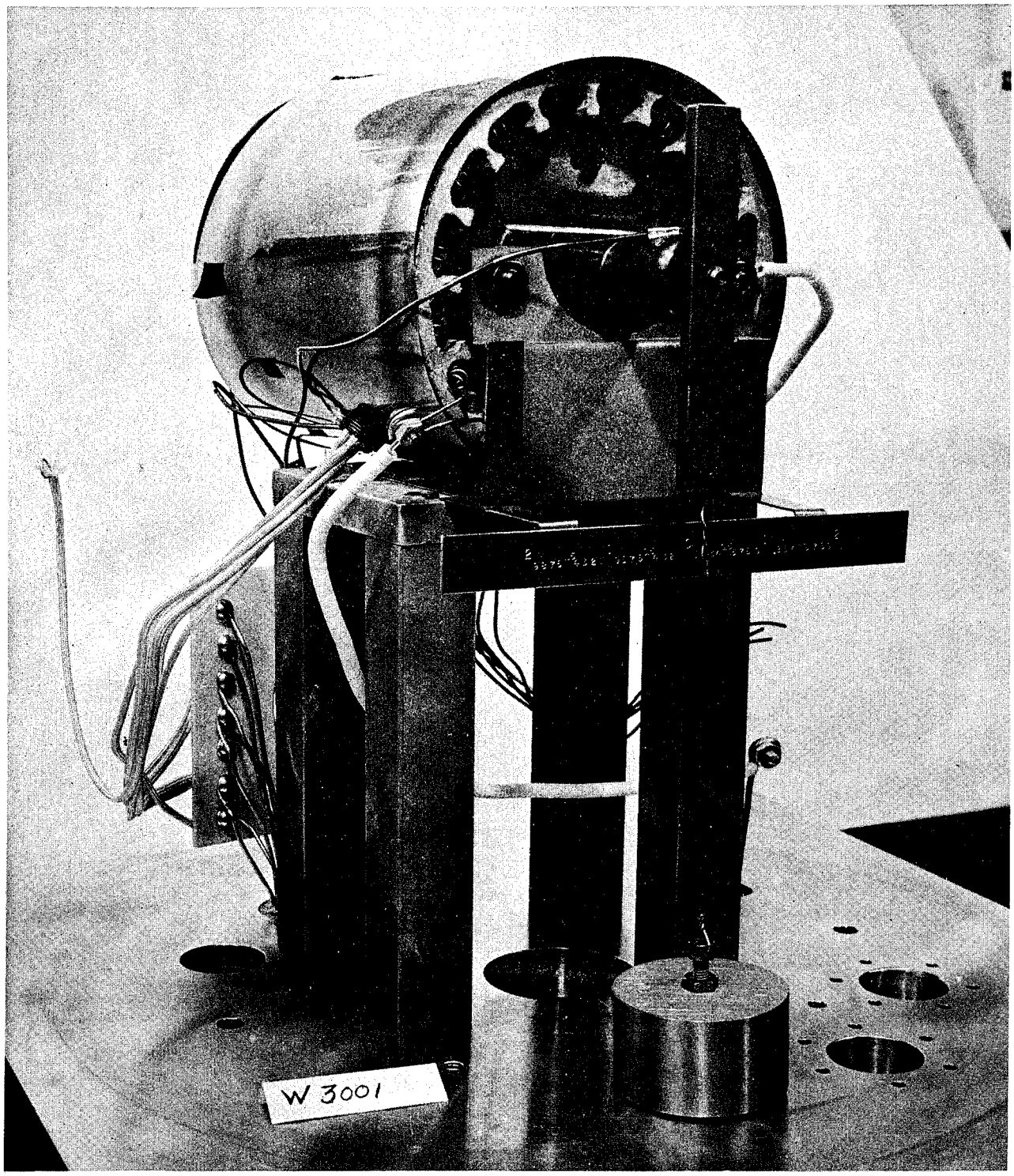

Figure 6. Vacuum-Temperature Test Fixture

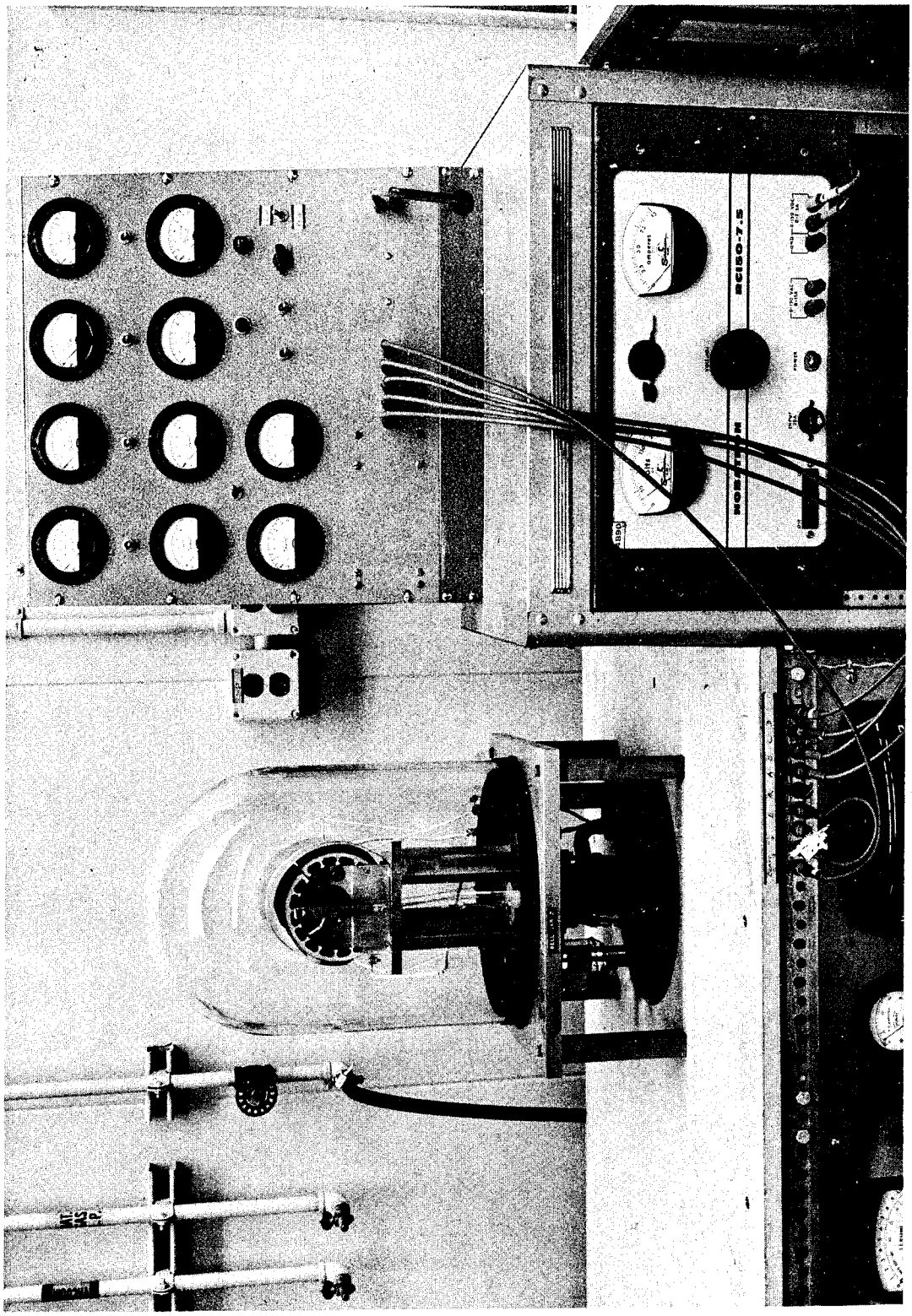

Figure 7. Vacuum-Temperature Test Assembly

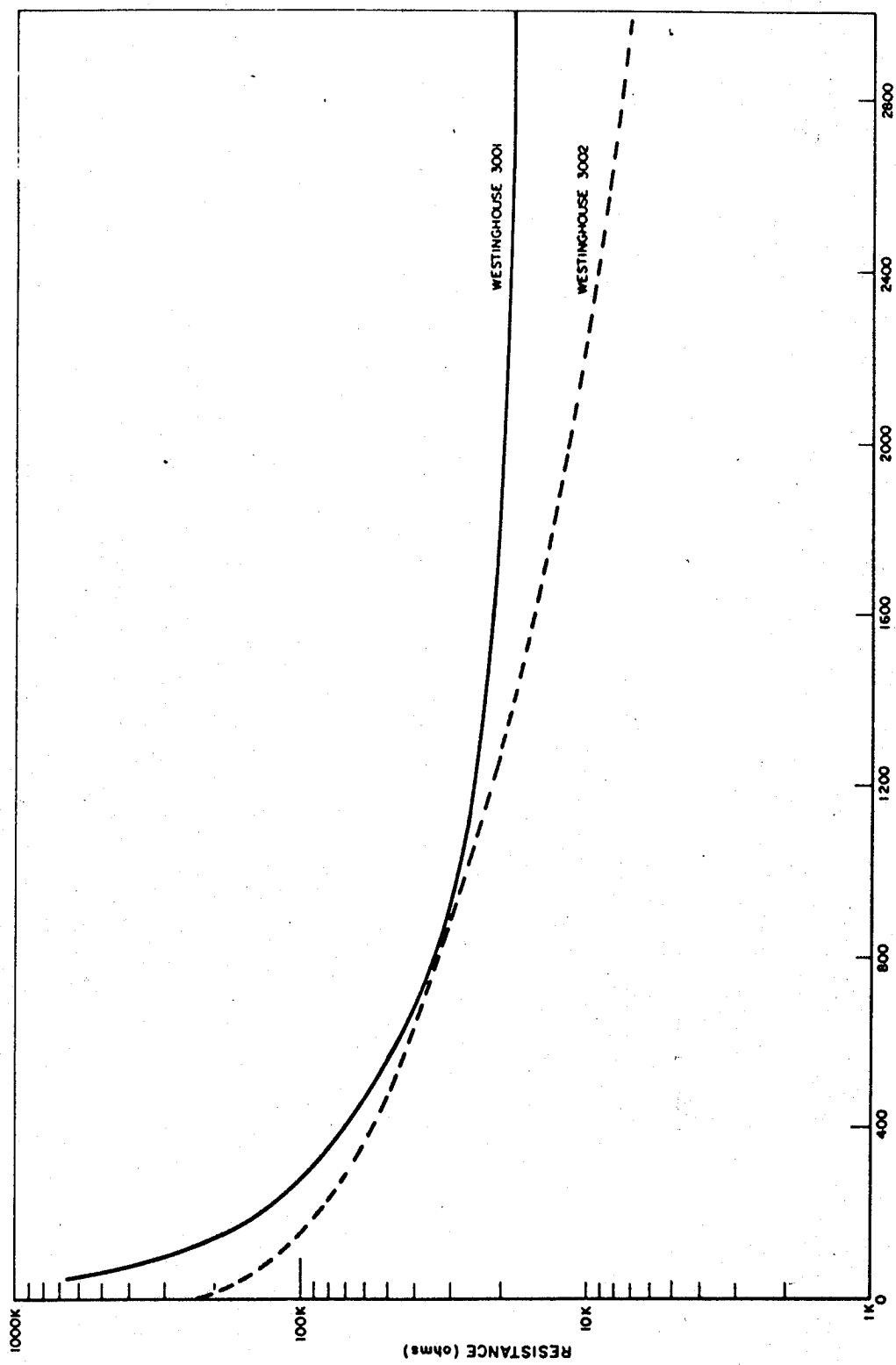

7568-55157

Figure 8. Vacuum-Temperature Test Results

6-17-63

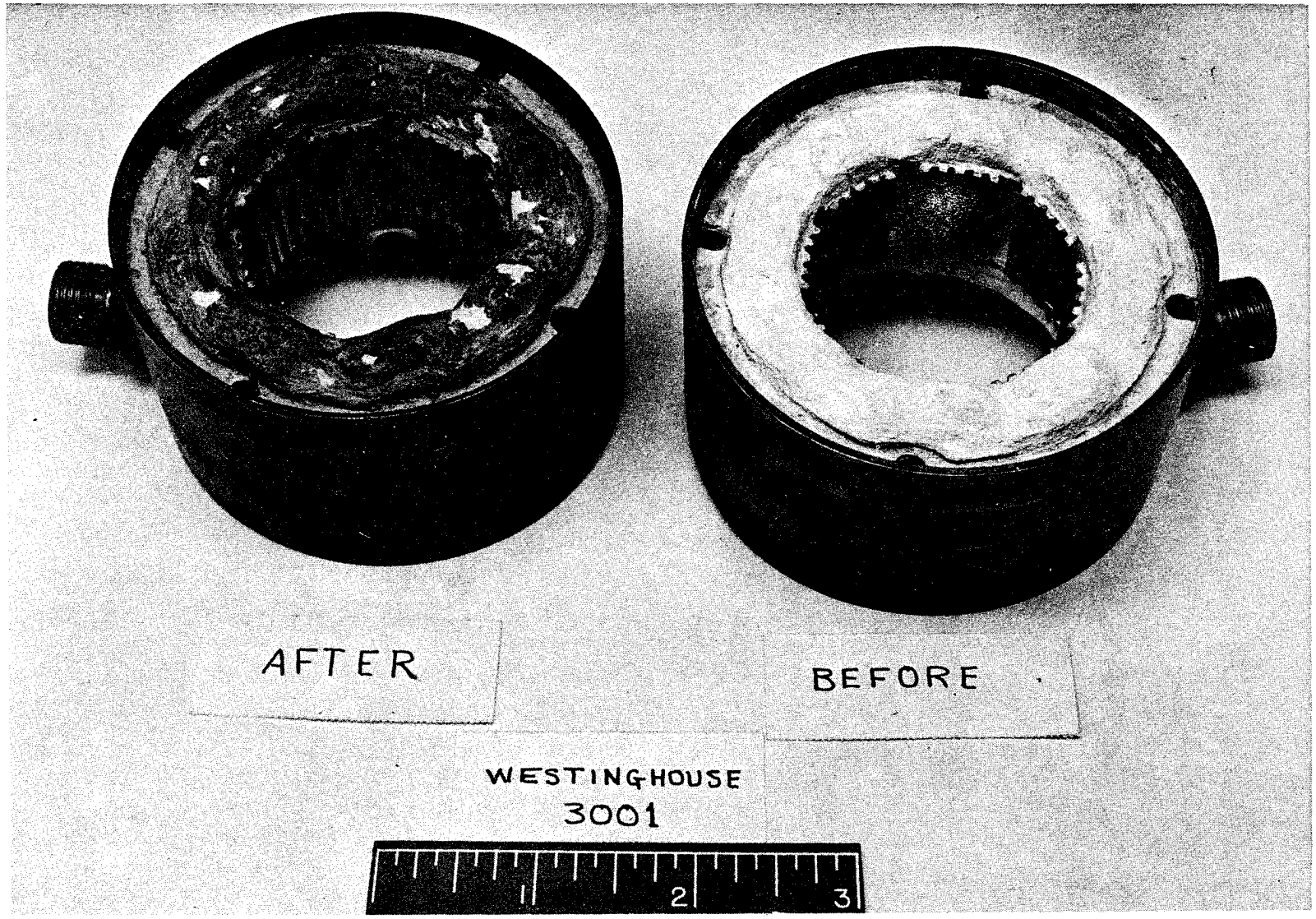

Figure 9. Test Stators Before and After 3000-hr Vacuum-Temperature Test

after testing. Scrapings of the residue were taken and a chemical analysis was made. These scrapings were found to contain lead, boron, and silica. The residue was cleaned from the stators by sandblasting the stator pole faces and wiping the stator end-turns. As much of the residue as possible was removed in this way. Chemicals and solvents were not used in the cleaning process, as this possibly could have been detrimental to the insulation material. After cleaning the residue from the stator end turns, the insulation resistance-to-ground was found to have increased markedly. The room temperature values of the insulation resistances were 7000 megohms and 333 megohms. One of the units was reassembled and placed back in test. The initial insulation resistance at 1000°F, after cleaning, was 1.17 megohms. The resistance decreased during the first 1000 hours of operation at 1000°F to 604 K ohms. Tests on this unit are continuing.

Figure 10 shows the test assembly that was irradiated. This assembly contained stainless-steel test spools with oxalloy wire coils which were encapsulated with the original Westinghouse insulating material and material free of Boron-10.

Inpile measurements at 8-hour intervals were made of the insulation resistance from coil-to-coil and from coil to the grounded spool core. These measurements were made with a 100-volt d-c potential. The temperatures were maintained at approximately 550 to 600°F for 27 days (577 equivalent full-power hours). The pressure was maintained at approximately 4×10^{-5} Torr. The gamma dose at the end of this time was about 2.7×10^{10}R. The neutron dose at this time was:

Energy	Total Neutron Dose (10^{18} nvt)
>0.1 Mev	3.9
0.017 - 0.1	0.6
0.4 ev - 0.017 Mev	4.7
<0.4 ev	0.06

The electrical insulation resistance as a function of time is shown in Figures 11 and 12. The data show that there is no significant difference between the insulation resistance exhibited by either of the encapsulating materials. There were no extreme changes in insulation resistance exhibited during reactor shutdown. This indicates that the insulation material is not seriously

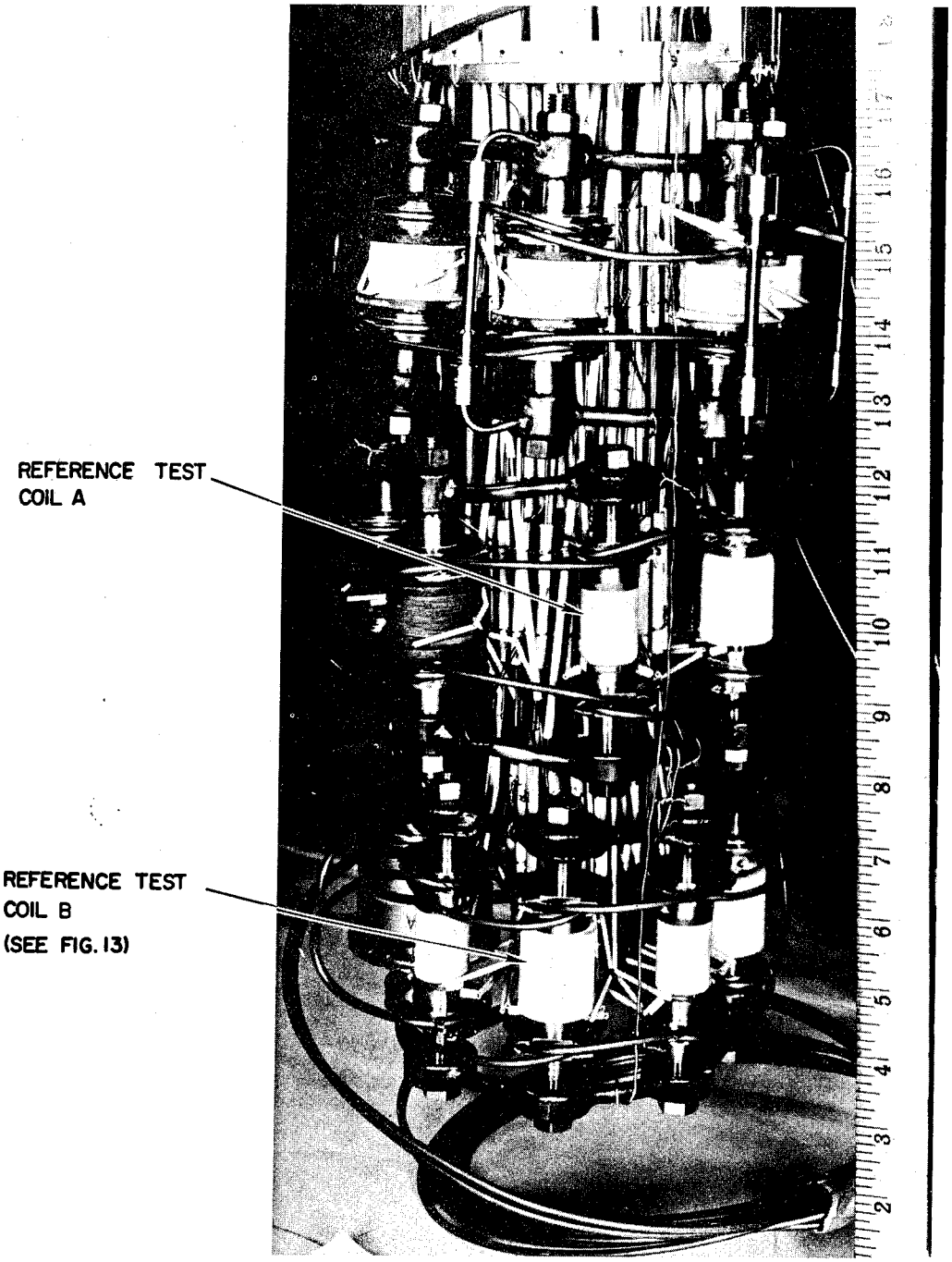

Figure 10. Irradiation Test Assembly

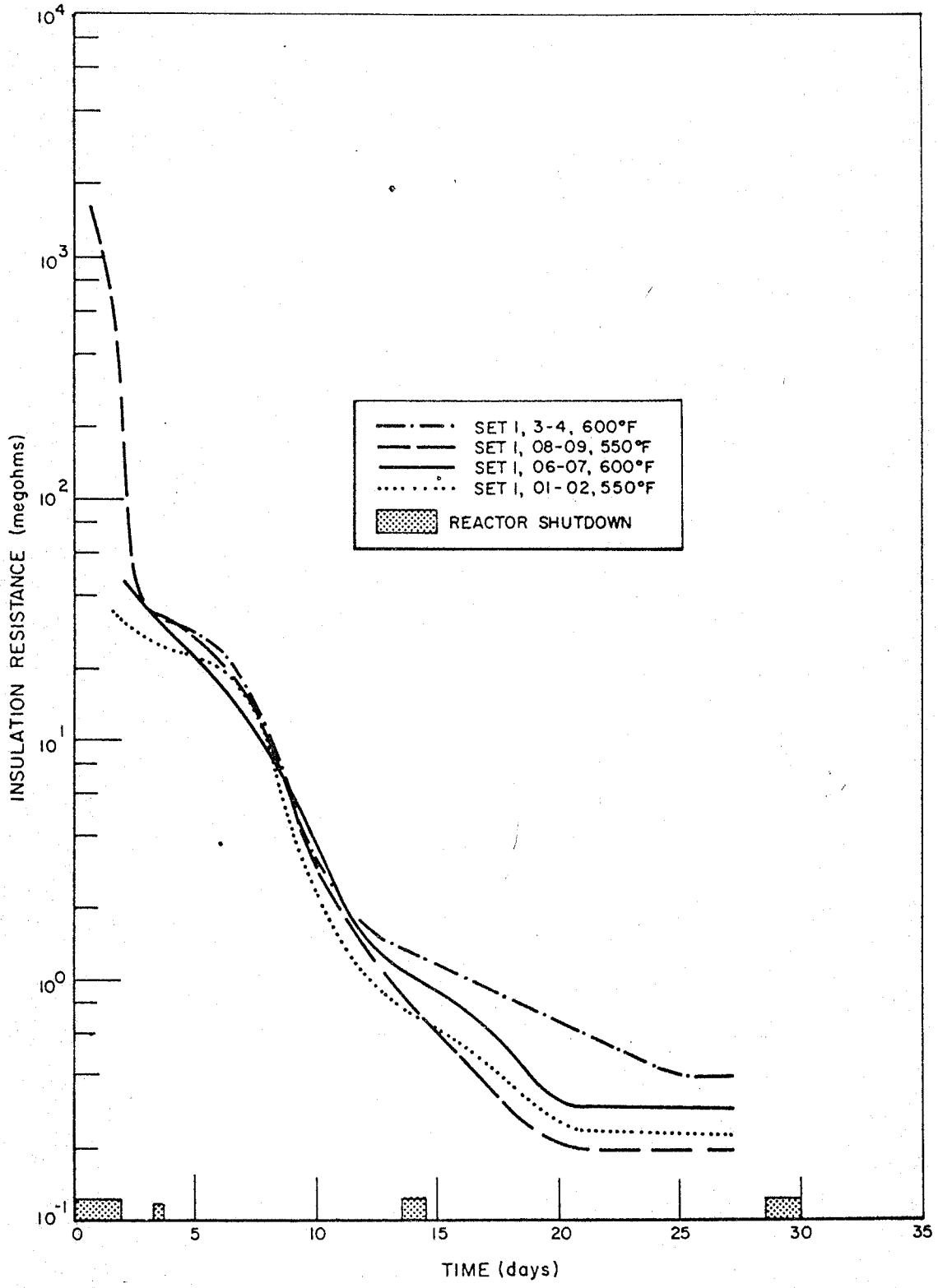

Figure 11. Resistance vs Irradiation, Conductor-to-Ground

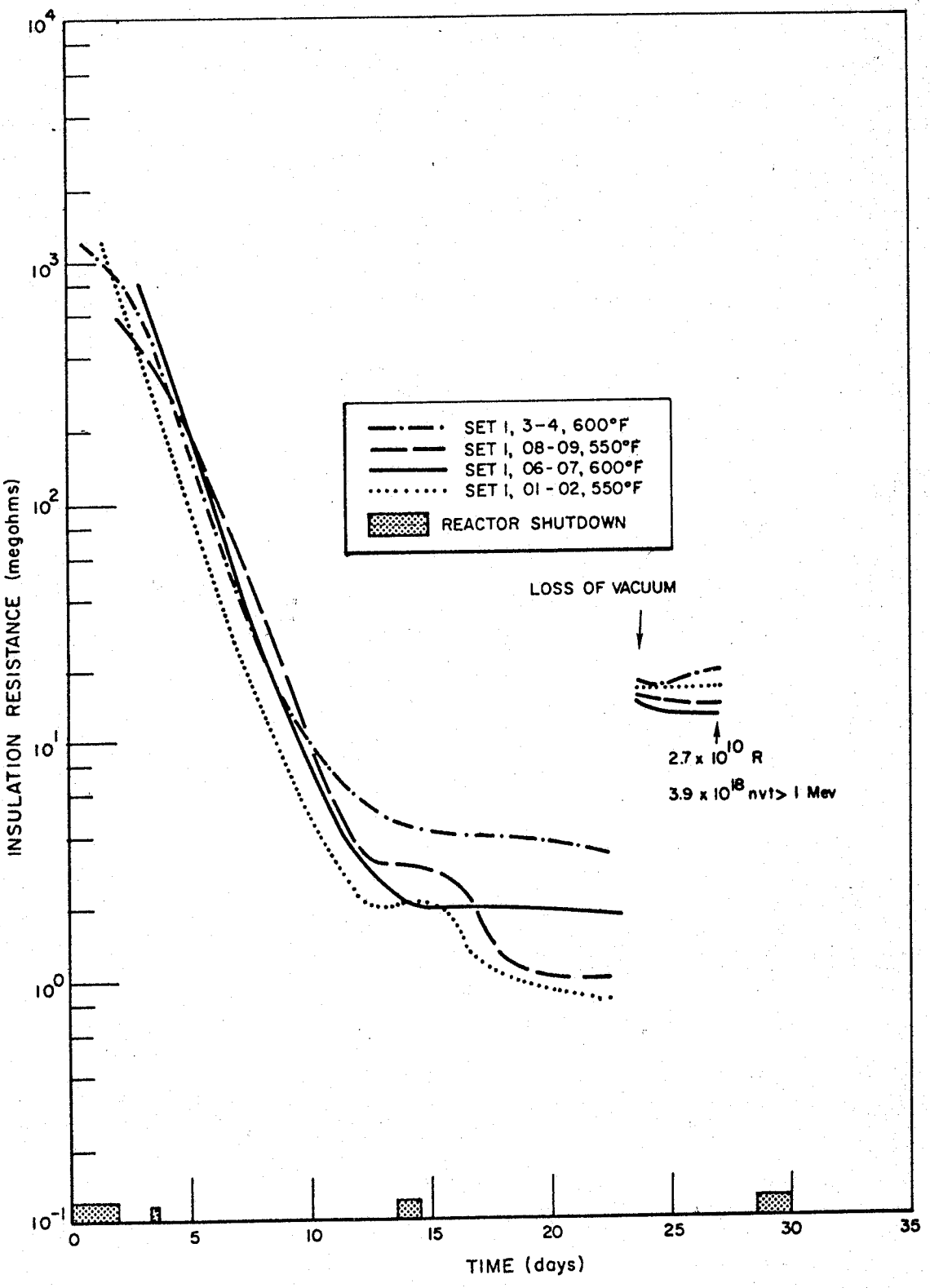

6-17-63

7568-55160

Figure 12. Resistance vs Irradiation, Conductor 1-to-Conductor 2

affected by the gamma dose rate. The sudden change in the rate of aging during reactor shutdown at the end of the first 12-day cycle of irradiation was due to a decrease in the spool temperature which was caused by the sudden decrease in gamma heating rate. The loss of gamma heat was partly compensated for by the heating coils within the irradiation capsule during reactor shutdown. The insulation resistance increased as the temperature decreased.

The sudden increase in insulation resistance during the 23rd day of the test was due to a power failure within the vacuum system which resulted in a rapid increase in capsule pressure. Experiments currently being undertaken have indicated that the increase in pressure possibly is the reason for the increase in insulation resistance.

Comparison of pre-irradiated photographs of the insulating materials with post-irradiation photographs (Figure 13) shows that neither insulating material was subject to physical damage due to the irradiation.

CONCLUSIONS

Except for the adverse effect of the conductive residue which volatilized out of the dielectric material, this insulation looks very promising for the environmental conditions of high-temperature space applications.

It appears that the initial stator under test had and maintained a high insulation resistance value because it was tested in a large volume chamber where there was ample opportunity for the volatile material to leave the stator and collect in the remote cooler regions of the chamber. In later tests, the stators were enclosed in end-housings more nearly simulating actual application. In this case, the volatile materials were restricted from escaping and eventually settled on the end-turns thus reducing the insulation resistance.

Future development work in dielectric materials for space should be directed to a material which has a strong chemical bond between its constituents and which is devoid of all high vapor-pressure materials such as boron and lead.

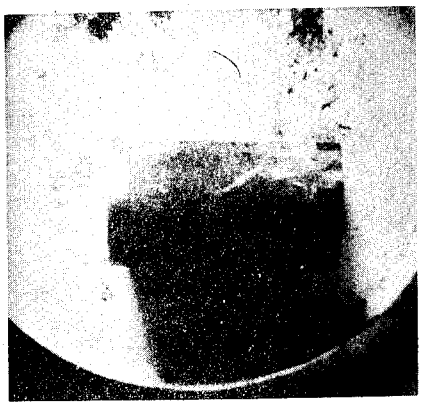

COIL A

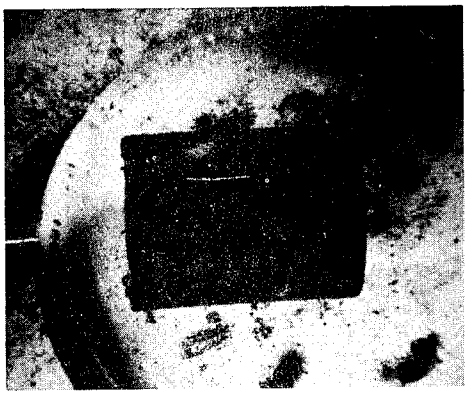

COIL B

Figure 13. Test Coils
After Irradiation

BERYLLIUM OXIDE DIELECTRIC COMPONENTS IN AEROSPACE APPLICATIONS

By P. S. Hessinger
B. Haura

National Beryllia Corporation
Haskell, New Jersey

(1) INTRODUCTION

The increasing emphasis on component reliability and stability under stringent environmental conditions has presented a challenge to the designer and fabricator of dielectric materials to be utilized in aerospace applications. The stability of a dielectric material over a wide range of temperatures, atmospheres, and mechanical stresses is dependent on a number of factors related to its basic chemical formula, internal structure, and proper utilization when integrated into the component.

Ceramic materials have been utilized for dielectric purposes for many years dating back to the early porcelain spark plug compositions, steatite as used in radio frequency applications, and more recently the high purity aluminum oxide used for a wide range of frequencies and electro-mechanical applications. As the parameters for space component dielectrics are established it becomes more and more evident that new problems are developing not heretofore encountered in the use of ceramic insulation. Of these, two of the most critical are, the ability to dissipate heat and the ability to withstand radiation. These properties are required in addition to the more common insulating requirements of low dielectric loss and high specific resistivity.

In addition, vibration and impact requirements dictate a need for high mechanical strength and the ability to withstand both thermal and mechanical shock conditions.

One of the ceramic materials which is being utilized for these advanced component applications is beryllium oxide in the form of a single-phase ceramic oxide body sintered to near theoretical density under closely controlled processing conditions. Beryllium oxide ceramic materials have been somewhat controversial since their inception, due primarily to the fact that the initial powder raw materials are toxic and must be handled with extreme care and cleanliness. Secondly, because of the relatively high initial cost of the starting materials, the resultant ceramic materials have been costly when compared to earlier more conventional steatite or alumina components.

In the past few years however, a rapid advancement of beryllium oxide handling, fabrication and the use of automatic processing techniques has greatly reduced both of these factors as far as their influence on the utilization of beryllium oxide in dielectric applications. These technological advances have now made possible the use of this material in a very wide range of electronic components from extremely miniaturized semi-conductor device packages up to fabricated aerospace radome structures.

The intent of this paper is to present the most recent available data on beryllium oxide ceramic dielectric materials presently being applied in aerospace systems and to review the factors which affect the critical dielectric and thermal properties when used in such applications.

(2) PROPERTIES OF BERYLLIUM OXIDE

Beryllium oxide (BeO) is presently the only known oxide of beryllium metal. Neither beryllium metal itself nor, for all practical purposes, beryllium oxide is found in the free state in nature. The primary source for beryllium and beryllium compounds is the mineral beryl, a double metasilicate of beryllia and alumina with the ideal formula $3BeO \cdot Al_2O_3 \cdot 6SiO_2$, which contains a theoretical beryllium oxide content of 14% by weight. Beryllium oxide is obtained from beryl ores through a complex thermal, chemical, and mechanical reduction process which accounts in part for the relatively high cost of the starting materials used in the ceramic fabrication process.

The BeO utilized in ceramic dielectric work is obtained as a white, extremely fine, crystalline powder ranging in ultimate particle size from 0.1 to 1 microns. The basic crystal structure of BeO is hexagonal, the structure corresponding exactly to the zinc sulfide (ZnS) lattice as found in wurtzite. Figure 1 illustrates in tabular form the fundamental properties of beryllium oxide which would be of interest in most applications. In comparing this material with other ceramic oxides it becomes obvious that it has an extremely high melting point of 4650°F and a relatively low density, 3.00 g/cc or .108 pounds/cubic inch. The high boiling point of 7030°F and extremely low vapor pressure make beryllia attractive as a stable material over a wide range of temperatures and pressures as may be encountered in space applications.

Probably the most outstanding single property of beryllium oxide is its extremely high thermal conductivity. At room temperature, the thermal conductivity of beryllium oxide is 0.63 $cal/cm^2/°C/sec/cm$ (150 $BTU/FT^2/°F/HR/FT$. This value when compared with other metallic

and non-metallic materials may be seen to be somewhat higher than aluminum metal, beryllium metal, nickel, iron, and virtually all dielectric materials. It is approximately 60% that of pure copper.

For the purposes of this paper, further references to beryllium oxide will, unless otherwise specified, imply a fabricated dense ceramic body having a beryllium oxide content of 99% or more and an average density of 2.85 g/cc which is 95% of the density of single crystal beryllium oxide. Figure 2 illustrates graphically the behavior of the thermal conductivity of beryllium oxide as a function of temperature, showing the characteristic decrease of the conductivity as temperature increases. It may be pointed out that even at temperatures of 1000°F the thermal conductivity is comparable to or slightly higher than that of nickel. Data recently published by several investigators, Burk and Powell, in the low temperature range indicates an extreme increase in thermal conductivity, and at -50°F the value is better than 1.0 $cal/cm^2/sec/^oC/cm$. While not shown on this specific plot, there are indications that a peak is reached at approximately -200°F having an order of magnitude of 1.5 $cal/cm^2/sec/^oC/cm$ with subsequent drop-off as the temperature approaches absolute zero. These values may be compared to the thermal conductivity of copper at room temperature which is 0.9 $cal/cm^2/sec/^oC/cm$.

The high thermal conductivity of fabricated beryllium oxide ceramic materials is primarily dependent upon the BeO content which must be of maximum value, preferably 99% or above, and the absence of porosity, thus requiring maximum densification during sintering. Because of these requirements, close control of micro-structure is a necessity in the fabrication of beryllium oxide components. Minor impurity amounts have been shown to reduce the thermal conductivity substantially, particularly in the presence of a glassy phase. For example, a 2% impurity level of alumina or silica will reduce the thermal conductivity of beryllium oxide by close to 20%.

The use of beryllium oxide in aerospace dielectric applications is predicated on the stability and control of its insulating properties. The three values of immediate importance are dielectric constant, dielectric loss tangent, and volume resistivity. The stability of the dielectric constant as a function of temperature is of primary importance in the design of antenna windows and waveguide windows which are required to operate over wide ranges of temperature varying from the cryogenic range up to several thousand degrees fahrenheit as experienced during re-entry. Measurements have been made on sintered beryllia at various frequencies and the characteristics of the material may be seen in Figure 3.

It may be noted on the curves that there is a reversal of the frequency effect in the relationship of the three curves, however, this may be related to variations in the test technique since the data was obtained from several sources. The 230 megacycle data was measured in a high temperature resonant cavity dielectrometer with a refractory metal heating element suitable for measurements to 3000°F. In this technique the dielectric constant is determined from displacement of the resonant frequency from the center frequency and the loss tangent from the change in width of the half power bandwidth. The 3140 megacycle and 8500 megacycle measurements were made using the slotted waveguide technique and measuring the shift in the standing wave due to the sample. With regard to the dielectric constant of beryllia it may be noted that it is approximately 6.5 at room temperature which is about 70% that of aluminum oxide and at 2000°F it has increased by approximately 18%. This increase however, is reproducible and dependent upon the control of purity of the material.

Figure 4 shows a plot of the dielectric loss tangent of beryllium oxide at the same three frequencies and over a wide temperature range. Behaving as most ceramic materials do, the loss tangent decreases as the frequency increases, particularly in the high temperature range as shown on the curves. It might be noted that data recently published Sutton & Bowlby, at 9375 megacycles has extended the measurements to 2500°F and at this particular frequency the loss tangent value of .0017 was determined for 99.5% purity beryllium oxide. The room temperature value for dielectric loss tangent of from .0003 to .0005 shows a high degree of stability out to 800°F at all frequencies. These low loss characteristics make possible the use of beryllium oxide in a number of high power window and high frequency device applications which will be described further in the paper.

The dielectric constant of beryllium oxide may be controlled primarily by its density and to a small extent by its chemical purity. Since in order to maintain the high thermal conductivity properties, the BeO content must remain at a level of 99% or better, chemical additions of higher dielectric constant oxides to BeO have a nominal effect on increasing its dielectric constant. The dielectric constant however, may be reduced by introduction of porosity and this has been done by foaming the material down to as low as 25 lbs/ft^3 or 13.5% of theoretical density with a resulting dielectric constant of 1.75. The curve shown on Figure 5 has been obtained at various density levels for sintered beryllium oxide. The scatter in data points may most likely be attributed to variation in pore shape and size however the trend of the curve is rather obvious. The measurements at 1 megacycle and 100 KC were made using a Boonton Radio 160-A Q-meter and the 9375 megacycle data was obtained using a waveguide termination tech-

nique. Further studies are being conducted to determine the physical parameters, which influence the frequency effects on dielectric properties of porous beryllia, however, the data obtained and shown on this curve does indicate that the available range of dielectric constant control is quite wide. Loss tangent data obtained on these materials fell within the range of the dense material. Such low density and foam ceramic dielectric bodies have potential application in light weight radome and electro-magnetic window structures for aerospace applications and are being developed for this intended purpose.

Figure 6 shows a plot of the volume resistivity versus temperature characteristics of 99% purity beryllium oxide made both in the pressed and sintered or extruded form. The volume resistivity of any pure oxide ceramic material is extremely sensitive to the presence of impurities and efforts are presently underway to reach maximum purity in beryllia utilized for applications where resistivity is critical. Such applications include ultra-high temperature thermocouple insulation and temperature sensing devices designed for operation at temperatures to 4000^{o}F. We know for example that the presence of alkali and alkali contaminants are extremely detrimental to pure oxides particularly in the presence of a silicious phase where ionic mobility can occur. Extreme care must therefore be exercised in the fabrication of ultra-high purity insulating bodies and this involves working with chemical reagent grade starting materials, all organic handling systems, and the elimination of physical contact of the material with any metallic processing equipment. It has been indicated that, by increasing the purity to a level approaching 99.9%, several decades of increased insulation resistance can be anticipated at the high temperature end of the curve.

One additional comment may be of interest on the dielectric properties of beryllium oxide and this is in relation to its dielectric strength which has been measured on various thickness samples. As with most ceramic materials the dielectric strength increases with decreasing thickness. It has been found that it will range from a low of 125 volts/mil in a.250 inch thickness to 300 volts/mil in a .050 inch thickness. Further research is needed however in the area of dielectric breakdown strength of beryllium oxide to relate micro-structure with this property. It is expected however that improvements in mechanical strength of beryllia will lead ultimately to higher dielectric strength values. High purity beryllium oxide manufactured several years ago ranged in flexural strength from 15,000 to 18,000 lbs/in^2. The material presently being utilized in aerospace applications ranges from 25 to 30,000 lbs/in^2. Material has been made under closely controlled laboratory conditions having a strength of

45,000 lbs/in^2 which is directly comparable to high purity aluminum oxide materials. This noticable increase in the physical properties of beryllia ceramics may be attributed directly to the increased requirements for the material as dictated by new missile and space applications which have emphasis on reliability in electronic components.

(3) FABRICATION OF BERYLLIUM OXIDE DIELECTRIC MATERIALS

Beryllium oxide may be fabricated into component shapes using relatively conventional ceramic processing methods. These methods include slip casting, extrusion, and cold-pressing or isostatic pressing. The starting material in all cases is a beryllium oxide powder which has been calcined, producing sufficient crystal growth, to limit extensive shrinkage during the densification process. The calcination of sub-micron size particles to temperatures between 900 and 1500^{o}C results in a powder product having controlled crystallite sizes ranging as high as 30 microns.

In the slip casting process the powdered materials are blended into an aqueous slurry containing various electrolyte materials to maintain the particles in suspension during the casting operation. Porous plaster molds are used, the material being introduced in a slurry condition allowing time for build-up of the BeO coating on the wall of the mold after which the excess slip is drained from the system. Following an initial drying shrinkage the piece can be removed from the mold with relative ease. This process finds somewhat limited use however, it is applicable to the fabrication of large three-dimensional pieces and has been applied to high purity crucibles, combustion boats, and more recently fabrication of beryllium oxide radome blanks.

The extrusion process utilizes beryllia in a similar form combined with organic lubricants and binders which, as a high solid-content plastic mass, allows the material to be extruded through an abrasion resistant nozzle into rods, tubes, and fine capillaries of extended length. Such tubular forms of beryllium oxide are used in thermocouple insulation, helix support rods, and various cylindrical insulator shapes.

Cold-pressing, which is sometimes called dry-pressing, is probably the most widely applied ceramic forming process for electronic beryllium oxide components. This method utilized the material in a granulated form with comparatively small amount of moisture or an organic binder. The material is fabricated in a steel die cavity and compacted under pressure using techniques similar to powder metallurgy. The advantage

of the cold-pressing technique is that small parts of comparatively complex geometry can be produced at a rapid rate with a high degree of uniformity and reporducibility. A modification of the cold-pressing technique which has lent itself to the formation of large dense shapes is isostatic pressing in which the powder is compacted inside of a plastic or rubber envelope which is sealed and suspended within a pressing medium of either water or oil. The advantage of such a process is that pressure is applied uniformly from all directions, and thus eliminates laminations and density differentials which sometimes occur in large cross-section ceramic shapes.

Care must be taken in the preparation of materials for all of these processes when dielectric properties are considered and the organic binders, lubricants, and compounds used in processing must not leave any residual metallic or carbonaceous residues which could be deleterious to the loss and resistivity characteristics of the ceramic body. Fabrication of 99.5% purity beryllium oxide ceramic materials is dependent upon extreme care in handling, mixing, and forming of the parts in all stages of the manufacturing process. Subsequent to the forming step the material is subjected to a high firing, reaching in some cases as high as 3400°F, to achieve densification. During the firing steps the beryllium oxide shapes must be handled with care and prevented from undergoing any interaction with the furnace components or the setter materials. For this purpose the material is generally fired on setters also of beryllium oxide.

Following firing when the parts are cooled to room temperature, if precise dimensional requirements exist they may be achieved using ceramic grinding techniques generally with diamond tooling. Methods such as surface grinding, centerless grinding, and drilling are common to precision fabrication of beryllium oxide dielectric parts.

Because of the high degree of purity and the need for elimination of any toxicity hazards in the finished product, a methodical cleaning procedure must be utilized for the finished parts prior to delivery to a user. The parts taken from machining are ultrasonically cleaned using carefully selected detergents which do not leave detrimental residues. They are subsequently given a series of wash steps and in mnay cases are subjected to a intermediate clean firing operation which removed any residual organic contamination developed during handling or machining of the shape. The cleaning procedures for beryllium oxide dielectric parts are especially critical if the material is to be metallized for subsequent plating and/or assembly operations where residual surface contamination could cause a blistering or loss of adherence. Finished parts to be used in such assembly work are

therefore packaged, sealed, and then handled with nylon gloves during any further processing on the part. One comment which could be made at this point is in connection with the toxicity aspects of beryllium oxide processing. This is the fact that beryllium oxide fabrication process must be conducted using complete hooding and glove box facilities and following stringent house-keeping requirements as recommended by the Atomic Energy Commission. Once the parts are high fired however, they are dense and there is no residual surface powder or any easily removeable beryllia material which could be considered hazardous. In grinding however, dust is generated and therefore the grinding operation must be done under hooded conditions. Following the above described cleaning procedures, the resultant parts may be handled as if they were any other ceramic material and no difficulty should be encountered because of the hazardous nature of the initial beryllium oxide starting materials.

(4) DIELECTRIC APPLICATIONS OF BERYLLIUM OXIDE MATERIALS

The successful use of beryllium oxide in dielectric applications is dependent upon the ability of the design engineer to use to full advantage the unique physical properties available in the material. High thermal conductivity can provide substantial improvements in power dissipation and reliability if the proper methods of joining the ceramic component to the metallic elements are utilized.

One of the early developments in the use of beryllium oxide for heat dissipation purposes was in the semi-conductor field where a need existed for a means of isolating the collector of various power transistor devices and at the same time to dissipate heat from the junction into an infinite heat sink or a comparable external cooling device. Because of the wide range of transistor case sizes being utilized under the various JEDEC designations, a series of beryllium oxide transistor heat sink pads were designed for direct combination with presently existing transistor cases. Figure 7 illustrates some transistor insulator types, the larger being a TO-3 wafer the smaller sizes being TO-5 and TO-18. It might be noted that some of the parts incorporate a metallized surface such that the heat sink pad can be soldered directly to the chassis for maximum removal of heat. When this cannot be done, mechanical clamping must be utilized to effect good interfaces between the beryllia, the transistor, and the chassis. Thermal resistance data on this type of dielectric heat sink have been measured and are shown in Figure 8. These measurements were made using a relatively simple circuit in which the current and voltage applied across the transistor were measured and various power levels generated in the device. Thermocouple measurements were then made between the copper transistor case (T_C) and the infinite heat sink directly below the transistor (T_S). Thermal

resistance was then calculated and expressed in ^{o}C per watt. These measurements were made with a TO-3 size transistor was $0.14^{o}C$/watt. Several thicknesses of beryllia were evaluated and it might be observed that if the interface resistance is removed from the value obtained, the thermal resistance of the beryllium oxide part is as much as 20 times lower than comparable and more common dielectric heat sink materials. It may be noted that in equal thicknesses, beryllia demonstrates a thermal resistance of approximately 30% that of aluminum oxide when used in a mechanically assembled system. Similar tests using metallized and brazed assemblies have reduced this factor to approximately 20% of the equivalent alumina insulator.

A modification of the external beryllia heat sink is shown in Figure 9 in which a beryllia insulator is brazed to the base of a beryllium-copper clip device. The transistor may then be mechanically forced into the clip and held so as to be stable under extreme conditions of vibration, and yet be removed for repair and replacement purposes.

A refinement of the external dielectric heat sink is utilization of beryllium oxide wafer within the structure of the transistor case itself. This has been achieved in stud-mount assemblies as shown in Figure 10. In this particular case the small beryllia disc in the center of the stud has been metallized with molybdenum-manganese, has been electro-plated and then attached to the stud by ceramic-to-metal brazing. Subsequent to this operation the semi-conducting die is placed on the pad and the entire unit hermetically sealed. It has been found that with devices having such an isolated collector design, up to 400% higher power levels can be reached over conventional assembly methods. In addition to the development of high power levels, increased reliability is achieved because of the removal of the thermal dissipation problem at the junction.

The maximum utilization of beryllium oxide in semi-conductor device packaging for high reliability systems may be achieved using a design which integrates the ceramic component directly into the basic package design itself. In order to achieve this, the geometry of the ceramic must be kept as simple as possible. In a minimum of thermal stresses must be introduced into the design and the package design must be flexible in its fabrication parameters such that it can be utilized for a wide range of devices. Figure 11 illustrates the beryllium oxide micro-power transistor package which utilizes a disc of BeO brazed to either a copper heat sink stud, or in a form to allow attachment to a flat heat sink surface. Leads are brought out through pin seals in the base of the beryllium oxide and the die is attached to a metallized pad area in the center of the insulation. The external copper flange

is brazed forming a hermetic package and the final device assembly is achieved by cold-welding. Such semi-conductor packages using high purity beryllium oxide have demonstrated 10 ampere capability at frequencies in the 200 megacycle range and have been applied to numerous devices for missile and ultimately satellite systems. In this particular package design the low dielectric loss and low capacitance of the beryllium oxide are used to maximum advantage in combination with its high thermal conducting properties.

Figure 12 shows several small device packages fabricated of beryllium oxide, metallized and brazed directly to copper connectors and seals. The use of BeO in such miniaturized diode assemblies takes advantage of the materials low dielectric constant and resulting low capacitance, thus reducing the frequency effects of the insulation on the circuit operation.

Printed circuit applications of beryllium oxide have been developed for micro-electronic module approach to miniaturization and have led to improvements in power dissipation characteristics within the mounting board itself. Figure 13 illustrates small metallized printed circuit boards of 99.5% beryllium oxide. Typical of these applications is the unit in the upper right hand corner which forms the base for a five watt thin-film amplifier. Through the use of such a heat dissipation technique, the entire servo-amplifier module has been reduced to less than 1/4 of a cubic inch; with no sacrifice in the characteristics of the components used.

Figure 14 illustrates a somewhat larger beryllium oxide circuit board development, these particular components being utilized in the transmitter assembly for the Telstar satellite. The larger board measures approximately 2 x 4", and the thickness of both is approximately 1/8". In the Telstar transmitter module, a number of these beryllium oxide printed circuit boards have been utilized, the heat being ultimately removed by heat-straps, and the entire transmitter assembly being encapsulated in an organic foam.

Recent improvements in the technology of fabrication and control of beryllium oxide properties has led to development of a number of micro-wave window and radome applications. The utilization of beryllium oxide in radomes for aerospace and missile systems is based on the low loss and stable dielectric properties of the material combined with thermal shock resistance which results from its high thermal conductivity. Radomes have been fabricated both by slip casting and by isostatic pressing in a number of conical and ogive shapes. Figure 15 illustrates some cast beryllium oxide radome ogives approximately 6" in length with .100" wall thickness. The casting process utilized for fabrication of the radomes has resulted in uniform density and strnegth throughout the full radome shape with a capacity to scale the operation to increased sizes while maintaining the desired dielectric properties. Figure 16

illustrates a small thin-wall radome of beryllium oxide which has been machined to a .050" wall thickness for an advanced prototype application. Similar beryllium oxide shapes have been subjected to stringent re-entry shock tests and have given strong promise as a window and radome material for aerospace systems where high heat fluxes are involved.

The use of beryllium oxide in advanced space power conversion systems has been considered by many investigators, and experimental data obtained to date indicates that with the high melting point, thermal shock resistance, and ability to be metallized and sealed, high purity BeO holds promise in devices such as magnetohydrodynamic systems and possibly thermionic generators. In the magnetohydrodynamic applications, high purity and high strength are of critical importance along with chemical stability. Beryllia itself has a sensitivity to high water-vapor concentrations at elevated temperatures and techniques are being studied to retard the resulting corrosion affects. In addition, fundamental crystallographic studies are being conducted on the behavior of beryllium oxide in the temperature range between 2,000°C and its melting point. Crystallographic inversions have been detected leading to what appears to be a cubic structure and for MhD systems operating in this temperature range, stabilizing of the material may be required to prevent degradation under long time exposure.

In thermionic systems, resistance to cesium vapor corrosion appears to be the critical area for materials to be used in both the envelope and seal of such devices. Beryllium oxide has been fabricated in a dense gas tight form suitable for such device applications. Again, however, in addition to maintaining its electrical resistance, it appears that an extremely high purity material is required to retard attack by alkalis vapor corrosion. If these fundamental problems can be overcome by additional research, the inherent nuclear radiation resistance of BeO combined with its unique thermal and dielectric properties will make possible material capabilities not presently available for such systems.

(5) SUMMARY

In conclusion we may summarize the information presented, by stating that continued efforts in the control and fabrication of beryllium oxide ceramic materials are leading to new areas of application in aerospace, and missile and satellite systems. Data obtained on materials presently being manufactured for such advanced applications indicates a desireable stability of dielectric properties over a fairly wide range of frequency and temperatures, and a unique capability to dissipate the heat from critical areas in many devices and systems. The stability and reliability of transistors, diodes, and other devices

to be used in present and future space applications may depend on the use of beryllium oxide insulation and present development efforts are expected to lead to several new concepts in device design. The mechanical and electrical stability of window and radome materials under conditions of re-entry may depend upon the use of beryllium oxide to provide the required dielectric and structural properties. Substantial advances have been made in recent years in the properties and fabrication of this material, and we hope continued research and development in this and related areas may provide a new family of highly stable dielectric materials for use by future aerospace designers.

REFERENCES

1. "Oxide Ceramics", by Dr. Eugene Ryshkewitch, Academic Press, New York and London, 1960.

2. R. W. Powell, Trans Brit, Ceram. Soc. 53, 389-397 (1954).

3. "Thermal Conductivity of Beryllia Ceramics from -200° to 150°C, by Maksymilian Burk, Journal of the American Ceramic Society, Vol. 46, No. 3, March 1963.

4. Newlan, B. M., "High Temperature Dielectric Measurements in the VHF Range", Lockheed Aircraft Corp., Calif., December 1961.

5. "Beryllium Oxide Radome Development", Summary Report on Contract NOw-60-0057-c.

6. Goldsmith, A., Hirchhorn, H. J., and Waterman, T. E., "Thermophysical Properties of Solid Materials, Volume III - Ceramics", Armour Research Foundation, November 1960, WADC Technical Report 58-476, ASTIA No. 265597.

7. Hessinger, P., Strott, A., and Haura, B., "Beryllium Oxide Dielectric Heat Sinks for Electronic Devices," Special Tech. Publication No. 300, Published by the American Society for Testing and Materials, 1961.

8. "Dielectric Properties of Electromagnetic Window Materials for Hypersonic Vehicles, presented at the 1962 National Aerospace Electronic Conference, Dayton, Ohio, May 14-16, 1962 by R. W. Sutton and C. W. Bowlby, Antennas and Radomes Unit, The Boeing Company, Aero-Space Division.

FIGURE 1

Fundamental Properties of Beryllium Oxide

Chemical Formula:	BeO
Crystal Structure:	Hexagonal, Wurtzite (ZnS) c/a Ratio 1.63
Theoretical Density:	3.008 g/cc
Melting Point:	2570°C (4650°F)
Boiling Point:	4000°C (7030°F)
Vapor Pressure:	mm. Hg. Torricelli

$$\log_{p} = 18.50 - \frac{34,230}{T} - 2 \log T$$

THERMAL CONDUCTIVITY OF BERYLLIUM OXIDE

SAMPLE DENSITY 2.85 G/CC; PURITY 99 + BeO

FIGURE 2

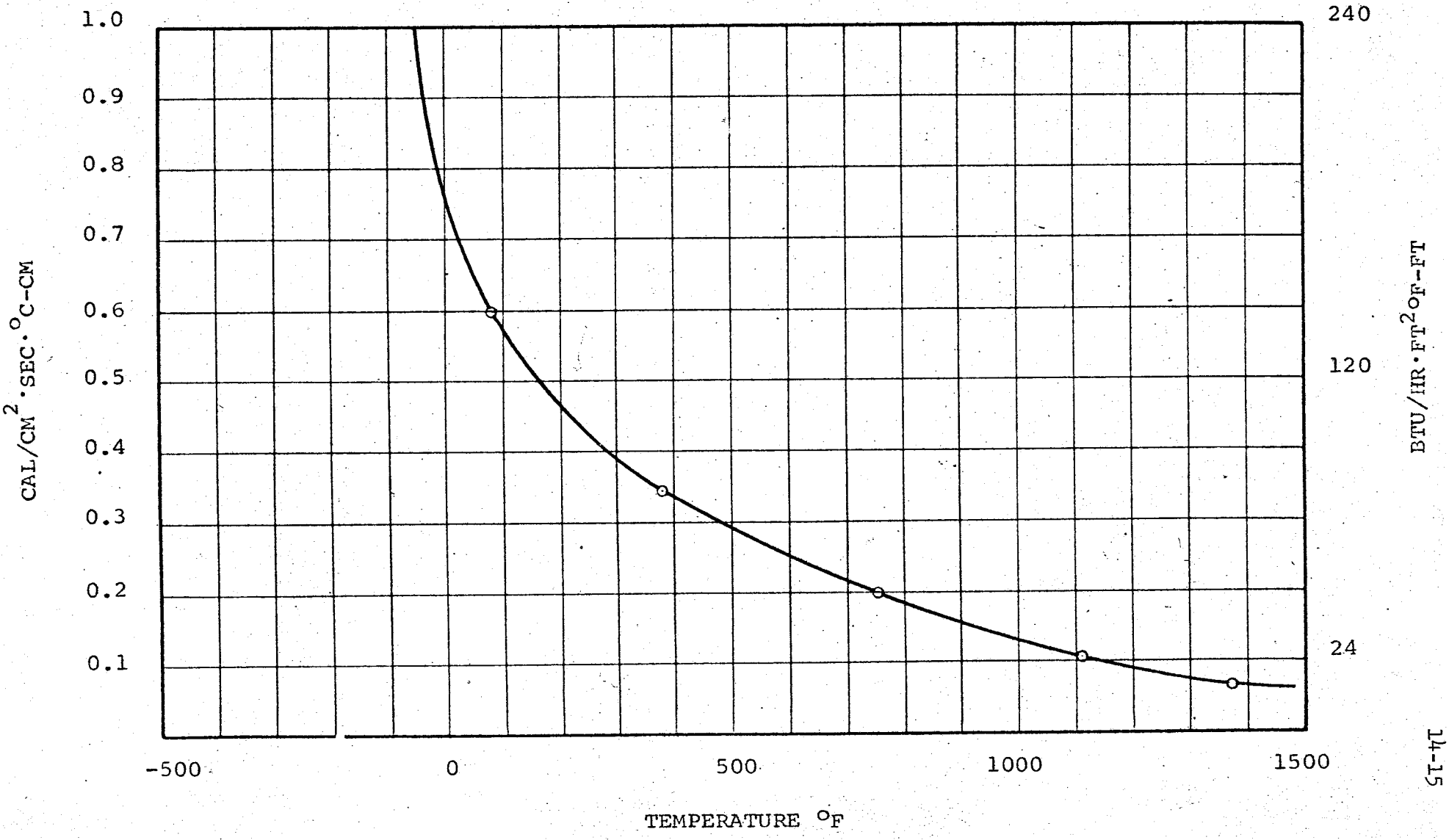

TEMPERATURE DEPENDENCE OF DIELECTRIC CONSTANT OF BeO

DATA CORRECTED FOR SAMPLE DENSITY 2.85 G/CC

FIGURE 3

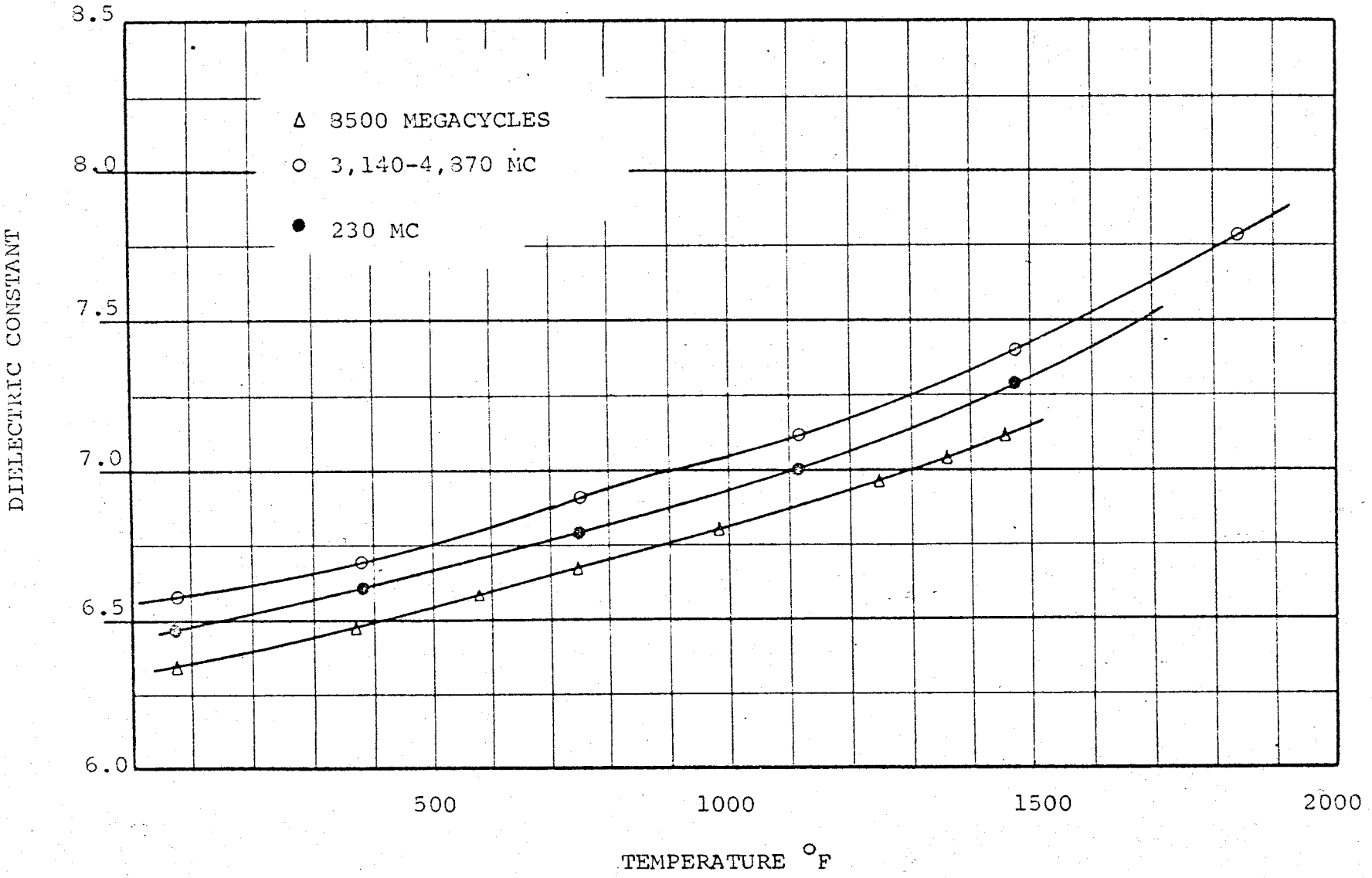

TEMPERATURE DEPENDENCE OF LOSS TANGENT OF BeO

FIGURE 4

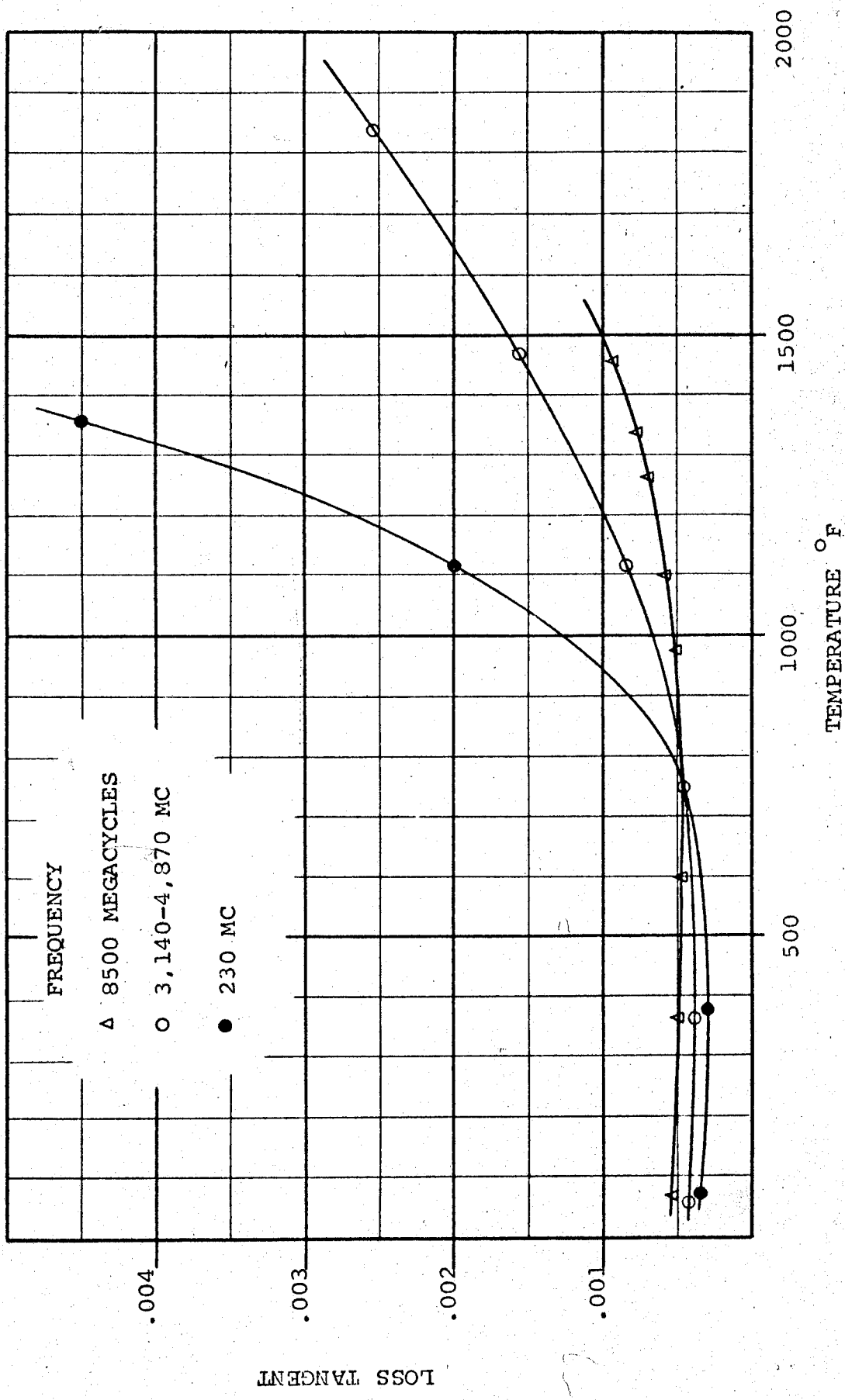

DENSITY DEPENDENCE OF DIELECTRIC CONSTANT OF BeO

FIGURE 5

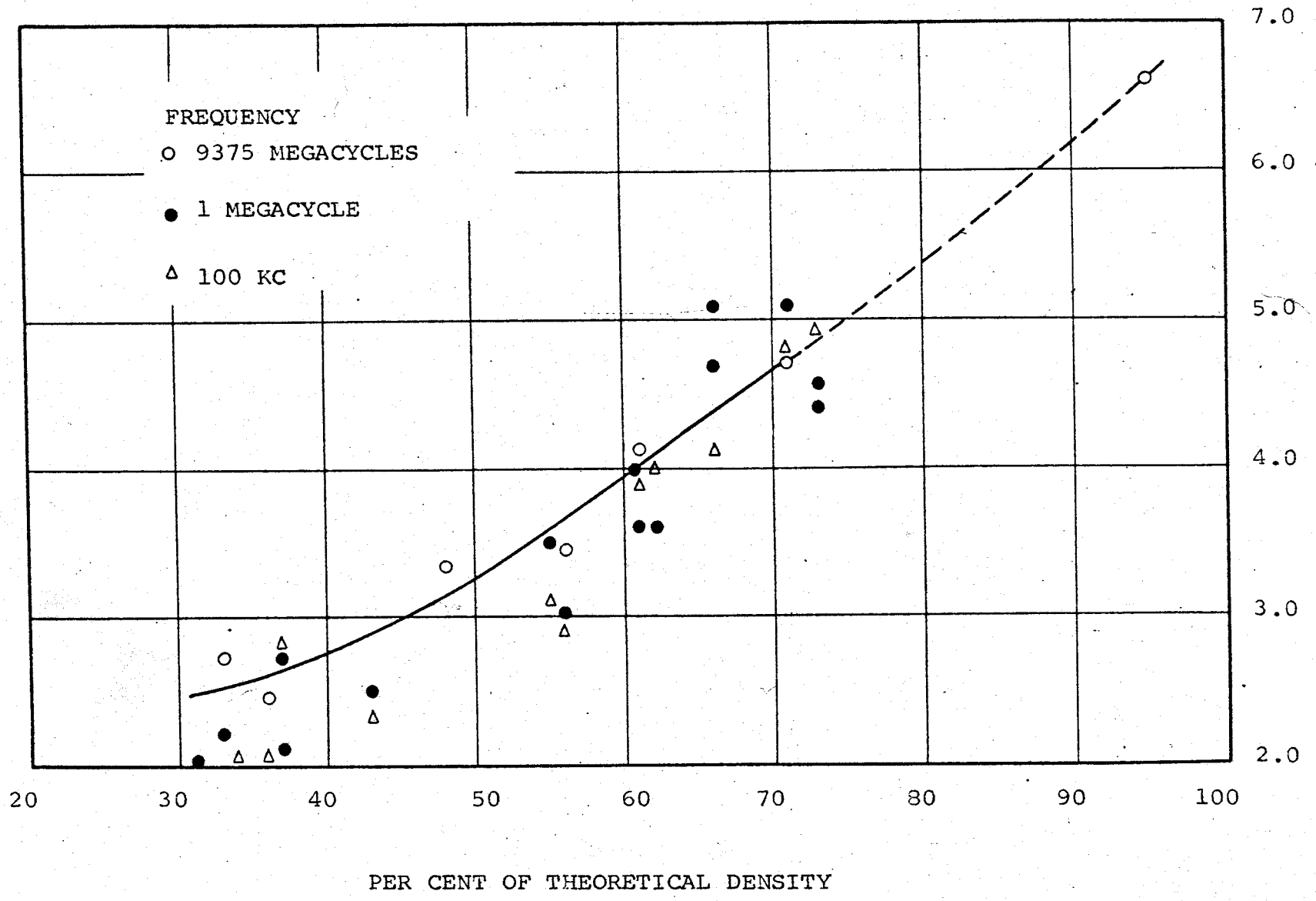

FIGURE 6

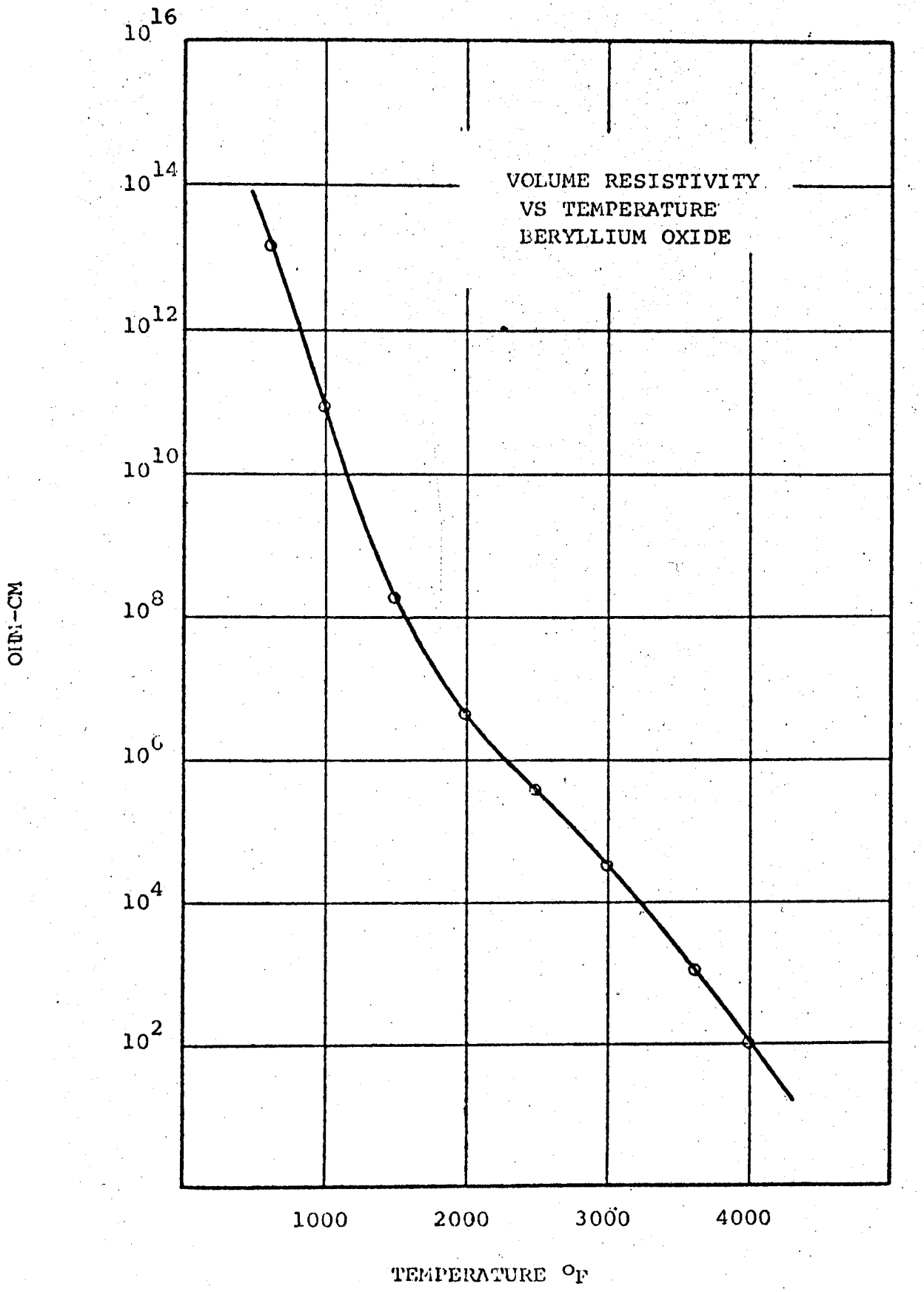
VOLUME RESISTIVITY
VS TEMPERATURE
BERYLLIUM OXIDE
10^{16}
10^{14}
10^{12}
10^{10}
10^{8}
10^{6}
10^{4}
10^{2}
OHM-CM
1000
2000
3000
4000
TEMPERATURE °F

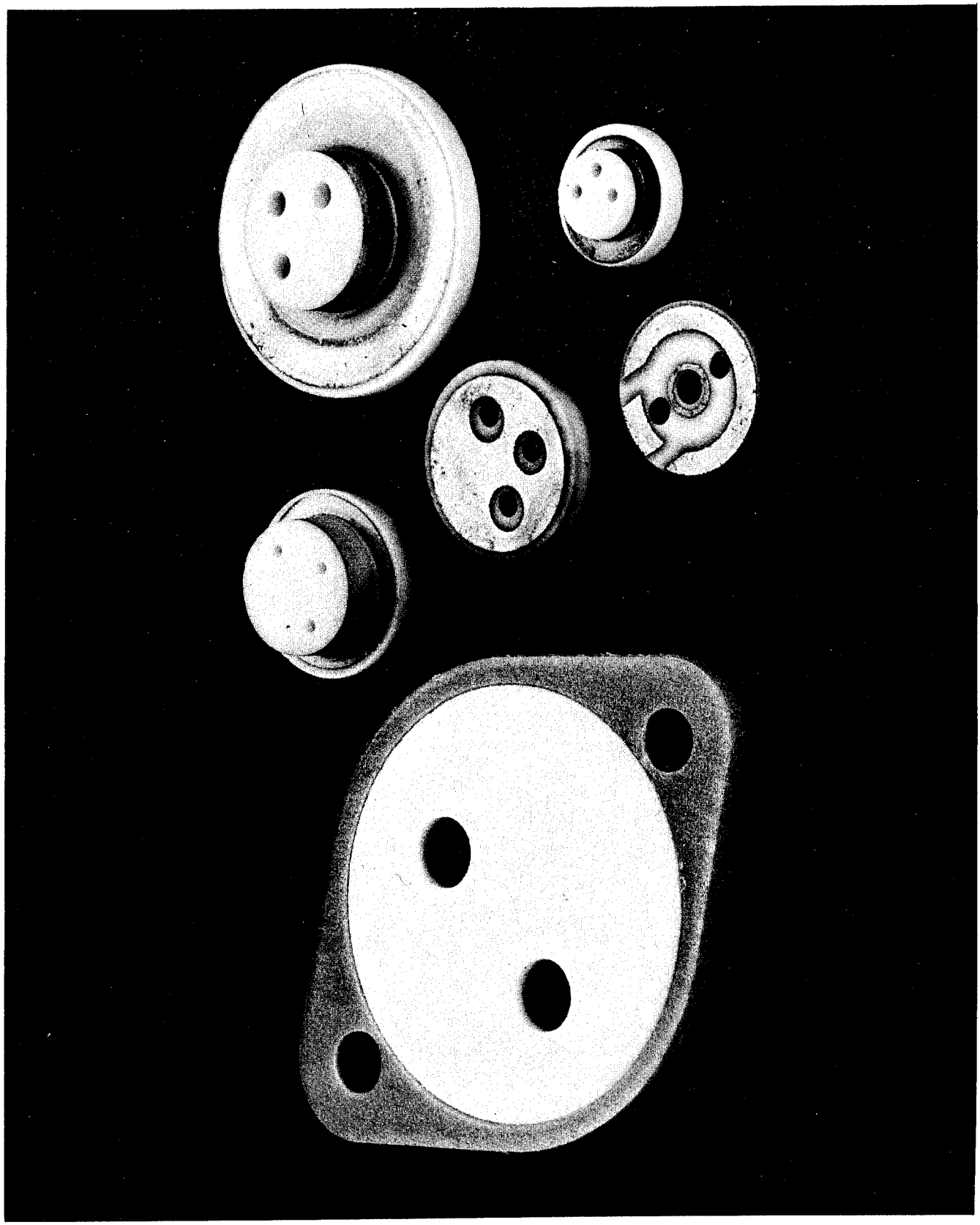

Figure 7

FIGURE 8

Thermal Resistance of Dielectric Heat Sinks
Power Transistor 2N554 at 12 Watts

Material And Thickness	Tc Case Temp. °C	Ts Sink Temp. °C	Thermal Resistance °C per Watt	Corrected for Interface Resistance
No Insulator	52.3	50.6	0.14	0
Mica .0025 in	57.8	50.0	0.65	.51
Anod. Aluminum .022 in.	55.5	49.5	0.50	.36
Glass Fabric .003 inc.	58.3	48.9	0.78	.64
Alumina Ceramic .062	57.8	50.0	0.65	.51
BERLOX BeO .094"	55.5	50.6	0.41	.27
BERLOX BeO .062"	54.4	51.1	0.28	.14
BERLOX BeO .031"	54.4	52.3	0.17	.03

Figure 9

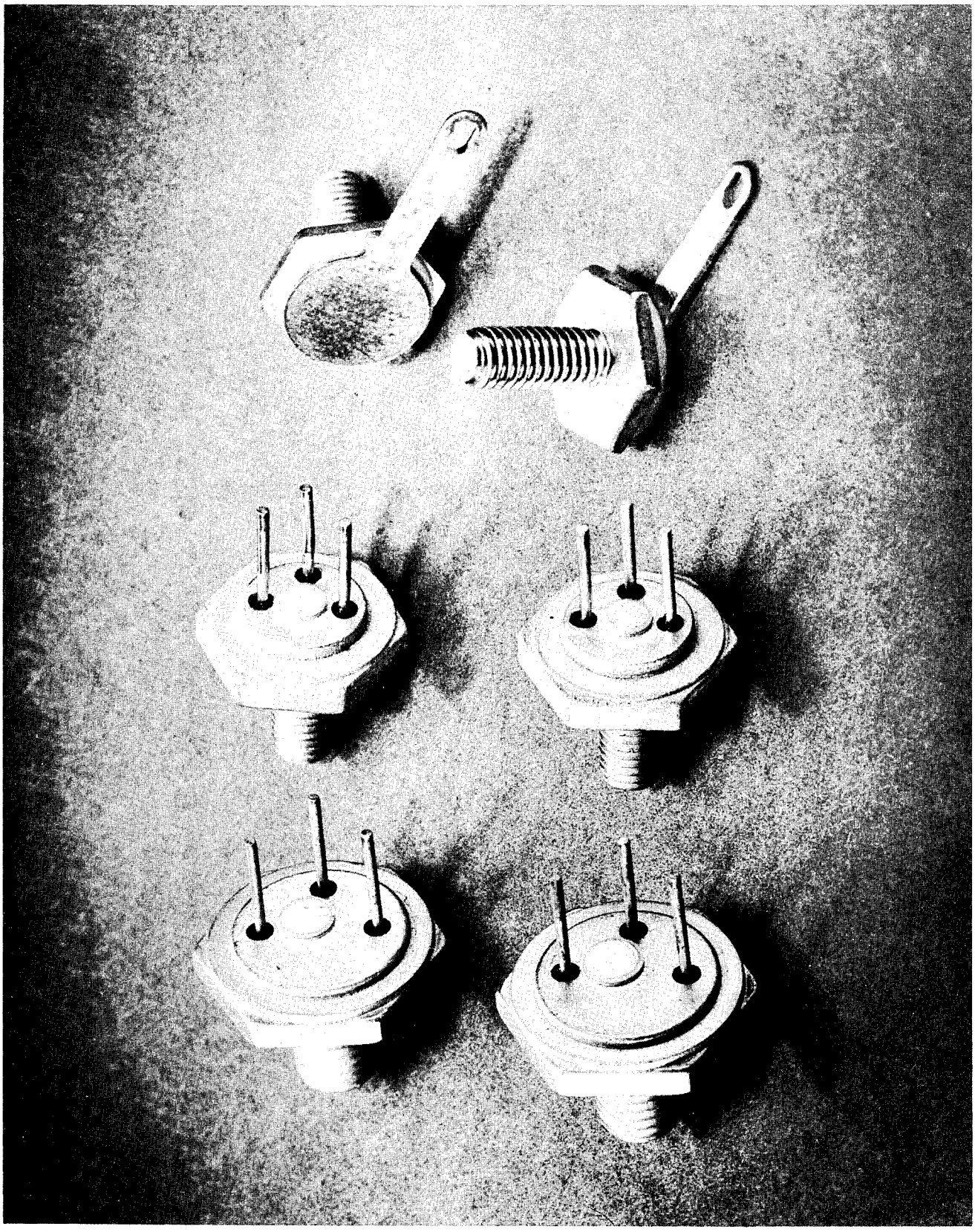

Figure 10

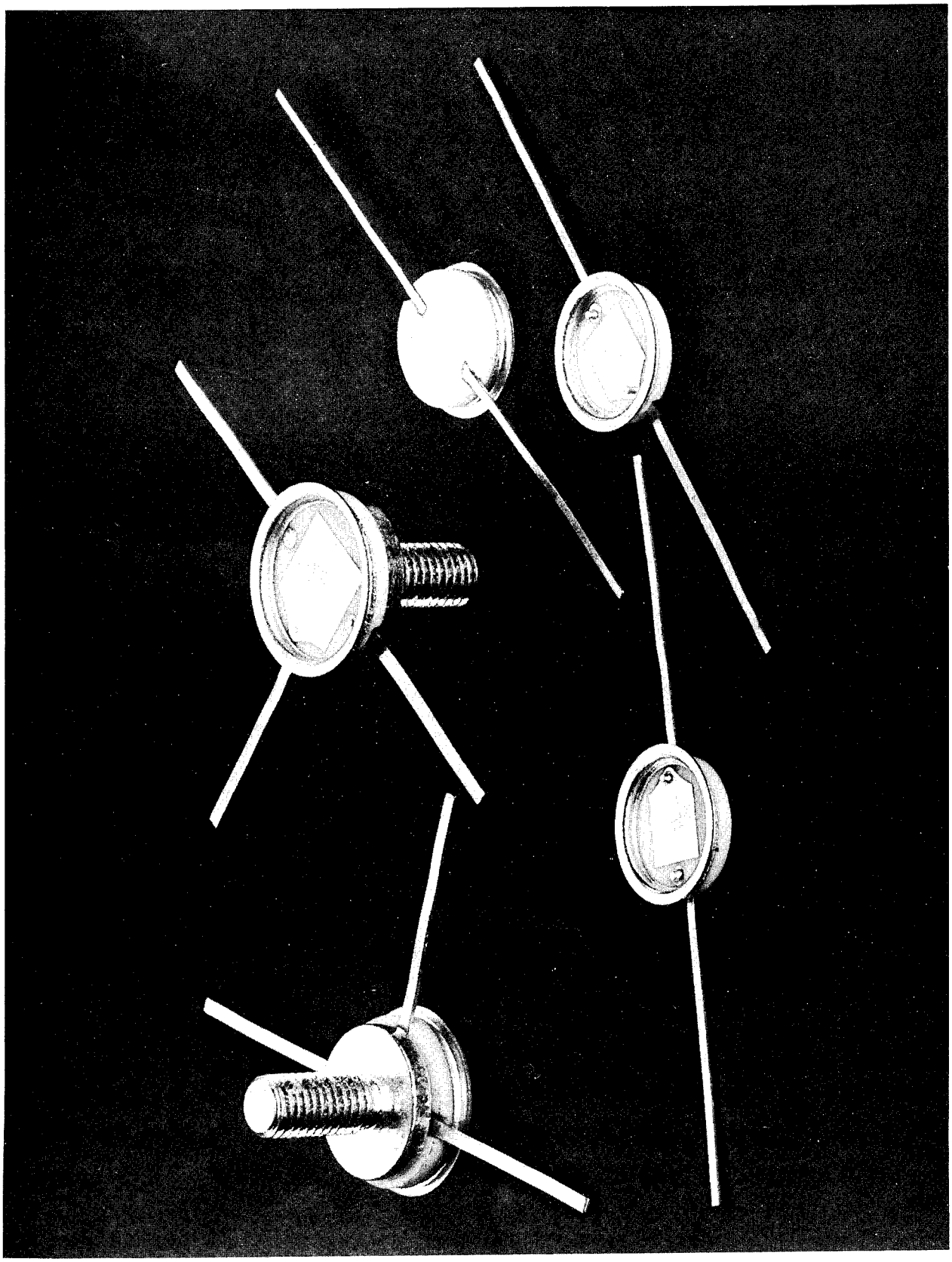

Figure 11

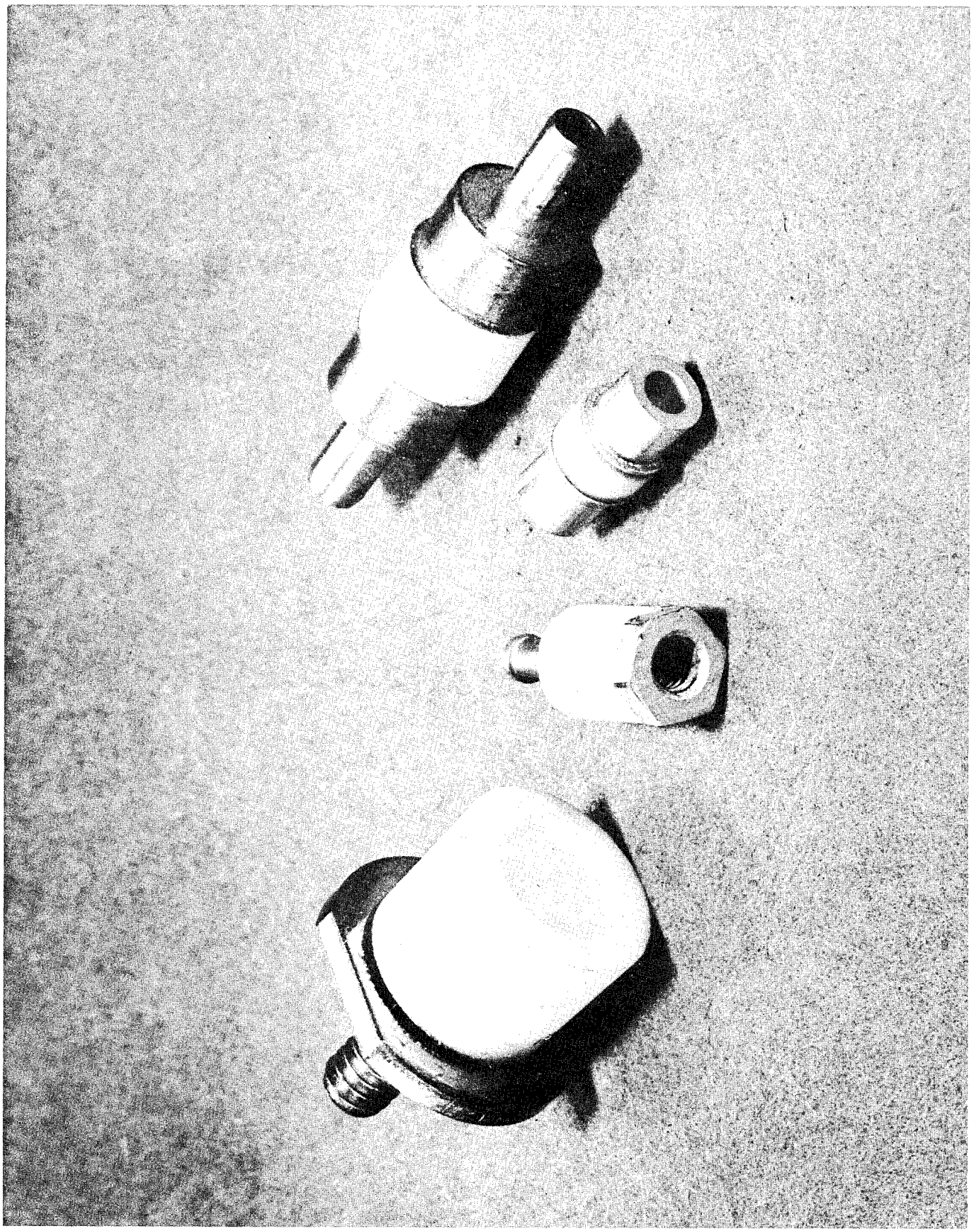

Figure 12

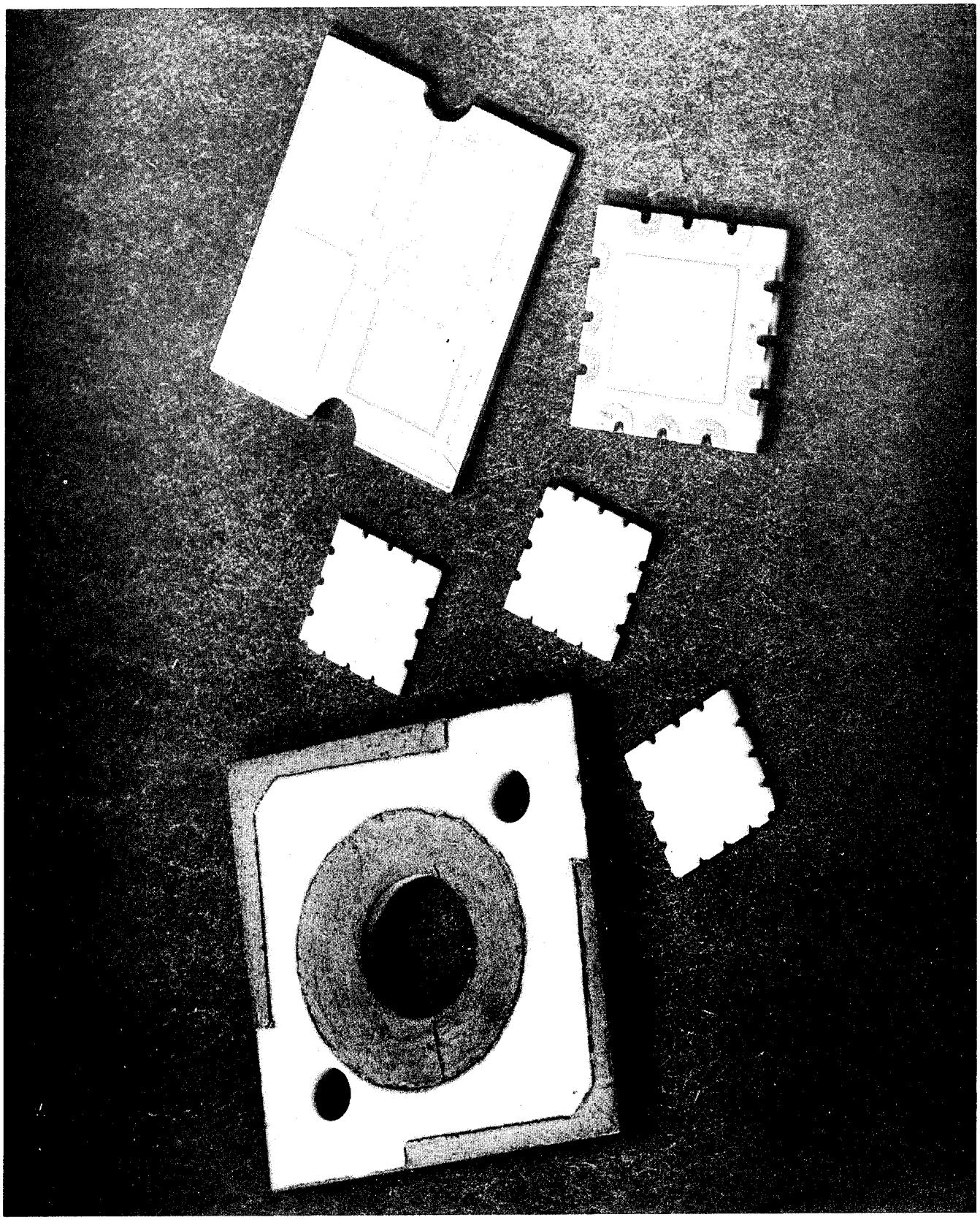

Figure 13

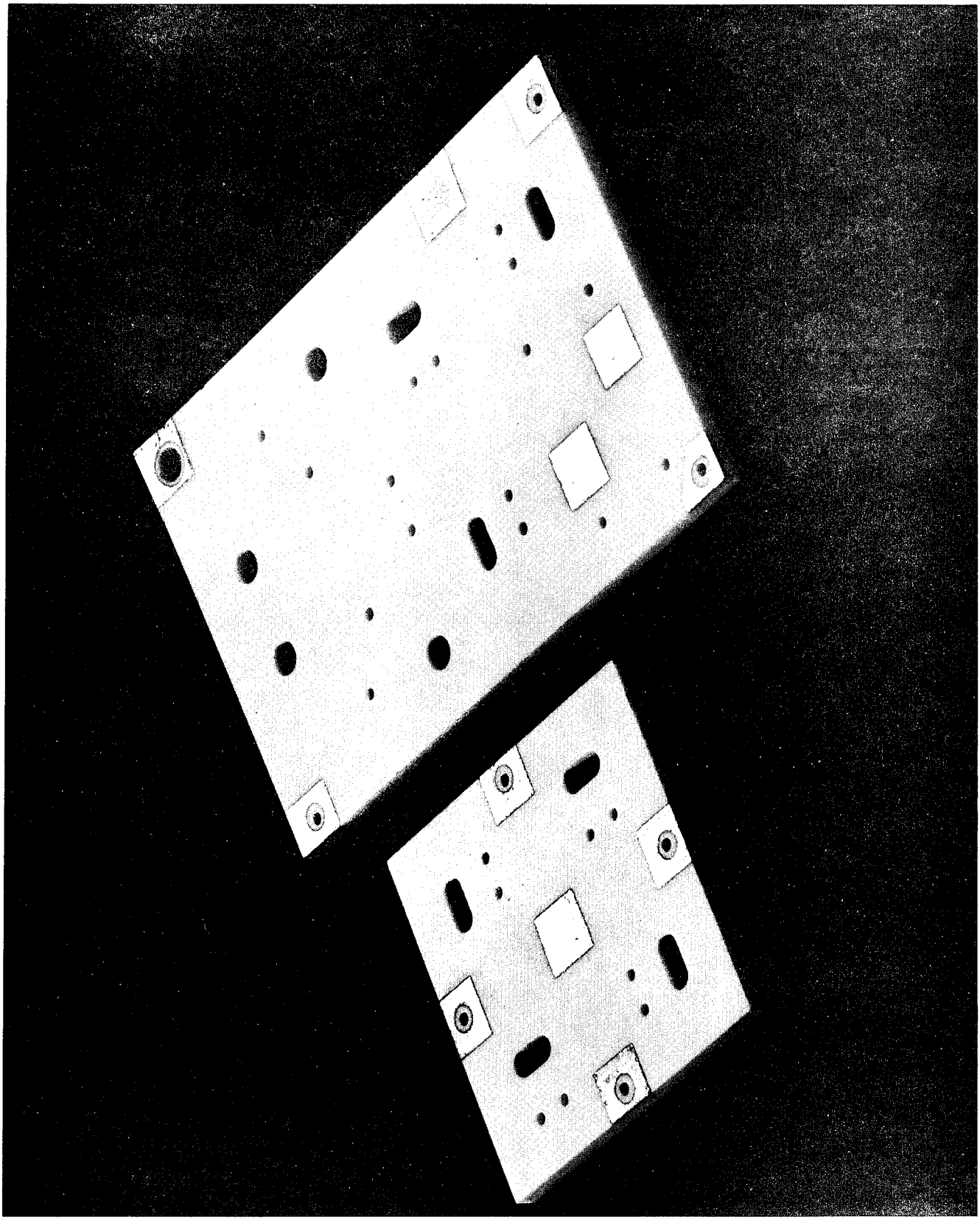

Figure 14

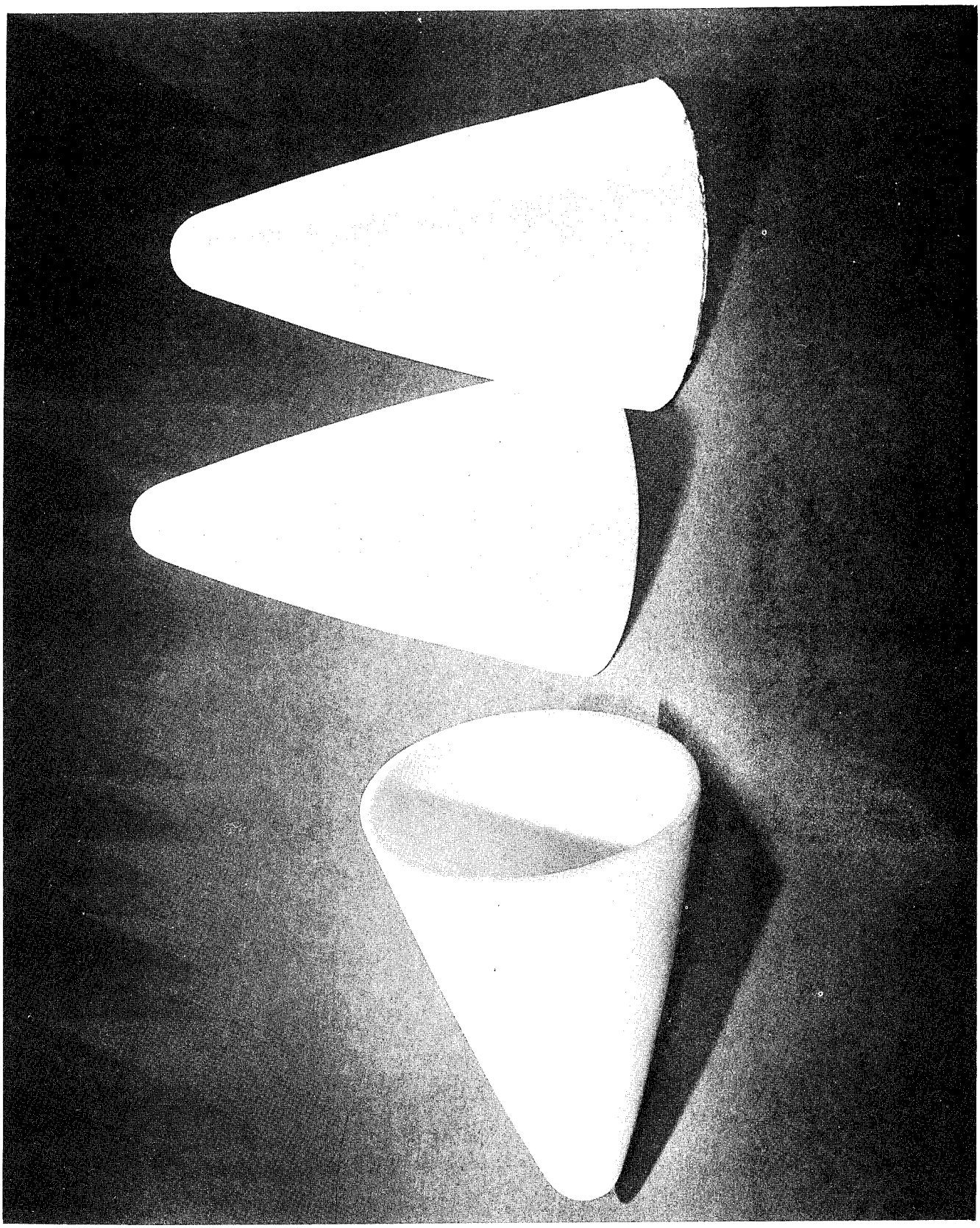

Figure 15

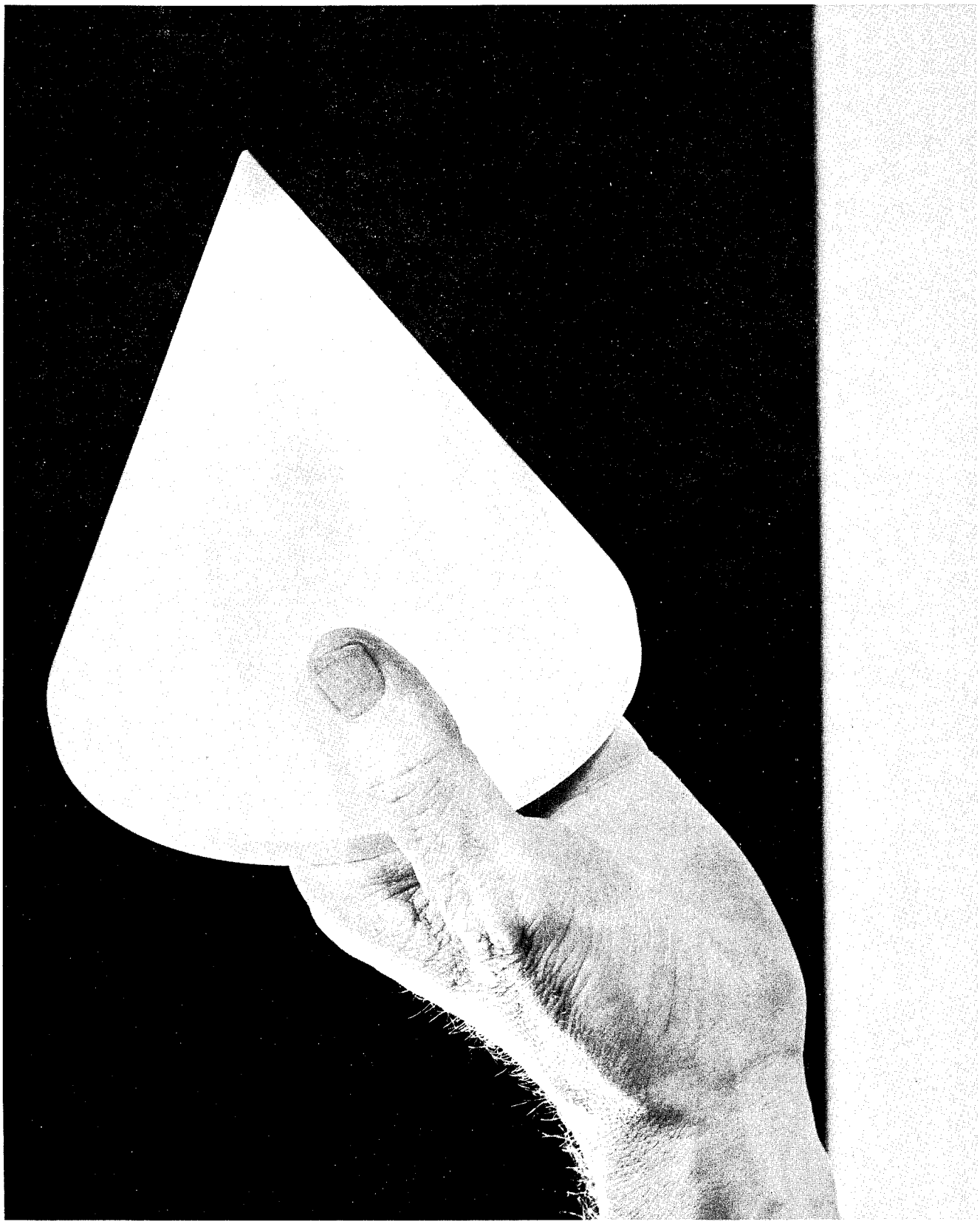

Figure 16

THE ELECTRONIC PROPERTIES INFORMATION CENTER

Emil Schafer
Hughes Aircraft Company, Culver City, California

So much has been said about the information problem, or as it is known, "the information retrieval problem", that no additional comments will be added here. However, the program being undertaken at Hughes Aircraft Co. under the sponsorship of the Information Processing Section of the Applications Laboratory at Wright-Patterson Air Force Base has been established as one of several technical information centers whose responsibility is to accumulate and index the literature and to organize the data collected in more useful form. This operation is called the Electronic Properties Information Center, and under the contract it is required to collect, index, and abstract the literature on the electronic/electrical properties of materials, and to evaluate and compile the experimental data.

This contract began in June 1961, and covers the following categories of materials: insulators, semiconductors, ferroelectrics, metals, ferrites, ferromagnetics, electroluminescents, thermionic emitters and superconductors. The first year-and-a-half were concerned only with the first two categories: insulators and semiconductors. Literature in these two categories was searched back to 1940; during this time more than 50,000 titles were examined of which some 6100 papers were accepted for inclusion in the system. The twelve properties of arc resistance, corona effects, dielectric absorption, dielectric constant, dielectric strength, dissipation factor, electrical conductivity, electrical resistivity, insulation resistance, irradiation effects, loss factor, and power factor as being representative of the properties defining an insulator. As may be imagined, there was some difficulty in defining these categories in terms of properties, and especially in defining a particular material as being in one category, when under various environmental conditions it exhibits properties which place it in two or more other categories.

Some other problems have been in the naming of materials. Basically, a system of chemical names rather than trade names has been settled upon. For example, "Teflon" is indexed under "POLYTETRAFLUOROETHYLENE PLASTICS". Oxide systems follow the nomenclature used in phase diagrams: e.g., "BARIUM OXIDE - ZIRCONIUM OXIDE SYSTEMS", rather than "barium zirconate". In the insulator category, composites of several materials present unique naming difficulties. Similar problems are to be found in the naming of materials and defining of properties chiefly in other than the insulator category. (In our complete system we have space in our computer coding for 99 property names; about 54 property names have been used so far.) Glossaries of properties and effects have been prepared identifying those names used and subsuming the others. For example, a tentative list of 140 properties in the semiconductor category was reduced to 29, with the remainder subsumed.

In searching, only papers containing experimental data have been accepted; theoretical or review papers, or papers devoted solely to the preparation of the materials have been excluded. Every material indexed is assigned a code number. Every property indexed is assigned a property code number. These two numbers, together with the paper accession number, are used to prepare a complete index resulting in a computer printout. It should be noted that the Center maintains a copy of every paper indexed, since the final evaluation and compilation are done from the complete paper, not from the abstract.

The insulator category contains more than 600 terms descriptive of ceramics, plastics, rubbers, glasses, gases, liquids, waxes and so on. Although the term "irradiation effects" has been included as a property, the interest is, of course, in it as another parameter with respect to the dielectric strength, loss factor, etc. Any parameter influencing the electronic/electrical property being examined is of interest in the compilations. Of the 600 insulator terms, it is expected that Data Sheets will be issued on most of them. For example, "DIALLYL PHTHALATE PLASTICS" are subdivided by filler material such as asbestos filled, glass fiber filled, etc. Depending on the literature, individual Data Sheets might or might not be issued.

In contrast to the data contained in the Landolt-Börnstein tables, the EPIC Data Sheets are arranged by material rather than by property. When the literature is evaluated, all papers pertaining to a given material are collated, the data contained in tables and graphs compared, and what are judged to be the best are used in compiling the final Data Sheets. Bibliographies and footnotes are carefully checked to be sure that any valuable and pertinent literature is not overlooked. Evaluation is confined to original, primary papers only. In the insulator category, however, much material of interest is derived from the manufacturer's catalogs and other trade literature. The resulting compilations are carefully reviewed by a group of senior scientists before the Data Sheets are approved and issued. If the data are found questionable because of what appear to be faulty or dubious measurements, unknown sample compositions, or if more reliable data are available, the suspect data are rejected. The data as presented in the Data Sheets are generally in the same form as in the primary publication; graphical matter or tables. Sometimes composite curves are drawn for data selected from various sources; in this case, individual data points are individually identified. Some data require a little care: one curve exhibited a discontinuity caused by the lunch hour and was so identified; in another graph, one scale was marked, 10^{-5}, 10^{-4}, 10^{-2}, and 10^{-1}, with no 10^{-3}. A quick computation was necessary to determine which end of the scale should be changed: the 10^{-2} and 10^{-1} should have been 10^{-3} and 10^{-2}.

The design engineer, in specifying materials for components in a space environment, is vitally interested in how parameters such as external gaseous or plasma pressure, particle and electromagnetic radiation, temperature, etc., affect the electronic properties. Unfortunately, he is also interested in the effect of these parameters on mechanical and other properties. Our work is limited, however, to the effects on electrical/electronic properties.

To date, Data Sheets have been prepared on several important insulation materials: Polyethylene Terephthalate (Mylar), Polytetrafluoroethylene (Teflon), Polytrichlorofluoroethylene (Kel-F), Aluminum Oxide, Magnesium Oxide - Silicon Oxide Systems (Steatite), Silicone Rubber, Pyroceram, Beryllium Oxide, Magnesium Oxide, Borosilicate Glasses and Aluminosilicate Glasses. New Data Sheets are being compiled and issued continually.

The active assistance of all research people is solicited by sending to us copies of papers and reports whose data could be incorporated into our Data Sheets. Every curve and table used is, of course, credited to the original author. Plans for the future include the division of property and parameter data into ranges for more specific retrieval and identification. It is hoped to be able to answer a query for a material given the required property and parameter specifications.

Requests for individual Data Sheets or to be placed on the distribution list should be made by writing to the Commander, Aeronautical Systems Division, Attn: ASRCEM-1, Wright-Patterson AFB, Ohio. Requests should state in which category/categories of materials (insulators, semiconductors, ferroelectrics, metals, ferrites, ferromagnetics, electroluminescents, thermionic emitters and superconductors) Data Sheets are desired. During 1963, it is expected that Data Sheets for the insulator and semiconductor categories only will be issued; issuance of Data Sheets for other categories will begin in 1964. Reciprocity in sending new data to us will permit the preparation of more complete and meaningful Data Sheets.

ROUND TABLE

PANEL DISCUSSION

R. D. Shelton
NASA - Marshall Space Flight Center

The things I wish to talk about are some special dielectric problems in space. (They are special because I am interested in them.) They might be grouped around the general heading of the interactions of charged particle radiation with dielectrics. One way we get into this area is as follows: In the process of coating satellites for heat balance and in performing certain experiments you find that some of your more rugged materials are insulators and dielectrics. In the case of one satellite they decided that in order to heat balance the thing properly so that the transistors would be at the right temperatures, they ought to paint some polka-dot pattern on the outside, and that one of the insulators would be a good material with the proper emittence, absorptance, and so forth. Somebody wanted to put a plasma probe experiment on the satellite and asked the following question: If the satellite with its insulator conductor surface is running into the solar wind and into the radiation belts, what is the difference in characteristics between a metal surface and an insulator surface? The charges strike the insulators, they are embedded in the insulator, and because they are not conducted away, they create stray electric fields which interfere with the plasma probe measurements.

One of the interesting things being looked at now is the potential assumed by a satellite moving through the solar wind. In order to answer this question you need to look at the interaction of the charged particle radiation with the dielectric surface which covers the satellite. The micrometeroid experiment will use a very large quarter mil Mylar capacitor with several square meters of area. When a meteroid penetrates this capacitor it will produce an ionized trail which causes the capacitor to discharge. But unfortunately you have several problems which I will just enumerate very briefly: There are essentially 3 regions, consisting of conductor, Mylar (or something else, if this doesn't work), and a conductor on the other side. You have radiation impacting on the capacitor. The radiation does a couple of things: If the electrons (or protons) stop in the material, you have charged particles in the material. The charged particles produce electric fields, and the electric fields produce breakdown. You get discharges sort of like the effects talked about on the plate glass yesterday. Another thing that happens, if you have either compton collisions or a photoelectric event, is that electrons are displaced by the radiation. This creates other electric fields in the dielectric which appear as induced voltages or induced currents. So I think one very interesting area would be the interaction of charged particle radiation with the various dielectrics that are used in spacecraft. This is a very poorly understood field. In fact, the electron penetration has been so poorly understood that someone has ended up misjudging the count rate on a detector by a factor of 100, just due to not knowing the penetration laws for electrons through materials.

Alexander Smakula
Massachusetts Institute of Technology

I should like to bring up a few questions. I will not provide any solutions; only suggestions. Hearing the papers yesterday and today, I think the majority of us have the impression that dielectrics in space constitute a very complicated problem. The question is: What shall we do with this complication? Something must be done. Of course it would be foolish to try to appoint some kind of committee that would decide what to do. In my opinion everyone of us should try to do by himself whatever he can. By personal contact with other fellows we might have a possibility to solve at least part of these very complicated problems. I was surprised that there is only one chemist who has been among us, even though he did present an excellent paper. Since the dielectric problems are so complicated, I should think that we need a very close collaboration of chemists, physicists and engineers. Most papers gave us an approach on more or less technical subjects. We definitely need it; we cannot wait until fundamentals will be solved. But we must not forget the fundamentals, and we must try to think very hard how to eliminate bottlenecks and find the most essential parameters. These have to be studied very carefully; one level of the problems cannot be completely separated from another one. It would be much better if, for instance, even such competitors as General Electric and Westinghouse would exchange ideas and even samples. This definitely would help (Laughter!!). As you know, impurities play a very important role; therefore it is not proper if everybody tries to buy, let us say, all the best materials, which are definitely from Du Pont (!), and then try to measure something, while the supplier will not tell you exactly what is in it. The next time you order even the same material, the company might have added something in order to improve some properties. This way we will not make any fast progress. Another thing: we should try to get good reproducibility, both of samples and methods. Also we should measure the essential properties not only at one temperature, but cover a whole range and eventually vary the time as well. We should take continuous measurements to see what happens between the points. Too often we are inclined to assume a smooth change but, as you know, it is not always so. Now radiation damage is of particular concern; we know it does not go linearly with time and dose. In this connection I should like to mention our experience. We did some radiation damage with 3-Mev electrons on various ionic crystals, simple crystals, and solid solutions. I expected that in solid solutions there would be much higher radiation damage or, let us say, higher trapping of electrons and holes because those crystals are definitely more disturbed. But it turned out that it was not the case. We found a trapping decrease of electrons in some systems by a factor of 5 or even 10. Temperature has a similar effect. The coloration by radiation at room temperature is generally quite strong but at liquid-nitrogen or liquid-helium temperature it is much weaker. Yet at about -80°C the effect is much higher than either at lower or higher temperatures. Thus one has to be very careful with interpolation.

Now one last remark. I would like to know: Why is this conference called "Dielectrics in Space"? Do we have dielectrics without space? You know we scientists, who are not philologists, are a little to lazy to think hard what kind of proper name to give; so we take just what we have at hand. I have to confess I did the same, with KRS-5, which we are treating so badly today. You probably do not know what KRS-5 means, but I will now tell you the secret, since the war is over and you now may know it: It is nothing but KR, the first two letters from the German word for crystal, S for synthetic, and 5, because it was my fifth experiment that succeeded.

Karl Martinez
The Boeing Company

Most of my comments will be around some of the basic research and the use of research results in space systems and components and the use of these in a nebulously defined environment and operational parameters. You can see as I go along why I would title this as a summary of problems that are faced by various types of vehicles that are to operate in leaving the face of the earth and going out and some time later returning. Some of the problems that are faced include a better definition of the combined natural and man-made environments, definition of the combined operational parameters, and definition of the rate of change of these parameters. Keeping the above in mind, along come the reliability boys who say they must have a high degree of reliability, long service life, maintainability, ease of operation, light in weight, no volume, and so forth. So some of the items that we are interested in specifically as applied to components are:

1. Improve the dielectric properties of various fluids that are used as coolants in electrical and electronic equipment.

2. Some applications require good thermal conductivity as well.

3. Many solid and flexible dielectrics in a vacuum show outgassing and embrittlement when combined with the other environmental parameters. What can we learn about these?

4. Use of inert gas itself as a dielectric in hermetically sealed equipment. The gas just doesn't stay sealed for some of the metals. What can we do to improve the containment of these gases inside of hermetically sealed units?

5. Use of vacuum itself as a dielectric instead of conventional dielectric materials. This may save weight.

6. We need dielectric materials that are not affected by such contaminants as ordinary dirt, fluids, fumes, lubricants.

7. One question that has been raised is the cold welding in a vacuum of dielectric materials to each other and dielectric to non-dielectric materials. Is this a problem? We don't know.

8. We need adhesives with good dielectric properties in themselves such that they will not deteriorate dielectric properties of other materials when applied.

9. There is need for dielectric insulating materials for use inside of cryogenic fluid tanks. The above are a number of uses being pioneered and we need to know more about them. Then comes the other question:

10. Will various radiation fields create transient voltages and, if so, how much?

11. The use of dielectric materials that are not as porous to such gases as oxygen, hydrogen, nitrogen, helium, and so forth.

12. Radome and antenna dielectrics with very low losses to stand temperature ranges from near absolute zero on up to about 5000°F.

13. Dielectric characteristics of materials over a wide frequency range combined with vacuum, radiation and temperature environment.

14. Dielectric materials with good thermal transport characteristics.

15. Then last but not least, laboratories are needed for synthesizing the combined environmental and operational parameters over the widest limit to be foreseen including the rate of change to be anticipated.

Included in the above is the interest in getting light weight materials. Just before the meeting I was intrigued in an item that a gentlemen sitting in the room has and I would like to call on him, Dr. Okaya. He has something in the way of an electronics item illustrating the trend towards microminiaturization of some of the things that we are after in order to save volume. This happens to be one of them so I hope you ladies and gentlemen don't mind my calling on him.

Akira Okaya
Westinghouse Research Laboratories

I would like to call your attention to the miniaturization of a dielectric resonator. The size of this resonator is 1/8" square x 1/16" thick. This small piece of rutile corresponds to this conventional bulky resonator having a volume of more than a cubic inch. The reason is very simple. This crystal has a high dielectric constant, about 100. The Q of this resonator is about the same as a metal cavity at room temperature. If you go down to liquid helium temperature the Q is much higher than the metal cavity. With some other crystals, we observe a Q of about 1 million, which is almost incredible. So I think we have quite a good example of miniaturization, and here is another example. This is another resonator. This is a resonator for 10 centimeter wavelength. I have a paper discussing this so I will not go into any detail here. The paper is published in the October 1962 Proceedings of IRE which covers the details. This is another example: a filter. It is a very simple structure and very easy to adjust and quite reliable. You could make a band pass filter and also band reject filter of high or low Q.

E. L. Brancato
F. J. Campbell*
U. S. Naval Research Laboratory

Space has introduced new dimensions to the demands imposed upon dielectric materials. These dimensions now include vacuum, ultraviolet, particle radiation, and broad temperature-range, from cryogenic to searing levels. As if this were not enough, there has been added the need to reduce size and weight and to increase performance reliability to a very high level. The one mitigating factor to this new trend is that performance life expectancy has been reduced--in many cases, to a matter of minutes. Thus, a comprehensive experimental study of dielectric materials should be made to obtain the short-time rating. It is expected that the performance index of dielectrics will vary markedly from long-time to short-time function.

Since dielectrics must function under a multiplicity of environments, the interaction of these ambients upon the degradation of materials makes it important that the properties of dielectrics be observed under more completely simulated space conditions. Properties obtained in ultraviolet alone, or under particle radiation alone, or temperature alone, may give misleading results. For example, a study in our laboratory has shown that while the thermal life of electrical insulation is influenced by radiation, this influence differs markedly on a given material between a concurrent exposure and sequential exposures to heat and radiation. We have experimented with both processes in a study of insulating enamels and varnishes on magnet wires and have found that for some materials the normal thermal lives are greatly increased by combining heat aging with a gamma radiation exposure. Twisted pair specimens were used on which the end-of-life was determined by a 1000-volt electric strength test. It was discovered that normal thermal life of polyvinyl formal was enhanced by 870% at 160°C in the combined environment, while a silicone-enamel-varnish combination increased 162% at 240°C and a polyester, 780% at 200°C. Of the wires still in progress, ML enamel (an aromatic polyimide) which was noted as a very thermally stable organic material in two of the papers given today, has been aging at 300°C and 5×10^5 Roentgens per hour for more than 400% of its normal thermal life with no failures to date. Increased life is not universal for all materials since several others in this study had much less than normal thermal lives. Thus, it is apparent that only by testing in the combined environment of the anticipated service can we obtain a reliable estimate of service reliability.

In another area, we feel that more work should be done in the exploration of organic dielectric materials to fulfill dynamic functions, such as was reported by Dr. Beam, where films are used as thermoelectrostatic solar energy converters. Also, more encouragement should be given to research into the understanding of the semiconductor properties of some organic compounds and to their synthesis. There are a few laboratories investigating this field. To our knowledge, a small amount of the research is being sponsored by the Bureau of Ships and investigated by Drs. W. H. Yanko and M. E. Gutzke of Monsanto Research Corporation.

---

*Discussion presented by Mr. Campbell.

Finally, one other materials area requiring greater attention is that of adhesives. They are significantly important in that they may serve as a mechanical binder (to attach thermal insulation to the walls of a liquid fuel tank) or as a dielectric barrier in the bonding of solar cells to metal substrate material, and in another function, to bond the glass shields to the front surface of solar cells. Here, of course, they must be transparent. If you recall in Mr. Cherry's talk following the banquet, solar cells are sensitive to radiation damage; some types more than others. Likewise, this is true for transparent adhesives and some types of glass currently being used for the shields. When degradation occurs, it is first observed as a decrease in the spectral transmittance characteristics in the violet and blue wavelength region; thus, we observe the material turning yellow as the radiation dose increases. Now the damage in a solar cell occurs as a decrease in the response to red wavelengths; thus effect of the combined damages is like closing the curtain from both ends of the spectrum to reduce the solar energy conversion efficiency of the solar cell. Some recent studies at NRL indicated that an ultraviolet exposure will reduce transmittance of a commonly used adhesive at the critical wavelength of 0.5 microns by as much as 45%, and an exposure to 1 Mev electrons, by as much as 24%. Exposures to 5-Mev protons produced similar damages. Just as solar cell research is aimed toward greater radiation resistance, more work is also needed to develop improved adhesives so necessary in the construction of solar cell systems powering today's satellites.

QUESTIONS

AND

ANSWERS

QUESTIONS AND DISCUSSION AFTER ROUND TABLE SPEAKERS

A. S. Denholm
Ion Physics Corporation

Q. In this discussion comments have been made on some vacuum tests being made at unnecessarily low pressures. I am sure that most of us realize that where surface effects are important there can be good reasons for testing in ultra high vacuum. At pressures below 10^{-9} torr it is possible to maintain surfaces free of adsorbed gas which can be significant to studies of vacuum discharges, friction, fatigue, etc.

We have already discussed the deleterious effects of radiation on solar cells. It may not be generally known that Ion Physics Corporation, and possibly others, are making solar cells using radiation techniques. Impurities are introduced into the base material by high energy bombardment with impurity ions. For example, boron ions are implanted in silicon this way. Varying the acceleration energy gives different penetration depths and gives better control of the fabrication process than the usual diffusion techniques. For example, the cells can have a better relative response to the solar spectrum than those fabricated in the usual way. Efficiencies of 8.5% have been obtained so far. Does the panel know of this technique?

F. J. Campbell
U. S. Naval Research Laboratory

This is a new technique to me but I might ask, does the pre-irradiation stabilize the solar cell to further radiation degradation which is one of the things that has been found once the radiation reaches a certain degradation level it sort of asymptotically goes on from there. Is this something that you might have found?

A. S. Denholm
Ion Physics Corporation

A. We are in the process of examining this effect for the ion implanted cells and results should be known shortly.

K. N. Mathes
General Electric Company

Q. I would like to make a comment and raise a question in respect to a comment made by several members of the panel. I personally have been very interested in what I once called functional evaluation; in other words, the evaluation of materials under the environmental conditions. Now I frankly have become scared and I think we may have opened up Pandora's box. As Frank Campbell points out: We need combined environment conditions such as radiation and temperature. I might add: voltage and physical strength and many other factors all combined at the same time. There was a point raised also about the fact that intensity--the degree of acceleration--is very important. Professor Smakula points out that not only does

he not wish to extrapolate, but he isn't even sure that he can interpolate. In the data I showed by Dr. Volger of Eindhoven, his (loss factor) peaks for quartz were found at 10 to 20°K. If he had made tests at only liquid helium (about 4°K) and at liquid N_2 (77°K) temperatures, the peaks would have been missed entirely. So we could go on and on. We could talk about the question of ultra high vacuum and I agree with the comment about the importance of high vacuum not only under some circumstances. Then comes the question about volume effects, and then the question about geometry and how geometry affects all of the other factors. I suddenly am getting awfully scared again. I recognize that we can't wait for fundamental understanding. If we just pile pages of mathematics on the board, we'll never get anywhere. (Maybe I wish I were 15 years older so I could retire!) I do think that maybe it is conferences like this which will begin to bring together new kinds of thoughts from many areas and inter-disciplinary feeling. It may be that out of this, by some miraculous approach, we do get some feeling of what to do under these circumstances, just as the bumblebee does fly. I wonder if there may be comment from the panel on this rather heterogeneous statement.

R. D. Shelton
NASA - Marshall Space Flight Center

A. I want to make a brief statement about some of these computations on the damage by charged particles. I've tried two computations during the last year: one was on the damage to solar cells and the other was on how long the dielectrics will stand up under space radiation. Looking at the environments to establish the important factors, I found out that, in the available spectrum of protons or electrons, a piece was missing in the spectrum between about 1 Mev down to 2 Kev. This was the most important part contributing to the solar cell and surface dielectric damage. So one big piece of missing information is the radiation environment.

J. R. Perkins
E. I. du Pont de Nemours & Co., Inc.

Q. I'd like to ask Frank Campbell about his continued work on the combined effects. We're talking about the thermal and radiation effects. The very logical thing would be to go ahead and to add vacuum to these. I was wondering if you had plans to do that, and secondly, if you do, based on your experience on the non-additive effects, what do you predict for the third?

F. J. Campbell
U. S. Naval Research Laboratory

A. From results of our studies, I can't predict a thing. Our chamber is adaptable to a vacuum, rather difficult though, because our radiation source is below 100 feet of water, but we can reach about 10^{-2} (mm) with the vacuum system we have now.

J. R. Perkins
E. I. du Pont de Nemours & Co., Inc.

Q. Don't forget the voltage, too.

F. J. Campbell
U. S. Naval Research Laboratory

A. I have to take my specimens out of the source and exposure to make voltage tests.

Alexander Smakula
Massachusetts Institute of Technology

I should like to mention the circumstance that we are really in the woods. What shall we do? In my opinion we have actually only two extreme possibilities: Either we wait until some genius finds a way and tells us what to do. Such things happen from time to time; some gifted scientists have a proper feeling for what is needed and in what direction to go. But this is so rare that we hardly can wait for it. So nothing remains for us but just to work very hard and try to do our best.

Karl Martinez
The Boeing Company

Hearing about the bewildered attitude that some of us have about being scared and wishing we were 15 years or so older so we could retire reminds me of an experience not too long ago when there was a certain company, an aircraft company, that was designing an airplane that became known as a B-17. There was a professor at one of the universities in aerodynamics that flatly told us back in the early 30's that such an airplane would never fly because it had a certain L/D and a wing span of such and such and it had a certain weight versus drag characteristics. He proved mathematically that that B-17 was never going to fly. Well, it's a good thing that human beings have pessimistic as well as optimistic views and like the bumblebee, we didn't know any better so somebody build the B-17 and it flew. Today we're still bewildered in a good many areas. Listening to the views here, the pros and cons of a very excellent cross-section of industry on materials reminds me of a comment made by Dr. Arthur Von Hippel not too long ago. He said that the men working on materials in the basic research are still not far removed from the alchemists or an excellent cook. A pinch of this and a pinch of that and a right amount of so and so and you stir it up and it comes out tasting delicious but what is it? Then somebody else has to take on the job of finding out what it is and why it is and what it can be used for. Primarily what it can be used for. This approach is necessary. We do not want to lose that capability in this country. But in addition to that, one of the

things that this meeting indicates is the need for some directed effort towards finding what the environmental parameters are so that we can go into the basic materials research and direct some of that research, not all of it, towards synthesizing materials towards the end utilization. I once told Dr. Von Hipple that we should put some effort into trying to get a basic method, a system whereby we could synthesize some of these future environmental parameters and then with that method, very broadly speaking, even put it into a computer so that we could find out what molecules had to be put together in order to come out with the characteristics that we needed in the end result. Of course, this is probably Utopia and I don't imagine that many people will appreciate that or even realize that something like that might be thought of. Maybe many of them have, but this has often come to my mind, to minds of several people. We have kicked it around and you should hear the fantastic approaches that have resulted. If you think we're bewildered now, you should wait until another half generation goes by, we will be really bewildered.

W. H. Redanz
National Carbon Company

Q. I would like to go back to the question I raised this morning, and perhaps bring back to my laboratory a little more specific definition of what I've heard during the last few days about the need for a high temperature insulator. We in our laboratories have scientists working in the area of high temperature chemistry and for other reasons than making insulators. They have come up with a commercial process to make what turns out to be a pretty good electrical insulator. Perhaps we can put the same kind of chemistry to work, to solve a problem in high temperature electrical insulation. I'd like to have some comments on the specific need for a high temperature insulator; such as what temperature? what metals at these temperatures would the insulator come in intimate contact with? I certainly have an idea of vacuum and voltage requirements. These chemical questions would help them, giving them a specific description of what is needed.

Karl Martinez
The Boeing Company

A. You mentioned some needs or examples of actual needs and uses for high temperature electrical insulating materials and metals they would be next to. Certain vehicles, some are ballistic in nature as far as leaving the face of the earth and returning back in a ballistic projectory and others that have a controlled re-entry back into the earth's atmosphere meet temperatures in different parts of the body that vary all the way from a temperature of around 4000°F down to a cool temperature of about 1700°. It is necessary to take measurements of temperature out of those areas. As a result, one application comes to mind: that of getting thermocouple electrical wires out there. This is a very real

application. Thermocouple wires, not to carry electrical power, but to carry instrumentation measuring currents. Can you imagine trying to use an ordinary chromel alumel and the more ordinary electrical insulating materials out there. When you realize that the specific resistivity of normal electrical insulating materials (I say the word normal, advisedly) around this wire have a specific resistivity that may be in megohms near room temperature; at a temperature of 1000°F higher the specific resistivity gets down in some cases to about 1 ohm. This would not be very good. There have been efforts to increase the specific resistivity at temperatures that I've mentioned. This has not been easy, however, over the years. The last two years specifically, there were 92 separate independent research and industry companies contacted to get such a wire. Out of those 92 I received 18 replies back, out of those 18 only 6 said that they would even consider to look at the problem and out of those 6 only 2 actually got serious, about wanting to look at the bids. This gives you an idea about what went on in this country in the past few years. We today do have the wire, electrical wire for primarily instrumentation purposes. The material is not copper, which melts at about 1700°. It is not chromel-alumel and it's not tungsten because tungsten becomes extremely brittle and oxidizes. It is a platinum alloy. One of the reasons for platinum alloy, not pure platinum, is that we wanted an almost flat resistivity at the temperatures that we're using: all the way from room temperature clear up to the high temperature. Most metals when you plot the resistance versus temperature have a fairly steep rise as the temperatures goes up. We don't want that if we can help it. There is an actual application. The secret was in the assembly of the entire combined wire, the techniques used. We have also found that it has been necessary for us to consider the use of this wire for power circuits which really threw us for a loop at first, but fortunately we have found ways and means to carry very modest amounts of power, and throw away our thoughts that we must have the specific resistivity of copper for these circuits. We have had to change our point of reference. This might help you in an actual application, as far as your company is concerned.

LIST

OF

ATTENDEES

LIST OF ATTENDEES

Amborski, L. E.	E. I. du Pont de Nemours & Co., Inc., Yerkes Research Laboratory, Buffalo 7, New York
Anton, H.	Cosmic, Inc., Washington 7, D. C.
Barney, W. H.	Corning Glass Works, Corning, New York
Beam, B. H.	NASA - Ames Research Center, Moffett Field, California
Bechtold, J. H.	Westinghouse R & D Center, Pittsburgh 35, Pa.
Berg, D.	Westinghouse R & D Center, Pittsburgh 35, Pa.
Blair, G. R.	Hughes Aircraft Co., Culver City, California
Bober, E. S.	Westinghouse R & D Center, Pittsburgh 35, Pa.
Brummet, B. D.	Thomas A. Edison Research Lab., West Orange, New Jersey
Burge, G. W.	Douglas Aircraft Co., Santa Monica, California
Byers, D. C.	NASA - Lewis Research Center, Cleveland 35, Ohio
Campbell, F. J.	U.S. Naval Research Lab., Washington 25, D. C.
Castle, J. G.	Westinghouse R & D Center, Pittsburgh 35, Pa.
Cherry, W. R.	NASA - Goddard Space Flight Center, Greenbelt, Maryland
Cole, Q. P.	General Electric Co., Erie, Pa.
Corcoran, C. S.	NASA - Lewis Research Center, Cleveland 35, Ohio
Dakin, T. W.	Westinghouse R & D Center, Pittsburgh 35, Pa.
Davis, E. K.	Westinghouse R & D Center, Pittsburgh 35, Pa.
Delacy, E.	Sylvania Systems Engrg., Waltham, Massachusetts
Denholm, A. S.	Ion Physics Corporation, Burlington, Massachusetts
Devaney, R. G.	Tennessee Eastman Co., Kingsport, Tennessee
Doyle, T. E.	Mellon Institute, Pittsburgh, Pennsylvania
Elbling, I. N.	Westinghouse R & D Center, Pittsburgh 35, Pa.
Elcox, R. E.	Ion Physics Corporation, Burlington, Massachusetts
Ellithorn, H. E.	Hughes Aircraft Co., Fullerton, California
Endicott, H. S.	General Electric Co., Philadelphia 1, Pa.
Ernst, W. A.	Westinghouse Air Arm Division, Baltimore, Maryland
Fertig, J. M.	Westinghouse R & D Center, Pittsburgh 35, Pa.
Flowers, L. C.	Westinghouse R & D Center, Pittsburgh 35, Pa.
Frederick, W. G. D.	Wright-Patterson Air Force Base, Ohio
Freeman, J. H.	Westinghouse R & D Center, Pittsburgh 35, Pa.
Frisco, L. J.	Johns Hopkins University, Baltimore 31, Maryland

Gail, H. R.	Westinghouse Gateway Office, Pittsburgh, Pa.
Gainer, G. C.	Westinghouse R & D Center, Pittsburgh 35, Pa.
Gilmore, A. L. E.	Westinghouse R & D Center, Pittsburgh 35, Pa.
Goba, F. A.	Canadian Westinghouse Corp., Hamilton, Ontario, Canada
Gregor, L. V.	IBM Research Center, Yorktown Heights, New York
Hardtke, F. C.	Argonne National Laboratory, Argonne, Illinois
Harrison, H.	NASA Headquarters, Washington 25, D. C.
Haura, B.	National Beryllia Corp., Haskell, New Jersey
Hayes, M. E.	Westinghouse Electronics Div., Baltimore, Maryland
Heacock, J. F.	E. I. du Pont de Nemours & Co., Inc., Yerkes Research Laboratory, Buffalo 7, New York
Herrmann, D. B.	Bell Telephone Labs., Murray Hill, New Jersey
Hespenheide, W.	Burroughs Corporation, Pittsburgh, Pa.
Hessinger, P. S.	National Beryllia Corp., Haskell, New Jersey
Hickam, W. M.	Westinghouse R & D Center, Pittsburgh 35, Pa.
Hirayama, C.	Westinghouse R & D Center, Pittsburgh 35, Pa.
Hofmann, C. F.	Westinghouse R & D Center, Pittsburgh 35, Pa.
Hogle, D. H.	Minnesota Mining & Mfg. Co., St. Paul 19, Minnesota
Izzo, C. P.	Westinghouse R & D Center, Pittsburgh 35, Pa.
Jolley, C. E.	E. I. du Pont de Nemours & Co., Inc., Wilmington, Del.
Kannam, P. J.	Westinghouse Semiconductor Div., Youngwood, Pa.
Kaputa, E. J.	NASA Headquarters, Washington 25, D. C.
Kelly, J. C. R., Jr.	Westinghouse R & D Center, Pittsburgh 35, Pa.
Kerr, D. R.	IBM Corporation, Poughkeepsie, New York
Klein, A. A., Jr.	Hughes Aircraft Co., Fullerton, California
Kofoid, M. J.	Boeing Company, Seattle, Washington
Kovac, Carl	ELECTRONIC NEWS - Pittsburgh, Pa.
Kueser, P.	Westinghouse Lima Works, Lima, Ohio
Lell, E.	Bausch & Lomb, Inc., Rochester 2, New York
Lewis, D. W.	Westinghouse R & D Center, Pittsburgh 35, Pa.
Lin, F. C.	Westinghouse R & D Center, Pittsburgh 35, Pa.
Litant, I.	Avco Corporation, Wilmington, Massachusetts
Littlefield, E. B.	Avco Corporation, Wilmington, Massachusetts
Malinaric, P. J.	Westinghouse R & D Center, Pittsburgh 35, Pa.
Martinez, K.	Boeing Company, Seattle, Washington

Mathes, K. N.	General Electric Co., Schenectady, New York
McCarthy, J. L.	INSULATION Magazine, Libertyville, Illinois
McGahey, R. V.	Westinghouse Gateway Office, Pittsburgh, Pa.
McIlvaine, D. K.	Westinghouse Lima Works, Lima, Ohio
McMahon, W.	Bell Telephone Labs., Murray Hill, New Jersey
Miille, R.	Westinghouse Lima Works, Lima, Ohio
Moberly, L. E.	Westinghouse R & D Center, Pittsburgh 35, Pa.
Molzon, A. E.	Picatinny Arsenal, Dover, New Jersey
Moses, G. L.	Westinghouse Electric Corp., East Pittsburgh, Pa.
Murphy, E. B.	Massachusetts Inst. of Tech., Lexington, Massachusetts
Neff, W. S.	Westinghouse Lima Works, Lima, Ohio
Novotny, G.	ELECTRONICS Magazine
Okaya, A.	Westinghouse R & D Center, Pittsburgh 35, Pa.
Parisi, G. I.	Bell Telephone Labs., Murray Hill, New Jersey
Pascale, J. V.	Bell Telephone Labs., Murray Hill, New Jersey
Pavane, M. M.	USAF Scientific & Tech. Liaison Office, New York, New York
Penny, G. W.	Carnegie Institute of Technology, Pittsburgh, Pa.
Perkins, J. R.	E. I. du Pont de Nemours & Co., Inc., Wilmington, Del.
Pezdertz, G.	NASA - Langley Research Center, Hampton, South Carolina
Pickett, J. H.	Westinghouse Electric Corp., Irwin, Pa.
Power, E. J.	Bell Telephone Labs., Whippany, New Jersey
Rao, D.A.A.S. Narayana	University of Saskatchewan, Saskatchewan, Canada
Redanz, W. H.	National Carbon Co., New York, New York
Rider, M.	Westinghouse Buffalo Division, Buffalo, New York
Riel, R. K.	Westinghouse Semiconductor Div., Youngwood, Pa.
Rowe, E.	B. F. Goodrich Research Center, Brecksville, Ohio
Ruffing, C. R.	Westinghouse R & D Center, Pittsburgh 35, Pa.
Runk, R. H.	Westinghouse R & D Center, Pittsburgh 35, Pa.
Sassano, D. R.	Westinghouse R & D Center, Pittsburgh 35, Pa.
Sattler, F. A.	Westinghouse R & D Center, Pittsburgh 35, Pa.
Schafer, E.	Hughes Aircraft Co., Culver City, California
Shelton, R. D.	NASA - Marshall Space Flight Center, Huntsville, Alabama
Sheppard, H. R.	Westinghouse Sharon Division, Sharon, Pa.
Shoupp, W. E.	Westinghouse R & D Center, Pittsburgh 35, Pa.

Skinner, S. M.	Westinghouse Air Arm Division, Baltimore, Maryland
Sletten, A. M.	Westinghouse R & D Center, Pittsburgh 35, Pa.
Smakula, A.	Massachusetts Inst. of Tech., Cambridge, Massachusetts
Smyth, D. M.	Sprague Electric Co., North Adams, Massachusetts
Snelling, G. R.	E. I. du Pont de Nemours & Co., Inc., Philadelphia, Pa.
Snyder, A. W.	Sandia Corporation, Albuquerque, New Mexico
Sommerman, G. M. L.	Westinghouse R & D Center, Pittsburgh 35, Pa.
Spoerer, C. G.	Westinghouse R & D Center, Pittsburgh 35, Pa.
Sprengling, G. R.	Westinghouse R & D Center, Pittsburgh 35, Pa.
Steel, O. P.	Atomics International, Canoga Park, California
Stevens, N. J.	NASA - Lewis Research Center, Cleveland, Ohio
Strier, M. P.	Thomas A. Edison Research Lab., West Orange, New Jersey
Sun, K. H.	Westinghouse R & D Center, Pittsburgh 35, Pa.
Swiss, J.	Westinghouse R & D Center, Pittsburgh 35, Pa.
Tarneja, K. S.	Westinghouse Semiconductor Div., Youngwood, Pa.
Tracy, J.	Celanese Research Labs., Summit, New Jersey
Tuckerman, A. J.	Hughes Aircraft Co., Culver City, California
Vest, C. E.	NASA - Goddard Space Flight Center, Greenbelt, Maryland
Vondracek, C. H.	Westinghouse R & D Center, Pittsburgh 35, Pa.
Wales, A. F.	American Enka Corporation, Enka, North Carolina
Warrick, F. E.	American Enka Corporation, Concord, Massachusetts
Weeks, R. A.	Oak Ridge National Lab., Oak Ridge, Tennessee
Werberig, C.	Thiokol Chemical Corp., Trenton 4, New Jersey
Winslow, J.	U.S. Naval Radiological Defense Lab., San Francisco, Cal.
Woodland, P. C.	Dow Chemical Company, Midland, Michigan
Works, C. N.	Westinghouse R & D Center, Pittsburgh 35, Pa.
Yeoman, F. A.	Westinghouse R & D Center, Pittsburgh 35, Pa.

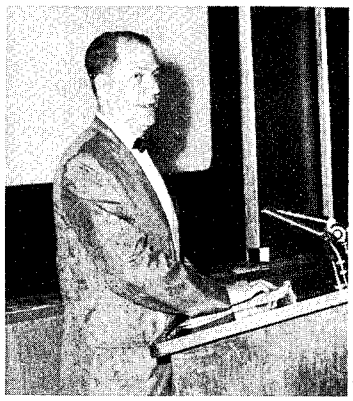

H. Harrison

A. S. Denholm

T. W. Dakin

M. J. Kofoid

L. J. Frisco

R. A. Weeks

K. H. Sun

D. B. Herrmann

A. W. Snyder

E. J. Kaputa

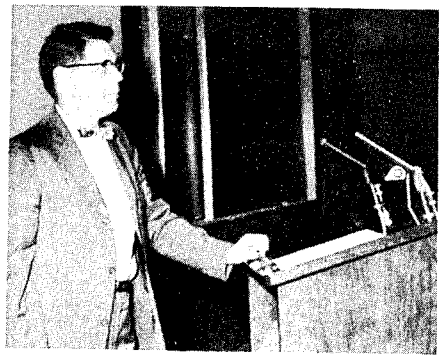

G. R. Blair

S. M. Skinner

K. N. Mathes

G. R. Sprengling

B. H. Beam

J. Swiss

O. P. Steele

P. S. Hessinger

MEMBERS OF THE ROUND TABLE

R. D. Shelton, K. Martinez, A. Smakula, F. J. Campbell
J. C. R. Kelly, Moderator

J. Swiss, D. Berg, W. E. Shoupp
Westinghouse

W. E. Shoupp I. N. Elbling
Westinghouse

J. Swiss, W. R. Cherry, NASA
(Banquet Speaker), W. E. Shoupp

W. E. Shoupp, Westinghouse
Vice President - Research
Banquet Toastmaster

W. R. Cherry, Head, Space Power
Technology, NASA - Banquet Speaker

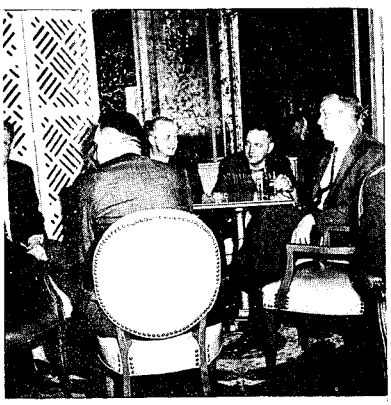

K. H. Sun, G. W. Penny, A. W. Snyder